AFRICA CENTER OF EXCELLENCE FOR WATER MANAGEMENT
ADDIS ABABA UNIVERSITY
SCHOOL OF GRADUATE STUDIES
COLLEGE OF NATURAL AND COMPUTATIONAL SCIENCES

Hydrological and Hydrodynamic Modelling of Flows to Support Establishment of Flood Adaptation Strategies for River Malaba Sub-Catchment in Uganda

By:

Ambrose MUBIALIWO

A Ph.D. dissertation submitted to Africa Center of Excellence for Water Management, the School of Graduate Studies of Addis Ababa University in partial fulfilment of the requirements for **The Degree of Doctor of Philosophy in Water Management (Hydrology and Water Resources Management)**

March 2022

Addis Ababa, Ethiopia

Africa Center of Excellence for Water Management

Addis Ababa University

School of Graduate Studies

Hydrological and Hydrodynamic Modelling of Flows to Support Establishment of Flood Adaptation Strategies for River Malaba Sub-Catchment in Uganda

By:

Ambrose MUBIALIWO

A Ph.D. dissertation submitted to Africa Center of Excellence for Water Management, the School of Graduate Studies of Addis Ababa University in partial fulfilment of the requirements for **The Degree of Doctor of Philosophy in Water Management (Hydrology and Water Resources Management)**

Declaration

I, Ambrose Mubialiwo (GSR/4334/11), hereby declare that this research dissertation titled ***"Hydrological and Hydrodynamic Modelling of Flows to Support Establishment of Flood Adaptation Strategies for River Malaba Sub-Catchment in Uganda"*** has been developed by me and has not been submitted to any other institution for award of any academic qualification. The content of the dissertation has not been plagiarized and where works of other researchers have been used, they have been appropriately cited.

Ph.D. Candidate	**Signature**	**Date**
Ambrose MUBIALIWO	_____	_____

AFRICA CENTER OF EXCELLENCE FOR WATER MANAGEMENT

ADDIS ABABA UNIVERSITY

Hydrological and Hydrodynamic Modelling of Flows to Support Establishment of Flood Adaptation Strategies for River Malaba Sub-Catchment in Uganda

By:

Ambrose MUBIALIWO

A PHD DISSERTATION SUBMITTED

TO
AFRICA CENTER OF EXCELLENCE FOR WATER MANAGEMENT
ADDIS ABABA UNIVERSITY

APPROVED BY BOARD OF EXAMINERS

The undersigned confirm that they have read this Ph.D. research Dissertation and that in their opinion; it is fully adequate, in scope and quality, as a PhD dissertation for **The Degree of Doctor of Philosophy in Water Management (Hydrology and Water Resources Management)**

Advisor
Name Dr. Ing. Adane ABEBE Signature _____ Date _____

Advisor
Name Dr. Charles ONYUTHA Signature _____ Date _____

Examiner
Name Prof. Yang HONG Signature _____ Date _____

Examiner
Name Dr. Alemseged TAMIRU Signature _____ Date _____

Chairperson
Name Dr. Feleke ZEGWE Signature _____ Date _____

Acknowledgements

I would like to Praise and Thank the Almighty God, for granting me uncountable blessings, knowledge, and capacity to complete the Ph.D. programme. I am heartily thankful to my advisors Assoc Prof. Dr. Ing. Adane Abene (Ph.D.) and Dr. Charles Onyutha (Ph.D.) whose inspiration, encouragement, direction, mentorship and support all through empowered me to develop an understanding of how to handle this research. May the Lord bless them. I am indebted to the Africa Center of Excellence for Water Management, Addis Ababa University, Ethiopia for funding my four-year Ph.D. studies, as it would not have been possible for me to attain it without their financial support. I extend my gratitude to the academic and administrative staff at Africa Center of Excellence for Water Management, Addis Ababa University, Ethiopia for their knowledge and administrative support.

I am so grateful to the Department of Civil and Environmental Engineering, Kyambogo University, Uganda for providing office space and computer laboratory services in addition to granting me a four-year study leave to pursue my Ph.D. studies in Ethiopia. In a special way, my heart is overwhelmed for my dear wife Eva, and children Praise, Pervin and Pearl for their love, support and tolerance of my absence for the four years. To my parents, brothers and sisters, I address my wholehearted appreciations for giving me the strength to reach for the stars and chase my dreams.

Special thanks go to my friends Eng. Joel Mubiru, Eng. Anthelem Iragena, Dr. Sam Bulolo, Eng. Willington Amanyire and their families for always loving me and my family. I am beholden to Mr. Enock Kajubi and Mr. Cyrus Chelangat for their substantial contributions during the execution of this research. To Mr. Andrew Mutenga of Butaleja District Local Government, his guidance during data collection and additional support whenever called upon are gratefully acknowledged. I extend my vote of thanks to the community of River Malaba sub-catchment for their active participation and information provided during the field activities. I am grateful to the Ministry of Water and Environment of Uganda and National Forest Authority of Uganda for providing part of the data used in this research.

Dedication

This work is dedicated to my parents, my siblings, my wife, my three beautiful daughters (Praise, Pervin and Pearl) and my Ph.D. Advisors.

Table of Content

List of Tables

List of Figures

Acronyms and Notations

ACRONYMS			
AMM	Annual Maxima Method	LP	Less Preferred
ANMS	Annual maxima series	LSA	Least Applicable
AMR	Annual Mean Rainfall	LSE	Less Effective
AMV	Annual mean value	LSP	Least Preferred
AWBM	Australian Water Balance Model	LULC	Land Use Land Cover
		MA	Most Applicable
ADF	Amplitude-Duration-Frequency	MAB	Model Average Bias
CL	95% Confidence Interval Limits	MAE	Mean Absolute Error
CMA	Coefficient of Model Accuracy	MAM	March-April-May
		MdA	Moderately Applicable
CSD	Cumulative Sum of rank Differences	MdE	Moderately Effective
		MdP	Moderately Preferred
CSI	Critical Success Index	ME	Most Effective
CUSUM	Cumulative Sum	MP	Most Preferred
CV	Contingent Valuation	MWE	Ministry of Water and Environment
BDDC	Double-bound dichotomous choice	NSE	Nash Sutcliffe efficiency
DEM	Digital Elevation Model	OCHA	Office of the Coordination of Humanitarian Affairs
EPIs	Extreme Precipitation Indices		
EVD	Extreme Value Distribution	OH	Oscillation Highs
FAR	False Alarm Ratio	OL	Oscillation Lows
FDF	Flow-Duration Frequency	OND	October-November-December
FGDs	Focus Group Discussions	POT	Peak-Over-Threshold
GDP	Generalised Pareto Distribution	PET	Potential Evapotranspiration
HEC-RAS	Hydraulic Engineering Center's River Analysis System	PGF	Princeton Global Forcing
		Q	Extreme Flow Quantile
HMSV	Hydrological Model focusing on Sub-flows' Variation	Q-Q	Quantile-Quantile
		RRM	Ratio of Root Mean squared error to the maximum event
HR	Hit Rate		
IDF	Intensity-Duration Frequency	SAC	Sacramento
IHACRES	Identification of Unit Hydrographs and Component Flows from Rainfall, Evaporation and Stream	SMAR	Soil Moisture Accounting and Routing
		UAV	unmanned aerial vehicle
		UGX	Uganda Shillings
ITZC	Inter-Tropical Convergence Zone	UQ	Upper Quantile
JJAS	June-July-August-September	VA	Very Applicable
JICA	Japan International Cooperation Agency	VE	Very Effective
		VP	Very Preferred
KGE	Kling–Gupta efficiency	WAI	Weighted Average Index
KIIs	Key Informants Interviews	WMO	World Meteorological Organisation
KWMZ	Kyoga Water Management Zone		
LA	Less Applicable	WTP	Willingness to Pay
LE	Less Effective	YRP	Year Return Period
LQ	Lower Quantile	YRPF	Year Return Period Flood

NOTATIONS

B_{cf}	*B*ias correction factor
B_e	Bias error
β^s	Regression coefficients
β^s	Starting bid
β^f	Follow-up bid
Ck	Coefficient of kurtosis
Cs	Coefficient of skewness
Cv	Coefficient of variation
H_o	Null hypothesis
H_1	alternative null hypothesis
I_a	Index of agreement
m	Trend Magnitude/slope
m.a.s.l.	Meters above sea level
m^3s^{-1}	Cubic meter per second
n	Samples size
NWD5	Wet days
NWD10	Very wet day
PRCPTOT	Annual total wet-day precipitation
SPre5	Sum of precipitation >5 mmday^{-1}
Spre10	Sum of precipitation >10 mmday^{-1}
T	Return Period
T_{CSD}	Trend statistic
ρ	Density
T_{max}	Daily maximum temperature
T_{min}	Daily minimum temperature
TPre10	Rainfall total >10 mmday^{-1}
R	Coefficient of determination
R10	Number of heavy precipitation days
R_e	Relative efficiency
US$	United States Dollar
Z	Standardised trend statistics
$Z_{\alpha/2}$	Standard normal variate
α	Significance level
p	Probability value
τ	Power parameter
σ	Standard deviation/error
2D	Two-dimensional
I_a	Index of agreement
γ	Scale parameter
x_t	Threshold
λ	Shape parameter
r	net rainfall

Abstract

Many people tend to live in the floodplains along River Malaba due to fertile soils which support agriculture. However, heavy rains in the highlands of Mount Elgon often lead to floods which end up affecting especially the local population in terms of loss of lives and destruction of infrastructure within the low-lying areas of River Malaba sub-catchment in Uganda. This research aimed at presenting a platform for understanding the impacts of flooding on the socio-economy while investigating perceived effectiveness of establishing flood adaptation strategies for predictive risk-based water resources management in the study area. The study had four specific objectives including; (i) to analyse changes in historical rainfall and potential evapotranspiration (PET), (ii) to perform hydrological modelling of extreme peak flows, (iii) to estimate impacts of flooding given the spatial extents of flooding inundations, and (iv) to analyse community willingness-to-pay (WTP) for flooding adaptation strategies. Changes in terms of trends and variability were analysed using nonparametric approach based on the cumulative sum of the difference between exceedance and nonexceedance counts of data points. The second specific objective consisted of determining which hydrological model could best reproduce observed extreme peak flows. Hydrodynamic modelling was performed using a two-dimensional Hydraulic Engineering Center's River Analysis System model. Double-bound dichotomous choice contingent valuation method was applied to assess the local population's WTP for flooding adaptation measures. The number of days with rainfall intensity > 5 mm/day and 10 mm/day had insignificant (p>0.05) decreasing trend. The sum of rainfall with intensities > 5 mm/day exhibited a significant (p<0.05) decreasing trend. However, annual maxima rainfall increased (p>0.05), indicating less frequent rains but some events having very high intensity. Variability of rainfall sub-trends was insignificant (p>0.05) and had a common pattern. PET had an insignificant (p>0.05) positive trend. The amplitudes in PET variability were insignificant (p>0.05) and though of generally common pattern. The Australian Water Balance Model exhibited the best performance in reproducing extreme peak flows and it had Nash–Sutcliffe efficiency (NSE) of 0.837. Land-use change had insignificant (p>0.05) influence on determining flood inundation extents. Inundation of rice gardens by the most severe 100-year flood was found to lead to an economic loss of about US$ 39 million. Amongst the infrastructure, churches showed the highest economic losses of US$ 1,623,832 due to flooding of 100-year return period. In general, the local community was aware of the flood citing rainfall variability and longer rainfall durations as main cause of flooding. Post-

flood strategies were more efficient than those practiced before- and during-floods. Among the suggested structural and non-structural strategies, “river training structures” and “flood forecasting and early warning” were highly preferred, respectively. 55% of the households expressed WTP an individual amount between Uganda shillings (UGX) 5,000 (US$ 1.35) to UGX 500,000 (US$ 135.14). Several demographic, social and institutional factors had significant (p<0.01) positive impact on community WTP. This study findings are relevant in supporting policy makers regarding predictive planning and development of flood risk adaptation pathways given the established destructions within the sub-catchment due to flooding.

Key words: River Malaba sub-catchment, extreme peaks flows, hydrological and hydrodynamic modelling, flood adaptation strategies, willingness-to-pay

Chapter One

1. Introduction

1.1 Background

The high productivity of soils along River Malaba tends to increase the desire for local population to settle adjacent to floodplain corridors. The areas around Mount Elgon are known for encroachment of gazetted forest reserve by the local population for human settlement and farming (Sassen and Sheil, 2013). The soil under massive deforestation experiences increased exposure to erosion by rainfall runoff. The heavy rainwaters received in the highlands of Mount Elgon result in the bursting of river banks, hence flooding the low-lying areas of Tororo and Butaleja as well as some parts of Namutumba and Bugiri districts. Within the same area, the highland areas of Manafwa and Bududa are vulnerable to rainfall-induced landslides (Mayega *et al.*, 2015; Ministry of Water and Environment, 2018a). These weather events leave devastating effects including loss of lives, destruction of property, infrastructures, and displacement of people (Ministry of Water and Environment, 2018b, 2014a).

Some of the devastating events caused by peak high rainfall intensities include (1) the May 2021 floods that affected thousands of the population (Floodlist, 2021); (2) the floods of December 2019 with at least 4 deaths and over 2000 people displaced, (Floodlist, 2019); (3) the severe floods and landslides in Bududa of October 2018, displacing 858 people, 51 deaths and a total of 12,000 people affected (Assessment Capacity Project (ACAPS), 2018). Similarly, the severe landslides of March 2010 killed over 400 and displaced 5,000 people in Bududa district (Atuyambe *et al*., 2011), and over 33,000 households affected in Butaleja (OCHA, 2010). These events have a tendency to occur annually.

Floods in River Malaba sub-catchment have one of the highest occurrence and geographical distribution (United Nations International Strategy for Disaster Reduction, UNISDR, 2018). With the recurrent floods in different parts of Uganda, the local and national economies are highly vulnerable due to the impacts on crucial sectors such as agriculture, water resources, forest, energy, health, infrastructure and settlement. Thus, the possibility of Uganda realising its "Vision 2040" targets still hangs in balance (Ministry of Water and Environment, 2018a, 2015). Due to the disastrous impacts including hindrance of sustainable development especially in the developing

world (Rakib *et al*., 2017), there is a need to come up with flood adaptation strategies (Thomas and López, 2015). Adaptation is the process of making transformation in the human systems in response to real or predictable climatic events and or their related impacts, aimed at reducing the harm or exploitation of beneficial opportunities (City of Vancouver, 2020; Levina and Tirpak, 2006). Formulation of adaptation strategies exclusively based on modelling may result in increased risks rendering the society more susceptible to infrequent but extremely impacting disasters (Ciullo *et al*., 2017). Baan and Klijn (2004) emphasised that effective management of floods requires investigation of both technical and socio-economic aspects which guide decision-making on the establishment of feasible flood protection strategies.

Despite the possible predictability of floods as they occur repeatedly, communities in River Malaba sub-catchment have continued to suffer the consequences. This could be attributed to inappropriate adaptation mechanisms being employed (Mayega *et al.*, 2015). Some communities in River Malaba sub-catchment have adopted good agricultural methods such as afforestation and introduction of terracing as a strategy for reducing the effects of floods and landslides (Osuret *et al*., 2016). However, like other parts in the country, the area still grapples with low adaptive capacity with respect to flooding impacts, mainly due to financial and technical constraints in addition to societal issues. Besides, in Uganda, there is a challenge in mainstreaming adaptations into sectoral strategies and plans as well as low capacity at district and community levels to engage in adaptation planning (Echeverría *et al*., 2016). Recently, to lessen the impacts consequent to occurrence of floods, the community support in monetary form and/or generosity (physical effort), has become crucial. This has been through the use of flood management mechanisms that rely on the Willingness to Pay (WTP) (see e.g. Arnal *et al*., 2016; Entorf and Jensen, 2020; Gravitiani and Suryanto, 2017; Maghsood *et al*., 2019; Reeser, 2016; Thistlethwaite *et al*., 2020).

1.2 Statement of the problem

The dramatic weather events identified in section 1.1 result in distressing effects, such as loss of human lives, displacement of local population, death of livestock and destruction of infrastructure. Such losses have affected various sectors, such as agriculture, water resources, forest, energy, health, infrastructure and settlement. To effectively manage the flooding impacts, policy-makers require vital information for vigilant and careful planning of risk-based water resources management strategies. These require an integration of hydrological/hydraulic modelling and social aspects, to incorporate all concepts obtained from various stakeholders especially the

vulnerable community. To generate information vital for the intended purpose by the policy-makers and other stakeholders involved in flood management, there is need to consider, as accomplished in this study,

a) Specific in context to River Malaba sub-catchment,
b) analyses of the changes in key climate variable (rainfall and potential evapotranspiration), considering extreme high conditions to guide the spatio-temporal mappings of floods,
c) evaluation of multiple hydrological models' performance on several "goodness-of-fit" metrics and select the best in simulating extreme peak flows,
d) application of 2D hydrodynamic model to evaluate the landscape effect on the magnitude of flooding,
e) integration of hydrology and societal understanding of floods, and
f) establishment of the community willingness-to-pay, and their influencing factors.

Several climate variability and flooding-related studies have been conducted. However, none of the studies had the aforesaid considerations (a), to d). For instance, the studies were not specific in context to River Malaba sub-catchment but rather, done at regional scales e.g., Kansiime *et al*. (2013); at large water basins e.g., Kizza *et al*. (2009), Nyeko-Ogiramoi *et al*. (2013), Alemu *et al.* (2015), Mugume *et al*. (2016); Onyutha *et al.* (2020), and country-wide scales e.g., Phillips and Mcintyre (2000), Nsubuga *et al*. (2014), Mwaura and Okoboi (2014), Majaliwa *et al.* (2015), Onyutha (2016a), Jury (2018), Onyutha *et al*. (2021b) and Ngoma *et al.* (2021). Furthermore, most studies focused on rainfall and temperature variability, except, Alemu *et al.* (2015) and Onyutha (2016b) that considered evapotranspiration. Whereas analysis of temperature can give an insight of the evapotranspiration, the end-user especially the farmers require specific information on evapotranspiration. In addition, most of the studies (Luwa *et al*., 2021; Mubialiwo *et al*., 2021c; Ngoma *et al*., 2021; Onyutha *et al*., 2021b, 2020) assessed trends on average values of climatic variables. On the other hand, a few studies (Barasa *et al.*, 2013; Onyutha, 2020a) have analysed changes in extreme meteorological variables. However, Barasa *et al.* (2013) focused on drought indices and did not suggest any adaptation strategies, while Onyutha (2020a) considered Lake Victoria Basin (outside the study area).

A few studies (Ednah, 2018; Onyutha and Willems, 2018) on hydrological modelling applied either one or very few hydrological models. On the other hand, the study by Onyutha *et al.* (2021) applied seven lumped conceptual models in the simulation of daily River Kafu flows. However,

this study was conducted in western Uganda and not in the eastern part of Uganda (where the study area is located). Besides, most of these studies applied either one or very few (maximum of 4) "goodness-of-fit" measures. There were no previous studies that applied 2D hydrodynamic models to simulate floods in River Malaba sub-catchment.

Bomuhangi *et al.* (2016), established the local community insights on climate variability based on the meteorological data trends. However, the study was confined to only two districts (Manafwa and Kapchorwa), for which, Kapchorwa falls outside the River Malaba sub-catchment. In addition, the study was not accompanied by any hydrological or hydrodynamic modelling to yield results which would be associated with the community perceptions to suggest adaptation strategies. The study which established the coping strategies and underlying causes of vulnerability to landslides and flooding in the Mount Elgon region (Osuret *et al.*, 2016), was only based on qualitative analysis of the social aspect with no hydrological and/or hydrodynamic concepts. Several studies which were conducted in Uganda to analyse the community willingness-to-pay (Angella *et al*., 2014; Banga *et al*., 2011; Hansen *et al*., 2013; Kikulwe and Asindu, 2020; Wright, 2012) did not focus on floods. Besides none of the studies were conducted in the River Malaba sub-catchment.

The need to address the gaps in the aforesaid studies related to flooding compelled the undertaking of this research. Therefore, this research aimed at employing the hydrological and hydrodynamic modelling to capture flooding extent, and the socio-economic study to assess the community attitude, response and willingness-to-pay for adaptation strategies.

1.3 Main objective and specific objectives

1.3.1 *Main objective*

To present a platform for understanding the impacts of flooding on the socio-economy, while investigating perceived effectiveness of establishing flood adaptation strategies for predictive risk-based water resources management in the RM S-C

1.3.2 *Specific objectives*

The specific objectives of the study were;

i) to analyse the changes in historical rainfall and potential evapotranspiration,
ii) to model extreme peak flows of River Malaba sub-catchment,

iii) to perform hydrodynamic modelling of floods while estimating socio-economic impacts of floods in River Malaba sub-catchment, and
iv) to analyse the community willingness-to-pay for flood adaptation strategies given the influencing factors.

1.4 Research questions

Multiple research questions were formed to address each specific objective.

i. *For specific objective one:* Were there significant trends and variabilities in rainfall & PET? What patterns of variabilities did rainfall & PET exhibit?
ii. *For specific objective two:* Which conceptual model best simulates observed extreme peak flows in the RM S-C? Can a hydrological model perform satisfactorily under the condition of data scarcity?
iii. *For specific objective three:* Did LULC changes significantly influence flood dynamics? What is the spatial extent of inundation due to severe flooding events? What are the socio-economic impacts of flood in the study area?
iv. *For specific objective four:* Is the community willing to pay for flood adaptation strategies? What factors influence the community WTP?

1.5 Significance of the study

The findings of this study are vital to policy makers, local community and future researchers in a number of ways including: (1) the study provides information of the changes in extreme rainfall and evapotranspiration which provide an insight into the influences of climate variability and anthropogenic factors on the hydrological processes. (2) The findings indicate the best performing model in reproducing observed extreme peak flows events. Output of the best performing model can be used for predicting quantiles to force hydrodynamic model in simulating extreme peak flows. (3) The findings can inform policy makers on the community willingness to pay for flood adaptation strategies. This can be used in supporting stakeholders' decision regarding predictive planning of flood adaptation strategies in the study area. (4) The findings of the study also provide estimates of the economic damage due to flooding impacts. (5) The findings from this study as well provide noteworthy clues for further research and baseline information in the development of more effective and holistic approaches for managing flooding impacts. Whereas this research was limited to a one River Malaba sub-catchment in Uganda, it is anticipated that the elementary

approaches and methods proposed can be applicable elsewhere in the world, particularly in Africa, and the research results can be beneficial in advancing the current knowledge in the new field of integrating hydrology and societal perception. For instance, scenario analysis comprising the application of hydrodynamic model to model spatial extent of flooding and inundation of crops with subsequent quantification of related economic losses can be vital for predictive adaptation of climate variability on food security.

1.6 Scope and limitation of the study

This study was limited to floods in River Malaba sub-catchment. Climate variability (and not climate change) was considered. Emphasis was on flood adaptation strategies in the flood-prone areas of River Malaba sub-catchment. The study main data was hydro-meteorological and spatial for the part of hydrologic and hydrodynamic modelling. The socio-economic data was for assessment of the society perception regarding floods and quantification of their WTP.

The study was limited to flooding events that occurred in the recent five to ten years. This was because, it may be difficult for the local community to clearly recall information in the distant past which could have miss-informed the research. However, in situations where an inventory could yield clear record of such incidences, the study considered extending beyond the ten years back in time. Besides, to quantify changes in rainfall and potential evapotranspiration, the study utilised longer historical period from 1948 to 2016. The study did not consider the river bed aggradations of sediment loads coming from upstream through embankment modification and erosion. This assumption might have consequently resulted in overestimation of the water surface elevation in the selected river sections. Due to lack of reliable ground-based meteorological data, the use of reanalysed products was adopted. Validity of reanalysed datasets was evaluated using some of the existing ground-based meteorological data. Besides, the unavailability of historical record of flood events extents affected the uncertainty of evaluation of the hydrodynamic model results.

1.7 Outline of the dissertation

Chapter One deals with introduction of this research in terms of the background, statement of the problem, main and specific objectives, research questions, study significance, and scope and limitation of the study.

Chapter Two includes description of the study area and the data used. The particular dataset (s) used to answer each of the stated research questions are clearly described.

In *Chapter Three*, the changes in long-term rainfall and evapotranspiration were analysed. Extreme conditions were considered for rainfall while PET was analysed at annual and seasonal timescales.

Chapter Four involved modelling of River Malaba flows from 1999 to 2016 using seven lumped conceptual rainfall runoff models. Performance of the models was evaluated and the model which best simulated the observed extreme peak flows events of River Malaba sub-catchment can be found clearly presented.

In *Chapter Five,* hydrodynamic modelling of flood and estimation of socio-economic impacts of floods in River Malaba sub-catchment was tackled.

Chapter Six presents results on the existing and preferred adaptation strategies. In the same chapter, there is quantification the community willingness-to-pay (WTP) and associated influencing factors for the restoration of River Malaba floodplain

In *Chapter Seven,* the general conclusion from the study answering the different research questions for various specific objectives are presented. In addition, recommendations for future research are also provided.

Chapter Two

2. Study area and data

2.1 Study area

The River Malaba sub-catchment (Figure 2.1) has a total transboundary drainage area of about 3,500 km^2, shared between Uganda (approximately 69% or 2,395 km^2) and Kenya (around 31% or 1,100 km^2). The sub-catchment stretches between latitudes 0º19'0N and 1º07'N, and longitudes 33º37'E and 34º37'E. The sub-catchment is part of the Mpologoma catchment within Kyoga Water Management Zone (KWMZ) (Ministry of Water and Environment, 2014b). It consists of River Malaba formed by two tributaries of Lwakhakha and Malakisi, and later joined by Lumbaka/ Kibimba, Osia and Mahanga tributaries. River Malaba originates from the Mount Elgon at about 4,315 meter above sea level criss-crossing through districts of Bududa, Manafwa, Tororo, Butaleja reaching the shores of Lake Kyoga on the western side at about 1,055 meter above sea level, where it discharges into River Mpologoma. The sub-catchment has a flow outlet at Budumba with latitude of 0º49'N and longitude of 33º47'N. At the national level, Uganda climate is mostly influenced by the Monsoons and Inter-Tropical Convergence Zone (ITCZ) (Ministry of Water and Environment, 2014a). However, locally, climate of the study area is somewhat influenced by the presence of large water bodies (such as Lake Victoria and Kyoga) and the Mount Elgon slope breezes that tend to affect the afternoon convection (Camberlin, 2009). This results in high variability of weather elements within the study area (Ministry of Water and Environment, 2018a).

The sub-catchment receives bimodal rainfall with the first and more intense rainy season occurring from March to May (MAM), and the second one and more variable from October to December (OND). The average annual rainfall over the sub-catchment is about 1,375 mm, though the districts of Bududa and Manafwa receive slightly higher rains (on average 1,800 mm per annum). The sub-catchment is generally a colder area compared to the rest of Uganda with relatively minimal seasonal temperature variations (Ministry of Water and Environment, 2018a). The average temperature ranges between 15.8 and 30.6 °C (Barasa *et al.*, 2013). The study area experiences frequent floods and landslides with substantial effects such as displacement of people, loss of lives and destruction of property including roads, bridges, schools and hospitals (Mayega *et al*., 2015; Osuret *et al*., 2016).

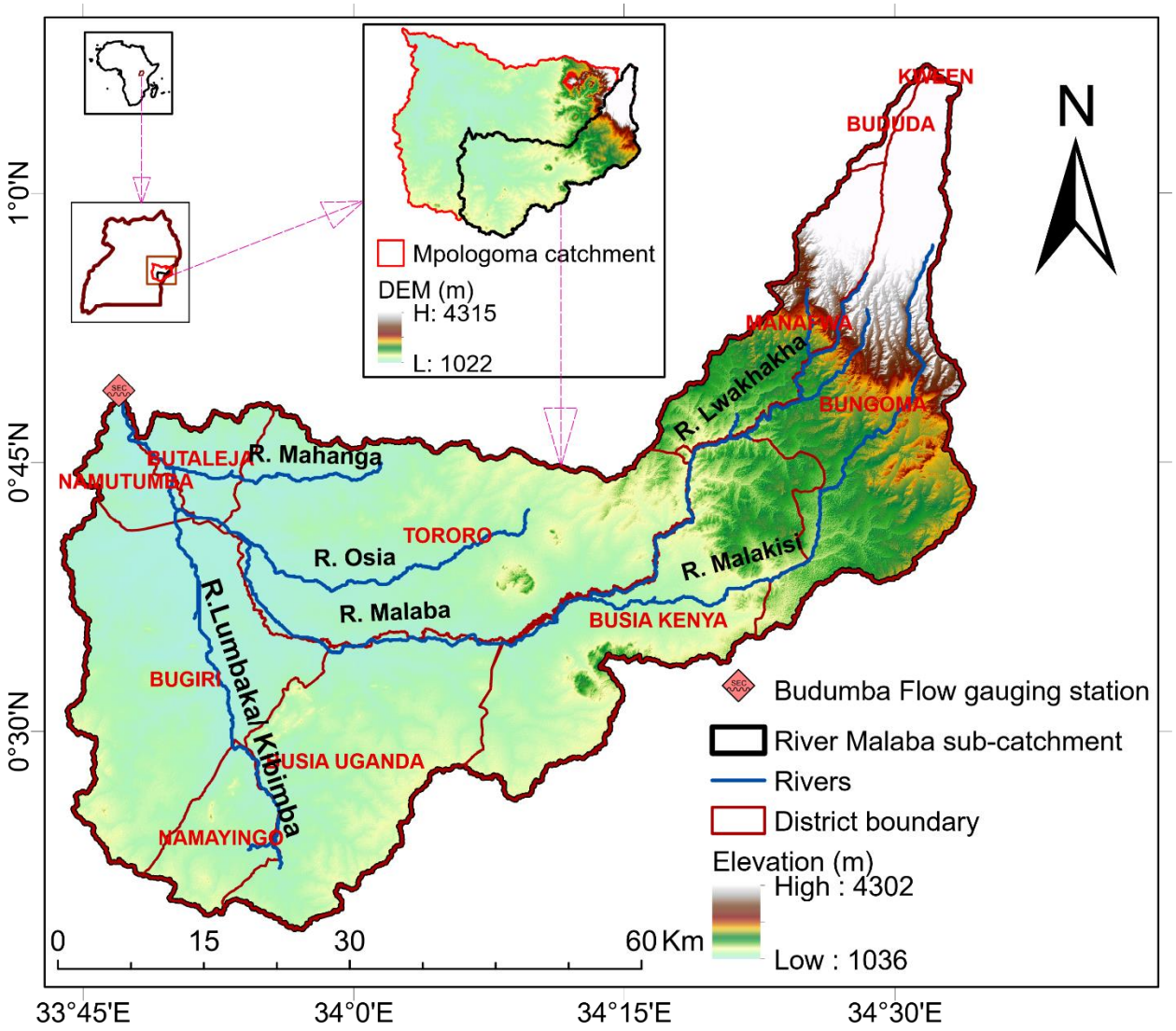

Figure 2.1 Location of River Malaba sub-catchment. The background map is the digital elevation model (DEM) acquired via https://asf.alaska.edu/data-sets/sar-data-sets/alos-palsar/ (accessed: 10 January, 2021).

Like the rest of Mpologoma catchment where the study area is located, the main occupation are rain-fed agriculture and livestock grazing (Ministry of Water and Environment, 2018a). While dense forests are found in the highlands of Mount Elgon, the remaining areas comprise of agricultural and grassland, fallow land, and isolated woodlots. Petric Plinthosols and Gleysols form the major soils types in the sub-catchment but with other categories including Lixic ferrasols, Acric ferrasls and Nitisols (Barasa *et al.*, 2017; Kitutu *et al.*, 2009). The area is occupied mainly by the indigenous Bagishu in the districts of Bududa and Manafwa, and Japadhola in Tororo districts.

Banyole are found in the district of Buteleja, while Busia and Namayingo districts have the Basamia. Bugiri and Namutumba districts mostly have the Basoga.

2.2 Data

This section described data types used in the research. Both primary and secondary datasets were considered (Figure 2.2). The study made use of hydro-meteorological data as well as community perception within the study area.

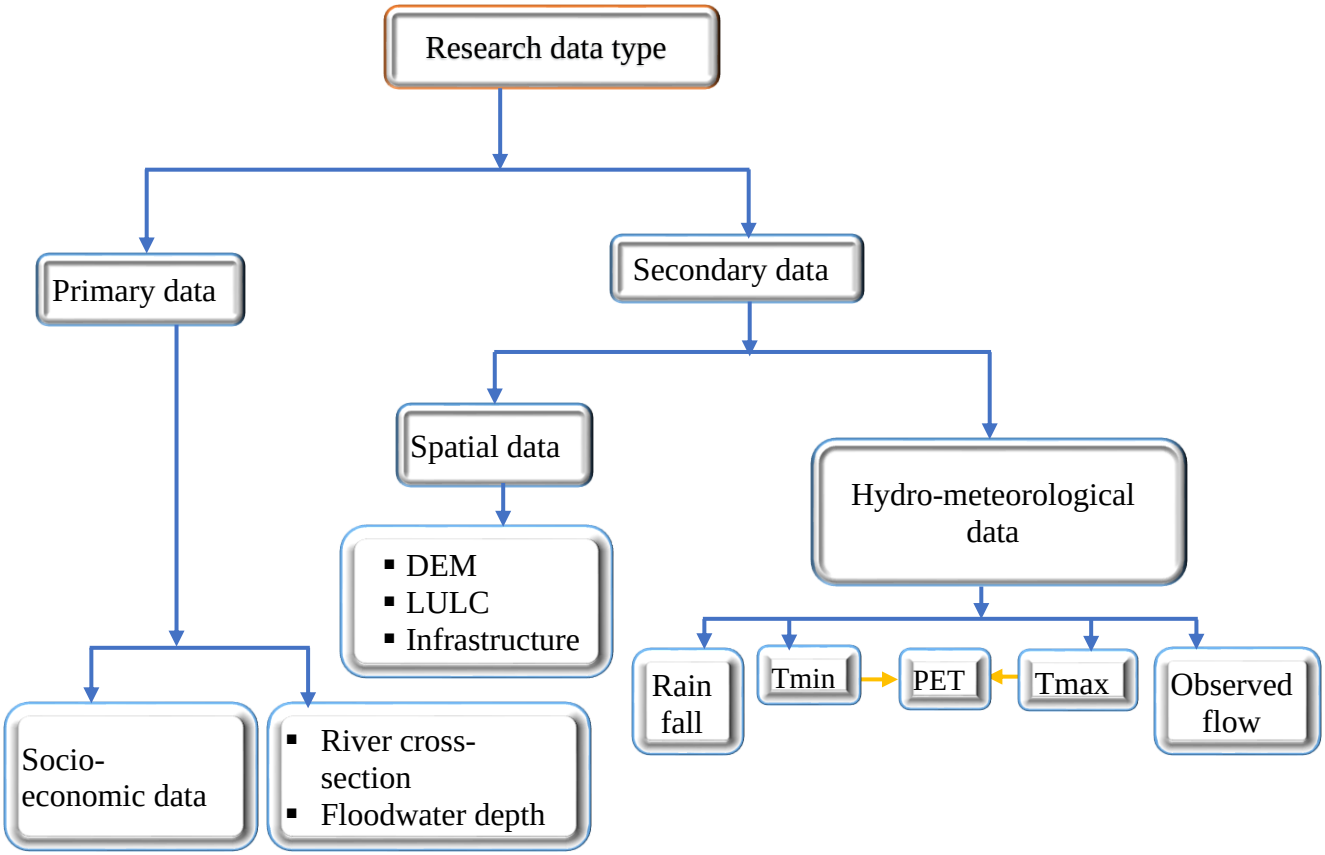

Figure 2.2 Overview of data used in this study.

2.2.1 *Hydro-meteorological*

Hydro-meteorological dataset including, rainfall, temperature and observed river flow were acquired from various sources as described shortly in the next sub-sections. The datasets were used to analyse changes in climatic conditions as presented in Chapter 3. Simulation of extreme peak flows (Chapter 4), and hydrodynamic modelling of floods (Chapter 5), were as well largely based on data presented in this sub-section.

2.2.1.1 Rainfall

In Uganda, most weather stations were damaged and some were neglected due to the political turmoil of the 1970s, according to the Japan International Cooperation Agency, JICA (2011). The study area is located within sub-Saharan Africa, a region well known to be characterised by data scarcity. The available observed data sets are from few weather stations characterised by short record length, large gaps of missing records, and uncertain or questionable quality. (Griensven *et al*., 2012; Onyutha and Willems, 2017a). This affects some investigations such as trend and variability analyses. To deal with this challenge, several global reanalyses or satellite climatic products can be used. Some of the freely available reanalyses temperature and precipitation products include, the Climate Research Unit (CRU) Time series version 4.0 (Harris *et al*., 2020), Precipitation Estimation from Remotely Sensed Information using Artificial Neural Networks Climate Data Record (PERSIANN-CDR) (Ashouri *et al*., 2015), Tropical Rainfall Measuring Mission (TRMM) Multi-satellite Precipitation Analysis (TMPA) (Huffman *et al*., 2007), African Rainfall Climatology (ARC) (Novella and Thiaw, 2013), Princeton Global Forcing (PGF) (Sheffield *et al*., 2006), Global Precipitation Climatology Project (GPCP) (Adler *et al*., 2018), etc. A number of these products have short-term records despite having data up-to the recent years. For instance, the PERSIANN-CDR, TRMM-TMPA, and ARC data series cover periods from 1983 (Ashouri *et al.*, 2015), 1998 (Huffman *et al*., 2007), and 1983 (Novella and Thiaw, 2013), respectively. However, some data products such as the PGF cover a long-term period (1948 to 2016) in addition to the high spatial resolution of 0.25° x 0.25° (Sheffield *et al*., 2006).

Recently, the CRU TS v4 monthly *PET* data calculated based on the standard Penman-Monteith method was released for use (Harris *et al*., 2020). The CRU TS v4 data are managed by the United Kingdom's Natural Environment Research Council (NERC). The earlier version of this *PET* data (CRU TS3.10) (Harris *et al*., 2014) was used by Onyutha (2016b). However, the CRU TS *PET* was in the form of country-wide average series in addition to having a low spatial resolution of 0.5° x 0.5° (Harris *et al.,* 2020, 2014) which was still deemed coarse with respect to the size of the sub-catchment considered in this study. For refined results across small catchments, high resolution spatial and long-term data is required. Eventually, the PGF was chosen because temperature and precipitation series with spatial resolution of 0.25° × 0.25° were available. PGF dataset is commonly used because of its high spatial and temporal resolutions, global coverage, and long-term record length, robustness particularly for trend and variability analyses, as

demonstrated in several studies (Khan *et al*., 2018; Li *et al.*, 2019; Nashwan *et al*., 2018; Nashwan and Shahid, 2019; Onyutha, 2016a; Onyutha *et al.*, 2020; Onyutha and Willems, 2017a, 2017b; Zhang *et al.*, 2016). PGF observational-based dataset was developed using a blend of National Centers for Environmental Prediction–National Center for Atmospheric Research (NCEP-NCAR) reanalysis dataset (Kalnay *et al*., 1996) and other several global, observational datasets including the Climate Research Unit (CRU) TS2.0, Tropical Rainfall Measuring Mission (TRMM), Global Precipitation Climatology Project (GPCP) and National Aeronautics and Space Administration (NASA) Langley Surface Radiation Budget (Sheffield *et al*., 2006).

Daily precipitation, minimum (T_{min}) and maximum (T_{max}) temperature data of the observational-reanalysis hybrid PGF (Sheffield *et al*., 2006), were acquired online in a gridded (0.25° × 0.25°) form via from http://hydrology.princeton.edu/data/pgf/ (accessed: 10 January 2020). The data covers a period from 1948 to 2016. The PGF data possessed no missing values over the considered period (1948 to 2016) at all the selected 48 grid pints (Figure 2.3). T_{min} and T_{max} were applied in computation of the potential evapotranspiration (section 2.2.1.2). The background map in Figure 2.3 is the annual rainfall total (mm) obtained by the ordinary kriging interpolation method (Wackernagel, 1995) based on data from 1948 to 2016. The choice of ordinary kriging was based on its ability to minimise the variance of the errors as it estimates the weighted linear combination of the available data and is unbiased as it strives to have a mean residual or error of zero (Mesić, 2016).

Reanalyses data sets, despite their wide usage, are known to be predisposed in replicating the observed extreme events (Ehret *et al*., 2012; Nair *et al*., 2009; Sharifi *et al*., 2018). Hence, it was deemed vital to assess the validity of PGF dataset. To do so, rainfall data recorded at nine rain gauging stations (Table 2.1) were obtained from the Uganda National Meteorological Authority (UNMA). For each station, statistical metrics including the coefficient of variation (Cv), skewness (Cs), actual excess kurtosis (Ck) and annual mean rainfall (AMR) were computed. From Table 2.1, the Cv values varied from 0.12 to 0.28 indicating a modest fluctuation on a year to year basis. Under ideal conditions, the Ck for normal distribution is zero. Similarly, a normal distribution is also characterised by Cs = 0. However, data, from the 9 stations were, on average, somewhat positively skewed (Cs = 0.50) and leptokurtic (Ck = 0.29) (Table 2.1). The highest values of Ck, Cs and Cv were obtained at Sukulu VTRO, Vukula and Butaleja prison, respectively. The AMR

varied between 1021.0 mm and 1640.7 mm. The highest and lowest AMR values were observed at Dabani catholic and Butaleja prison, respectively.

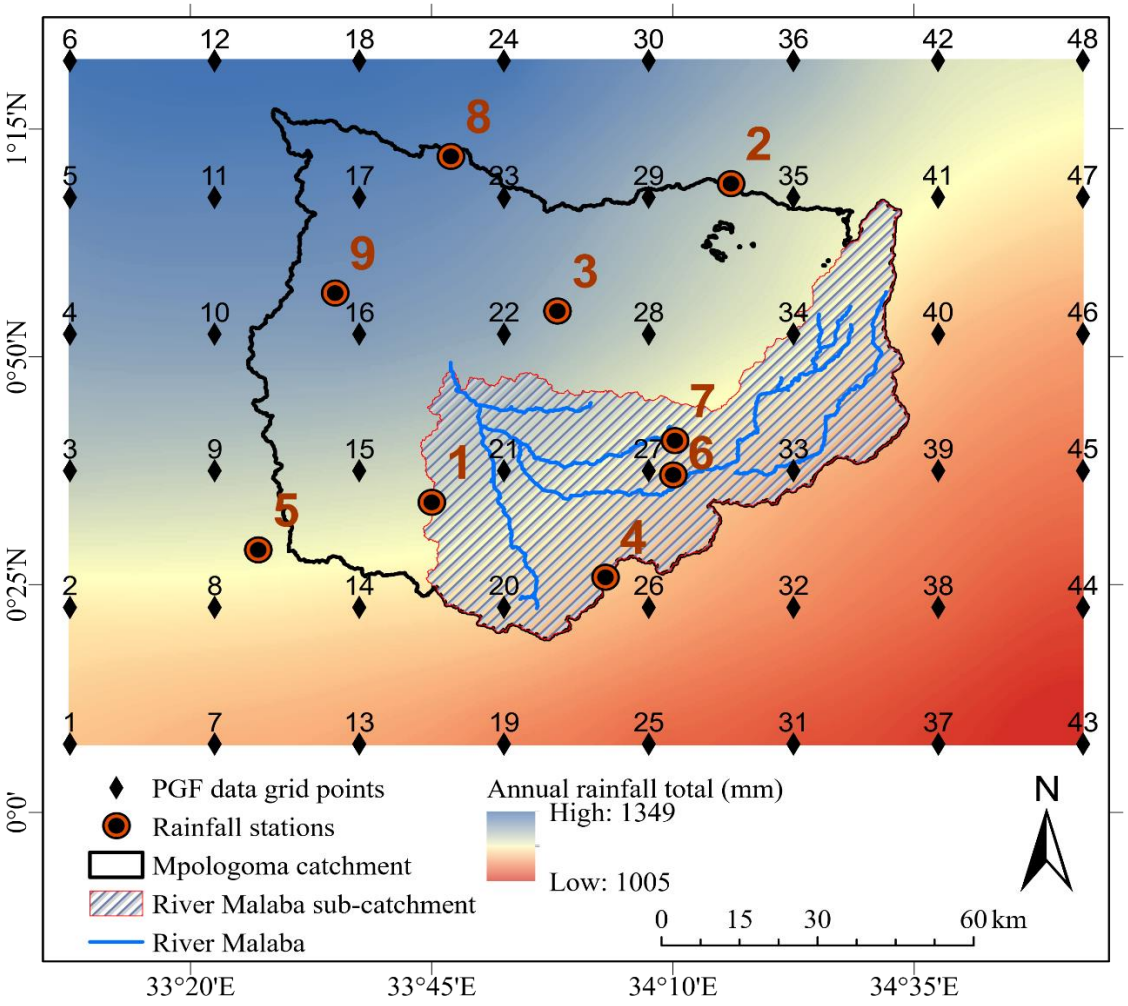

Figure 2.3 Map showing the PGF grid points and locations of the selected rainfall stations detailed in Table 2.1.

From Table 2.1, the period of available data varied from one station to another with most stations having data ending in the 1980s except Tororo, mainly due to the reason mentioned in the first paragraph of this sub-section (JICA, 2011). Since validation required the same period of PGF and observed data, this study considered a period from 1948 to 2016.

As a quality control procedure**,** infilling of missing records was done using the Inverse Distance Weighted (IDW) interpolation technique developed by Shepard (1968) (Equation 2.1). Due to its robustness, the IDW technique has been applied in several studies (Chen *et al*., 2017; Das, 2019; Lam *et al*., 2015; Onyutha, 2017a; Pellicone *et al*., 2018).

Table 2.1 Selected rainfall station, their coordinates, data record period and statistical metrics

S/N	Station Name	Coordinate		Data Record		Statistical metrics			
		Lat. [°]	Long. [°]	From	To	Ck [-]	Cs [-]	Cv [-]	AMR [mm]
1	Bugiri	0.57	33.75	1948	1975	0.20	0.63	0.26	1389.2
2	Bugusege Coffee Res Station	1.15	34.27	1948	1982	-0.21	0.73	0.18	1533.2
3	Butaleja Prison	0.92	33.97	1948	1981	-0.07	0.04	0.28	1021.0
4	Dabani Catholic	0.43	34.05	1948	1983	-0.52	0.66	0.17	1640.7
5	Imanyiro	0.48	33.45	1948	1974	-0.21	0.41	0.22	1351.6
6	Sukulu VTRO	0.62	34.17	1963	1986	0.29	0.86	0.19	1543.8
7	Tororo	0.68	34.17	1981	2016	0.07	0.34	0.12	1506.4
8	Kibale VTC	1.20	33.78	1948	1980	1.98	-0.18	0.20	1369.6
9	Vukula	0.95	33.58	1948	1980	1.05	1.03	0.17	1424.8

Lat. and Long. denote latitude and longitude, respectively.

The missing rainfall depth/intensity R_M at station M for a given period was determined using rainfall values R_j at the q neighbouring stations considering the same period.

$$R_M = \sum_{j=1}^{q} R_j \times d_j^{-\tau} \left(\sum_{j=1}^{q} d_j^{-\tau} \right)^{-1} \tag{2.1}$$

where; d_j is the distance between station M with the missing data record and one of the q neighbouring station used for interpolation. The term τ is the power parameter which determines the dependability of the IDW interpolations. A small value of τ results in an average value considering input from all the neighbouring stations. On the other hand, a large value of τ distant station are assigned a smaller weight hence ignoring their contribution (Lu and Wong, 2008; Pellicone *et al*., 2018). While using daily or monthly data, τ = 2 is recommended. However, when hourly or annual data is to be used, τ =3 and τ =1 are suggested. Consideration of the above values minimises the interpolation errors. As suggested by Lloyd (2005), a value of τ =2 was applied in this study.

a) Homogeneity testing of the observed precipitation data

Climactic data extremes can result in severe influences on the hydrological systems and human society. If data are realised to be inhomogeneous, a correction factor is applied prior to their application and further analysis to avoid vague results. Several studies (Caloiero *et al*., 2018; Kocsis *et al.*, 2020; Onyutha *et al*., 2021b; Pandžić *et al*., 2020) have tested homogeneity of hydro-climatological data sets prior to applying it for additional analysis. Four homogeneity testing techniques including the Pettit's test (Pettitt, 1979), the Standard normal homogeneity test (SNHT) (Alexandersson, 1986), the Buishand's test (Buishand, 1982), and the von Neumann's test (Neumann, 1941) were applied. Considering the significance level α to be 0.05, the null hypothesis H_0 (homogeneous precipitation data) was not rejected for *p*-value greater than α. As an alternative null hypothesis H_1, the four homogeneity testing approaches adopt a step-wise shift in the long-term mean at a certain point in time. Furthermore, a jump in precipitation data was examined using the non-parametric test dubbed the cumulative sum (CUSUM) charts test (Page, 1961). On the constructed CUSUM charts, the upper and lower limits were superimposed based on standard deviation (σ) and in terms of the mean $\pm 2\sigma$ of the CUSUM data points

The homogeneity testing of data can be found in Table 2.2. The four test methods indicate an acceptable match. Except station 1 (Bugiri) where H_o was rejected ($p < 0.05$) for all the four homogeneity tests, the remaining stations had H_o not rejected ($p > 0.05$). In addition to the statistical presentations, Figures A.1 and A.2 of Appendix A show the graphical representation of Buishand's test and CUSUM charts used to indicate any regime shift in the dataset. From the results, still only one station (Bugiri) had inhomogeneous precipitation. Since all stations are from the same climatic region, the inhomogeneity exhibited at Bugiri station could not be attributed to spatial difference in precipitation characteristics, but rather could be attributed to measurement errors. This is because H_o (homogenous precipitation data) was not rejected ($p > 0.05$) from 8 out of 9 stations (Table 2.2). Therefore, it can be deduced that rainfall over the study area is homogenous. These results are consistent with the findings from the study by Onyutha *et al*. (2021b) that reported homogenous precipitation at the two stations within KWMZ where the study area is located. The regime shifts (positive and negative) displayed in the CUSUM charts (Figure A.2) imply possible influence of climate variability on the study area precipitation. Therefore,

knowledge of variability in extreme precipitation is crucial for predictive planning and management of water resources applications in River Malaba sub-catchment.

Table 2.2 Homogeneity test on annual maxima precipitation

S/N	Station Name	*p*-value			
		Pettit's test	SNHT	Buishand's test	Von Neumann test
1	Bugiri	0.043*	0.037*	0.025*	0.014*
2	Bugusege Coffee Research Station	0.540	0.816	0.715	0.490
3	Butaleja Prison	0.481	0.201	0.157	0.538
4	Dabani Catholic	0.643	0.760	0.510	0.645
5	Imanyiro	0.466	0.422	0.568	0.532
6	Sukulu VTRO	0.656	0.628	0.549	0.530
7	Tororo	0.585	0.724	0.701	0.782
8	Kibale VTC	0.311	0.168	0.162	0.519
9	Vukula	0.442	0.516	0.403	0.479

*Denotes that H_o (homogenous precipitation data) was rejected ($p < 0.05$).

b) Validation of PGF data

The validity of PGF precipitation was analysed using observed rainfall from the selected stations and this was by testing the H_o (no correlation between PGF-based precipitation and observed rainfall) at a significance level α of 5%. The H_o was rejected if the absolute correlation coefficient between observed and PGF-based precipitation was greater than the critical value of correlation at a α. Validation was done for extreme conditions considering five extreme precipitation indices. The indices included Sum of precipitation above 5 mm/day (SPre5), Sum of precipitation above 10 mm/day (SPre10), Annual maxima series (ANMS), and number of days with precipitation intensity greater than 5mm/day (NWD5) and 10mm/day (NWD10). Detailed description of the indices can be found in section 3.2.1. The correlation of the extracted anomalies between PGF and observed indices is shown in Table 2.3. The correlation is as well presented graphically in Figures A.4 to A.8 of Appendix A. Similarly, the critical values of the coefficient of correction are

indicated in Table 2.3. At stations 5 and 8, PGF and observed rainfall had positive correlation for the five indices. At station 5, H_o (no correlation) was rejected ($p < 0.05$) for ANMS and NWD10. H_o (no correlation) was rejected ($p < 0.05$) for NWD10 and NWD5 at station 8. Stations 2, 6 and 7 had negative correlation for ANMS, NWD10 and NWD5. Station 2 and 7 had H_o (no correlation) rejected ($p < 0.05$) for NWD10 and ANMS, receptively. Except for NWD10, at station 1, PGF and observed rainfall were positively correlated.

Table 2.3 Correlation of PGF gridded and observed rainfall

S/N	Station (above) PGF Grid (below)	Correlation Coefficient					Corr. Crit.
		ANMS	NWD10	NWD5	SPre10	SPre5	
1	Bugiri PGF_15	0.08	-0.19	0.05	0.24	0.16	0.37
2	Bugusege Coffee PGF_35	-0.19	-0.35*****	-0.04	0.12	0.19	0.33
3	Butaleja Prison PGF_22	-0.13	0.01	0.07	0.11	-0.03	0.33
4	Dabani Catholic PGF_26	0.17	-0.07	0.12	-0.18	0.31	0.33
5	Imanyiro PGF_8	0.39*****	0.39*****	0.11	0.28	0.17	0.38
6	Sukulu VTRO PGF_27	-0.14	-0.02	-0.14	0.28	0.28	0.40
7	Tororo PGF_27	-0.38*****	-0.06	-0.28	0.03	-0.13	0.37
8	Kibale VTC PGF_23	0.08	0.34*****	0.52*****	0.19	0.20	0.33
9	Vukula PGF_16	0.03	0.20	-0.20	-0.21	-0.21	0.34

Note: Corr. Crit, denotes correlation critical value at α of 0.05. ***** indicated that H_0 (no correlation) was rejected ($p < 0.05$).

From Figures A.4 to A.8 of Appendix A, PGF rainfall overrates and/or underestimates the oscillations highs and lows from the observed rainfall at different times. The positive (negative) correlation implies that when the observed rainfall displayed a rise (reduction) over a certain period, the PGF rainfall exhibited a decrease (an increase). This behaviour was also reported by Onyutha (2016a). Table 2.5 shows the comparison of trend magnitude/slope between observed

and nearby PGF rainfall series. The comparison of trend direction between observed and nearby PGF rainfall series can be found in Table 2.5. The criteria to reject (not reject) H_o (no trend) is explained later in Chapter 3, sections 3.2.2 and 3.2.3. From Table 2.5, at 5 out 9 stations (2,4,6,7,9, both PGF and observed data had positive trends in ANMS. The PGF and observed rainfall had contrasting trend slopes for NWD10 except stations 7 and 8. Similarly, for NWD5, PGF and observed rainfall exhibited different trend slopes except stations 1, 5 and 9. Both PGF and observed rainfall had H_o (no trend) rejected ($p < 0.05$) for SPre5. At station 1, 2 and 5, observed rainfall had H_o (no trend) rejected ($p < 0.05$) but the corresponding nearby PGF series had H_o (no trend) not rejected ($p > 0.05$) for ANMS, NWD10 and NWD5. In general, PGF data had H_o (no trend) not rejected ($p > 0.05$) at different stations except for SPre5.

Table 2.4 Trend magnitude / slope, *m* in observed and nearby PGF series

S/N	Observed (above) PGF grid (below)	ANMS	NWD10	NWD5	SPre10	SPre5
1	Bugiri	-0.71	0.00	-0.03	10.11	4.41
	PGF_15	0.05	-0.03	-0.001	-1.79	-6.97
2	Bugusege Coffee Res Stat.	0.33	0.02	0.06	5.71	6.40
	PGF_35	0.08	-0.08	-0.07	-2.32	-7.74
3	Butaleja Prison	-0.29	0.00	0.00	-5.64	-6.65
	PGF_22	0.06	-0.04	-0.001	-2.55	-7.72
4	Dabani Catholic	0.23	0.01	0.01	1.69	2.25
	PGF_26	0.05	-0.001	-0.001	-1.21	-6.04
5	Imanyiro	-0.78	0.03	0.03	5.27	5.60
	PGF_8	0.04	-0.03	0.00	-1.31	-6.14
6	Sukulu VTRO	0.08	0.03	0.05	-19.55	-20.43
	PGF_27	0.05	-0.01	-0.001	-1.64	-6.71
7	Tororo	0.05	-0.03	-0.02	2.32	2.12
	PGF_27	0.05	-0.01	-0.001	-1.64	-6.71
8	Kibale VTC	-0.63	-0.001	-0.001	-1.186	-1.419
	PGF_23	0.07	-0.03	-0.06	-2.64	-8.31
9	Vukula	0.44	0.00	0.00	3.25	2.92
	PGF_16	0.06	-0.02	0.00	-2.64	-7.67

Table 2.5 Trend direction Z in observed and nearby PGF series

S/N	Observed (above) PGF grid (below)	ANMS	NWD10	NWD5	SPre10	SPre5
1	Bugiri	-5.18*	5.30*	-1.98*	3.28*	2.52*
	PGF_15	1.05	-0.63	-1.23	-2.04*	-2.08*
2	Bugusege Coffee Res Stat.	4.60*	2.17*	5.03*	1.61	3.84*
	PGF_35	1.14	-1.36	-1.60	-2.03*	-2.08*
3	Butaleja Prison	-2.15*	1.70	2.79*	-3.50*	-2.69*
	PGF_22	1.10	-0.53	-1.37	-2.10*	-2.09*
4	Dabani Catholic	1.25	0.81	2.51*	2.54*	2.43*
	PGF_26	1.13	-0.51	-0.92	-1.75	-2.16*
5	Imanyiro	-6.87*	2.20*	2.20*	2.31*	2.66*
	PGF_8	1.04	-0.71	-1.16	-1.84	-2.12*
6	Sukulu VTRO	0.51	-5.05*	2.37*	-5.09*	-4.36*
	PGF_27	0.98	-0.18	-1.17	-1.90	-2.13*
7	Tororo	1.12	-3.33*	-2.89*	3.53*	2.29*
	PGF_27	0.98	-0.18	-1.17	-1.90	-2.13*
8	Kibale VTC	-3.65*	-1.27	-1.27	-2.58*	-2.62*
	PGF_23	1.15	-0.92	-1.80	-1.93	-2.11*
9	Vukula	4.02*	1.60	8.24*	2.74*	2.83*
	PGF_16	1.13	-0.47	1.56	-2.08*	-2.06*

***** Indicates that H_0 (no trend) was rejected ($p < 0.05$).

The results presented in Table 2.3, Table 2.5, Table 2.5 and Figures A.4 to A.8 indicate that the performance of PGF rainfall series in reproducing the variability of observed rainfall varies from one area to another. This disparity could be attributed to the effect of various regional features such as the water bodies (like Lake Victoria and Lake Kyoga), mountains and topographical changes (Camberlin, 2009; Onyutha, 2016a). However, PGF application after filtering of the inequalities in the data using appropriate temporal scale can provide an insight about general summary of statistical information regarding changes in the climate variables (WMO, 2009). Besides, conducting bias correction on PGF data series can greatly improve its performance (Zhang *et al.*, 2020). In this study, bias correction of the PGF data was done as detailed in section 2.2.1.1(c).

c) Bias correction of PGF data

From section 2.2.1.1(b), it is evidenced that PGF dataset possess bias and random errors. Therefore, to make PGF data adequate for the purpose of this research, bias correction was done (Sharifi *et al*., 2018). Observed rainfall data in and around the study area (Table 2.1 and Figure 2.3) was applied. The study by Tian *et al*. (2013) compared the two common error methods (additive and multiplicative) and recommended the use of multiplicative bias correlation method for bias removal. Thus, the bias correction followed the simple multiplicative bias correction method (Nielsen, 1998). This method was adopted because of the poor distribution of the rain gauge networks within the study area. The monthly bias correction factor B_{cf} was used to adjust the daily PGF precipitation data. The B_{cf} was obtained as follows:

$$B_{cf} = \frac{P_{obs,i}}{P_{PGF,i}} \tag{2.2}$$

where $P_{obs,i}$ and $P_{PGF,i}$ are station-based and PGF-based rainfall data at monthly time scale, respectively.

One bias factor was calculated for each month in a year and applied to daily data. The study by Saber and Yilmaz (2018) applied a similar approach with monthly bias factors used to correct hourly data.

The bias corrected PGF precipitation was computed as follows

$$P_{PGF\_after(x,y),T_i} = B_{cf} \times P_{PGF\_before(x,y),T_i} \tag{2.3}$$

where $P_{PGF\_before(x,y),T_i}$ and $P_{PGF\_after(x,y),T_i}$ are the PGF products for day T_i at grid (x, y) before and after bias removal, respectively.

Monthly bias factors were computed considering the station(s) that is(are) located in a particular grid cell or the closest station(s). It is noticeable from Table 2.1 that only the Tororo station had data of corresponding period to the PGF-based precipitation. The computed bias factor at Tororo station did not exhibit noticeable variability for the period before and after 1983. Therefore, since all stations were from the same climatic region, they were presumed to exhibit minimal variation in the bias factors. Consequently, the available periods of station-based data (Table 2.1) were used to compute monthly bias correction factors, and applied to daily PGF data from 1948 to 2016. This approach was previously used by Piani *et al.* (2010) on statistical bias correction of daily precipitation in regional climate models over Europe. In the study (Piani *et al*., 2010), bias

correction factors were calculated using data from 1961 to 1970 and applied to data of a different period (from 1991 to 2000). The sub-catchment-wide rainfall averages (applied in extreme peak flow modelling in Chapter 4) were obtained using the Thiessen polygon (Thiessen, 1911) constructed from the 14 grid points (Figure 2.4).

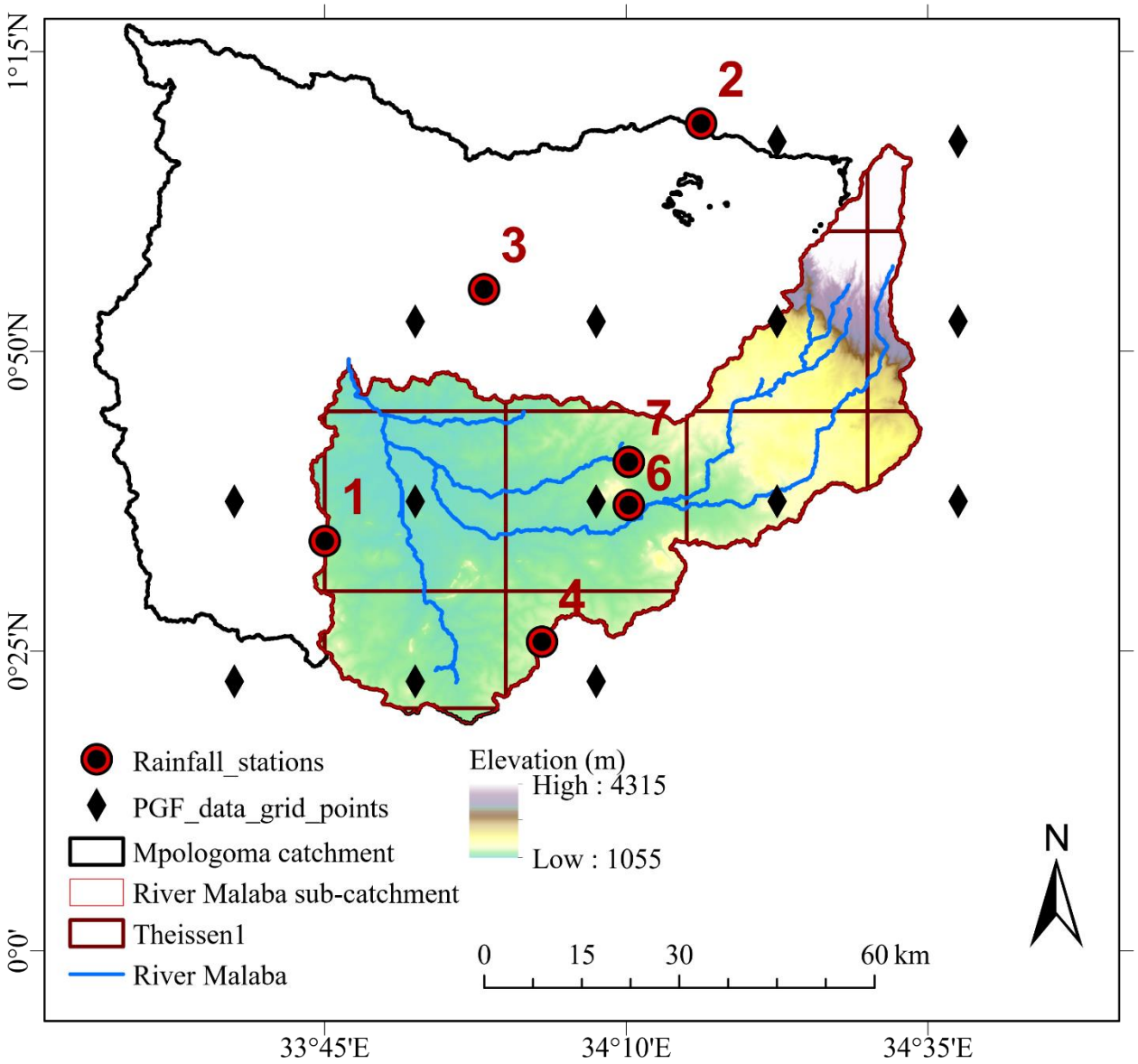

Figure 2.4 The Theissen Polygon obtained from the 14 PGF data points in and around River Malaba sub-catchment.

Five (05) PGF grid points fell inside the study area, while an additional nine were situated outside but very close (on average, less than 10 km from the sub-catchment boundary). All the 14 grids were used in obtaining the average rainfall over the sub-catchment. The sub-catchment daily

rainfall time series used in modelling of extreme peak flows (Chapter 4) can be found Figure 2.5a. The precipitation data from 1999 to 2016 was selected based on the available flow data of the same matching period (detailed in section 2.2.1.3).

2.2.1.2 Computation of PET

Due to lack of observed long-term evaporation and temperature data, potential evapotranspiration *PET* used in this study was estimated. A number of methods for estimating *PET* exist and they are categorically based on the combined energy-mass balance (Food and Agricultural Organization of the United Nations (FAO), Penman- Monteith method (Allen *et al.*, 1998)), temperature (Hargreaves (Hargreaves and Samani, 1985, 1982), Thornthwaite (Thornthwaite, 1948), Hamon (Hamon, 1963), Linacre (Linacre, 1977), and Blaney–Criddle (Blaney and Criddle, 1950)), radiation Abtew (Abtew, 1996), Priestly-Taylor method (Priestley and Taylor, 1972), and Makkink (Makkink, 1957)), and mass-transfer Rohwer (Rohwer, 1931)). Because of its physical meaning, the Penman-Monteith method has attracted wide applications (Allen *et al*., 1998; Li *et al*., 2018; Seong *et al*., 2018), particularly in regions with available weather data, making it unique compared with other methods which may require local calibration (Tabari and Talaee, 2011). The Hargreaves method necessitates only the measured minimum and maximum temperature data, is easy to use, and it is unlikely to be affected when data is obtained from arid or semi-arid, un-irrigated sites than the Penman-Monteith method (Hargreaves and Allen, 2003).

Seong *et al.* (2018) compared five different methods in approximating *PET* including the Hargreaves (Hargreaves and Samani, 1985, 1982), Hamon (Hamon, 1963), Thornthwaite (Thornthwaite, 1948), Priestley–Taylor (Priestley and Taylor, 1972) and Penman–Monteith (Allen *et al*., 1998). The Hargreaves method yielded comparable results with the FAO Penman-Monteith method when applied to the Susquehanna River Basin in the north-eastern United States (Seong *et al*., 2018). Li *et al*. (2018) applied both the Penman-Monteith and Hargreaves method in estimating *PET* for hydrological modelling. The Hargreaves method yielded remarkable streamflow simulation results when applied to the Ganjiang River Basin and was recommended to be an alternative to the Penman-Monteith method (Li *et al*., 2018). The choice of a *PET* method depends on the required temporal resolution, quality of the available weather data, and the required level of analysis (Hargreaves and Allen, 2003). Subsequently, Hargreaves and Allen (2003) recommended the use Hargreaves method in situations where data quality is uncertain, and/or where historical weather data is missing. In the same line, the Hargreaves method was recently

applied in a study by Onyutha *et al*. (2020) that analysed evapotranspiration in the region where the study area is located. Eventually, based on the analysis of the aforesaid *PET* methods, the lack of adequate weather data, such as solar radiation, relative humidity and/or wind speed in the study area, and the coarse resolution of the available *PET* CRU TS v4 data (Harris *et al*., 2020), the Hargreaves method (Hargreaves and Samani, 1985, 1982) was adopted in this study. The *PET* (mm/day) was computed at each grid point using the following equation:

$$PET = 0.0023\left(T_{mean} + 17.8\right)\left(T_{\max} - T_{\min}\right)^{0.5} Ra \tag{2.4}$$

where: R_a measures the extra-terrestrial solar radiation in (W/m^2) and this was estimated based on the location's latitude and the calendar day of the year, T_{mean} in $\left(^{\circ}C\right)$ is the mean temperature.

Only two years (1977 to 1978) of observed PET data at Tororo weather station were available. This data was considered insufficient to bias correct the PGF-based PET. However, a quick comparison of PGF-based PET and the one observed at Tororo station revealed a close agreement, hence the quality of the PGF-based PET was deemed adequate for the purpose of this study.

2.2.1.3 Flow data and processing

To perform hydrological modelling extreme peak flows (Chapter 4), observed river flow series were required for calibration and validation of the simulated flows from the rainfall-runoff models. Daily flow series at Budumba gauging station (with station ID 82217, latitude = 0º49'N and longitude = 33º47'N) (Figure 2.1), from 1999 to 2016 were obtained from the Ministry of Water and Environment (MWE), Uganda. The data was checked for quality assurance using visual inspection and statistical methods to ensure only satisfactory and quality data was used in the research. Only eighteen (18) years of recent flow data (from 1999 to 2016) for River Malaba were used (Figure 2.5c). Their selection was linked to the hydrodynamic modelling of flood extents (Chapter 5) which required recent information. Nevertheless, the eighteen years of data were considered very sufficient because longer calibration data series do not certainly yield better model performance (Li *et al*., 2010). The study by Li *et al.* (2010) revealed that only eight years of data are adequate to get a stable approximation of model performance. Since hydrological modelling of extreme peak flows (Chapter 4) required the same period of rainfall, PET and flow data, the period from 1999 to 2016 was considered here. This was because PGF-based data was ending in 2016.

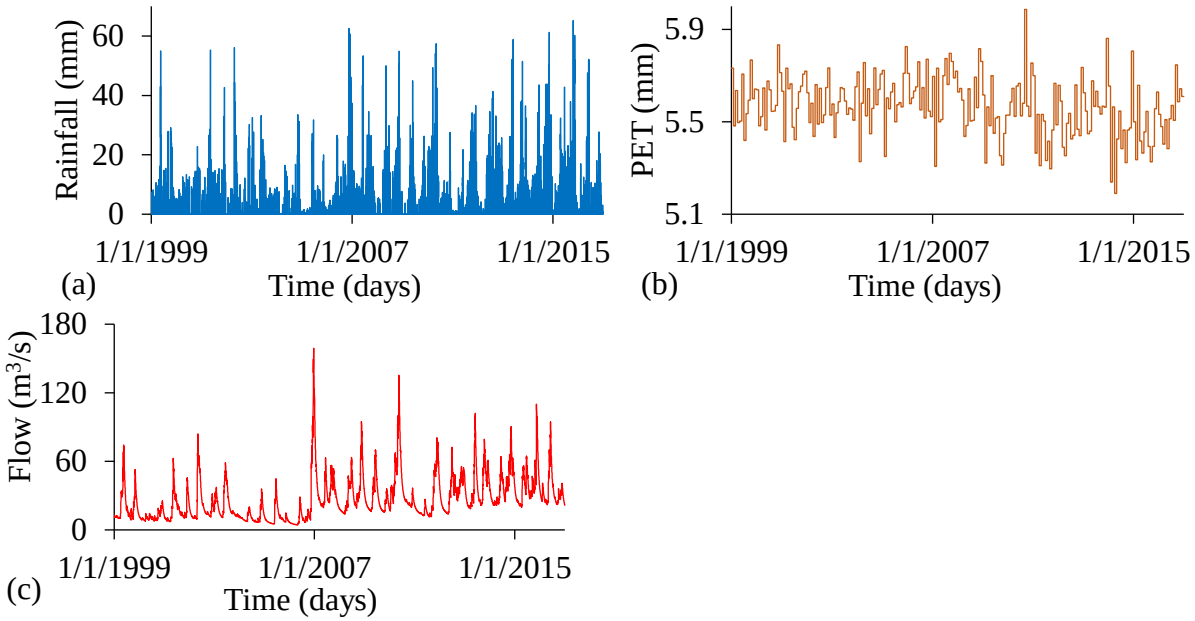

Figure 2.5 Time series of (a) daily rainfall, (b) daily PET, and (c) daily observed flow used in modelling of extreme peak flows (Chapter 4)

Similar to the observed rainfall data, statistical metrics in the PGF-based precipitation, computed PET and observed flow (Table 2.6) were estimated.

Table 2.6 Statistical metrics in PGF rainfall, PET and observed flow

Data	Statistical metric			
	Ck [-]	Cs [-]	Cv [-]	AMV
PGF rainfall	-0.7	-0.42	0.29	1125.25 mm
PET	-0.9	-0.65	0.01	5.57 mm
Observed flow	-1.04	-0.22	0.34	10436.15 m^3s^{-1}

AMV: Annual mean value.

Precipitation, PET and observed flow were negatively skewed (negative Cs values) and platykurtic (negative Ck values) compared with the normal distribution, for which Cs = 0 and Ck = 0. However, their Cv values indicated that there is slight variation on a year to year basis. The average annual rainfall was 1125.25 mm with mean annual *PET* of 5.57 mm, and annual mean flow of 10,436.15 m^3s^{-1} (Table 2.6).

From Figure 2.5c, there is a noticeable step jump in the flow. The step jump in river flow follows step jump in precipitation. Therefore, the unexpected jump in flow was due to the step jump in precipitation. Furthermore, from 2007 onwards, as there was step jump in mean of river flow and precipitation, PET was characterized by a negative sub-trend from 2007 till the end of the data.

Thus, 2007 marked the change point where there was a shift from meteorologically dry to wet conditions. Importantly, the step jump in precipitation can be linked to changes in large-scale ocean-atmosphere conditions. Therefore, applying the same approach as in section 2.2.1.1(a), homogeneity testing was performed on flow data. The results can be found in Figure A.3 and Table A.1 of Appendix A. Flow exhibited inhomogeneity. A step jump in flow could as well be due to changes in the data acquisition procedure, such as changes in rating curves, or faulty recording devices.

The simulated daily rainfall runoff discharge calibrated against river flow observed at Budumba hydrological station (Chapter 4), were adopted for hydrodynamic modelling of flood extents (Chapter 5). Rainfall runoff discharge was adopted instead of observed river flow to capture the dynamics of modifying land use types and their corresponding effect on hydrology. Besides, observed river flow cannot reflect the amount of flow in the floodplain as it is only measured at one location. It is vital to differentiate between rainfall runoff discharge and river flow. Rainfall runoff discharge refers to the inflowing discharge into the river, and was considered (in a lumped way) upstream of a given location along the river; or along a given river stretch. In other words, rainfall over the catchment generates runoff which flows into the river. The amount of runoff depends on the intensity of the rainfall. In turn, the magnitude of flooding event depends on the amount of runoff generated. The river flow (at a given point) comprises the transformation of the rainfall-runoff discharges (upstream of that point, and at previous time steps), after being routed through the river network.

2.2.2 ***Physiographic data***

The study on hydrodynamic modelling of flooding events (Chapter 5) was further based on physiographic data including Digital Elevation Model (DEM), river geometry and flood plain extent, and land use land cover (LULC). These are described shortly next.

2.2.2.1 Digital elevation model and river geometry and floodplain extent

The digital terrain model (DEM) of the study area with a resolution of 12.5 m was obtained from the ALOS PALSAR database, managed by the Alaska Satellite Facility (via https://asf.alaska.edu/data-sets/sar-data-sets/alos-palsar/; Alaska Satellite Facility, 2021). (accessed: 10 January, 2021). The river geometry including cross sections with an interval of 500

meters were obtained using the Engineer's Geographic Positioning System Real-Time Kinematic (GPS-RTK). The floodplain extents of the October 2007 and March 2010 events at various locations were obtained by establishing the flood marks (mainly flood depth) following well-documented approaches (Koenig *et al.*, 2016). This information was used to validate the flood inundation polygons. Furthermore, information about structures along the river such as bridges within the floodplains was obtained. In this study (especially in low-lying flood prone areas), most of the bridges were simple structures. Based on this, culverts were applied as an estimate, representing the simple bridge openings.

2.2.2.2 Land Use Land Cover maps

Figure 2.6a,b,c shows the study area land use land cover maps.

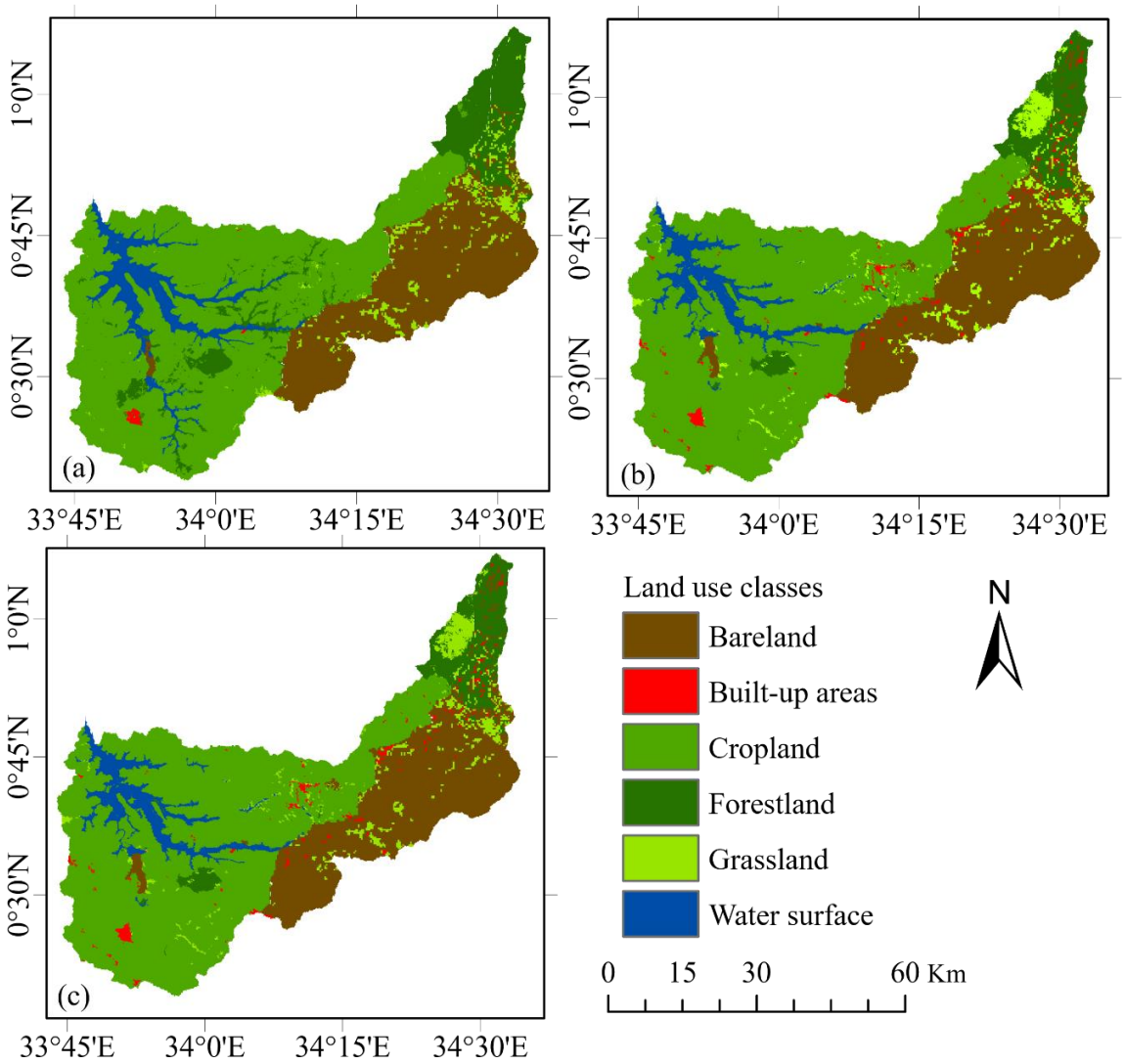

Figure 2.6 LULC maps for (a) 2010, (b) 2015 and (c) 2017. The legend applies to all sub-figures.

The LULC maps with a resolution of 30 m for three different years (2010, 2015 and 2017) (Figure 2.6a,b,c) were obtained from the National Forest Authority (NFA) of Uganda. The obtained maps were already classified by NFA by unsupervised classification. This approach was recently recommended by Ma *et al.* (2020) due to the lower field data sample requirements as compared to the supervised method.

LULC changes over the study area from 2010 to 2017 were quantified prior to hydrodynamic modelling (Figure 2.7). Bare land, built-up areas and cropland increased from 2010 to 2017, while water surface decreased (Figure 2.7). A decrease in water surface indicated reduced available water. Despite a decrease in forestland from 2010 and 2015, a slight increase occurred from 2015 to 2017. Forestland exhibited the highest decrease from 2010 to 2015, while crop land had the highest increase from 2010 to 2017. Grassland increased from 2010 to 2015 and later decreased.

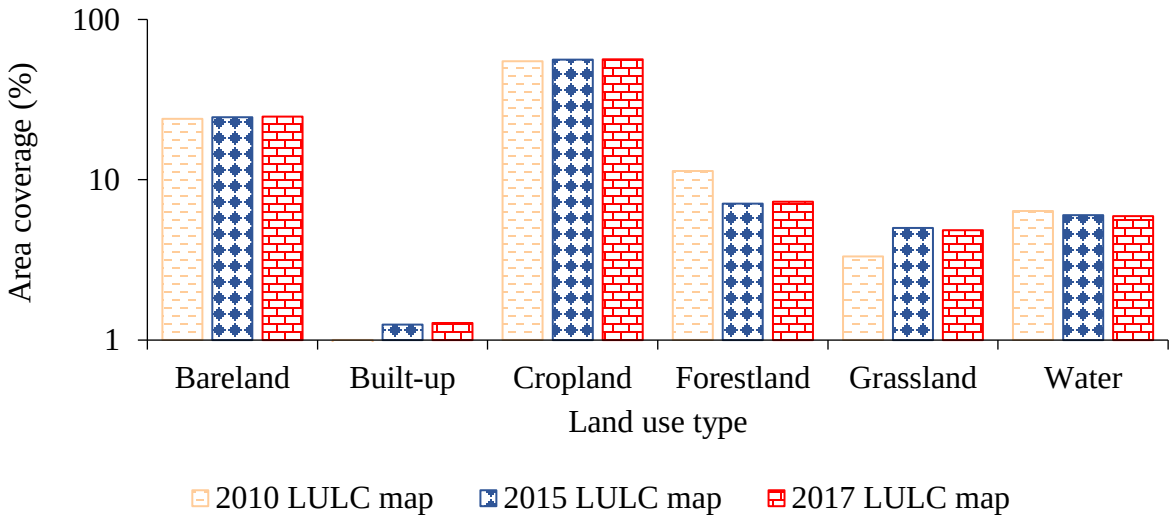

Figure 2.7 Land use changes from 2010 and 2017

2.2.3 *Physical infrastructures*

The study on hydrodynamic modelling of floods presented in Chapter 5 quantified the socio-economic impacts of floods on a number of physical infrastructures (Figure 2.8). The distribution of settlement clusters, and location of physical infrastructures (such as churches mosques, education institutions, health facilities) were obtained from the Uganda Bureau of Statistics (Uganda Bureau of Statistics, 2020, 2018).

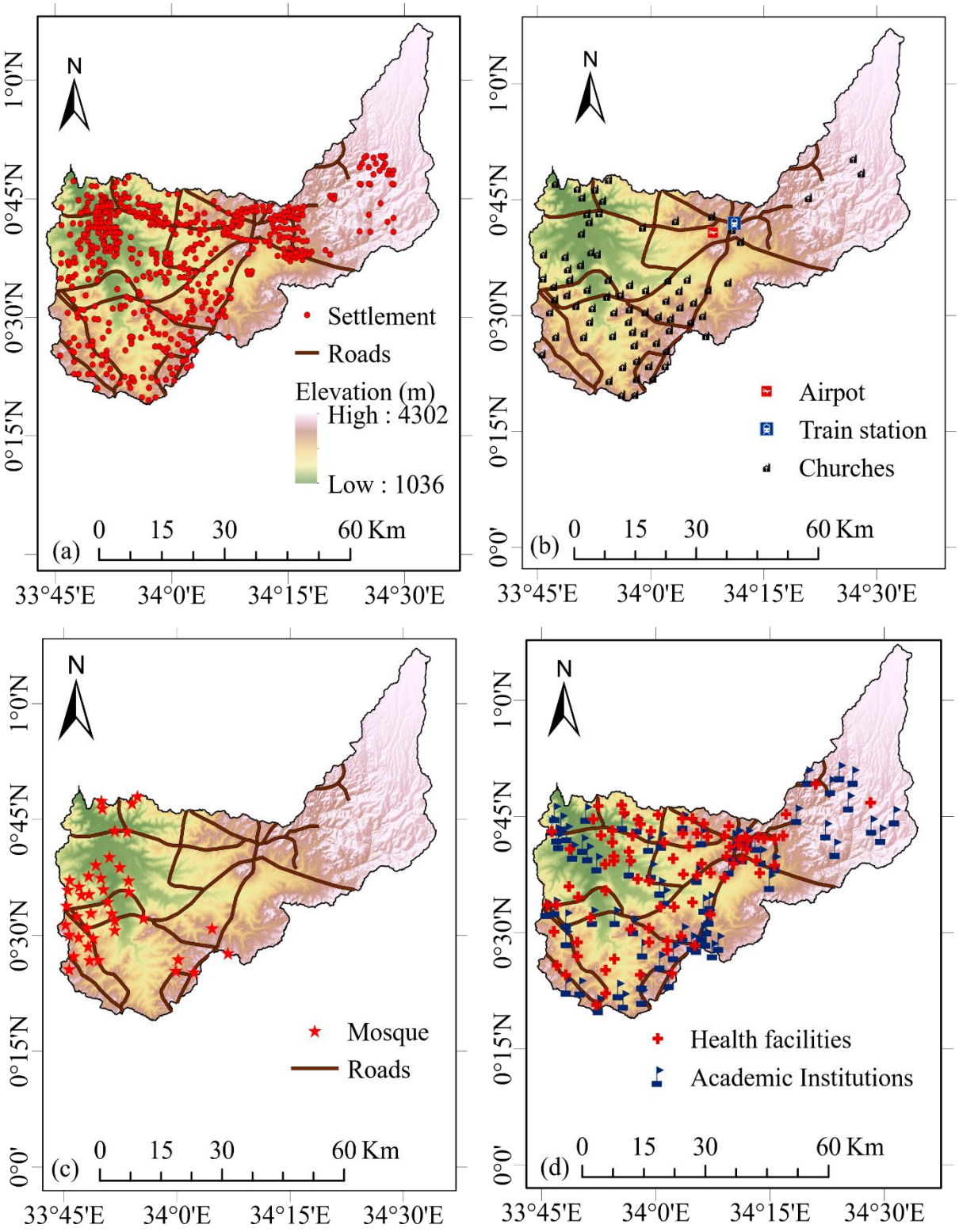

Ground measurements were also taken using the GPS-RTK to confirm the location of some infrastructures especially the airport, train station and some roads.

Figure 2.8 The distribution of physical infrastructures including (a) human settlement, roads (b) airport, train station, churches, (c) mosques (d) health facilities, academic institutions. The elevation on (a) as well applies for (b,c,d).

2.2.4 *Socio-economic data and collections methods*

The study on analyses of community willingness-to-pay and influencing factors towards restoration of River Malaba floodplains (Chapter 6) was based on socio-economic data. The data was partly used in Chapter 5. This data supports the understanding of community insights regarding the level of flooding and related impacts in the study area. Information concerning the current and preferred adaptation measures was acquired. Several approaches, including reconnaissance surveys, household surveys, focus group discussions (FGDs), key informant interviews (KIIs) and observations study were used as described shortly next in sections 2.2.4.1 to 2.2.4.5.

2.2.4.1 Reconnaissance surveys

Reconnaissance surveys were conducted for two weeks (27 October to 7 November, 2020) to achieve the all-purpose community perception regarding flooding. Both male and female were interviewed separately to achieve unbiased perception. The surveys were conducted by asking the households to define flooding events and related impacts that occurred in recent past 5 to 10 years. The limitation of 5 to 10 years was vital not to miss-inform the research as the local community may not clearly recall long ago information. However, in situations where responds had clear records of long-ago incidents, the study considered extending beyond the 10 years back in time. The flood adaptation strategies that have been in existence were as well generated. This information guided the development of both qualitative and quantitative survey questionnaires (Mathers *et al.*, 2007). To guarantee high quality data, the survey was carried out by educated and well-trained field assistants from Kyambogo University and Busitema University. Baseline data about the study area was obtained and used in determining the sample size. The survey also utilised secondary data such as internet articles, government and agencies reports (e.g., Uganda bureau of statistics (2020, 2018), Ministry of Water and Environment (2018a). Information such as socio-economic, demography of the society was obtained and used in WTP analyses.

2.2.4.2 Sample size and Household survey

Sampling enabled the selection of a representative number of individuals from a large population (Alvi, 2016). Several methods for determining the sample size exist including (1) the use of census for a small population (up to 200), (2) using a sample size of similar studies, (3) applying values in published tables, and (4) use of formulae to estimate sample size to a certain level of precision, confidence and variability (Glenn, 1992; Singh and Masuku, 2014). With the large and unknown population variability in proportion over the study area, the sample size used was obtained using the Cochran's sample size formula (Cochran, 1977, 1963) in equation (2.5). The Cochran formula computes an ideal sample size given the desired level of precision or margin error e such that;

$$N = \frac{Z^2}{e^2} pq \tag{2.5}$$

where N is the sample size, Z is the standard normal distribution indicating the degree of confidence level of p. In this study, a confidence level of 95% (Z=1.96) was adopted. The term p is the estimated proportion of the entire population. Finally, q is $(1-p)$, and e is the margin of error (level of precision). The Z of 1.96 assumes that approximately 95% of the sample will have a true value within the specified range of accuracy under a normal distribution (Singh and Masuku, 2014). Considering maximum variability and/or heterogeneity of the population in the study area, the value of p equal to 50% was assumed. e determines the level of accuracy of the sample size, the range in which the true value of the population is estimated to fall (Singh and Masuku, 2014). In this study, e of ±0.042 was adopted. The studies by Charan and Biswas (2013) and Naing *et al*. (2016) applied a value of 0.05 to determine the sample sizes. Considering the above parameter values, the computed sample size was 550. The use of Cochran's formula has been embraced by several studies (Feizollahi *et al.*, 2014; Kroonenberg and Verbeek, 2018; Lehmann *et al*., 2013; Makwinja *et al.*, 2019). In Uganda, some of the studies that applied the Cochran formula include Wafana *et al.* (2019), Wasswa *et al.* (2015), Odongo *et al*. (2014).

As the study intended to capture attention of the local community comprised of mostly illiterates, the face-to-face interview method was adopted (Mathers *et al.*, 2007). Mainly, households close and normally affected by floods were considered. However, consideration was also made for those households that are indirectly affected (households in highland area). The sampling procedure ensured that household were at least 150 m apart to reduce the self-styled *herd attitude effect*, where individuals' particular behaviours are influenced by their neighbours. This arrangement

further improved the diversity of the samples regarding flooding impacts. Household questionnaires were developed using information from the reconnaissance survey. Through a dry run of the survey on a small representative set of the targeted respondents, questionnaires were pre-tested and checked to identify and correct potential response errors which guaranteed their strength and dependability. The questions were designed not to cause any ethnical, political, social or environmental uncertainty that could otherwise jeopardise the research. Though the questionnaires were designed in English, an official language in Uganda, during the process of interview, translation into words or language locally suitable to the respondents was done. The survey gathered information such as (i) socio-economic activities in the area, (ii) existing mitigation and adaptation strategies including their rankings and (iii) community willingness and ability to pay for adaptation strategies, etc.

2.2.4.3 Focus group discussions (FGDs)

Ten FGDs having not more than 12 participants for effective management (Nyumba *et al.*, 2018), were used to gather data from a community. FGDs targeted the highly flood susceptible regions. FGDs helped to address particular concerns related to flooding; build community consensus about flood adaptation strategies; to cross-check information with a specific category of people having concrete knowledge on flooding events and existing adaptation strategies; and to obtain reactions to hypothetical and/or intended actions. FGDs focused on farmers, women groups, youth groups, schools, local government leaders and non-government organisations. Generated information included history of major past flooding events, the highly flooded areas and frequently affected sectors, existing pre-flood, during and after flood adaptation strategies, and monetary value of land and animals.

2.2.4.4 Key informant interviews (KIIs)

KIIs were conducted at districts and local levels targeting leaders, politician, civil servants and NGO working on projects related to management of rain-induced floods. Their selection was based on experience and expertise. Kumar (1989), urges that KIIs yield information of doubtful meaning and low trustworthiness, as key informants are not cautiously nominated, interview guides not prior prepared, and responses are poorly captured. However, in this study, participants to KIIs were carefully chosen to guarantee the proper representation of conveyed community ideas (McKenna and Main, 2013). The generated information included traditional methods to predict rains and

floods, previous disastrous flood events, trend of flood events, adaptation strategies and their effectiveness, prospective plans to restore the floodplains, community involvement in flood management.

2.2.4.5 Observations study

Direct observations enabled the collection of qualitative data and to develop an in-depth understanding of rain-induced floods. It yielded information on the current flooding challenges. The study was based on looking, listening, asking questions and keeping detailed field notes. Useful information on the history of land use land cover, major flood events, current flood problems and existing flood adaptation strategies considered in the study area were acquired. This method provided information that could not be obtained by the other methods that largely depend on self-report (Morgan *et al*., 2017).

Chapter Three

3. Changes in historical rainfall and potential evapotranspiration

This chapter is based on the published paper:

Mubialiwo A, Onyutha C, Abebe A. 2020. Historical rainfall and evapotranspiration changes over Mpologoma catchment in Uganda. *Advances in Meteorology* 2020 (Article ID 8870935): 1–19. https://doi.org/10.1155/2020/8870935

The chapter is further based on the manuscript titled *"Changes in extreme precipitation over Mpologoma catchment in Uganda, East Africa"* submitted for publication.

3.1 Introduction

Heavy rainfall and high variability in rainfall pattern are known key drivers of flood risk in East Africa and this is where the study area is located (Macleod *et al*., 2021). Besides, evapotranspiration provides an insight into the water balance of an area. For instance, it can regulate humidity, infiltration and flood peaks during rainfall (Krishnaswamy *et al*., 2013; Rodrigues *et al*., 2019). Changes in evapotranspiration together with rainfall variations can contribute to fluctuations in hydrological indices, such as river flow (Obada *et al*., 2017). These changes can intensify the occurrence of flooding events. The alteration in catchment characteristics by flooding events could implicate possible impacts of human factors on the hydrology. Alongside the human factors, there could also be the influence of climate variability on hydro-meteorology of the study area. Analysis of the changes in rainfall and potential evapotranspiration is vital for predictive planning of water resources management applications. Extreme meteorological amplification may increase the intensity and frequency of flooding and associated risks, resulting in huge costs to human societies and economy. Therefore, for relevance of application in flood analysis, changes in meteorological variables, especially precipitation need to be done for extreme conditions to generate quite more reliable information.

Spatial and temporal changes can be examined in terms of trend and variability. Some of the variability analyses methods include Autocorrelation Spectral Analysis (ASA) (Blackman and Tukey, 1959), the Quantile Perturbation Method (QPM) (Ntegeka and Willems, 2008), the Empirical Orthogonal Functions (EOF) (Lorenz, 1956), etc. Similarly, trend analyses can be

performed using parametric or non-parametric methods. Some of the parametric methods include the Least-squares linear regression (Haan, 1977), Sen's robust slope estimator (Sen, 1968), etc. The common non-parametric methods include Mann–Kendall (MK) (Kendall, 1975; Mann, 1945), Spearman rank correlation (Lehmann, 1975; Sneyers, 1990; Spearman, 1904). Another non-parametric method of trend analyses is by using the Cumulative Sum of the Difference (CSD) between exceedance and non-exceedance counts of data points (Onyutha, 2021a, 2016c, 2016b). The CSD method utilises both statistical and graphical approach making in unique from the traditional methods like Mann-Kendall (MK) (Kendall, 1975; Mann, 1945) and Spearman rank correlation (Lehmann, 1975; Sneyers, 1990; Spearman, 1904) which are purely statistical. Besides, the CSD method can as well be applied to analyse for both trend and variability analyses. Some of the recent studies that applied the CSD method include by Ma *et al*. (2021), Onyutha *et al*. (2021b), Onyutha (2021b), Mubialiwo *et al*. (2021c), Onyutha *et al*. (2020), Cengiz *et al*. (2020), Vido *et al.* (2019), Tang and Zhang (2018), Pirnia *et al*. (2018). This, the CSD method was adopted in this study.

Therefore, this study aimed at analysing the rainfall and evapotranspiration trends and variability across Mpologoma catchment where River Malaba sub-catchment is located. For precipitation, the relevant indices considered in the analysis are the ones that explain floods along rivers and in the low-lying areas. Analyses were based on the PGF series of daily resolution, while considering a study period of 1948-2016. Rainfall data observed at a number of stations was used for validation and bias correction of the PGF data (see section 2.2.1.1 (b), (c)).

3.2 Methodology

3.2.1 *Extraction of extreme precipitation indices (EPIs)*

Five EPIs were computed from the PGF precipitation dataset (Table 3.1). Four of the five indices including Sum of precipitation above 5 mm/day (SPre5), Sum of precipitation above 10 mm/day (SPre10), Very wet days (NWD10), and Annual maxima series (ANMS) were respectively equivalent to Rainfall total >5 mm/day (TPre5), Rainfall total >10 mm/day (TPre10), Very wet day (NWD10), and Annual maxima series (AMS) indices included in Onyutha (2020a). Similarly, NWD10 equates to Number of heavy precipitation days (R10) listed in Zhang *et al.* (2011). While several indices are recommended by World Meteorological Organization (WMO), some of them may not necessarily reflect very severe weather conditions. For instance, Annual total wet-day

precipitation (PRCPTOT) as listed in Zhang *et al.* (2011) may just indicate conditions very close to mean climatic situation. PRCPTOT could be suitable for analyses that provide agriculture related information. Therefore, selection of indices should be based on a specific purpose of application (Persson *et al*., 2007). In this study, the five indices (SPre5, SPre10, NWD5, NWD10 and ANMS) were selected for relevance of application in flood analysis which is a key component in water resources management.

Table 3.1 List of precipitation indices

S/N	ID	Name	Definition
1	SPre5	Sum of precipitation above 5 mm/day	Annual total precipitation considering days with precipitation > 5 mm
2	SPre10	Sum of precipitation above 10 mm/day	Annual total precipitation considering days with precipitation > 10 mm
3	NWD5	Wet days	Annual count of consecutive days when precipitation > 5 mm
4	NWD10	Very wet days	Annual count of consecutive days when precipitation > 10 mm
5	ANMS	Annual maxima series	Series comprising the maximum precipitation intensity in each year

3.2.2 *Trend Analyses*

Trend magnitude or slope (*m*) was computed at each grid using Theil (1950) and Sen (1968) in the following equation:

$$m = median\left(\frac{x_j - x_i}{j - i}\right), \forall i < j \tag{3.1}$$

Considering n as the sample size, x_j and x_i denote the j^{th} and i^{th} value, respectively, such that $1 < i \le (n-1)$ and $1 < j \le n$.

The significance of the non-zero was evaluated by testing the null hypothesis H_o (no trend) using the method of cumulative sum of the difference (CSD) between exceedance and non-exceedance counts of data points developed by Onyutha (Onyutha, 2021a, 2016c, 2016b).

To apply the CSD method, the given dataset (denoted by X) of size *n*, was rescaled to transform it into another series becoming d_x such that (Onyutha, 2021a).

$$d_{x,i} = n - k_{x,i} - 2t_{x,i} \quad for\ 1 \le i \le n \tag{3.2}$$

where $t_{x,i}$ is the number of times the i^{th} observation exceeds other data points in *X*, while $k_{x,i}$ represents the number of times the i^{th} observation appears within *X*.

The CSD trend statistic T_{CSD} can be calculated using the following equation (Onyutha, 2021a)

$$T_{CSD} = \sum_{j-1}^{n} \sum_{i-1}^{i} e_{x,i} \tag{3.3}$$

where

$$e_{x,i} = d_{x,i} \times \sqrt{\frac{(n-1)}{\sum_{i=1}^{n} \left(d_{x,i}\right)^2}} \quad for 1 \le i \le n \tag{3.4}$$

Positive $(T_{CSD} > 0)$ and negative $(T_{CSD} < 0)$ values of T_{CSD} indicate increasing and decreasing trends, respectively. Trend statistic T_{CSD} is computed to assess the existence of either monotonic trend or seasonal component in hydro-meteorological data, which guides its further use, for instance in hydrodynamic modelling. The distribution of T_{CSD} is approximately normal with the mean of zero and variance given by:

$$Var\left(T_{CSD}\right) = \frac{n\left(n^2 - 1\right)}{12} \tag{3.5}$$

The standardized CSD trend statistics Z which follows the standard normal distribution with mean (variance) of zero (one) is calculated using the following expression

$$Z = \frac{T_{CSD}}{\sqrt{Var\left(T_{CSD}\right)}} \tag{3.6}$$

The values of $Var\left(T_{CSD}\right)$ applied in estimating Z are corrected from the influence of persistence in the data by applying the approach in Onyutha (2021a). Considering $Z_{\alpha/2}$ as the standard normal variate, the H_o (no trend) is rejected $(p < \alpha)$ for $|Z| > |Z_{\alpha/2}|$, otherwise, the H_o (no trend) is not rejected $(p > \alpha)$ for $|Z| < |Z_{\alpha/2}|$. In this study, α was taken to be 5% which has a corresponding Z value of 1.96.

3.2.3 *Variability analyses*

To compute variability using the CSD method, the given data X is divided into subsets each starting from the p^{th} to the f^{th} value of X (equation (3.7)). To each sub-series, the sub-trend statistic Z is computed using equation (3.7). To do so, a time slice of length h is moved from the beginning to the end data record. h is the considered relevant time scale. For instance, h =10 would represent assessment of decadal oscillations affect. For the selected h, $s = 0.5 \times (h+1)$ and $s = 0.5 \times h$ in the cases when h is odd and even, respectively such that (Onyutha, 2018). h is the considered relevant time scale.

$$Z_i^h = f\left(x \subset X \mid x_p \le x \le x_f\right) \quad \text{for} \, t = 1, 2, \ldots, n \tag{3.7}$$

where Z_i is the i^{th} value of Z, while the terms p and f can be given by:

$$\left.\begin{array}{l} \text{if } t < s, \quad p = 1, \; f = h + t - s - 1 \\ \text{if } t \ge s \text{ and } i \le (n-s), \quad p = t - s + 1, \; f = t + s \\ \text{if } t > (n-s) \text{ and } t \le n, \quad p = t - s + 1, \; f = n \end{array}\right\} \tag{3.8}$$

The values of Z_i (equation (3.7)) are plotted against the corresponding i^{th} data year. The $Z = 0$ line becomes the reference representing the data with completely no trend. Variability in the data is considered in terms of the occurrences of the positive and negative sub-trends. The (100-α) % Confidence Interval limits (CL) are constructed in terms of $Z_{\alpha/2}$ at α. The H_o (natural randomness) is rejected if the scatter fall outside the (100-α)% CL limits or if $|Z| > Z_{\alpha/2}$ at α, otherwise, the H_o is not rejected. CL is computed to test the significance of trend.

3.3 Results and Discussion

3.3.1 *Trend analyses in extreme precipitation*

Figure 3.1 presents the linear trend slope/magnitude (mm/year) in various EPIs. Decreasing trend in the SPre5 and SPre10 were exhibited across the entire catchment (Figure 3.1a,b). Similarly, the entire area was characterised by decreasing NWD5 and NWD10 (Figure 3.1c,d). The study by Ongoma *et al*. (2016) reported a reduction in number of wet days for precipitation greater than 10 mm an equivalent to NWD10. The decreasing sum of precipitation may be attributed to declining number of wet days. Here, one would think that reducing number of wet days and decreasing sum

of precipitation imply a tendency to shift towards dry climatic conditions, pointing a high risk of drought in the area. This circumstance can only be true when general average statistics are considered. However, the annual maxima series (ANMS) (something of concern regarding water resources management), indicated an increase (Figure 3.1e). This inferred that chances of experiencing rare but highly impacting events are very high. The above findings were in agreement with the report by Ministry of Water and Environment (2018a) which indicated erratic and unpredictable rainfall over Mpologoma catchment, both in amount, duration, and intensity.

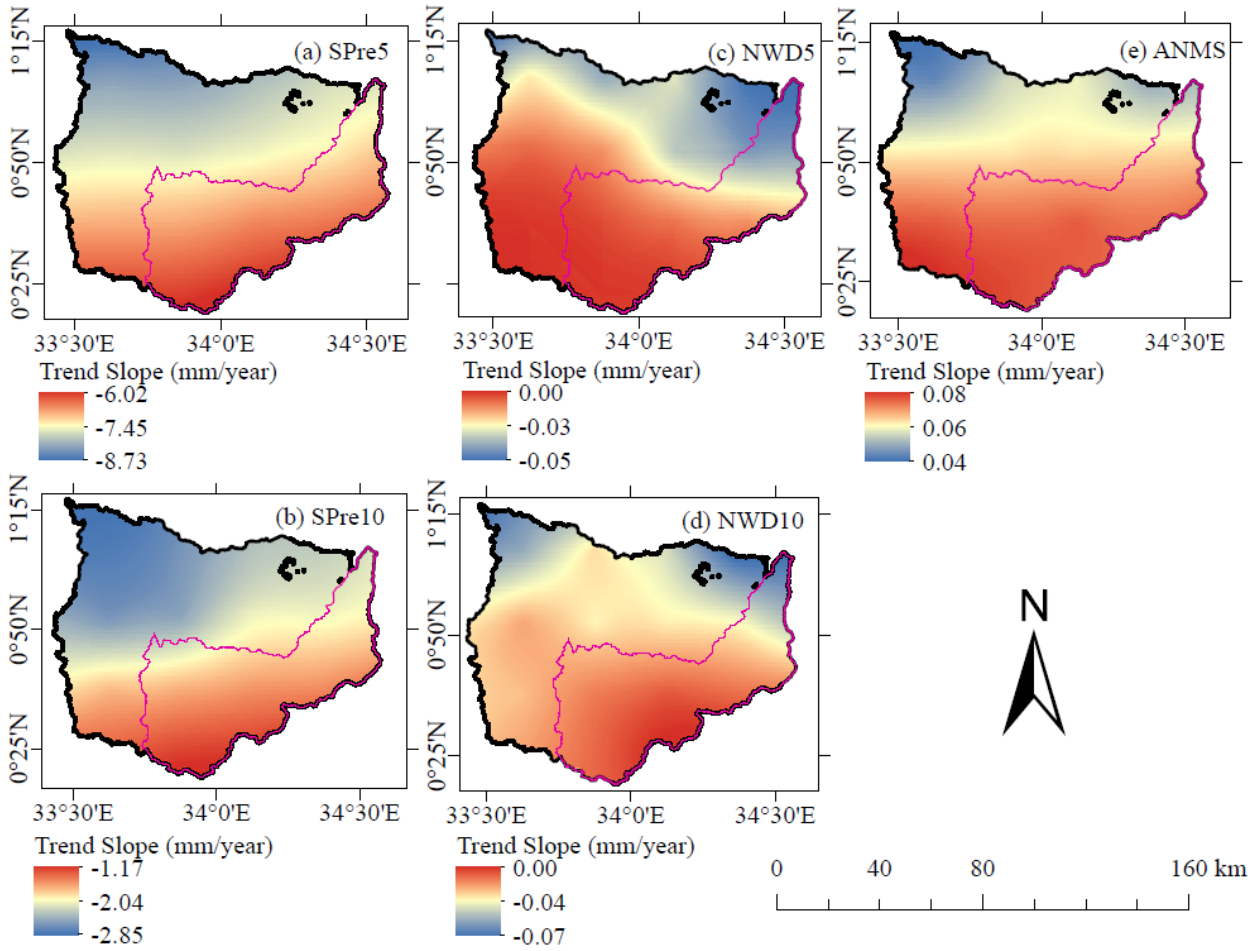

Figure 3.1 Trend slope/magnitude (mm/year) for (a) SPre5, (b) SPre10, (c) NWD5, (d) NWD10 and (e) ANMS

Erratic and unpredictable rainfall can result in flooding events which leave devastating effects, such as loss of lives, destruction of property, infrastructure and displacement of people. Therefore, with such disastrous impacts, well-thought adaptation strategies developed based on an integrated understanding of the extreme weather events and social perception are vital (Thomas and López,

2015). In addition, the presence of trends and shifts in the rainfall embrace the need to consider non-stationarity (Onyutha, 2017b; Salas and Obeysekera, 2014), while planning and designing of risk-based water resources management structures as opposed to conventional methods of deriving design quantiles based on stationary climate.

Figure 3.2 shows the standardised trend statistics Z for various EPIs corresponding to the linear trend slope/magnitudes in Figure 3.1.

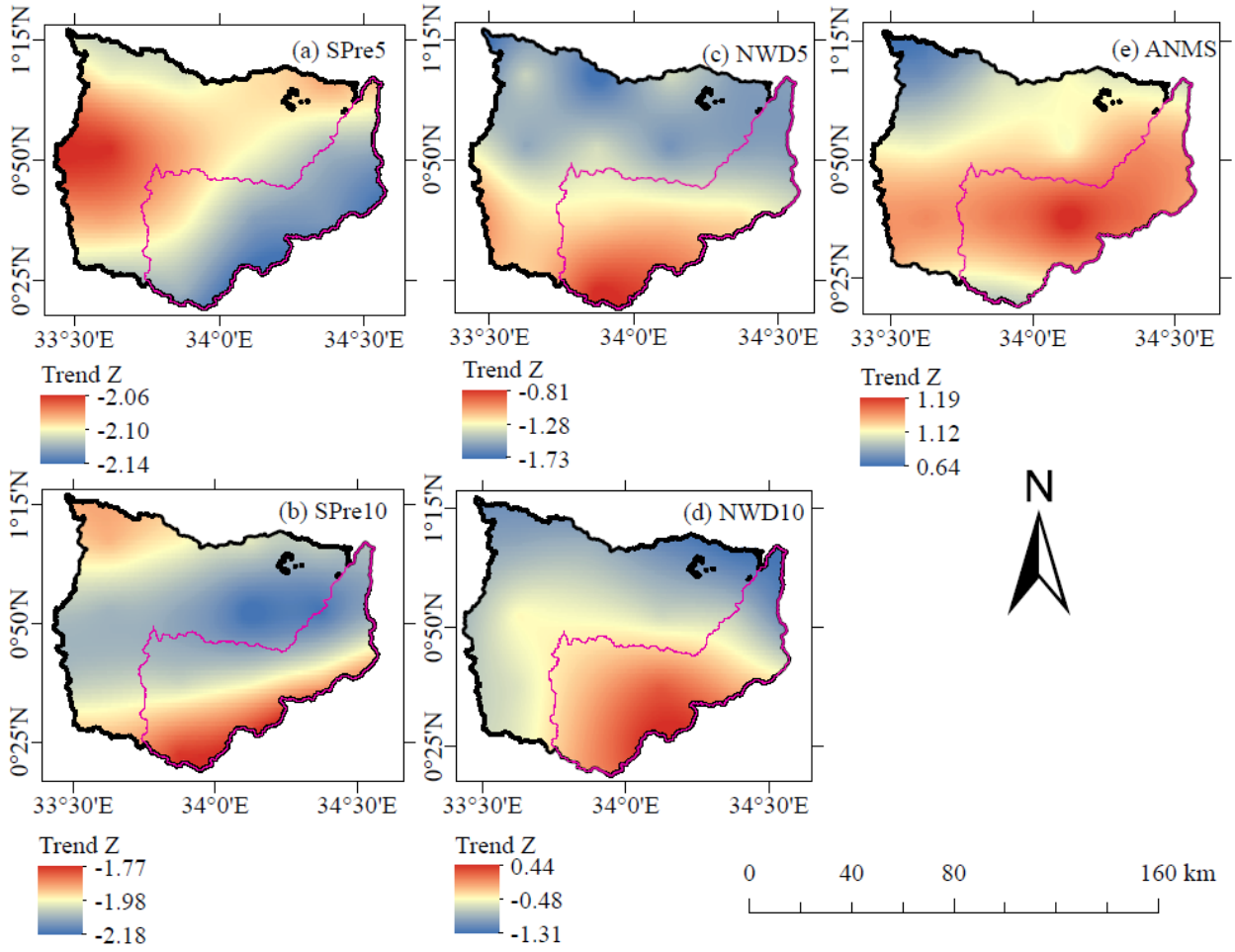

Figure 3.2 Standardised trend statistics Z (trend direction) for (a) SPre5, (b) SPre10, (c) NWD5, (d) NWD10 and (e) ANMS.

The H_o (no trend) was rejected ($p < 0.05$) for decreasing SPre5, with corresponding standardised trend statistics Z values range of $-2.14 \leq Z \leq -2.06$ (Figure 3.2a). Similarly, except the south and south eastern part of the catchment (largely in River Malaba sub-catchment) where $Z < 1.96$, H_o (no trend) was rejected ($p < 0.05$) for decreasing SPre10 (Figure 3.2b). On the other hand, H_o (no

trend) was not rejected ($p > 0.05$) for decreasing NWD5, NWD10 (Figure 3.2c,d). Similarly, the increasing ANMS had the H_o (no trend) not rejected ($p > 0.05$) (Figure 3.2e).

3.3.2 *Spatio-temporal Variability Analyses on extreme precipitation*

Spatio-temporal variability is explained in terms oscillation highs (OH), which indicates a variable higher than the long-term mean and oscillation lows (OL), which designates a variable below the long-term mean. The long-term mean corresponds to the trend statistic Z value of zero. The null hypothesis H_o (natural randomness) is not rejected (rejected) if variability statistics falls inside (outside) the 95% confidence interval limits. When H_o is not rejected (rejected), this indicates that OH and/or OL is insignificant (significant). Figure 3.3 to Figure 3.7 show the differences in spatio-temporal variation in the extreme precipitation across the study area for the considered five EPIs.

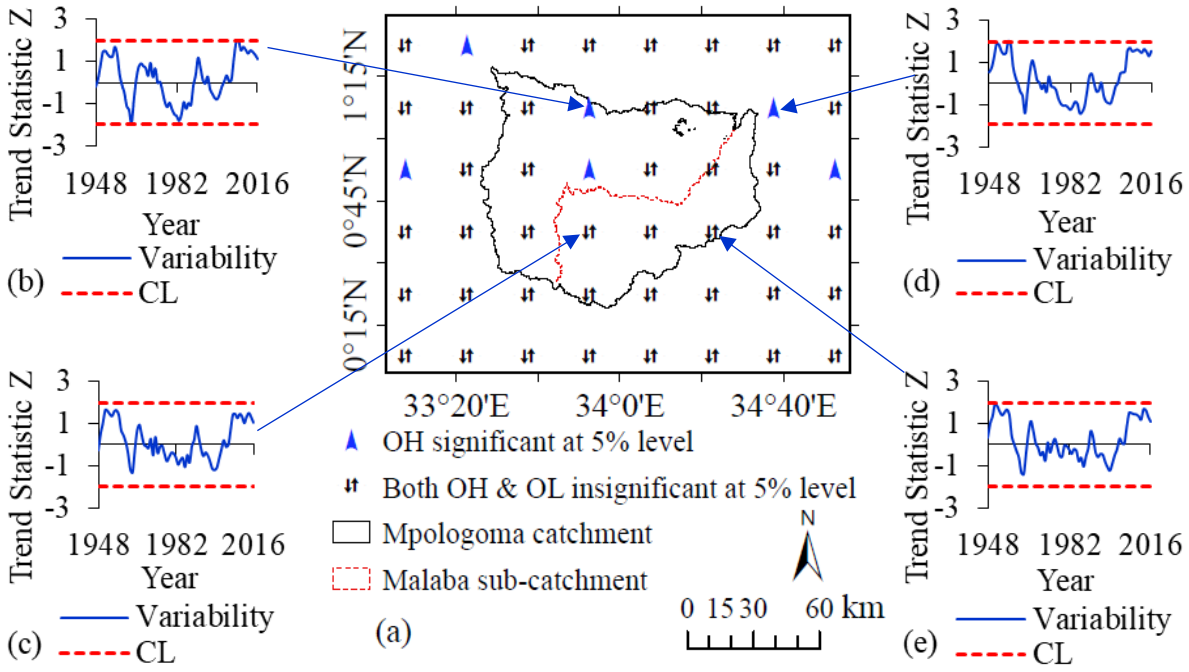

Figure 3.3 (a) spatial differences in the significance of rainfall variability and (b-e) temporal variability in ANMS EPI at different locations of the study area. "CL" corresponds to the dotted horizontal lines denoting the 95% confidence interval limits.

Except in a few locations, the entire study area experienced both insignificant ($p > 0.05$) OH and OL (Figure 3.3(a)), of generally similar pattern with strong frequency fluctuations (Figure 3.3(b-e)) for ANMS. The significant OH within the study area occurred between 2007 and 2008 (Figure

3.3(b)). The northeastern part (close but outside the study area) had significant ($p < 0.05$) OH around 1956 (Figure 3.3(d)).

Figure 3.4(a) shows significant OH ($p < 0.05$) in the southern region and eastern part (close but outside the study area) in the NWD10. The long-term mean was surpassed by NWD10 around 1951 (Figure 3.4(c,e)) The northern part of Tororo district experienced a significant ($p < 0.05$) OL around 1998 (Figure 3.4(d)). For the rest of the study area, NWD10 were characterised by both insignificant ($p > 0.05$) OH and OL. In general, the anomalies in NWD10 displayed a common pattern going above and below the long-term mean (Figure 3.4(b-d)).

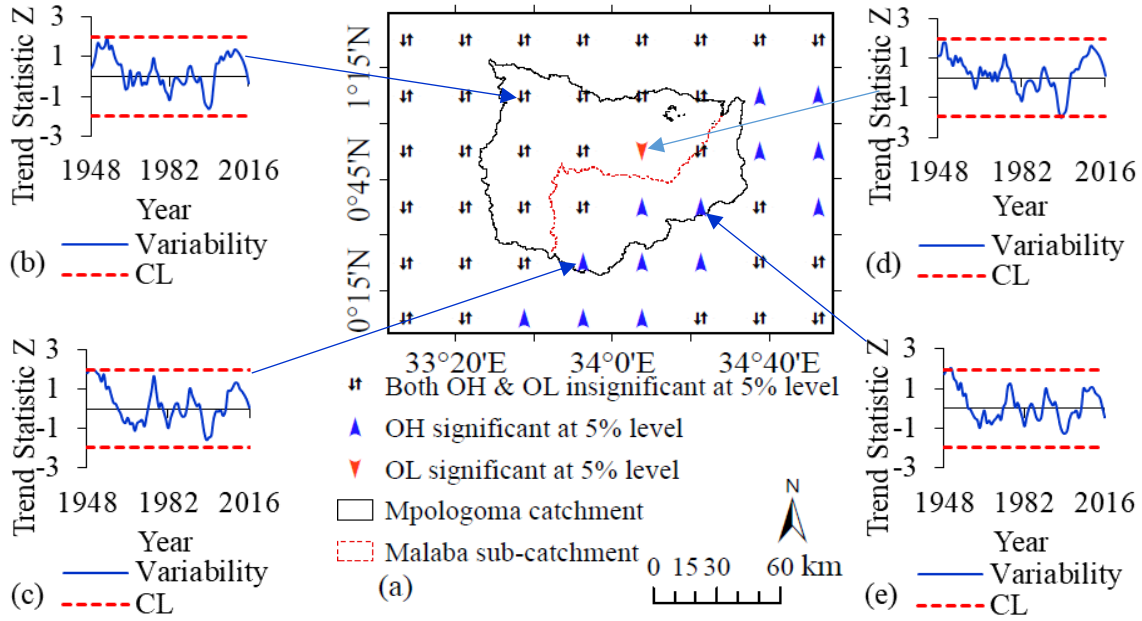

Figure 3.4 (a) spatial differences in the significance of rainfall variability and (b-e) temporal variability in NWD10 EPI at different locations of the study area. "CL" corresponds to the dotted horizontal lines denoting the 95% confidence interval limits.

In Figure 3.5(a), NWD5 exhibited significant ($p < 0.05$) OH in the West, central and Southern regions. The significant OH occurred in the early 1950s (Figure 3.5(b, c, e)). The North eastern region around Manafwa experienced significant OL in NWD5 around 1981 (Figure 3.5 (d)). Similar to NWD10, the oscillations in NWD5 exhibited a common pattern (Figure 3.5(b-d)).

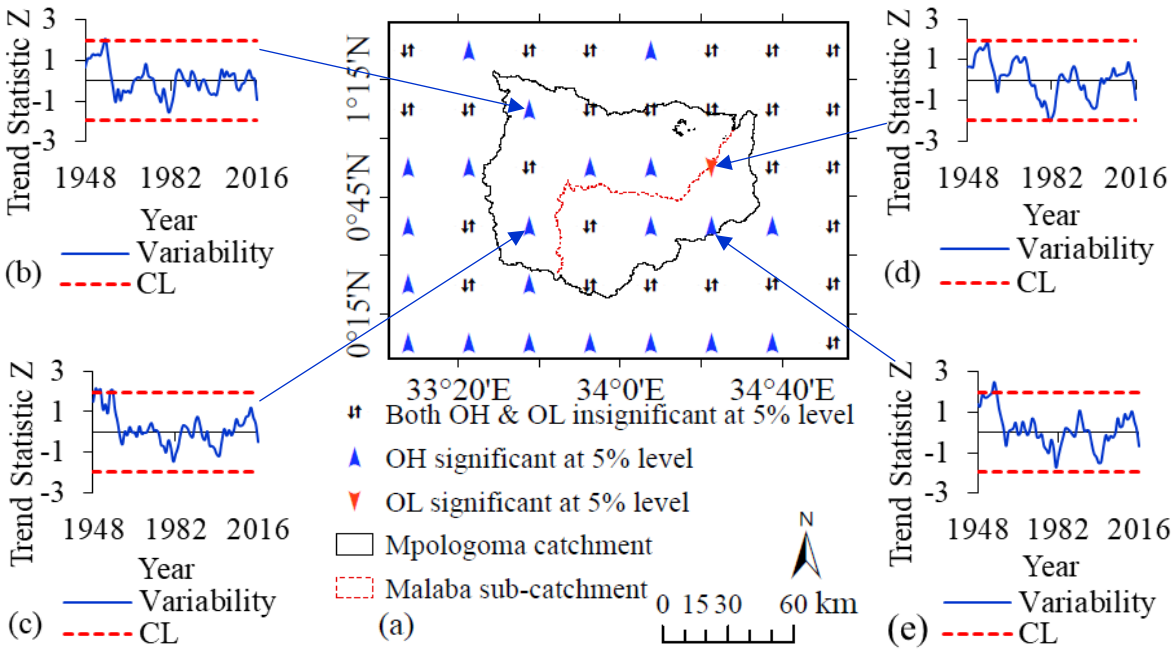

Figure 3.5 (a) spatial differences in the significance of rainfall variability and (b-e) temporal variability in NWD5 EPI at different locations of the study area. "CL" corresponds to the dotted horizontal lines denoting the 95% confidence interval limits.

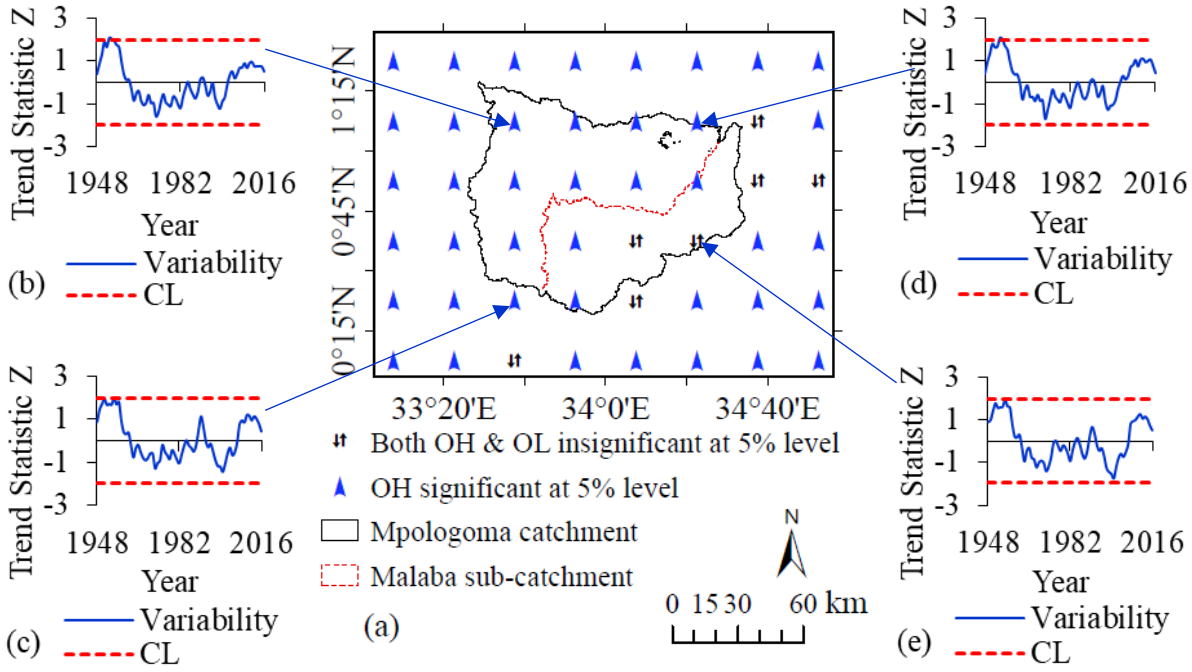

Figure 3.6 (a) spatial differences in the significance of rainfall variability and (b-e) temporal variability in SPre10 EPI at different locations of the study area. "CL" corresponds to the dotted horizontal lines denoting the 95% confidence interval limits.

Figure 3.6(a) shows that the entire areas had a significant ($p < 0.05$) OH in SPre10, while a small area exhibited both insignificant ($p > 0.05$) OH and OL. Similar to NWD10 and NWD5, 95% confidence limit upper limit was surpassed in the early 1950s (Figure 3.6 (b-d). SPre10 was above the long-term from late 1940s to early 1960s and as well from early 2001 till end of the study period (2016) (Figure 3.6 (b-e). The SPre10 oscillations over the entire study area displayed a common pattern.

In Figure 3.7(a) SPre5 over the entire area except around Northern part of Mbale was characterised by both insignificant ($p > 0.05$) OH and OL. Similarly, the SPre5 was above the long-term from late 1940s to early 1960s and as well from early 2001 till end of the study period (2016) (Figure 3.7(b-e).

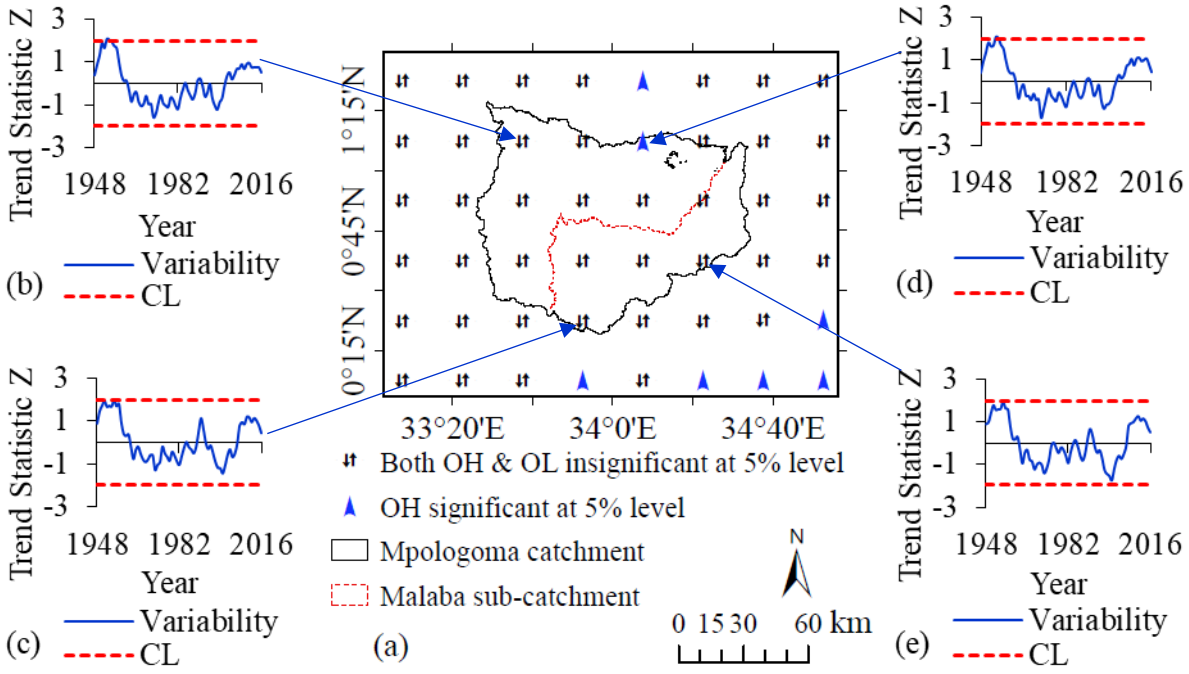

Figure 3.7 (a) spatial differences in the significance of rainfall variability and (b-e) temporal variability in SPre5 EPI at different locations of the study area. "CL" corresponds to the dotted horizontal lines denoting the 95% confidence interval limits.

OHs in extreme precipitation indicate possibilities of high intensity and severe flooding conditions and these may increase in future. Despite the observed decrease in some of the EPIs, intensified monitoring of extreme weather events in the study area is necessary. The finding from Ongoma *et al*. (2016) established that the study area exhibited high values of simple daily intensity index

which could be associated with the recurrent floods and landslides. The study area mainly suffers from recurrent and severe floods which destroy property and lead to loss of lives. It could be possible that the severe floods and landslides of March 2010 that killed over 400 people, displacing 5000 people in Bududa district with over 33000 households affected in Butaleja were due to an increase in ANMS.

3.3.3 *Statistical Trend Analyses on Evapotranspiration*

The trends in annual and seasonal evapotranspiration are shown in Figure 3.8. The western region (close but outside the catchment) as well as the northeast part far outside the catchment, had a positive significant trend (H_o rejected) ($p < 0.05$) in the annual evapotranspiration (Figure 3.8(a)). The rest of the study area experienced a negative insignificant trend at the 5% level.

Like the annual evapotranspiration, the western part (close but outside the catchment), as well as the northeast and northwest regions had a positive significant trend (H_o rejected) ($p < 0.05$) in the OND evapotranspiration. The rest of the catchment had a positive insignificant ($p > 0.05$) (Figure 3.8(b)). During the JJAS season, the region near the southeast and the far western part of the study area (approximately 30 km away), had a negative significant trend (H_o rejected) ($p < 0.05$) in the evapotranspiration (Figure 3.8(c)). The rest of the study area experienced a positive but insignificant trend at the 5% level. During the MAM season, the entire study area exhibited only a positive insignificant ($p > 0.05$) trend in the evapotranspiration (Figure 3.8(d)).

In general, evapotranspiration over the entire area exhibited an increase at the seasonal scales although not significant at the 5% level. A similar result was found by Onyutha (2016b), that indicated an increase of evapotranspiration over the entire Uganda. Similarly, the results were in agreement with the findings from Alemu *et al.* (2015). Th study by Onyutha *et al*. (2021a) as well reported an increase in PET across entire Uganda. The increase in evapotranspiration could be attributed to the increasing temperature as well as the varying rainfall from region to region over the study area. In addition, for the entire period (1948 to 2016), there was no negative trend in the OND and MAM evapotranspiration (Figure 3.8(b, d)). An increase in seasonal evapotranspiration although not significant would imply potential impacts on the soil water balance which might influence flood peaks.

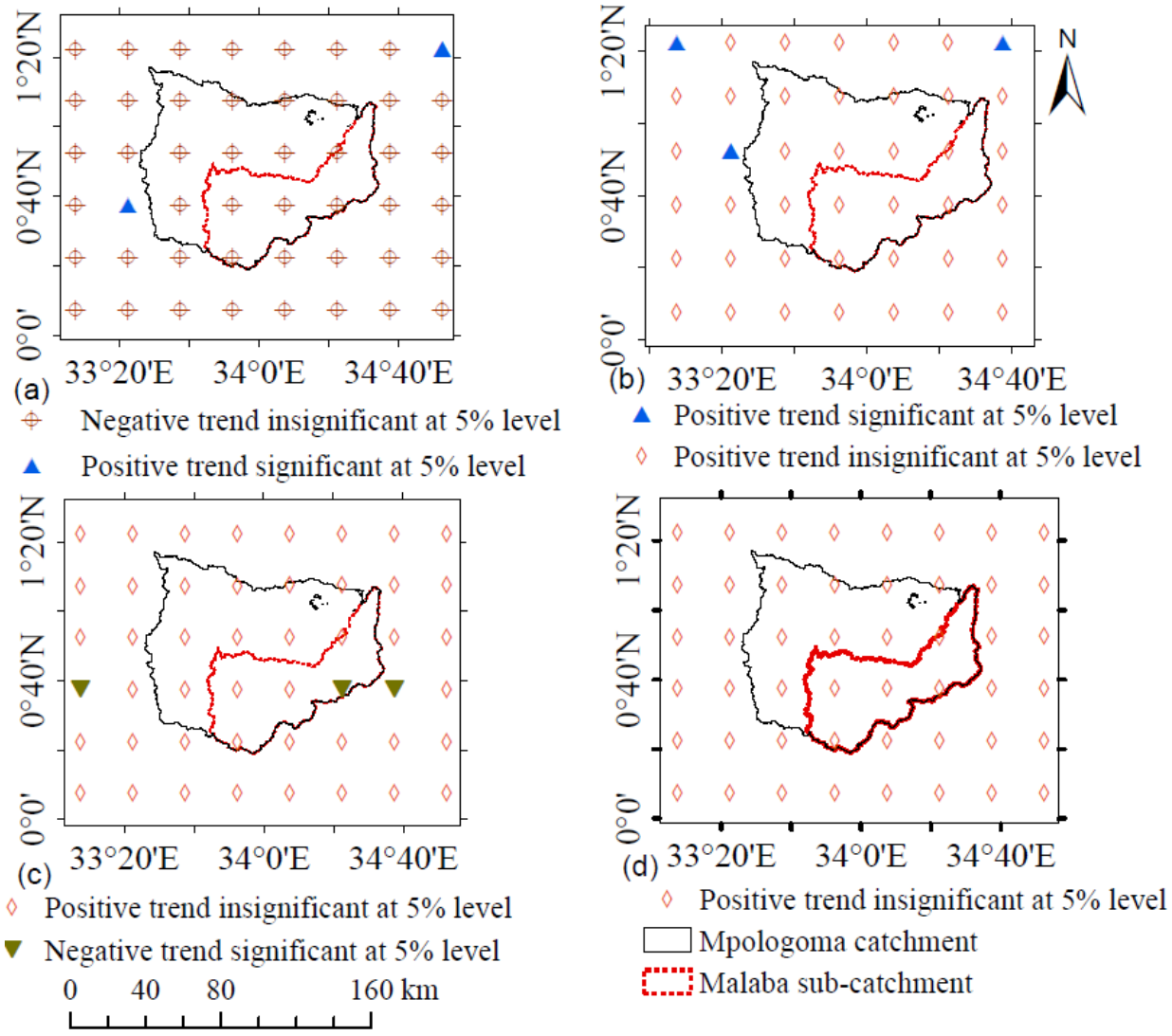

Figure 3.8 Trend in evapotranspiration (a) annual, (b) OND, (c) JJAS and (d) MAM

3.3.4 *Spatio-temporal Variability Analyses on Evapotranspiration*

Figure 3.9 to Figure 3.12 show the differences in spatial variation in the annual and seasonal evapotranspiration across the study area. At the annual scale, some region in the north, as well as areas near the southeast had significant OH (H_o rejected) ($p < 0.05$) (Figure 3.9(a).

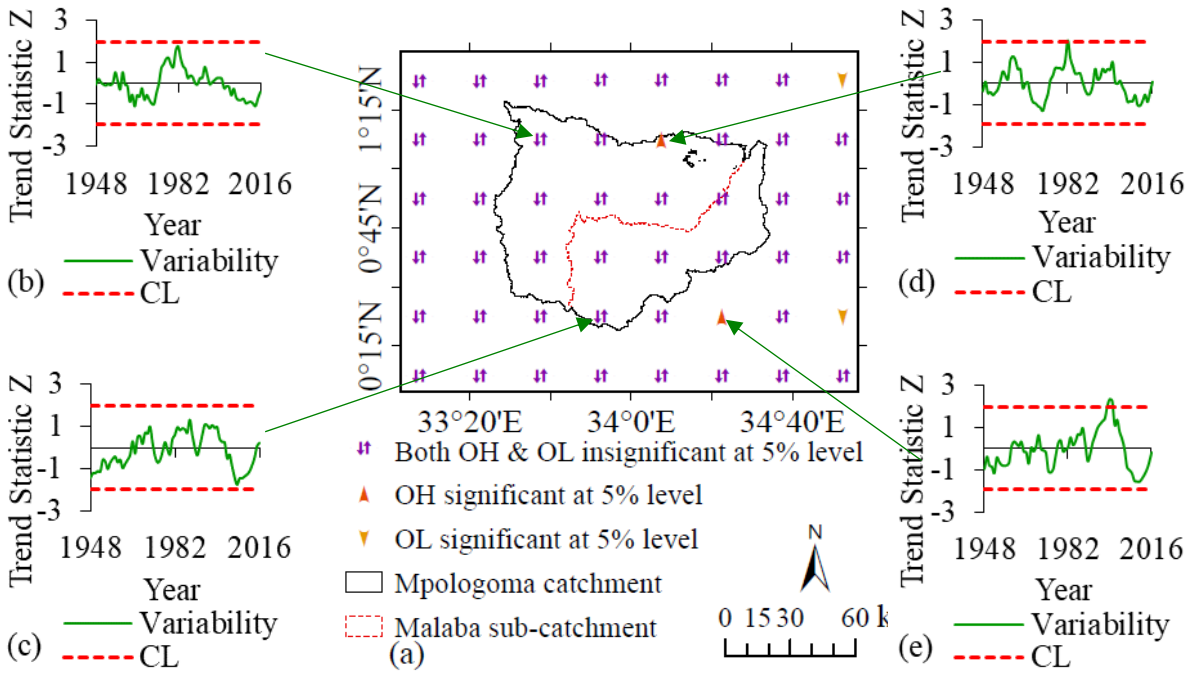

Figure 3.9 Spatial differences in the significance of annual evapotranspiration variability (a) and temporal variability in annual evapotranspiration (b-e) at different locations of the study area. "CL" corresponds to the dotted horizontal lines denoting the 95% confidence interval limits.

The far northeast and southeast regions (outside the study area) experienced significant OL (H_o rejected) ($p < 0.05$). The rest of the area experienced both insignificant OH and OL ($p > 0.05$) (Figure 3.9(a)). From Figure 3.9(b-e), annual evapotranspiration was characterised by both increase and decrease for the entire study period (1948-2016) but the northern region exhibited more of an increase in the mid-1970s till the late 1980s (Figure 3.9(b-d)).

Figure 3.10(a) shows that only the southern region of the catchment and an area approximately 30 km North of the study area experienced significant OL and OH ($p < 0.05$), respectively during the OND season. The rest of the catchment had both insignificant OH and OL during the OND season. The temporal variation of OND evapotranspiration was characterised by both increase and decrease but more pronounced increase (Figure 3.10(b-e)).

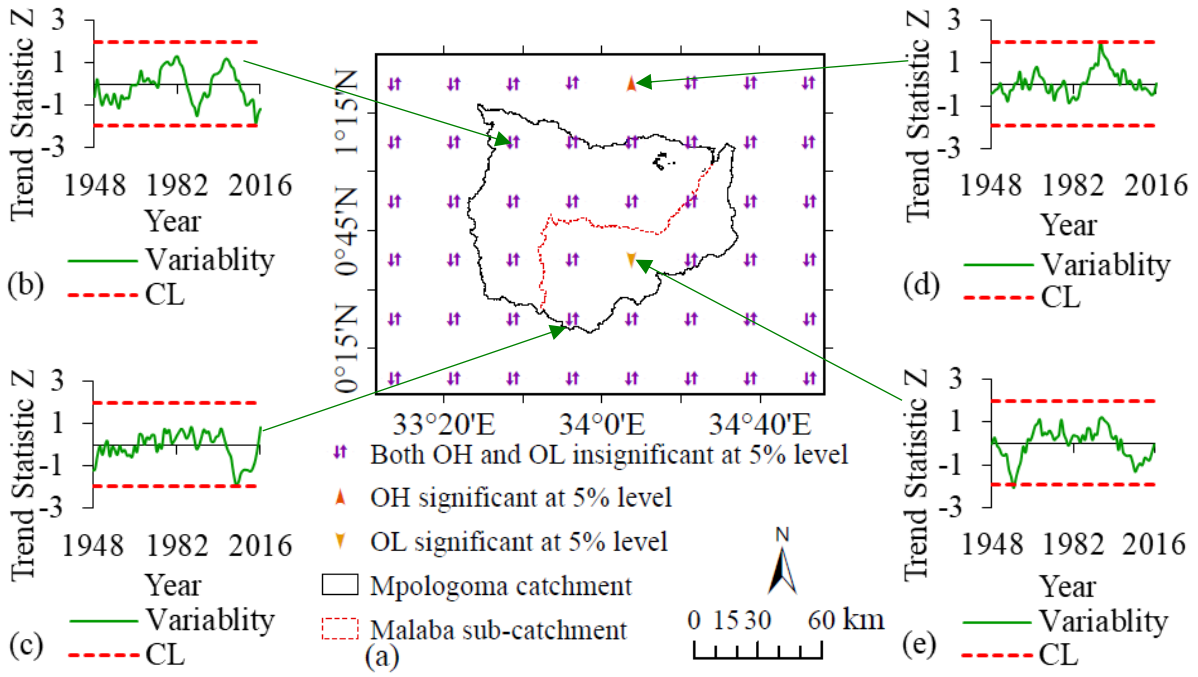

Figure 3.10 Spatial differences in the significance of evapotranspiration variability (a) and temporal variability (b -e) in OND evapotranspiration at different locations of the study area. "CL" corresponds to the dotted horizontal lines denoting the 95% confidence interval limits.

Figure 3.11(a) shows that during the JJAS season, the southeast region had significant OH ($p < 0.05$). The southwest/western region outside the catchment was characterised by both significant OH and OL ($p < 0.05$). However, the rest of the catchment had both insignificant OH and OL ($p > 0.05$) in the JJAS evapotranspiration. Evapotranspiration was generally above the reference except from the mid-1990s till the end of the study period (2016) when it was more below the long-term mean (Figure 3.11(b-e)).

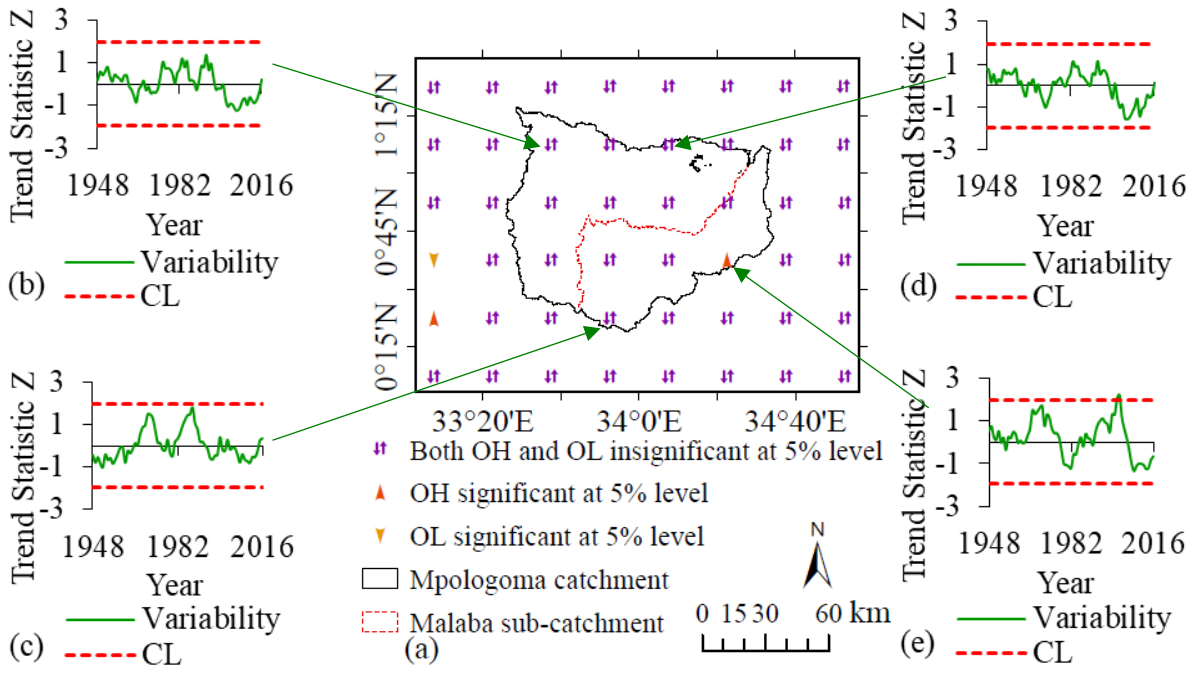

Figure 3.11 Spatial differences in the significance of evapotranspiration variability (a) and temporal variability (b-e) in JJAS evapotranspiration at different locations of the study area. "CL" corresponds to the dotted horizontal lines denoting the 95% confidence interval limits.

For the MAM season, significant OL ($p < 0.05$) was in the West, East, Southeast and far Northeast (outside of the catchment) regions (Figure 3.12(a)). The rest of the area experienced both insignificant OH and OL ($p > 0.05$). MAM evapotranspiration exhibited both an increase and decrease going above (below) the long-term mean for the entire study period (Figure 3.12(b-e)).

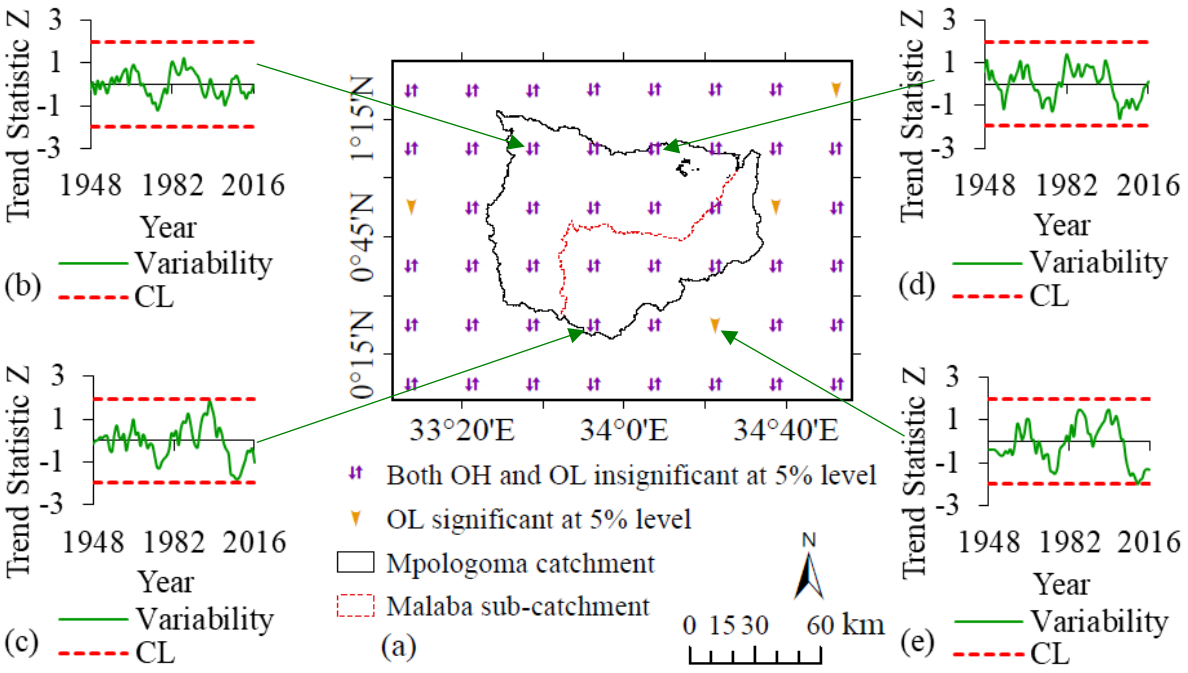

Figure 3.12 Spatial differences in the significance of evapotranspiration variability (a) and temporal variability (b-e) in MAM evapotranspiration at different locations of the study area. "CL" corresponds to the dotted horizontal lines denoting the 95% confidence interval limits.

3.4 Conclusion and implication of the findings

3.4.1 *Research questions addressed in this chapter*

For specific objective one: Were there significant trends and variabilities in rainfall & PET? What patterns of variabilities did rainfall & PET exhibit?

3.4.2 *Conclusion*

The number of wet days and sum of rainfall exhibited a decreasing trend with ($p > 0.05$) and ($p < 0.05$), respectively. However, annual maxima rainfall series had an increase ($p > 0.05$). This indicate that it may be raining less frequently but with some events having very high intensity. The decreasing sum of precipitation may be linked with decreasing number of wet days. For decreasing SPre5 across the entire catchment, H_o (no trend) was rejected ($p < 0.05$). Similarly, except the South and South Eastern parts, H_o (no trend) was rejected ($p < 0.05$) for decreasing SPre10. However, the decreasing NWD5 and NWD10, and increasing ANMS had H_o (no trend) not rejected ($p > 0.05$). Except in the late 1950s, oscillation in rainfall variability were insignificant ($p > 0.05$) but with a common pattern.

The sub-catchment PET had an insignificant ($p < 0.05$) positive trend. Similar to rainfall, the amplitudes in PET variability were insignificant ($p < 0.05$), and occurred in a clustered way.

3.4.3 *Implication of the study findings*

ANMS trend magnitude increasing over time. If this is to continue in the future, floods of greater magnitude may be experienced in the study area. Therefore, planning of flood adaptation strategies need to be more intensive and thorough. Rainfall extreme events over the study area occur in a clustered way (consecutively positive and negative) in time varying from decadal to multidecadal timescale. This indicates that rainfall variability is not random. Therefore, design of flood adaptation measures should consider the fact that over some periods, frequency can be higher than others. Besides, presence of rend and shifts call for non-stationarity in the design of water resource infrastructures, such as bridges. In periods of rainfall above the normal conditions, through sensitisation, the community in flood prone areas can relocate to safe places. To support communities to predict upcoming periods of wet conditions, it is vital to quantify the possible driver of rainfall variability. This could be done in future research to investigate if the large-scale atmospheric conditions can result in a delayed influence on the rainfall and evapotranspiration variability.

Chapter Four

4. Extreme peak flows in River Malaba sub-catchment

This chapter is based on the published paper:

Mubialiwo, A., Abebe, A., Onyutha, C., 2021. Performance of rainfall – runoff models in reproducing hydrological extremes: a case of the River Malaba sub-catchment. *SN Applied Sciences* 3, 24. https://doi.org/10.1007/s42452-021-04514-7

4.1 Introduction

To facilitate predictive planning and operation of risk-based water resources management within the study area, there was need to perform hydrodynamic modelling. Hydrodynamic modelling of floods, necessitate understanding the hydrologic processes with focus on the extremes. Hydrological modelling can be performed using either lumped conceptual, semi-distributed or distributed models. Distributed models consider the spatial distribution of rainfall, evapotranspiration and watershed characteristics at a resolution normally selected by the modeller to reflect the spatio-temporal variability of runoff. Some of the distributed (physically-based) hydrological models include the Gridded Surface Subsurface Hydrologic Analysis (GSSHA) (Downer *et al*., 2002), Systeme Hydrologique Europeen, "SHE" (Abbott *et al*., 1986), European Hydrological System Model (MIKE-SHE) (Refsgaard and Storm, 1995), Modular Modelling System (MMS) (Leavesley *et al*., 1996). Some models are not physically based but rather semi-distributed e.g., Soil and Water Assessment Tool (SWAT) (Arnold *et al*., 2012) which is operated on hydrological response unit (HRU) and necessitates parameter calibration. Whereas the physically-based (distributed) models have better computational capacity and are robust, with well implemented numerical methods, their application particularly, in rainfall-runoff simulations is still inadequate. Huge amount of data inputs may undesirably result in a more complex model which may lead to high prediction uncertainty especially if a model has large number of parameters (Pande *et al*., 2014).

On the other hand, lumped conceptual models are based on average spatial characteristics of the system, whose basis is to simulate flow at the outlet of the catchment (Asadi, 2013; Tassew *et al*., 2019). Examples of lumped conceptual models include the Australian Water Balance Model (AWBM) (Boughton, 2004), Sacramento (SAC) (Burnash, 1995), TANK (Sugawara, 1995),

Identification of Unit Hydrographs and Component Flows from Rainfall, Evaporation and Stream-flow data (IHACRES) (Croke *et al*., 2005; Jakeman *et al.*, 1990), SIMHYD (Porter and McMahon, 1971), Soil moisture accounting and routing (SMAR) (O'Connell *et al*., 1970), Hydrological Model focusing on Sub-flows' Variation (HMSV) (Onyutha, 2019), Pitman model (Pitman, 1973), Hydrologic Engineering Center-Hydrologic Modelling System (HEC-HMS) model (David Ford *et al*., 2008), Hydrologiska Byråns Vattenbalansavdelning (HBV) model (Bergström, 1992). The high capacity to simulate runoff with easy to use methods, and the minimum data requirement, has made the lumped conceptual models prevalent to distributed models for rainfall-runoff modelling. Lumped conceptual models have widely been applied (Adnan *et al*., 2020). Rainfall-runoff modelling can be done based on event-based or continuous approach. Recently, there is a transition from event-based to continuous hydrological modelling. For instance, Grimaldi *et al*. (2020) applied the Continuous Simulation Model for Small Ungauged Basins (COSMO4SUB) to ungauged catchment and the results were comparable with the event-based approach. Similarly, several studies have reported superior performance of Artificial Neural Network *(*ANN*)* models (Adnan *et al*., 2020; Aghelpour and Varshavian, 2020; Ebtehaj *et al*., 2020)

Within Uganda (where the study area is located), a few studies (Ednah, 2018; Onyutha and Willems, 2018) on hydrological modelling applied either one or very few hydrological models. On the other hand, Onyutha *et al.* (2021) compared the performance of seven lumped conceptual models in the simulation of daily River Kafu flows. However, this study was conducted in western Uganda and not in the eastern region (where the study area is located). Furthermore, most of the studies applied either one or very few (maximum of 4) "goodness-of-fit" measures. The selection and application of a particular model and "goodness-of-fit" measure from the several can result in a huge bias while concluding on the worthiness of the obtained model results (Onyutha, 2020b). This could be attributed to the varying structures and parameters amongst different model (Tegegne *et al.*, 2017). In addition, a particular "goodness-of-fit" measure may not provide information on some analyses components such as model residuals, making them insufficient in assessing model performance (Onyutha, 2020b; Zhou *et al*., 2019).

Reliable hydrological modelling results are vital for decision makers to avoid profligate expenditures resulting from wrongly informed predictive planning. Prior to this research, studies conducted to evaluate several lumped conceptual models' performance based on multiple "goodness-of-fit" statistics to model extreme peak flows in River Malaba sub-catchment were

lacking. Therefore, to address the aforesaid research gap, this study evaluated the performance of seven rainfall-runoff models in simulating extreme peak flows of River Malala sub-catchment while assessing model performance using nine "goodness-of-fit" metrics. In this study, focus was on high flow extreme for relevance of application in flood analysis.

4.2 Methodology

4.2.1 *Rainfall-Runoff Modelling*

This study used seven lumped conceptual rainfall-runoff models. Of the seven models, the six are internationally well-known including the Australian Water Balance Model AWBM (Boughton, 2004), SACRAMENTO (Burnash, 1995), TANK (Sugawara, 1995), Identification of Unit Hydrographs and Component Flows from Rainfall, Evaporation and Stream (IHACRES) flow data (Croke *et al*., 2005; Jakeman *et al*., 1990), SIMHYD (Porter and McMahon, 1971), and Soil Moisture Accounting and Routing SMAR (O'Connell *et al.*, 1970). These six models were obtained from the "eWater Toolkit" of the Cooperative Research Centre for Catchment Hydrology in Australia via http://www.toolkit.net.au/ (accessed: 08 February 2021). Detailed description of these six models can be found in the RRL (Podger, 2004). The seventh model or HMSV with details in Onyutha (2019) was accessed freely via https://sites.google.com/site/conyutha/tools-to-download (accessed: 10 February 2021). These models were selected because they (1) are freely available online, and (2) were found to be robust for rainfall-runoff modelling under various climatic conditions as demonstrated in several recent studies (Birhanu *et al*., 2018; Chelangat and Abebe, 2021; Goodarzi *et al*., 2020; Onyutha. *et al*., 2021; Onyutha, 2019; Pérez-Sánchez *et al*., 2019; Tiwari and Balvanshi, 2020).

Here is a brief mention of each model's parameters. AWBM has 8 parameters, but three of them (Baseflow index, baseflow recession constant, surface flow recession constant) are considered the major ones. SAC model has 17 parameters, with three designed for direct runoff simulation, other 3 for water capacity in upper zone, 2 for percolation into lower zones, while the remaining 9 are designed for water capacity in the lower zone. TANK model has 18 parameters categorised under 7 classes. The model has 3 major parameters (i.e. water levels in the tanks, height of outlets at tanks and runoff coefficients. IHACRES model has 11 parameters. SIMHYD model has 9 parameters, with 4 sensitive ones (i.e. infiltration coefficient and shape, interflow coefficient, and base flow coefficient). SMAR model has five water balance parameters and 4 routing parameters.

HMSV has total of 10 parameters. 4 parameters are for baseflow, 2 for interflow and 4 for overland flow simulation. A combination of the 10 parameters is used to calibrate the full model to simulate the total runoff. Higher values of recession constants imply delayed contributions of different components to the total runoff. Higher values of initial soil moisture storage signify faster contribution of run off from the catchment.

Modelling was done using meteorological data (rainfall and potential evapotranspiration) as described in sub-section 2.2.1.1. Prior to inputting the data into the models, it was converted into formats required by each of the seven rainfall runoff models. The Initial model parameters for each model as provided in Podger (2004) (for AWBM, TANK, SAC, SIMHYD and SMAR), Croke *et al*. (2005) (for IHACRES), and Onyutha (2019) (for HMSV) were set and the models ran to generate outputs. Sensitivity analysis on the model parameters was done prior to calibration. This was done to establish the contribution of a particular parameter variation to model output in order to identify which parameters have a great or less impact on the model response. This study adopted the use of local sensitivity analysis (LSA) method because, it is simple, fast and can yield results similar to the global sensitivity analysis (GSA) (Link *et al.*, 2018). The LSA method focuses of the impact on model output caused by a single parameter, while other parameters are fixed.

The model parameters were calibrated using the observed river flow data (sub-section 2.2.1.3) from 01/01/1999 to 31/12/2009, until there was a reasonable match between the simulated and observed flow. Model calibration can be based on manual or automatic strategy. With manual calibration, there is a trial and error adjustment of parameters based on the modellers' visual inspection of simulated and observed values, making it is very difficult to yield a hydrologically sound and unbiased results, and the process is tedious, time consuming, especially for models with many parameters (Amir *et al.*, 2013). When comparing models, manual calibration also yields subjective results. Thus, in this study, calibration was done using the automatic calibration strategy with model parameters automatically adjusted following systematic search algorithms based on the set objective function. In the rainfall-runoff models' frameworks, Nash-Sutcliffe efficiency (NSE) (Nash and Sutcliffe, 1970) was used as the optimisation objective function, while the models' performance was further assessed based on other eight "goodness-of-fit "metrics as described shortly next. Five models (AWBM, SACRAMENTO, TANK, SIMHYD, and SMAR) were calibrated based on shuffled complex algorithm (SCE) (Duan *et al*., 1993). The calibration of IHACRES followed the approach described by Croke *et al*. (2005). Similarly, the HMSV was

automatically calibrated based on the Generalized Likelihood Uncertainty Estimation (GLUE) developed by Beven and Binley (1992). HMSV framework allows a "step-wise" calibration strategy, first by calibrating parameters based on each of the sub-flows (baseflow, interflow and overland flow). The full model run is then performed combining parameters from the sub-flow models. This approach allows modelling of quick flows focusing on high flows while baseflow considers variation of the low flows. The models were validated using the observed river flow data for a record outside the calibration period (from 01/01/2010 to 31/12/2016). During validation, the same parameters and corresponding values used for calibration were maintained.

The models performance were evaluated based on nine widely used statistical indicators, including, Nash-Sutcliffe efficiency (NSE) (Nash and Sutcliffe, 1970)**,** model average bias (MAB) (%), Ratio of Root Mean squared error to the maximum event (RRM), relative efficiency (R_e) (Krause *et al.*, 2005), index of agreement (I_a) (Willmott, 1981), coefficient of determination (R) (Bartlett, 1993), mean absolute error (MAE), coefficient of model accuracy (CMA) (Onyutha, 2020b), and Kling-Gupta efficiency (KGE) (Gupta *et al*., 2009) as shown in equations (4.1) to (4.9). For all the seven model, NSE was used as the optimisation objective function for calibration. Consider $Q_{obs}, Q_{sim}, \bar{Q}_{obs}$, and $\bar{Q}_{sim}$ as the observed, modelled, mean of observed, and mean modelled flows, respectively. Furthermore, take $Q_{\max}, \sigma_{obs}, \sigma_{sim}$ and n, to denote the maximum observed flows, standard deviation in observed, standard deviation in modelled flows, and sample size, respectively. Lastly, consider r as the rank-based Spearman correlation coefficient between Q_{obs} and Q_{sim}. The various "goodness-of-fit" metrics were computed using:

$$NSE = 1 - \frac{\sum_{i=1}^{n}\left(Q_{sim,i} - Q_{obs,i}\right)^2}{\sum_{i=1}^{n}\left(Q_{obs,i} - \bar{Q}_{obs}\right)^2} \tag{4.1}$$

$$MAB = \frac{1}{n}\sum_{i=1}^{n}\left(\frac{Q_{sim,i} - Q_{obs,i}}{Q_{obs,i}} \times 100\right) \tag{4.2}$$

$$RRM = \frac{1}{Q_{\max}}\left(\frac{1}{n}\sum_{i=1}^{n}\left(Q_{sim,i} - Q_{obs,i}\right)^2\right)^{0.5} \tag{4.3}$$

$$R_e = 1 - \frac{\sum_{i=1}^{n} \left| Q_{sim,i} - Q_{obs,i} \right|^{f_p}}{\sum_{i=1}^{n} \left| Q_{obs,i} - \bar{Q}_{obs} \right|^{f_p}} \tag{4.4}$$

$$I_a = 1 - \frac{\sum_{i=1}^{n} \left| Q_{obs,i} - Q_{sim,i} \right|^{f_p}}{\sum_{i=1}^{n} \left(\left| Q_{sim,i} - \bar{Q}_{obs} \right| + \left| Q_{obs,i} - \bar{Q}_{obs} \right| \right)^{f_p}} \tag{4.5}$$

$$R = \frac{\sum_{i=1}^{n} \left(Q_{obs,i} - \bar{Q}_{obs} \right) \left(Q_{sim,i} - \bar{Q}_{sim} \right)}{\sqrt{\sum_{i=1}^{n} \left(Q_{obs,i} - \bar{Q}_{obs} \right)^2} \times \sqrt{\sum_{i=1}^{n} \left(Q_{sim,i} - \bar{Q}_{sim} \right)^2}} \tag{4.6}$$

$$MAE = \frac{\sum_{i=1}^{n} \left| \left(Q_{obs,i} - Q_{sim,i} \right) \right|}{n} \tag{4.7}$$

$$CMA = |r| \times \frac{min\left(\bar{Q}_{sim}^2, \bar{Q}_{obs}^2 \right)}{max\left(\bar{Q}_{sim}^2, \bar{Q}_{obs}^2 \right)} \times \frac{\sum_{i=1}^{n} min\left(\left(Q_{obs,i} - 3\bar{Q}_{obs} \right)^2, \left(Q_{sim,i} - 3\bar{Q}_{obs} \right)^2 \right)}{\sum_{i=1}^{n} max\left(\left(Q_{obs,i} - 3\bar{Q}_{obs} \right)^2, \left(Q_{sim,i} - 3\bar{Q}_{obs} \right)^2 \right)} \tag{4.8}$$

$$KGE = 1 - \sqrt{\left(r - 1 \right)^2 + \left(\frac{\sigma_{sim}}{\sigma_{obs}} - 1 \right)^2 + \left(\frac{\bar{Q}_{sim}}{\bar{Q}_{obs}} - 1 \right)^2} \tag{4.9}$$

where: f_p is the power factor.

NSE demonstrates how fit the simulation mimics the observation, and it varies between –∞ and 1.0, with the value of 1.0 denoting a perfect match. A value greater than 0.5 for NSE is considered acceptable (Santhi *et al.*, 2001). MAB and MAE denote the bias and mean error magnitude between modelled and observed values. The value of MAB and MAE equal to 0 signifies an unbiased model (Onyutha, 2016d). RRM was considered in this study instead of the root mean squared error because it is unitless and has a small value, making it suitable to compare with MAB. The values of R_e and I_a range between 0 and 1. A value of 1 designates perfect match between simulated and observed, while 0 implies total divergence. I_a is known for its insensitivity to systematic model overestimation and underestimations (Willmott, 1981). The values of f_p = 1 can be used to balance between high flows and low flows (Krause *et al.*, 2005; Onyutha, 2016d). However, in this study, the value of f_p was taken to be greater than 1 since the model evaluation focused on high flows. R quantifies how much the observed dispersion is explained by the

simulation. *R* ranges between 0 and 1. A value of 1 means perfect prediction of the modelled dispersion to the observed, and 0 indicates no correlation. This indicator has a weakness, as it only measures the dispersion, hence it is not recommended to be used solely (Krause *et al*., 2005). The values of CMA range from 0 to 1 with CMA equal to 1 signifying a perfect model, while CMA equal to 0 indicates that the model simulations do not match the observations (Onyutha, 2020b). Similar to NSE, a value of KGE equal to one denotes a perfect agreement between observations and simulation (Knoben *et al*., 2019).

4.2.1.1 Comparison of the model performance based on the "nine goodness-of-fit" measures

For the three periods of calibration (01/01/1999 to 31/12/2009), validation (01/01/2010 to 31/12/2016), and entire data period (01/01/1999 to 31/12/2016), models were ranked from 1 to 7 denoting the best and worst performance, respectively. Ranking was initially done based on individual "goodness-of-fit" statistic. For instance, a model with the highest (lowest) KGE was allocated rank 1 (7), indicating best (worst) model. This was done for all the nine metrics. The summation of ranks for the three periods (calibration, validation and entire period) were obtained for the nine metrics (NSE, MAB, MAE, RRM, R_e, I_a, R, CMA, and KGE). The model with the smallest (largest) sum of ranks for each individual metric was considered the best (worst).

4.2.2 ***Amplitude-Duration-Frequency Analyses***

To facilitate planning, design and operation of various water management projects against weather events, such as floods, and/or to reduce human and economic losses, there is need to understand the extreme peak flows and their frequency at selected temporal scales (Devkota *et al*., 2018; Nhat *et al.*, 2006). This can be through extreme value analysis on the hydrological time series for different aggregation levels, which generates Amplitude-Duration-Frequency (ADF) relationships. ADF for discharge and rainfall are called Flow-Duration Frequency (FDF) and Intensity-Duration Frequency (IDF), respectively. In this study, only the FDF are developed for both observed and modelled flow for each of the seven hydrological models. Aggregation simply converts fine resolution data into coarser time units e.g., from daily to monthly, which hydrologically implies representing a delayed response of a watershed (Onyutha, 2012). Here, aggregated hydrological time series were obtained by use of *n*-day moving window. Aggregation levels are selected with the consideration of appropriate water resources management of floods. The considered aggregation levels ranged from 1 day to 3 months (1, 3, 5, 7, 10, 30, 60, 90 days).

The adopted aggregation levels were applied and/or recommended in previous studies (Insitute of Hydrology, 1980; Onyutha, 2016d; Onyutha and Willems, 2013).

Taking $x_t, \gamma,$ and λ as the threshold, scale and shape parameters, respectively, calibration of the exponential extreme value distribution, above the defined threshold x_t, follows the following probability distribution, $G(x)$ (Pickands, 1975).

$$G(x) = 1 - \left\{1 + \lambda\left(\frac{(x - x_t)}{\gamma}\right)\right\}^{\frac{-1}{\lambda}} \tag{4.10}$$

With λ taking a value of zero, the cumulative distribution function (CDF) of the exponential distribution becomes:

$$G(x) = 1 - \exp\left\{-\left(\frac{(x - x_t)}{\gamma}\right)\right\} \tag{4.11}$$

The subsequent step after aggregation of the time series was the extraction of independent extreme high events. Two main approaches exist for extracting extreme hydrological events and these include the Peak-Over-Threshold (POT) and the Annual Maxima Method (AMM) techniques (Lang *et al*., 1999; Langbein, 1949). While the AMM is simple and generates extreme events that have high independence, the number of events can be few particularly for the short data record length as they generate only one event per year. On the other hand, the POT technique generates a satisfactory number of extreme events above the set threshold (Far and Wahab, 2016). Nevertheless, closely successive flood peaks could actually be a one flood, because the damage results from the highest and the related peaks may only have indirect contribution effects (Langbein, 1949). In this study, both the AMM and POT approaches were used. The AMM-generated independent events were used to compare the model performance in reproducing annual maxima, while the POT-generated independent events were used for frequency analysis of hydrological high extremes (in construction of FDF curves).

Several tools for extracting POT values exist including the WETSPRO: Water Engineering Time Series Processing tool (Willems, 2009), and Frequency Analyses considering Non-Stationarity (FAN-Stat) (Onyutha, 2017b). Chapter 3 revealed presence of trends and shifts in the rainfall and potential evapotranspiration over the study area. Since the same meteorological datasets (rainfall and potential evapotranspiration) were used as inputs in the hydrological models, the generated flows were presumed to exhibit non-stationarity (later confirmed in section 5.3.1 of chapter 5).

Therefore, the FAN-Stat tool that considers non-stationarity was adopted to obtain the independent POT value. The FAN-Stat tool was downloaded freely online via

https://sites.google.com/site/conyutha/tools-to-download (accessed: 10 February 2021). Using the extracted POT events, the extreme value distribution (EVD) was fitted to the independent extreme high flow events. According to Segers (2005), in extreme value theory, a conditional probability distribution of independent extreme events follows a Generalized Pareto Distribution (GPD), if only values above an appropriately high threshold x_t are used such that (Pickands, 1975):

$$G(x) = 1 - \exp\left\{-\frac{(x - x_t)}{\gamma}\right\} \quad \text{for } \lambda = 0 \tag{4.12}$$

and

$$G(x) = 1 - \left\{1 + \lambda\frac{(x - x_t)}{\gamma}\right\}^{-1/\lambda} \quad \text{for } \lambda \neq 0 \tag{4.13}$$

For values of $\lambda = 0$, the generated shape of the distribution tail is "normal" but when $\lambda > 0$ or $\lambda < 0$, the tail is heavy or light, respectively. For normal tail $(\lambda = 0)$, the GPD matches the exponential distribution.

Following the above concept, the distribution tail analysis in River Malaba sub-catchment is done for the high extreme river flow events. The weighted linear regression method recently applied by Baig *et al.* (2020) was used to determine the EVD parameters. To compute the EVD parameters in equation(4.12), exponential quantile plot with $-\ln\left[1 - G(x)\right]$ in the abscissa and x in the ordinate is adopted. The distribution assumes a straight line with a slope equal to γ that can be computed using equation (4.14) by implementing the weighting factors suggested in Hill (1975).

$$\gamma_t = \frac{1}{t-1}\left[\sum_{i=1}^{t-1}(x_t)\right] - x_t \tag{4.14}$$

where t denotes the number of POT events above the selected threshold x_t.

On the other hand, for parameters of a GPD as in equation (4.13), the plot with $-\ln\left[1 - G(x)\right]$ in the abscissa and x in the ordinate is used. The GPD appears as a line and the slope approximated to λ.The slope value of γ in the GPD expression (equation (4.13)) can be computed using equation (4.15), and the shape parameter λ can be estimated by the least square weighted linear regression assuming the weights suggested in Hill (1975) as shown in equation (4.16).

$$\gamma_t = \lambda_t \times x_t \tag{4.15}$$

$$\lambda_t = \frac{1}{t-1}\left[\sum_{i=1}^{t-1}\ln\left(x_i\right)\right] - \ln\left(x_t\right) \tag{4.16}$$

The finest value of x_t is selected from the exponential Q-Q plot at the point with minimum mean squared error (MSE). The MSE of the respective weighted linear regressions in EVD and GPD can be obtained from equations (4.17) and (4.18), respectively (Beirland *et al*., 1996).

$$MSE_t = \frac{1}{t-1}\left[\sum_{i=1}^{t-1}\left(-\ln\left(\frac{i}{t}\right)\right)^{-1}.\left(x_i - x_t - \gamma_t \ln\left(\frac{t}{i}\right)\right)^2\right] \tag{4.17}$$

$$MSE_t = \frac{1}{t-1}\left[\sum_{i=1}^{t-1}\left(-\ln\left(\frac{i}{t}\right)\right)^{-1}.\left(\ln\left(\frac{x_i}{x_t}\right) - \lambda_t \ln\left(\frac{t}{i}\right)\right)^2\right] \tag{4.18}$$

After calibration of the distribution and establishing the parameters, flow quantiles were computed. By taking n to be the data record length in years (in this case 18 years) and r as the rank of the generated POT extreme events (with 1 allocated to the highest POT values), the theoretical return period T based on the calibrated distribution was computed (equation (4.19)) (Rosbjerg, 1985). Similarly, the empirical return period (equation (4.20)) was determined (Onyutha and Willems, 2015a).

$$T(years) = \left(\frac{n}{t}\right)\frac{1}{1-G\left(X_T\right)} = \frac{n}{t \times \exp\left(-\frac{\left(x-x_t\right)}{\gamma}\right)} \tag{4.19}$$

$$T(years) = \left(\frac{n}{r}\right) \tag{4.20}$$

where X_T is the flow value corresponding to T obtained from equation (4.20). t was previously defined as the rank of the threshold values. $\left[1-G\left(x\right)\right]$ is the fitted EVD.

To carry out an extrapolation of the flow quantiles, equations (4.21) and (4.22) can be used for exponential distribution and generalise Pareto Distribution, respectively (Willems *et al*., 2007).

$$X_T = x_t + \gamma\left\{\ln(T)\right\} - \ln\left(\frac{n}{t}\right) \quad for \;\; \lambda = 0 \tag{4.21}$$

$$X_T = \exp\left(\ln(x_t) + \lambda\left\{\ln(T) - \ln\left(\frac{n}{t}\right)\right\}\right) \quad for \;\; \lambda \neq 0 \tag{4.22}$$

The high flow quantiles were extrapolated to different return periods (2, 10, 25, 50, 100 years). It is worth noting that in this study, extrapolation of quantiles is based on data od 18 years (1999 to 2016). However, the study by Schulz, Bernhardt (2016) discovered that extrapolations of quantiles for higher return periods (say 100 years) based on series of short-term can bring about large uncertainties. To minimise the possible uncertainties resulting from a small sample size, extrapolation of quantiles should not be for a return period greater than three times the record length (in years) of the data being used for analysis (Onyutha and Willems, 2013).Using the calibrated distribution parameters, the FDF relationships comprising of the accumulated values of flow for all the aggregation levels at three return periods (25, 50 and 100 year) were developed. Lastly the average model biases in replicating the observed high flow quantiles at different aggregation levels were computed based on equation (4.2).

4.3 Results and Discussion

4.3.1 *Comparison of model performance under moderate hydrological conditions*

Figure 4.1 shows the graphical comparison of observed and simulated river flow timeseries from the seven rainfall-runoff models. The set of parameters used to attain results in Figure 4.1are included in Table B.1 to B.7 of Appendix B. It is noticeable from Table B.1 to B.7 that optimised parameters were all with in the allowable ranges for each model. There is noticeable underestimation of the peaks especially by TANK, IHACRES, SMAR and HMSV (Figure 4.1c-d, f-g). In general, all the models well reproduced the pattern in the observed flow events (Figure 4.1a-g).

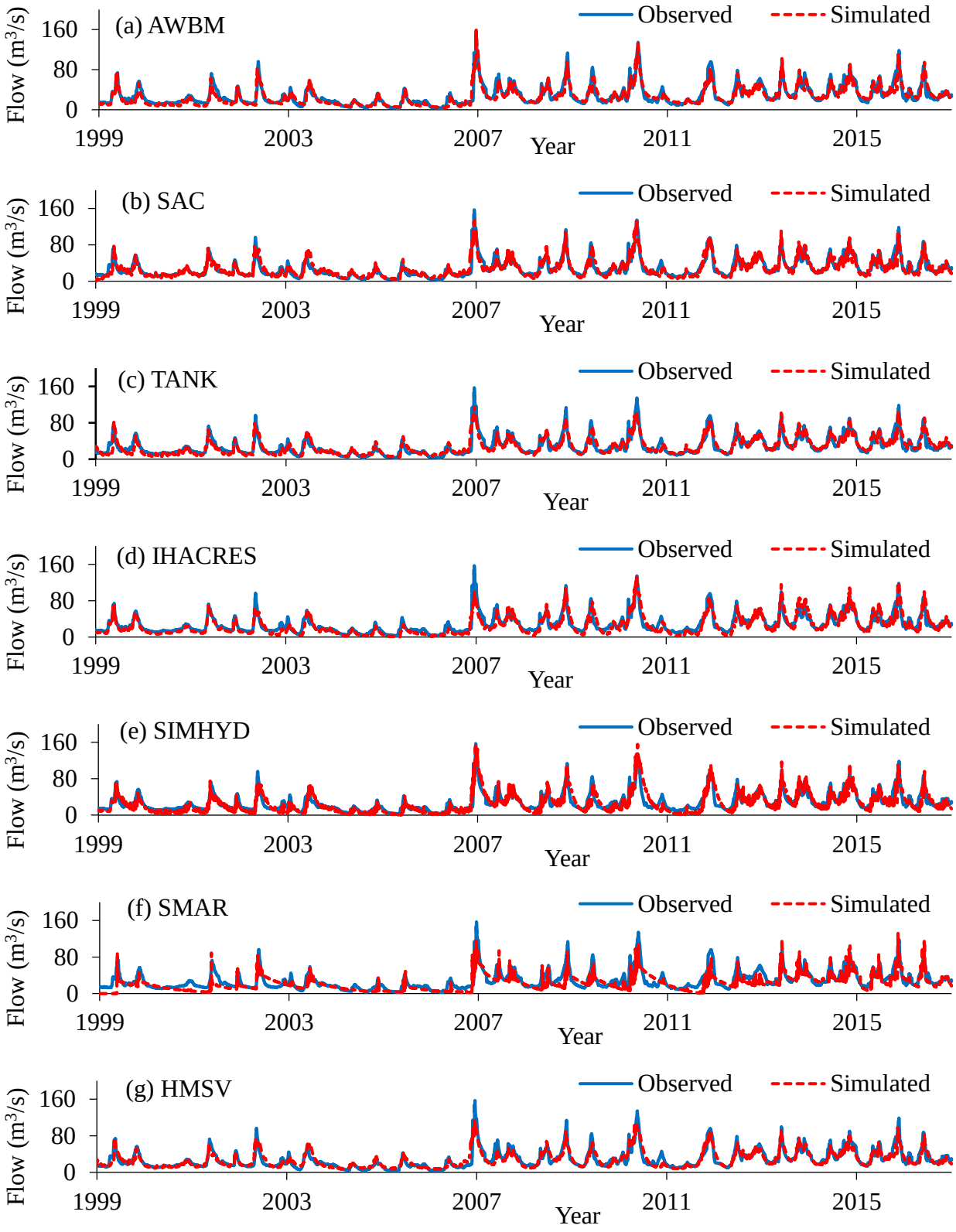

Figure 4.1 Observed discharge and simulated flows using the 7 hydrological models

In general, all the models well reproduced the pattern in the observed flow (Figure 4.1a-g). Figure 4.2(a-i) shows ranking of the model performance based on the nine "goodness-of-fit" statistics. Generally, AWBM had the smallest rank (1) hence, exhibiting the best performance (Figure 4.2 (a-i). However, when based on CMA (Figure 4.2 (i), AWBM ranked third after SAC and Tank. In several past studies (Onyutha. *et al*., 2021; Onyutha, 2016d), AWBM exhibited superlative performances. On the other hand, SMAR exhibited unsatisfactory performance with NSE of 0.46, 0.28 and 0.44 for calibration, validation, and entire period, respectively (Figure 4.2and Table 4.1). All models had NSE values above 0.50 (except SMAR).

The nine "goodness-of-fit" measures used for the calibration, validation and entire periods of the seven models are shown in Table 4.1. All models (except SMAR) exhibited laudable performance in simulating flows in the sub-catchment. The values of NSE varied between 0.46 to 0.83, 0.28 to 0.81, and 0.44 to 0.84 for calibration, validation, and entire period, respectively. The best performance was obtained with the entire period, followed by the calibration period. Statistically, the best model performance would be shown by MAB of 0%. However, in this study, the MAB values varied amongst the models with some exhibiting negative, while others showed positive. This discrepancy in the MAB value amongst the models could be attributed to the varying model structures used to convert rainfall into runoff. The values of RRM ranged between 0.048-0.085 and 0.069-0.133, for calibration and validation, respectively. Of the seven models, AWBM had the smallest value, while SMAR exhibited the largest values of RRM (Table 4.1). Based on R_e and I_a, the best performance of a model would be indicated by a value of 1. Nevertheless, highest R_e and I_a values of 0.595 and 0.798, respectively were obtained by AWBM. The lowest R_e and I_a values of 0.242 and 0.635, respectively were realised by SMAR. This further attests the unsatisfactory performance of SMAR. The values of R ranged between 0.712-0.917 and 0.552-0.901 for calibration and validation periods, respectively. This indicates that for all the models, the modelled dispersion to the observed was generally well predicted. The MAE values did not vary much amongst the models, except for SIMHYD and SMAR that slightly varied from other models. The values were within the ranges of 5.0-9.6 m^3s^{-1} and 6.6-14.2 m^3s^{-1} for the calibration and validation periods, respectively.

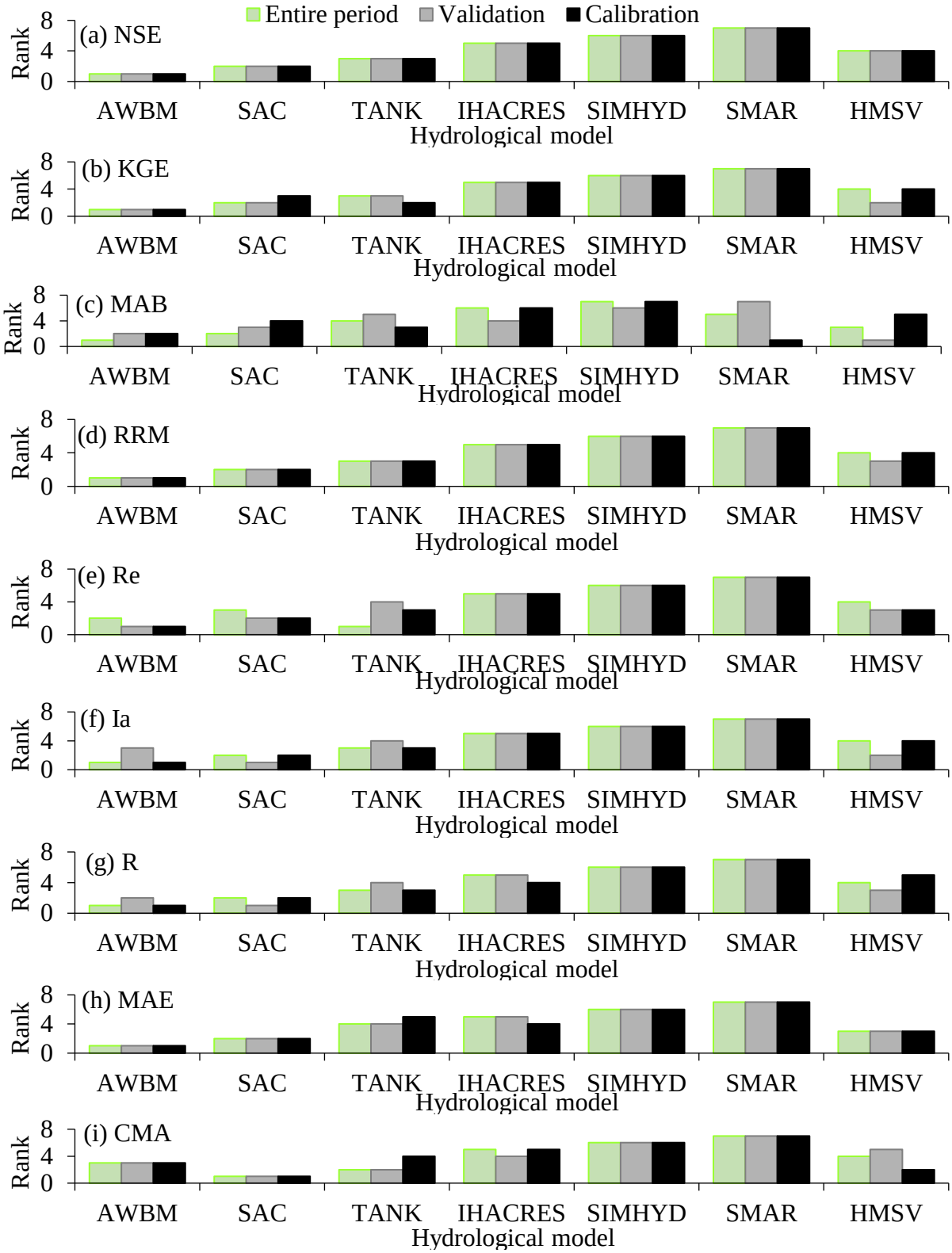

Figure 4.2 Model performance in terms of ranking. Ranks 1 and 7 denotes best and worst performing model, respectively. The same legend on (a) applies to (b-i).

By using the CMA, the best model performance would be shown by the value of 1. In this study, SAC had the highest value (0.791) followed by HMSV (0.725) for the calibration period (Table 4.1). Considering the validation period, SAC still had the highest value (0.807) followed by TANK (0.745). For both calibration and validation periods, SMAR had the smallest values of 0.466 and 0.293, respectively. Considering the KGE metric, AWBM performed best followed by SAC and TANK while SMAR performed last for all the periods. Generally, it can be concluded that the SMAR model performed worst, while AWBM performed finest based on the nine considered statistical indicators. However, in some studies e.g., Onyutha *et al*. (2021), SMAR generally performed better than SAC and TANK models. This could be attributed to the varying spatial resolution of catchments such as the size, climate, geology, landscape, and hydrological data (Onyutha, 2016d; Podger, 2004). In some cases, the lumped conceptual models have been found to perform better than physically-based models. For instance in the study by Jaiswal *et al.* (2020), for calibration, AWBM and TANK yield NSE values of 0.76 and 0.84, respectively, while SWAT had NSE of 0.75. However, in other areas, some rainfall-runoff models can exhibit unsatisfactory performances. For instance, in the study by Pérez-Sánchez *et al.* (2019), that compared six hydrological balance models (Témez, ABCD, GR2M, AWBM, GUO-5p, and Thornthwaite-Mather) in several basins within Spain, AWBM model did not perform well.

Table 4.1 Statistical performance evaluation of the models

S/N	Model	Calibration	Validation	Entire Period
	Nash-Sutcliffe Efficiency (NSE)			
1	AWBM	0.828	0.808	0.837
2	Sacramento (SAC)	0.808	0.795	0.822
3	TANK	0.799	0.791	0.816
4	IHACRES	0.741	0.700	0.749
5	SIMHYD	0.630	0.502	0.612
6	SMAR	0.458	0.281	0.436
7	HMSV	0.778	0.787	0.804
	Model Average Bias (MAB, %)			
1	AWBM	-3.121	4.910	0.186
2	Sacramento (SAC)	11.478	-4.935	4.721
3	TANK	3.555	9.625	6.053
4	IHACRES	-23.452	-6.020	-16.274
5	SIMHYD	-24.060	-10.563	-18.502
6	SMAR	-2.433	25.300	8.986
7	HMSV	12.010	-3.065	5.802
	Ratio of Root mean squared error to Maximum event (RRM)			
1	AWBM	0.048	0.069	0.053

S/N	Model	Calibration	Validation	Entire Period
2	Sacramento (SAC)	0.051	0.071	0.055
3	TANK	0.052	0.072	0.056
4	IHACRES	0.059	0.086	0.065
5	SIMHYD	0.070	0.111	0.081
6	SMAR	0.085	0.133	0.098
7	HMSV	0.055	0.072	0.058
	Relative efficiency (Re)			
1	AWBM	0.595	0.594	0.627
2	Sacramento (SAC)	0.569	0.580	0.608
3	TANK	0.547	0.567	0.692
4	IHACRES	0.477	0.460	0.510
5	SIMHYD	0.338	0.310	0.377
6	SMAR	0.242	0.130	0.250
7	HMSV	0.547	0.570	0.590
	Index of agreement (I_a)			
1	AWBM	0.798	0.782	0.809
2	Sacramento (SAC)	0.783	0.795	0.803
3	TANK	0.774	0.774	0.794
4	IHACRES	0.758	0.756	0.776
5	SIMHYD	0.706	0.679	0.714
6	SMAR	0.635	0.479	0.615
7	HMSV	0.765	0.783	0.791
	Coefficient of determination (R)			
1	AWBM	0.917	0.901	0.918
2	Sacramento (SAC)	0.901	0.902	0.909
3	TANK	0.896	0.892	0.903
4	IHACRES	0.895	0.881	0.895
5	SIMHYD	0.856	0.797	0.843
6	SMAR	0.712	0.552	0.685
7	HMSV	0.882	0.893	0.898
	Mean absolute error (MAE) (m^3s^{-1})			
1	AWBM	5.079	6.609	5.709
2	Sacramento (SAC)	5.411	6.842	6.000
3	TANK	5.688	7.040	6.245
4	IHACRES	6.571	8.764	7.474
5	SIMHYD	8.316	11.299	9.544
6	SMAR	9.510	14.160	11.425
7	HMSV	5.689	6.962	6.213
	Coefficient of model accuracy (CMA)			
1	AWBM	0.707	0.730	0.761
2	Sacramento (SAC)	0.791	0.807	0.839
3	TANK	0.705	0.745	0.834
4	IHACRES	0.560	0.726	0.688
5	SIMHYD	0.519	0.548	0.573
6	SMAR	0.466	0.293	0.554
7	HMSV	0.725	0.719	0.737
	Kling-Gupta efficiency (KGE)			

S/N	Model	Calibration	Validation	Entire Period
1	AWBM	0.888	0.890	0.900
2	Sacramento (SAC)	0.854	0.843	0.883
3	TANK	0.873	0.826	0.879
4	IHACRES	0.779	0.804	0.837
5	SIMHYD	0.756	0.745	0.772
6	SMAR	0.669	0.459	0.653
7	HMSV	0.821	0.847	0.841

Figure 4.3 shows the performance of models based on compiled values of ranking from all the nine "goodness-of-fit" measures constrained to the sub-catchment total water balance. This followed a procedure described in section 4.2.1.1. Production of Figure 4.3 considered the performance of models during calibration, validation and entire period (Table 4.1). It is noticeable from Figure 4.3 that AWBM performed best followed by SAC, while SMAR performance last. Performance of these models can vary based on the catchment of application. For instance, while TANK was among the best 3 models in this study, the study by Onyutha *et al*. (2021), that compared the performance of several lumped conceptual models in the simulation of daily River Kafu flows, TANK did not perform better. In the same study (Onyutha. *et al.*, 2021), SMAR generally performed well.

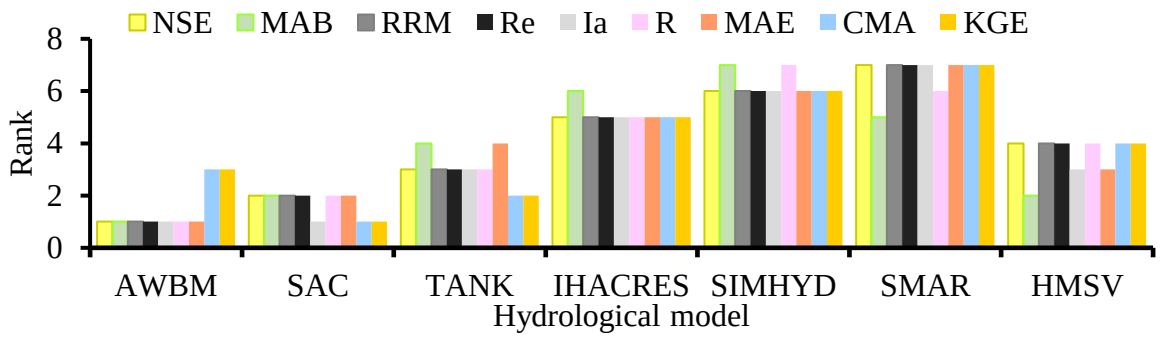

Figure 4.3 Assessment of model performance by ranks based on the combination on ranks from all the nine "goodness-of-fit" metrics considering the overall water balance. The best performing model is ranked 1 while the worst takes rank 7.

4.3.2 *Comparison of model performance in simulating annual maxima flow events*

Figures 4.4 the performance of models to simulate annual maxima flow events in each year. For a superlative model, all the observed and simulated scatter points would be plotted along the 45° line. All the hydrological models agreeably simulated high flows (Figure 4.4). AWBM model performed better in simulating annual maxima flow events (Figure 4.4a), followed by

SACRAMENTO (Figure 4.4b), while IHACRES performed last (Figure 4.4d). The annual maxima observed flow events beyond 100 ms^{-1} were slighted under-estimated by HMSV and TANK models (Figure 4.4c,g).

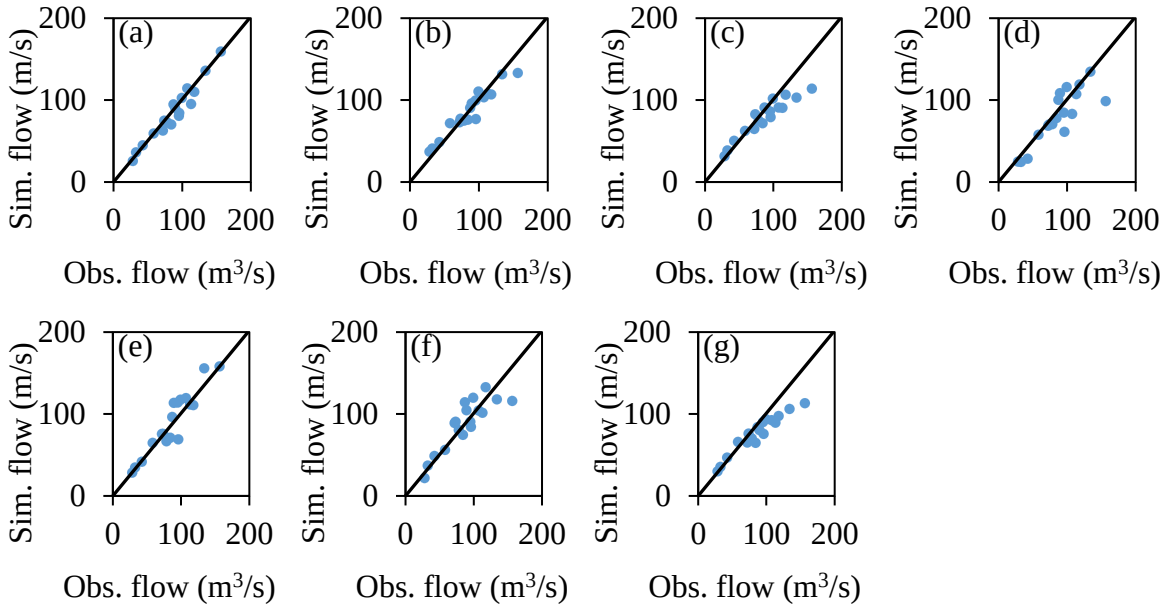

Figure 4.4 Model performance assessment based on comparison of observed and simulated annual maxima flows in each year for (a) AWBM, (b) SAC, (c) TANK, (d) IHACRES, (e) SIMHYD, (f) SMAR, (g) HMSV, Sim. stands for simulated, while Obs. means observed

The performance of hydrological models based on compiled values of ranking from all the nine "goodness-of-fit" measures considering the annual maxima flows in each year is shown in Figure 4.5. As for overall water balance, Figure 4.5 was obtained based on the procedure explained in section 4.2.1.1. Similar to the observations in Table 4.1 and Figures 4.1 to 4.3, AWBM model performed better than other models in simulating annual maxima series, except when based on the MAB statistical indicator (Figure 4.5). Similarly, SAC model performed second best. While Figure 4.3 shows that SIMHYD and SMAR performed last, these two models exhibited commendable performance in simulating annual maxima flows. Instead, IHACRES, TANK and HMSV portrayed the worst performances (Figure 4.5).

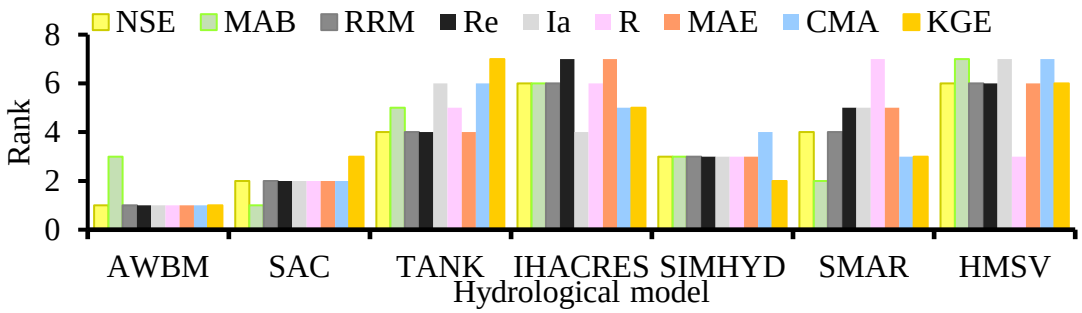

Figure 4.5 Assessment of model performance based on compiled values of ranking from all the nine "goodness-of-fit" metrics considering the annual maxima flows. The best performing model is ranked 1 while the worst takes rank 7

4.3.3 *Amplitude-Duration Frequency Analyses*

In this study, the extreme value distribution tail analysis at all aggregation levels showed a normal tail for the exponential quantile-quantile (Q-Q) plot for the high flow events. For instance, results of the calibrated exponential distribution obtained at 1-day aggregation level can be found in Figures 4.6. In the same figure, empirical and extrapolated quantiles are presented. In all cases, linearity behaviour in the quantiles was realised towards the tail of the distributions. While the exponential plot was adopted to obtain the linear behaviour of the quantiles, log-transformation was applied to the return period T on the x-axis. Towards the tail of the distribution, the mismatch between the empirical and modelled quantiles get systematically larger than those for small return periods. This tends to result from the influence of flooding on flow measurement stemming from the bias in rating curve extrapolation or the difference between the river discharge and the catchment rainfall-runoff discharge (Onyutha and Willems, 2013). Censoring out outliers prevents underestimation of flow which could result from assuming a light instead of normal tail. Assuming a light tail may result in underestimation of design quantiles for sizing water infrastructures such as bridges. In the Appendix C, exponential Q-Q plots obtained at different aggregation levels for high flows (5, 30 and 90 days) (C.1 to C.3) are provided. The frequency curve for SIMHYD and SMAR showed substantial deviations from the observed curve for the estimated flows especially at higher return periods, while AWBM, SAC, TANK, IHACRES and HMSV frequency curves did not display significant deviations (Figure 4.6).

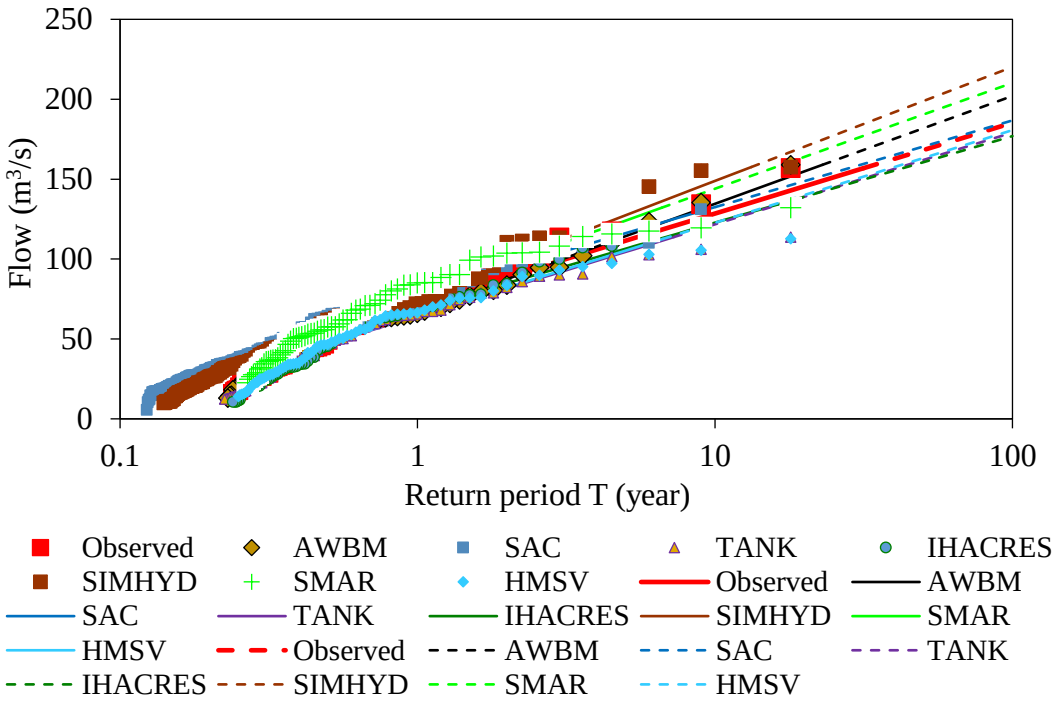

Figure 4.6 Comparison of exponential quantile-quantile plot for the high flow POT events considering 1-day aggregation level. The markers represent the empirical, solid lines signify theoretical (calibrated distribution), while dashed lines represent extrapolated quantiles

The return period for an average 1-day flood of 150 m^3s^{-1} is 24 years based on the observed flow curve (Figure 4.6), while the same event has a return period of 17 years for an evaluation based on AWBM model. However, when considering the HMSV model, the same event will have a return period of 30 years, while for the SIMHYD model, the return period is 10 years. The extrapolated quantiles for high flows can be relevant for vigilant flood analysis which can guide the planning and designing of risk-based water engineering structures such as bridges, slipways, etc.

The ADF relationships considering all the aggregation levels are shown in Figure 4.7. These were generated from the quantiles projected based on the EVD. It is shown that SMAR (Figure 4.7f) overestimated the high flow quantiles for the aggregation level of 1-day. However, for aggregation levels higher than 3-days, SMAR underestimated the high flow quantiles, except at 60- and 90-days.

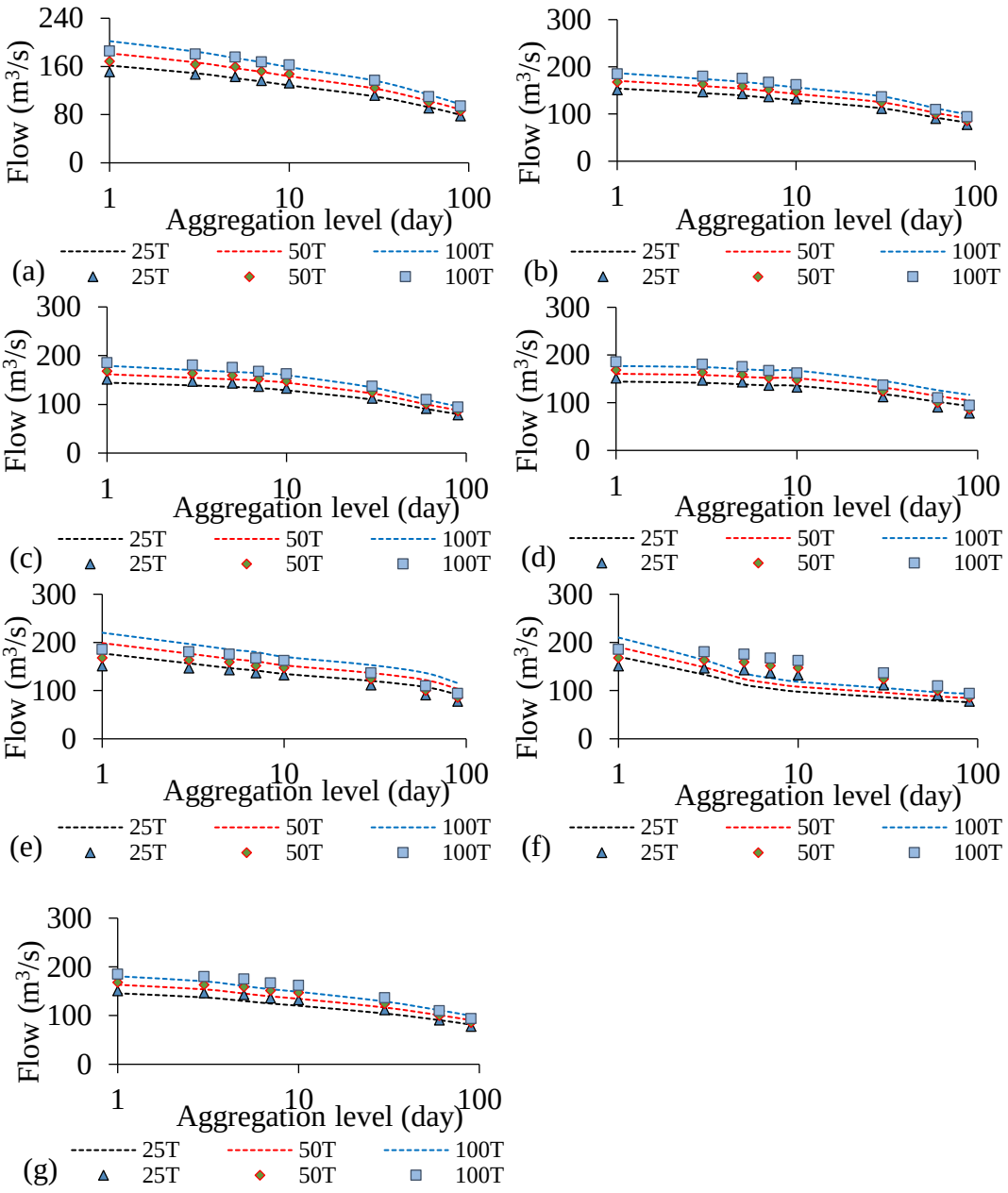

Figure 4.7 The FDF plots for high extreme observed and simulated flows obtained at different aggregation levels (1-90 days) for (a) AWBM, (b) SAC, (c) TANK, (d) IHACRES, (e) SIMHYD, (f) SMAR, (g) HMSV obtained at 25, 50 and 100 year return periods. In the legend, dashed lines denote simulated flow, while the markers signify observed flow

For all aggregation levels, SIMHYD (Figure 4.7e) overestimated the high flow quantiles particularly for the return periods of 25- and 100-years. For all aggregation levels, considering the AWBM, SAC, TANK, HMSV (Figure 4.7a-c,g), the observed and simulated high flow quantiles were generally in close agreement. The underestimation of high flow quantiles at higher

aggregation levels by SMAR could be attributed to the model inadequacy in capturing higher quantiles in the extreme value distribution tail. Similarly, the overestimation or underestimation of flow quantiles at 1-day aggregation level could be linked to the high noise in flow time series at low aggregation levels, resulting in uncertainties in calibration of the extreme value distribution.

The model biases in reproducing high flow quantiles at different aggregation levels are shown in Tables 4.2. From Table 4.2, SIMHYD exhibited positive biases at all aggregation level indicating an overestimation of high flow quantiles. Except for the 1-day aggregation level, SMAR showed an underestimation of high flow quantiles (Table 4.2).

Table 4.2 Model biases (%) in simulating high flow quantiles

Model	Aggregation Level [day]							
	1	3	5	7	10	30	60	90
AWBM	7.99	1.96	-1.26	-0.52	-2.44	-0.83	2.26	2.68
SAC	1.37	-2.52	-3.36	-2.35	-3.14	0.37	2.04	5.39
TANK	-3.79	-5.47	-5.02	-2.02	-2.03	-1.62	-0.38	2.10
IHACRES	-4.50	-3.29	-3.01	0.09	2.75	6.06	13.58	21.72
SIMHYD	18.11	8.00	4.25	5.83	3.41	9.79	21.26	20.35
SMAR	13.11	-9.27	-21.93	-23.96	-26.58	-22.74	-12.58	-1.31
HMSV	-2.98	-5.96	-8.80	-8.23	-8.72	-6.24	0.41	5.23

4.3.4 *Explanation of the differences in performance of the various models*

As earlier noted, all the seven rainfall-runoff models (AWBM, SAC, TANK, IHACRES, SIMHYD, SMAR and HMSV) reasonably simulated the high flows events. Li *et al.* (2015) also stressed that the structure of a model may influence its performance. However, in this study, the variability in model performance could not evidently be attributed to the differences in model structures. This is because various models performed either better under the consideration of total water balance and/or extreme hydrological conditions. Generally, four models (AWBM, SAC, TANK and HMSV) performed well regarding simulating flows in the sub-catchment. Considering the total water balance, AWBM had the highest NSE values of 0.828 and 0.808 for calibration and validation periods, respectively. In addition, AWBM had the lowest MAB value of 0.186% for the

entire period (1999-2016). Equally, AWBM performed better than other models in simulating the annual maxima flows.

Model performance in simulating flows could as well be associated with model parameters (Zhang *et al*., 2017). In this study, models' parameters exhibited varying sensitivity. AWBM was highly sensitive to higher values (close to 1.0) of base flow recession constant and also relatively sensitive to surface flow recession constant, storage capacity of third store, and fraction of catchment area for the first store. However, fraction of catchment area for the second store, and storage capacity of second store were almost insensitive parameters with minimal variation in the NSE values. The baseflow index, baseflow and surface runoff recession constant parameters in AWBM could justify the laudable performance of the model in reproducing the flows. Previous studies (Onyutha. *et al.*, 2021; Onyutha, 2016d; Yu and Zhu, 2015), revealed good performance of AWBM. However, in some cases, the AWBM may not yield better results. For instance, in the study by Pérez-Sánchez *et al.* (2019), that compared six hydrological models including the AWBM, revealed poor performance of the AWBM.

Similarly, the SACRAMENTO model with a set of seventeen parameters had the second-best performance in simulating flows during calibration and validation and mimicking of the annual maxima flows. Some of the SACRAMENTO parameters exhibited high sensitivity only at small values (e.g., additional fraction of pervious area, exponential percolation rate) while others had high sensitivity at higher values (e.g., fraction of base flow which is groundwater flow, lower zone free water primary maximum). Other parameters were almost insensitive (e.g., upper zone Free water maximum, fraction of water unavailable for transpiration).

The performance of SIMHYD model with nine parameters was not adequately better. The study by Li *et al*. (2015), that compared three hydrological models (HBV, SIMHYD and XAJ), revealed lower efficiency of the SIMHYD model. While SMAR model generally had well-identified parameters, three parameter (unit hydrograph linear routing, unit hydrograph linear routing component, infiltration rate) exhibited low sensitivity. This might have resulted in the lower performance of the model. In some studies (e.g., Bashar (2012)), SMAR model yielded sufficiently better results. The performance of a model may not be associated with the number of parameters it has (Jakeman and Hornberger, 1993). This is because, SACRAMENTO model that could be regarded as being over-parameterised with 17 parameters, performed better than other models with relatively fewer parameters e.g. SIMHYD (9 parameters), IHACRES (11 parameters), SMAR (9

parameters) and HMSV (10 parameters). Besides, AWBM with the smallest number of parameters (eight), performed better than other models. Although the calibration of HMSV was based on the "step-wise" (sub-flow variation) strategy (separate calibration of baseflow, interflow and overland flows), the model did not perform very well in simulating annual maxima. However, the credible ranking of HMSV in reproducing annual maxima flow could be linked to the overland and interflow parameters in the model.

Interestingly, the performance of a model may as well be attributed to the selected "goodness-of-fit" measures (Onyutha, 2020b, 2016d). For instance, for annual maxima flows, AWBM performed far better than other models. However, when based on the MAB, SAC and SMAR models performed better than AWBM. Besides, under the consideration of total water balance, using the CMA and KGE statistical indicators, SAC and TANK model performed better than AWBM, despite AWBM displaying overall superlative performance. Hence, to strongly conclude on the efficacy of a particular rainfall-runoff model, it is vital to assess its performance using various "goodness-of-fit" statistics as implemented in this study.

4.4 Implication of the findings

4.4.1 *Research questions addressed in this chapter*

Which conceptual model best simulates observed extreme peak flows in the RM S-C? Can a hydrological model perform satisfactorily under the condition of data scarcity?

4.4.2 *Implication of the study findings*

Overall, AWBM performed better than other models in simulated the extreme high flows with an NSE of 0.837. This implied that outputs of the AWBM can assertively be inputs for hydrodynamic modelling. Besides, the model outputs can as well be used for scenario analyses. However, choice of a model for any analysis should be done with careful consideration. This sis attributed to the uncertainties exhibited by different models. Satellite data set performed well for the study area. This was after validation and bias correction. Therefore, reanalyses or satellite datasets can perform well especially in poorly weather instrumented areas. However, the use of prior to its use, satellite data should be evaluated on a case-to-case basis. Differences in model structure can influence how satisfactory they can reproduce observations as it was indicated by under & over-estimation by different models.

Chapter Five

5. Hydrodynamic modelling of River Malaba floods and assessment of their socio-economic impacts

This chapter is based on the published paper:

Mubialiwo, A., Abebe, A., Kawo, N.S., Ekolu, J., Nadarajah, S., Onyutha, C., 2022. Hydrodynamic modelling of floods and estimating socio-economic impacts of floods in Ugandan River Malaba sub-catchment. *Earth Systems and Environment* 6, 45–67. https://doi.org/10.1007/s41748-021-00283-w

5.1 Introduction

In River Malaba sub-catchment and the neighbouring areas, rainfall exhibits an increasing trend and multi-decadal variability (Mubialiwo *et al.*, 2020; Onyutha *et al*., 2020). The positive trends in rainfall have resulted in more recurrent floods over the recent periods (e.g., 2010-2019) than from 1960 to 2009 (Onyutha *et al*., 2020). Flooding events result in considerable socio-economic impacts including damage of crops, destruction of infrastructures including roads, bridges, schools, and loss of livestock and human lives. The possibility of experiencing more floods of varying magnitudes in future in the study area presents worrying situation for water resources management. To effectively manage the associated impacts of flooding, there is need for predictive planning and operation of climate change adaptation measures (Xu *et al*., 2017). Such planning can be supported by provision of comprehensive information or maps of flood inundation and extents of infrastructure and property that can be affected by flooding as well as vulnerability of the local population. In addition, to reduce the effects of natural disasters, there is need to evaluate their socio-economic impacts and to consider management strategies (structural and non-structural).

Flood inundation mapping can be achieved by mimicking the physics of floodwaters in the river systems through hydrodynamic modelling using a number of numerical tools. Numerical (hydrodynamic) models can be categorised as one-dimensional (1D), two-dimensional (2D) or three-dimensional (3D) (Teng *et al.*, 2017). 1D models consider one directional flow along the centreline of the river channel and are suitable when detailed analysis is not essential (Alkema, 2007). 2D models make it possible to evaluate the landscape effect on the magnitude of flooding especially in near-flat topography (Alkema, 2007), such as the present study area. 3D models are

rarely used, since 2D shallow water approximations are considered adequate especially in areas with limited high resolution data, such as the current study area (Teng *et al*., 2017). 2D models have exhibited commendable performance. For instance, the study by Dhungel *et al.* (2019) revealed superior performance of 2D model in simulating flow depth and velocity in the lower Provo river, USA. Ghimire (2019) established that with fine resolution survey data and availability of local data, 2D models can present sound performance.

There are various 2D hydrodynamic models, such as the Hydraulic Engineering Center's River Analysis System (2D HEC-RAS) (Brunner, 2016), SOBEK Suite DELFT3D (Deltares systems, 2019), MIKE 21 (DHI, 2017), TUFLOW HPC (Heavily Parallelised Compute) (BMT-WBM, 2018). Whereas most hydrodynamic models are commercial, 2D HEC-RAS is freely available for use. HEC-RAS is a popular modelling program that computes water surface profiles in natural rivers and other channels applicable in floodplain management. Recently, 2D HEC-RAS model has attracted extensive applications in flood risk assessment. For instance, Pinos and Timbe (2019) compared the performance of four two-dimensional hydraulic models 2D HEC-RAS included, in regard to estimation of flood inundation maps. The study revealed reliable performance of 2D HEC-RAS (Pinos and Timbe, 2019). Ongdas *et al*. (2020) presented commendable performance of 2D HEC-RAS when applied for flood hazard maps generation for Yesil (Ishim) river in Kazakhstan. Other studies that applied 2D HEC-RAS include (Garcia *et al*., 2020; Kumar *et al*., 2019; Rangari *et al*., 2019).

2D models have been identified to provide suitable information to policymakers as they can clearly indicate which areas are to be inundated faster to make proper evacuation and/or resettlement plans (Alkema, 2007). To the best of the authors' knowledge, by the time of conducting this study, there were no previous studies that performed hydrodynamic modelling of floods in the study area which could contribute to establishment of sustainable risk-based water resources management strategies. Therefore, this study applied the 2D HEC-RAS hydrodynamic model for the purpose of identifying the inundation extents across the study area during flooding events of varying return periods. The study further assessed the socio-economic impact of floods on the society.

5.2 Methodology

5.2.1 *Trend analyses in rainfall runoff discharge and extraction of flow quantiles*

Presence of either monotonic trends in rainfall runoff discharge were assessed. The approaches already described in section 3.2.2 were used to analyse trend.

An important step in the hydrodynamic modelling is the selection of return periods for hydrographs to drive the model. For designs of various hydraulic structures such as those along sewer and river systems including bridges, and culverts, return periods between 5- and 100-years tend to be practically used (Onyutha and Willems, 2015b). The use of return periods around 100-years can be used for floodplain development, and medium-sized flood protection works (Onyutha and Willems, 2015b). Eventually, from the fitted extreme value distribution (EVD) as per the study (Mubialiwo *et al*., 2021a) and as already described in Chapter 4, sections 4.2.2 and 4.3.3, the extreme flow quantiles (return levels) at six different return periods (2-, 5-, 10-, 25-, 50-, and 100-years) were extracted. Apart from using the extreme flow quantiles (Q), the lower (LQ) and upper (UQ) quantiles corresponding to the 95% confidence interval limits were computed to determine uncertainties in the flooding extents (Ialongo, 2019). Synthetic hydrographs were developed for each return period and used as model input boundary conditions at the upstream of reaches (Bedient and Huber, 2002; Sule and Alabi, 2013).

5.2.2 *Description of the used model*

As stated before, the Hydrologic Engineering Center's River Analysis System (HEC-RAS) was applied. The model can simulate both steady and unsteady flow components. The steady flow element has the competence of modelling the subcritical, supercritical as well as mixed flow regime, water surface profiles. On the other hand, the unsteady flow component of HEC-RAS is capable of modelling independent 1D or 2D unsteady flow or combined 1D and 2D unsteady flows (Brunner, 2016). Herein, 2D HEC-RAS model 5.0.7 was used to simulate floods. The study involved computation of flood depth, and assessment of inundation extent on population, crops and infrastructure. The model simulated floods according to the following expressions (Brunner, 2016):

$$\frac{\partial H}{\partial t}+\frac{\partial p}{\partial x}+\frac{\partial q}{\partial y}=r \tag{5.1}$$

$$\frac{\partial p}{\partial t}+\frac{\partial}{\partial x}\left(p^2h^{-1}\right)+\frac{\partial}{\partial y}\left(pqh^{-1}\right)=-n^2kgh^{-2}\left(p^2+q^2\right)^{0.5}-gh\frac{\partial H}{\partial x}+pk+\frac{\partial}{\rho\partial x}\left(h\lambda_{xx}\right)+\frac{\partial}{\rho\partial y}\left(h\lambda_{xy}\right) \quad (5.2)$$

$$\frac{\partial p}{\partial t}+\frac{\partial}{\partial x}\left(pqh^{-1}\right)+\frac{\partial}{\partial y}\left(q^2h^{-1}\right)=-n^2qg\left(p^2+q^2\right)^{0.5}h^{-2}-gh\frac{\partial H}{\partial y}+qk+\frac{\partial}{\rho\partial x}\left(h\lambda_{xy}\right)+\frac{\partial}{\rho\partial y}\left(h\lambda_{yy}\right) \quad (5.3)$$

where h is the water depth (m), p and q denote the specific flow in the directions of x and y measured in m^2s^{-1}. r is the net rainfall in m. H is the surface elevation in *m*, while g stands for acceleration due to gravity measured in ms^{-2}. n is the manning's coefficient $\left(sm^{-1/3}\right)$, ρ is the density in kgm^{-3}. λ_{xx}, λ_{xy}, λ_{yy} represent the effective shear stress components while k is the Coriolis measured in s^{-1}. For the case when the analysis considered diffusive wave equation, then the inertial components in equations (5.2) and (5.3) is left out.

HEC-RAS has the capability to analyse either a fully 2D Saint Venant equation or the 2D diffusive wave equation following an implicit finite-volume approach (Brunner, 2016). Both 2D diffusive wave and Saint Venant equations can exhibit close performance (Dhungel *et al*., 2019; Ongdas *et al*., 2020; Shustikova *et al*., 2019). However, in this study, the 2D diffusive wave equation was adopted, because it supports longer time steps, is faster, and produces stable and accurate solutions than the Saint Venant equations (Ongdas *et al*., 2020; Sarchani *et al.*, 2020).

5.2.3 *Uncertainty analysis and calibration of Manning's roughness coefficients*

The possible uncertainties induced in the flow/flood simulation by changes in land use from 2010 to 2017 were assessed. This was done by evaluating the difference between the three LULC maps with respect to Manning's roughness coefficients. First, calibration was performed on the six major land use types (Figure 2.6) by applying the Manning override regions function in HEC-RAS (Brunner, 2016). Subsequently, the calibrated parameters were then used to simulate the floods in HEC-RAS. Because of the small sample size n of 6, the Student's $t-$distribution was adopted (Brereton, 2015). Statistical significance was set at $p<0.05$. The analysis considered three combinations of 2010 and 2015, 2010 and 2017, and 2015 and 2017. The test statistics t is computed as follows:

$$t = \frac{\bar{x}_1 - \bar{x}_2}{s_p \sqrt{\frac{1}{n_1} + \frac{1}{n_2}}} \tag{5.4}$$

with

$$s_p = \sqrt{\frac{(n_1 - 1)s_1^{\,2} + (n_2 - 1)s_2^{\,2}}{n_1 + n_2 - 2}} \tag{5.5}$$

where s_p is an estimator of the collective standard deviation of the two samples, s_1 and s_2 denotes the standard deviation, $\bar{x}_1$ and $\bar{x}_2$ are the mean values, n_1 and n_2 are the sample size of the manning's roughness coefficients from say 2010 and 2015, respectively. The p value can be computed using Ms Excel function TDIST (value, df ,tail). Considering the period of flow data (1999-2016), the 2015 LULC map (Figure 2.6b) was adopted in defining the manning's coefficient in the HEC-RAS model.

5.2.4 *Hydrodynamic modelling of floods*

Modelling was done using the inputs as DEM, 2015 land cover map (for manning's coefficients), and synthetic hydrographs for different return periods (see sections 2.2.1.3 and 2.2.2 for details). The 2D flow area covered the low-lying region which is prone to flooding (Figure 5.1). Two different boundary conditions (hydrograph and normal depth) were defined. Composite hydrograph boundary conditions were defined upstream of every reach representing the runoff discharges. The normal depth boundary conditions were defined at the downstream of the river and at the edges of the model where the runoff is presumed to flow. 2D HEC-RAS calculated the outflow, flood depth, water surface elevation, and velocity for each grid as the flood-water propagated throughout the domain to the normal boundary conditions.

The 2D computational mesh was set up with a cell size of 12.5 x 12.5 m. This selection of grid was to ensure minimal or no deviation from the DEM resolution (12.5 × 12.5 m). Selection of particular time steps in HEC-RAS may influence the results. Small time steps can result in very long computation times, while too large time steps may as well cause numerical diffusion hence model instability (Brunner, 2016). In this study, stability of the model was ensured by estimating the time step based on the Courant-Friedrichs-Lewy approach as follows (Brunner, 2016)

$$C = \frac{w_s \Delta t}{\Delta x} = \leq 1 \tag{5.6}$$

where C stands for the Courant number (dimensionless), V is the flood wave velocity (ms^{-1}), Δt is the computational time step (s), Δx denotes the grid size (12.5 m).

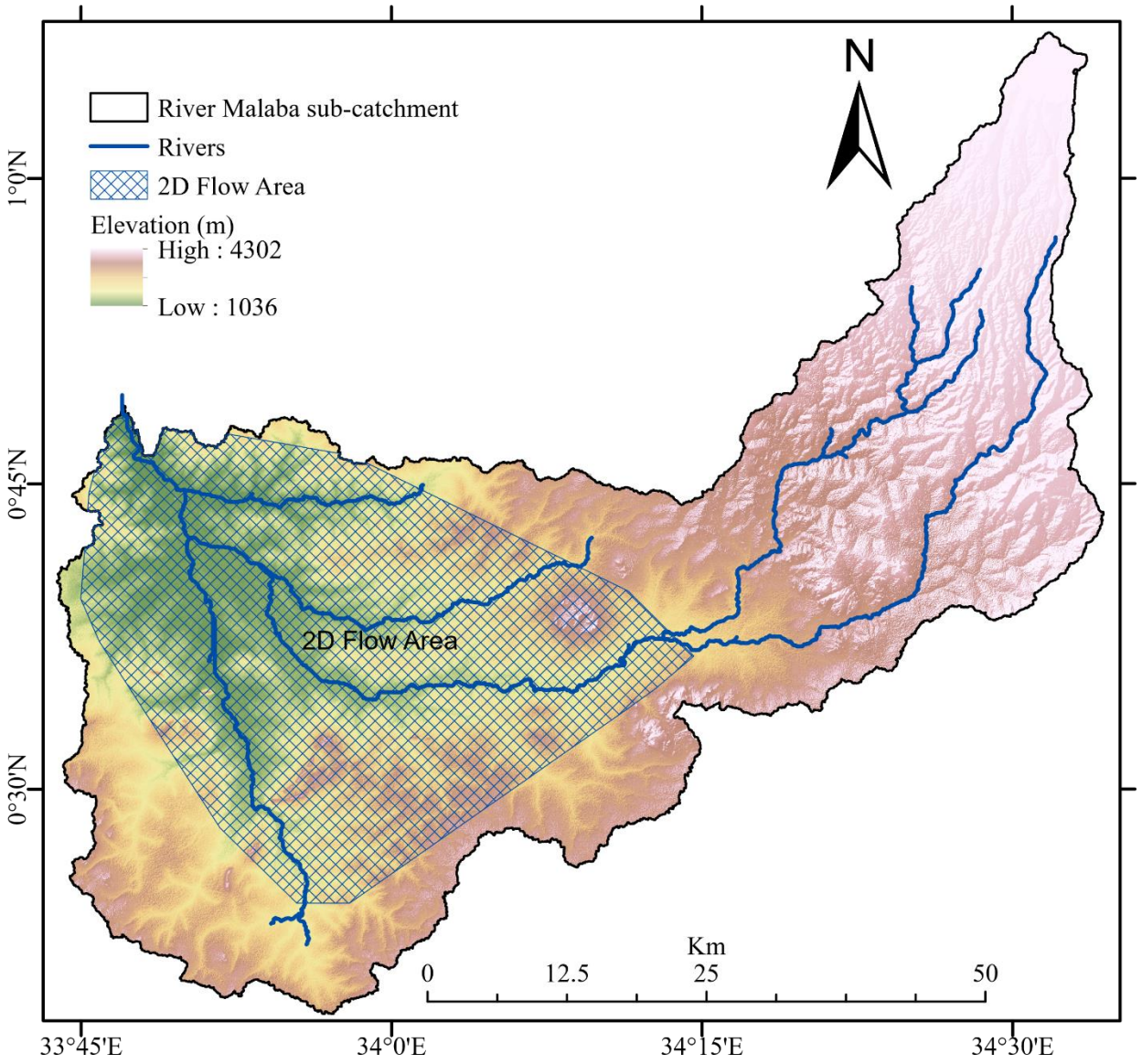

Figure 5.1 2D HEC-RAS flow area

Evaluation of model results is an essential component to measure performance. Evaluation of the 2D HEC-RAS model necessitated historical record of flood events. This could be in form of delineated extent from observations or remote sensing images. Unfortunately, it is worth noting that there are no official historical records of observed flood events extents for the current study

area despite the recurrent disasters. Even the available satellite images do not clearly capture the entire study area. Nevertheless, the flood image for the 20 October 2007 flood by Red cross was used (accessed: 11 July, 2021). This event affected almost the entire Uganda (Reliefweb, 2007). Prior to its use in evaluation of the model, the flood image (map) was corrected with guidance of the information obtained from community as per section 2.2.2.1. The image was also compared with another one of 06 May 2020 (Reliefweb, 2020) (accessed: 11 July 2021). Model performance was assessed based on several metrics including False Alarm Ratio (FAR), Hit Rate (HR), Critical Success Index (CSI) and Bias Error (B_e) as shown in Eqns. (5.7) to (5.10) (Sampson et al., 2015). These performance criteria have been applied in recent studies (Costabile *et al.*, 2020; Ongdas *et al.*, 2020; Sampson *et al*., 2015). Consider A_{sim} , A_{obs} as the simulated and observed flooded areas, respectively. Assume A_{cor} , A_{over} , A_{under} denote the correctly-, over- and under-predicted flood areas, respectively, all measured in km^2.

$$FAR = \frac{\left(A_{sim}/A_{obs}\right)}{\left(A_{cor} + \frac{A_{sim}}{A_{obs}}\right)} \tag{5.7}$$

$$HR = \frac{\left(A_{cor}\right)}{A_{obs}} \tag{5.8}$$

$$CSI = \frac{\left(A_{cor}\right)}{\left(A_{cor} + A_{over} + A_{under}\right)} \tag{5.9}$$

$$B_e = \frac{\left(A_{sim}/A_{obs}\right)}{\left(A_{obs}/A_{sim}\right)} \tag{5.10}$$

FAR is a measure of model overprediction and it varies between 0 and 1. A value of 1 implies "all false alarm", while 0 denotes "no false alarm". HR shows how well a model mimic the benchmark inundation without necessarily chastising for overprediction. HR ranges between 0 and 1, with 1 indicating that all wet areas in the benchmark inundation map are as well wet in the simulated output. CSI gives the combined effect of FAR and HR catering for both overprediction and underprediction. A value of 1 means perfect match between simulated and benchmark, while 0

indicates no match between the two. Lastly, B_e has two ranges (0 to 1 and 1 to ∞). The range of 0 to 1 indicates underprediction of the model and 1 to ∞ shows propensity of a model to overpredict (Sampson *et al*., 2015).

5.2.5 *Flood damage estimation*

Determination of economic losses due to flooding necessitated the flood depth and flood depth-damage functions for each infrastructure. The flood depths for individual infrastructure (churches, mosques, academic institutions and health facilities) spatially distributed within the inundated area were obtained from the generated flood depth map for each return period. We estimated the flood economic damage values for the extreme flow (Q) conditions. There are no site-specific damage functions for River Malaba sub-catchment, neither for the neighbouring areas. Therefore, depth-damage functions from other areas of similar topographical representation were applied to estimate the economic damage value for each of the selected infrastructure. The depth-damage function were adopted from (Chen, 2007; Pinos *et al.*, 2020; Scorzini and Frank, 2017). These were applied in conjunction with the flood damage functions and damage values provided by Huizinga *et al.* (2017) at national level. The depth-functions for a particular infrastructure at each depth location (e.g. church 1, church 2) were obtained by interpolating from the known depth-functions. The applied depth-damage functions for each infrastructure at different return period can be found in Table 5.1. Finally, the composite economic losses for each type of infrastructure were obtained as a summation of individual losses for the respective return periods. It is worth noting that these were mainly estimates and not necessarily the true ground economic loss values. Several studies (Amadio *et al*., 2019; Martínez-Gomariz *et al*., 2020; McGrath *et al*., 2019; Molinari *et al*., 2020; Romali and Yusop, 2021; Scorzini and Frank, 2017; Zarekarizi *et al.*, 2020) have embraced the use of flood depth-damage functions in different areas across the word.

Table 5.1 Depth-damage function for each infrastructure at different return periods obtained for each location

Infrastructure	Return Period (year)	Depth-functions																			
		1	2	3	4	5	6	7	8	9	10	11	12	13	14	15	16	17	18	19	20
Churches	2	0.44	0.39	0.76	0.49	0.23	0.16	0.26	0.32	0.30	0.29	0.33	0.37	0.60	0.45	0.63	0.68	0.26	0.40	0.24	
	10	0.44	0.45	0.77	0.52	0.30	0.23	0.28	0.38	0.40	0.35	0.36	0.45	0.65	0.64	0.69	0.69	0.26	0.48	0.35	
	50	0.50	0.47	0.80	0.54	0.34	0.51	0.31	0.39	0.44	0.37	0.38	0.54	0.67	0.65	0.70	0.77	0.74	0.70	0.75	0.19
	100	0.59	0.54	0.85	0.60	0.41	0.60	0.32	0.46	0.53	0.45	0.43	0.65	0.75	0.75	0.79	0.78	0.84	0.78	0.84	0.23
Academic institutions	2	0.36	0.57	0.24	0.26	0.25	0.59	0.36	0.24	0.27	0.54	0.54	0.13	0.27	0.37						
	10	0.56	0.63	0.35	0.32	0.31	0.59	0.47	0.54	0.42	0.59	0.56	0.53	0.39	0.55	0.15					
	50	0.65	0.64	0.38	0.33	0.35	0.65	0.49	0.55	0.50	0.76	0.56	0.58	0.44	0.66	0.26					
	100	0.71	0.72	0.45	0.40	0.37	0.68	0.58	0.62	0.63	0.84	0.64	0.61	0.53	0.75	0.31					
Mosques	2	0.13	0.17	0.26	0.31	0.55	0.66	0.60	0.63	0.68	0.48	0.25	0.35								
	10	0.21	0.23	0.39	0.36	0.59	0.68	0.66	0.69	0.74	0.58	0.30	0.44								
	50	0.27	0.28	0.67	0.40	0.59	0.73	0.69	0.72	0.78	0.83	0.34	0.47								
	100	0.29	0.31	0.72	0.43	0.63	0.79	0.74	0.77	0.83	0.86	0.37	0.51								
Health facilities	2	0.70	0.14	0.53	0.25	0.30	0.33	0.72	0.40	0.10	0.07	0.49	0.40								
	10	0.75	0.27	0.65	0.34	0.30	0.39	0.75	0.42	0.16	0.14	0.51	0.62								
	50	0.78	0.32	0.66	0.35	0.31	0.40	0.79	0.43	0.35	0.15	0.55	0.70								
	100	0.84	0.38	0.75	0.41	0.35	0.47	0.84	0.52	0.42	0.19	0.57	0.71								

5.3 Results and Discussion

5.3.1 *Trend analyses in annual maxima rainfall runoff discharge and extracted flow quantiles*

Rainfall runoff discharge exhibited significant positive trends considering the annual maxima series. The increasing rainfall runoff discharge had H_o (no trend) rejected ($Z>1.96$, $p<0.05$) (Table 5.2). This could be attributed to the increasing precipitation intensity. Significant positive sub-trends occurred from around 2007.

Table 5.2 Trend in simulated annual maxima rainfall runoff discharge

Trend magnitude/slope, *m* (m^3 $year^{-1}$)	Trend direction, Z
2.84	5.38

The extracted extreme flow (Q), lower flow (LQ) and upper flow (UQ) quantiles are presented in Table 5.3.

Table 5.3 Simulated extreme discharges (m^3s^{-1}) at varying return periods and corresponding upper and lower quantiles at 95% confidence interval limits of extreme values

Return period (year)	2	5	10	25	50	100
LQ (m^3s^{-1})	47.14	83.00	104.99	128.25	139.69	143.76
Q (m^3s^{-1})	95.64	122.34	142.55	169.25	189.45	209.65
UQ (m^3s^{-1})	144.14	161.69	180.10	210.25	239.21	275.54

5.3.2 *Uncertainty analysis and calibration of Manning's roughness coefficients*

The land use types and their calibrated manning's roughness coefficients are shown in Table 5.4. Calibration was intended to improve the HEC-RAS model performance. The computed *p*-values of 0.061, 0.064 and 0.379 for the combinations of 2010 and 2015, 2010 and 2017, and 2015 and 2017, respectively were greater than α (0.05) implying that H_o was not rejected. This implies that changes in LULC from 2010 to 2017 was insignificant. Therefore, the river flow variation and or damage from floods within River Malaba sub-catchment could be attributed to other factors beyond LULC changes such as climate variability. Previous study by Onyutha *et al*. (2021d) revealed that changes in LULC contributed only 8% to the River Mpanga flow variation. This contribution was smaller compared to other factors, such as climate variability (70%) (Onyutha *et*

al., 2021d). Furthermore, uncertainties in flood inundation simulations may result from the adopted manning's roughens coefficient values. In most cases, uniform instead of spatially varying values of roughness coefficient are assumed which could be a source of uncertainties (Huang and Qin, 2014). However, characteristic of flooding (extent and depth) may possess a low sensitivity to changes in manning's roughness coefficient (Höffken *et al.*, 2020).

Table 5.4 Calibrated Manning's roughness coefficients for each land use type

Land use type		Cropland	Bareland	Forestland	Water	Grassland	Built-up areas
Calibrated Manning's roughness coefficient	2010	0.039	0.035	0.170	0.370	0.035	0.070
	2015	0.041	0.034	0.150	0.350	0.040	0.060
	2017	0.045	0.031	0.155	0.310	0.038	0.063

5.3.3 *Model performance in mimicking the historical flood event*

The performance of the HEC-RAS model in capturing the historical flood image are presented in Table 5.5. The value of *CSI* indicates that the simulated flooded areas generally concur with the observed data. The value of *HR* above 0.5 and close to 1 further confirms an acceptable fit of wet areas in both simulated and observed dataset. However, values of B_e above 1 indicate an overestimation of the model.

Table 5.5 Model performance in flood simulation

Performance metrics			
False Alarm Ratio, *FAR*	Hit Rate, *HR*	Critical Success Index, *CSI*	Bias Error, B_e
0.65	0.71	0.62	1.6

5.3.4 *Spatial inundation extent analyses*

Vulnerability analyses were done to identify the extent of flooding on settlement, land cover, roads and other infrastructures. Figure 5.2 shows the inundation extent of settlements considering the LQ, Q and UQ for varying return periods. An enlarged illustration of inundation extent considering the extreme flows (Q) at 2-year and 100-year return period can be found in Figure D.1 of Appendix D. Flooding was highly noticeable in the low-lying areas. The spatial comparison established that inundation extent of settlements in the study area varies significantly. Settlement clusters are much concentrated in the lowest part of the flood-prone area. This could be attributed to the societal

stalemates such as less onerous way of setting up buildings with always profitable investments. This statement conforms with the findings by Kiyengo *et al*. (2019). The study focused on establishing the spatio-temporal distribution of flash floods and evaluate why people preferred settling in flood-prone area in Lubiji micro-catchment, a Kampala suburb (Kiyengo *et al.*, 2019). The escalating settlements in flood-prone areas by low-income communities worsens their vulnerability and habits. The poor land use management further contributes to increasing floods in such areas (Ramiaramanana and Teller, 2021).

It is noticeable that the difference between results of 50- and 100-year return periods in terms of the spatial coverage of flooded area was small even though it was expected to be large. This can be explained in three ways. First, the difference between quantiles of two return periods depends on the scale parameter (or the slope of the weighted linear regression line in quantile-quantile plot) especially for normal tailed EVD (Beirlant *et al*., 1996; Onyutha and Willems, 2015b; Willems *et al*., 2007). A large-scale parameter indicates high extreme flow variations (Onyutha and Willems, 2015b). The second explanation of the small difference between 50- and 100-year quantiles is due to the uncertainty in the statistical estimation of quantiles. In extreme value analysis, uncertainty in estimated flow quantiles increases as the considered return period goes higher than the length of the observed data series (Onyutha and Willems, 2013). In this line, extrapolation of quantiles is recommended to be limited for return periods not exceeding two or three times the length of the observed data (Kangieser and Blackadar, 1994). If, say, a series longer than 50-years was used, the 100-years return level could have probably been larger than the one used in this study. Third, the topography/bathymetry which can influence LULC of the study area cannot change very much in these few years, unless the region as suffered a natural disaster. This is justified by the insignificant LULC changes from 2000 to 2014 over two catchments within Uganda (Onyutha *et al.*, 2021d, 2021c). Thus, although the 100-year return period was considered for relevance,

corresponding results should be cautiously interpreted given the uncertainty involved in the estimation of the extreme quantiles.

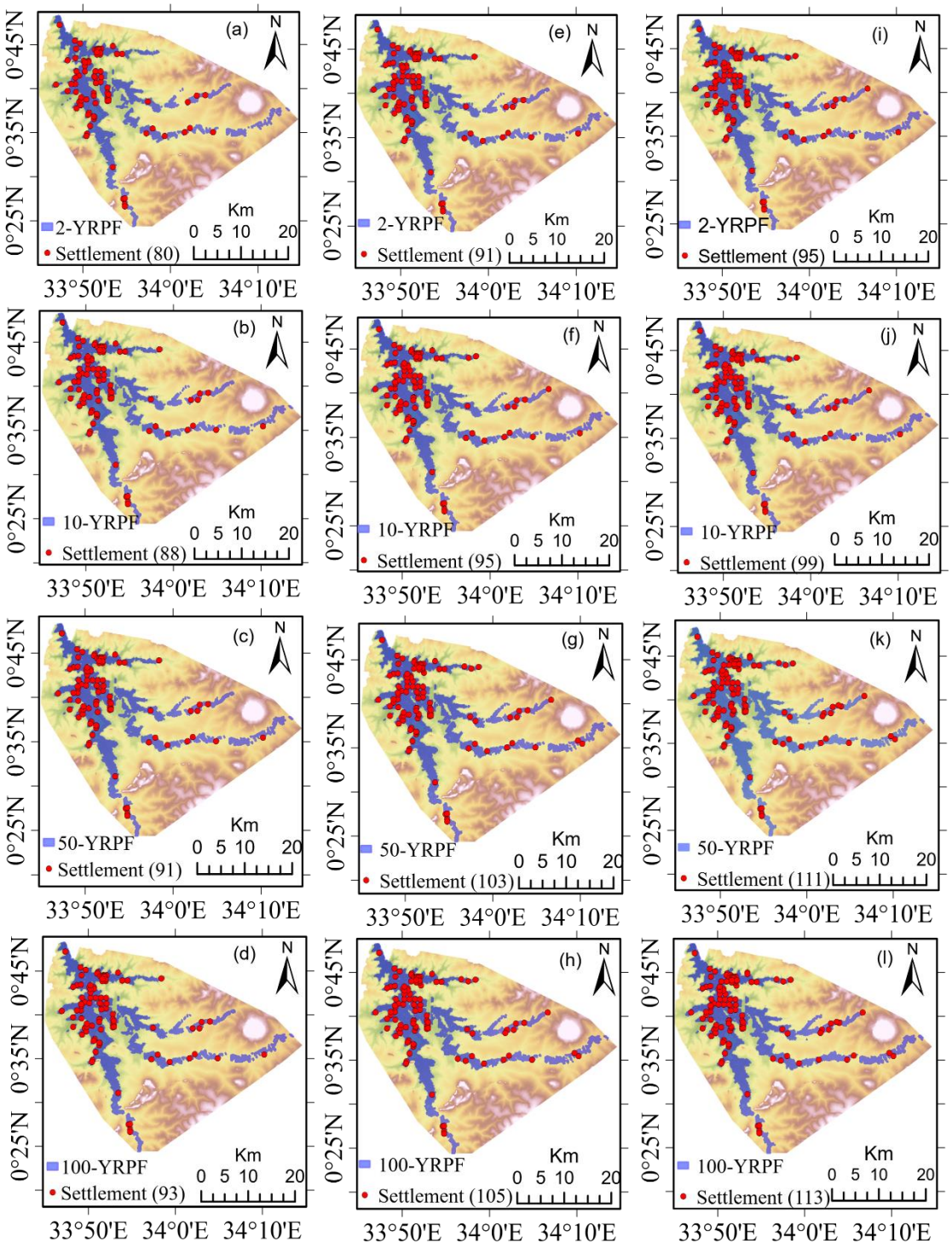

Figure 5.2 Inundation extent of human settlement based on (a-d) LQ, (e-h) Q and (i-l) HQ, at (a,e,i) 2-YRP, (b,f,j) 10-YRP, (c,g,k) 50-YRP and (d,h,l) 100-YRP. "YRPF" denotes "year return period flood". The number of settlements in the brackets represent number of settlement clusters with each cluster having an average 10 households (Mubialiwo et al., 2021b)

Field activities revealed that on average, a settlement cluster had 10 households, with an average household size of 9.7 people in the study area (Mubialiwo *et al*., 2021b). These values were adopted in estimating the population exposed to floods (Figure 5.3). It should be noted that this number excludes those affected by landslides in the highland areas of Bududa and Manafwa districts. At 2-years return period, at least 7,760 people are exposed to floods considering the lower limit of extreme flow at 95% confidence interval. The exposed population would increase by 12% and 16% for extreme and upper limit of extreme flow at 95% confidence interval, respectively considering the 2-year return period (Figure 5.3). To avert future loss of lives, authorities could make arrangement for relocation of population from risky to safer places.

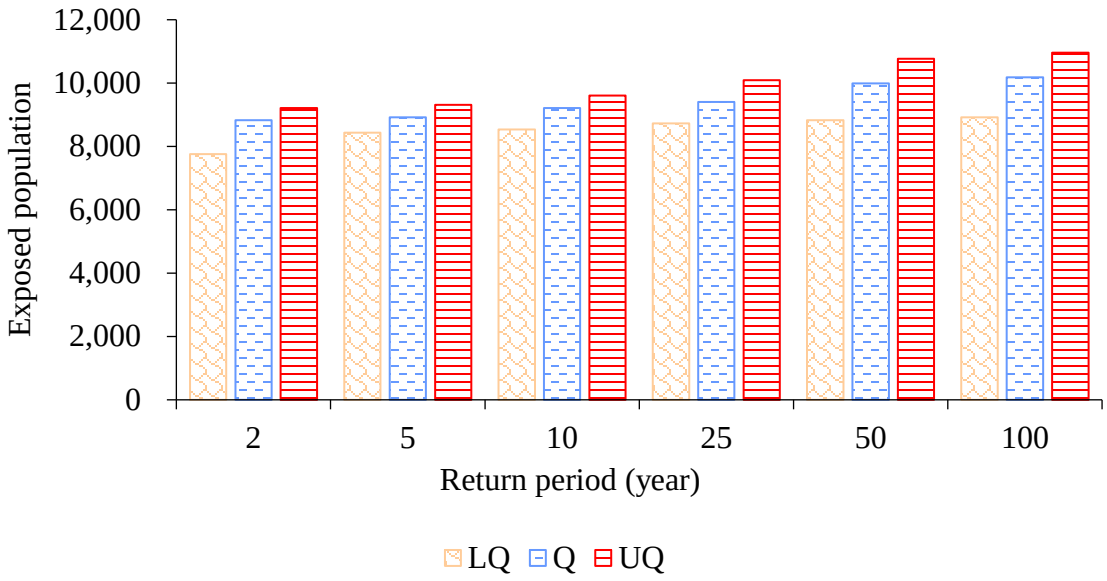

Figure 5.3 Estimated populations exposed to floods computed for 2- to 100-year return periods. LQ, Q and UQ are defined in section 2.2.1.3.

There was an increase of about 13.0%, 13.3% and 15.9% for LQ, Q and UQ, respectively, of the exposed population from 2- to 100-year return period (Figure 5.3). The government through ministry of relief, disaster preparedness and refugees has always resettled people from high risk areas in the gazetted refuge settlements (Reliefweb, 2019). However, the population relocated to safe places usually returns to flood-prone areas. The key underlying reasons could include (1) population pressure in refugee camps, (2) inappropriate information on disaster preparedness, (3) cultural beliefs influencing people's ability to cope with the new environment, (4) poor service delivery in the camps, and (5) infertile land in refugee settlements (Osuret *et al*., 2016). Successful

resettlement necessitates sensitisation of the community about its rationale as a way of building trust in the government (Neema *et al.*, 2018).

Figure 5.4 shows the variation of flooding depth across the study area simulated for different return periods (2- to 100-years). The maximum depth varied from 3.79 to 4.53 m at LQ for 2- to 100-years return period and 4.62 to 5.36 m at UQ for 2- to 100-years return period. As earlier observed with flooding extent, the difference between the 50- and 100-years return periods results in terms of flood depth is small despite if being expected to be large. The same reasons according to Beirlant *et al*. (1996), Onyutha and Willems (2015b), Willems *et al*. (2007) and Onyutha and Willems, (2013) still apply for this situation. The section with deepest flood water levels is observed approximately 1.6 km downstream of where bypass of Bugiri-Tororo road crosses Lumbaka/Kibimba tributary. The floodwater depths were obtained by subtracting the terrain from the water surface level.

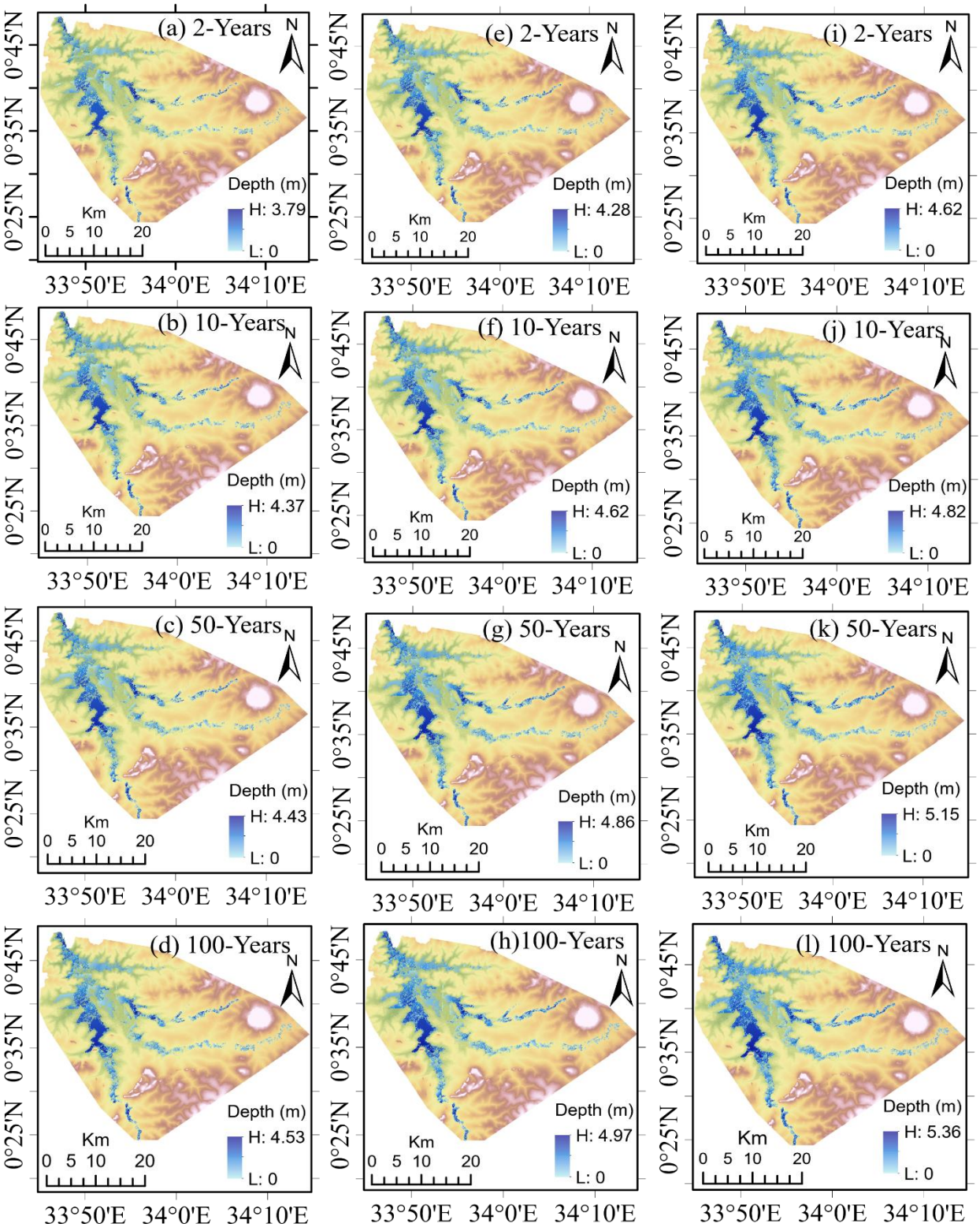

Figure 5.4 Flooding depth based on (a-d) LQ, (e-h) Q and (i-l) HQ, at (a,e,i) 2-YRP, (b,f,j) 10-YRP, (c,g,k) 50-YRP and (d,h,l) 100-YRP. "YRP" denotes "year return period". "L" and "H" denote high and low depth, respectively

The flooding extent on various land cover types is shown in Figure 5.5 for the extreme flows.

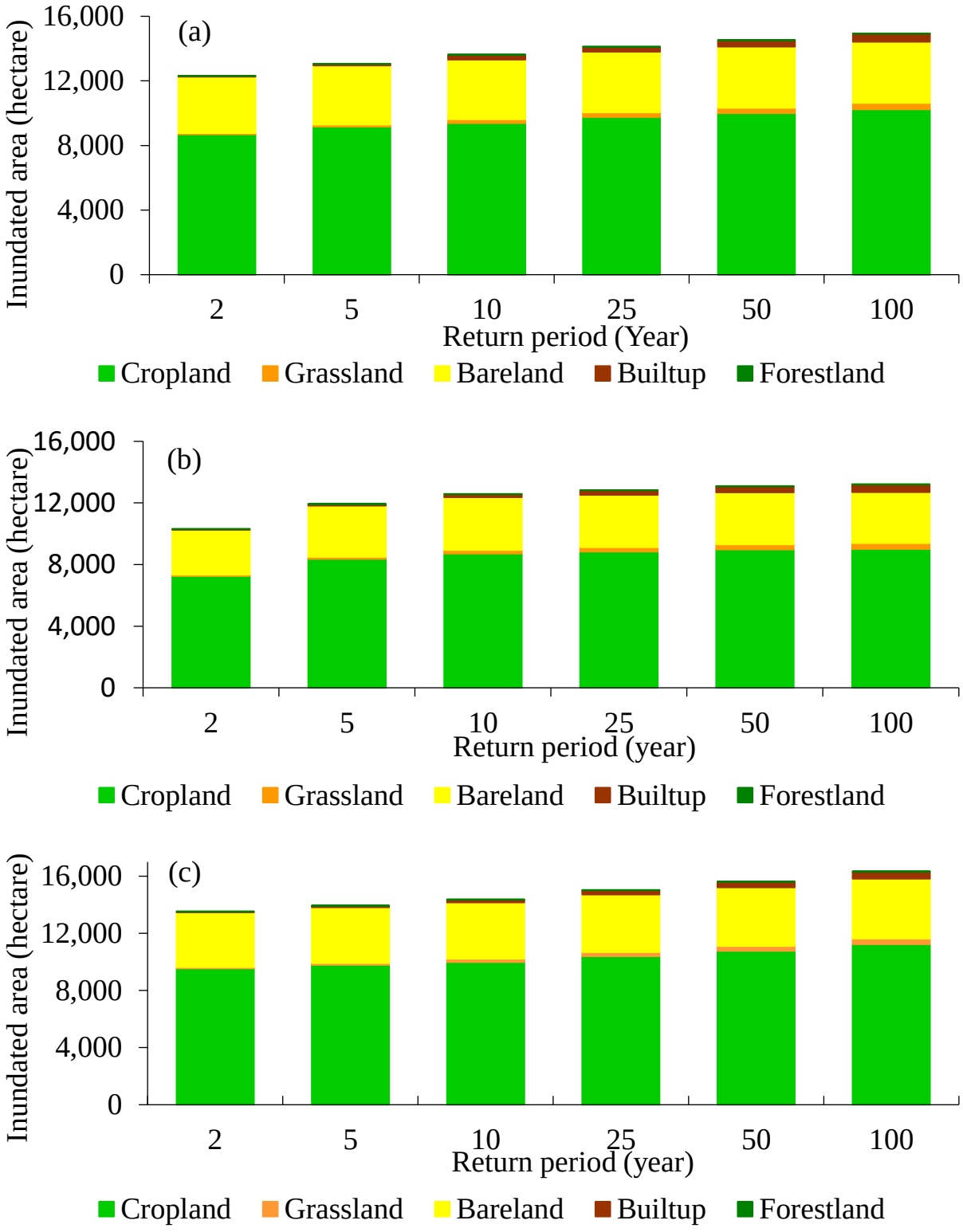

Figure 5.5 Flooding extent on different land cover types in the sub-catchment considering various return periods based on (a) LQ, (b) Q, (c) UQ

Flood vulnerability analyses results conform with the October to November 2020 field survey indicating highest percentage of vulnerability in the low-lying areas. The highest vulnerability percentage occurred in the cropland (cultivated land) with 10,234.8 hectare (ha) flooded by 100-YRP, followed by 3,793.9 ha of bare land. Inundation of cropland increased by 15% from 8,685 ha at 2-years to 10,235 ha at 100-years. Despite the relatively small areas of inundated built-up, these places have high population density mainly staying along the river banks. Besides, the inundated built-up land-use type exhibited the highest vulnerability percentage increase (90%) between 2- and 100-YRP followed by grassland (80%) (Figure 5.5). Therefore, in the low-lying areas, effective land-use conservation and management should be emphasised.

For the inundated cropland, field survey analyses done in October to November 2020 revealed that rice is the most cultivated crop taking approximately 40%, followed by maize (20%), millet/sorghum (15%). The other crops grown include beans, ground nuts, sweet potatoes, cassava sharing the remaining percentage. Rice which mainly doubles as both food and cash crop has been taken as an example to quantity the would-be loss if the land is inundated. Focus group discussions conducted with Namunasa stream rice farmers cooperative society limited revealed that on a good season (without inundation), one hectare of land can on average, yield 2.74 tons. This value is not much different from the country-wide rice yields of say 2.84 ton/ha in 2019 (Knoema, 2021). The average cost of a ton is approximately UGX 2,400,000 (US$ 675)[1]. By adopting these figures, the estimated loss on rice at varying return periods was computed as shown in Figure 5.6.

[1] UGX 3,554 is equivalent to 1 US$ (approximated based on the Bank of Uganda rate on 23 June 2021). UGX denotes Uganda Shilling and US$ stands for United States Dollar

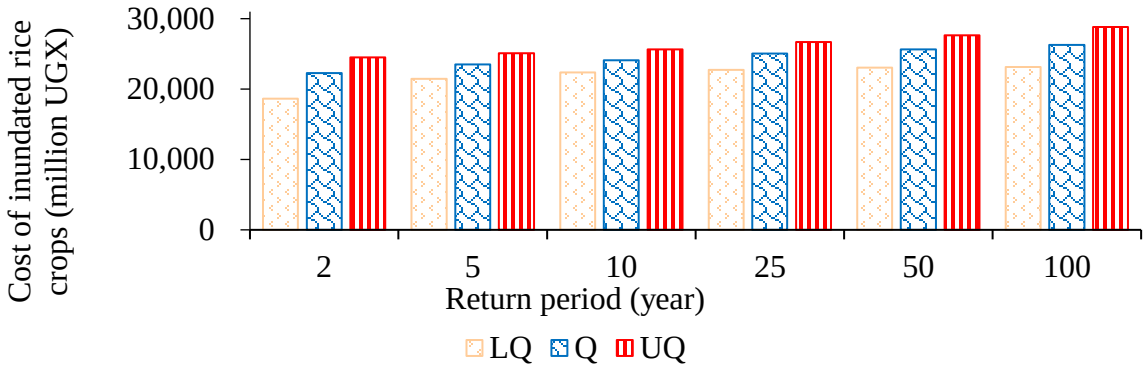

Figure 5.6 Cost of inundated rice crops at various return periods

Destruction of plantation signals a high risk of food insecurity and poverty in the area. In 2019, gardens were destroyed in Tororo and Butaleja district leaving the community in looming fears of famine (Daily Monitor, 2019). A similar event happened in 2020 (Uganda Radio Network, 2020). With the above, communities may need to develop best management practices such as restoration of wetlands and embracing of cover crops (Antolini *et al*., 2020). Alternatively, farmers may need to opt cultivating low yielding traditional crops that are rather resistant to flooding instead of experiencing total losses. Besides, observation of flood trends may help famers adjust their agricultural activities in the flood prone areas.

Figure 5.7 (a,b) shows the inundated infrastructures (churches, mosques, academic institutions and health facilities). There was no noticeable difference in the number of inundated infrastructures at the six different return periods (2-, 5-, 10-, 25-, 50- and 100-years). Therefore, in Figure 5.7 (a,b), only results obtained at 100-YRP are presented considering the extreme flow (Q). For the 100-YRP, fifteen academic institutions, twelve health facilities were inundated and remain susceptible to future inundation (Figure 5.7a). Similarly, twelve mosques and twenty churches are at a risk of flooding (Figure 5.7b).

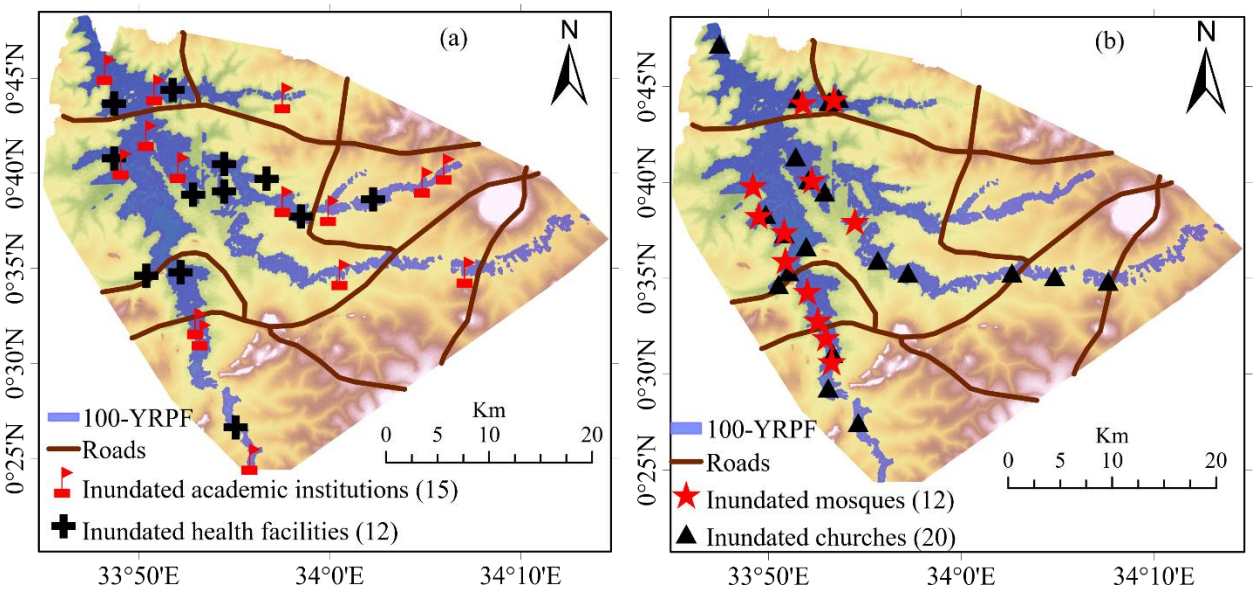

Figure 5.7 Inundation extent of (a) academic institutions, health facilities roads and (b) mosques, churches for the 100-YRP obtained using the extreme flows (Q)

Based on the available information, economic losses due to flooding of infrastructures were estimated following the procedure in section 5.2.5. The estimated economic losses for various infrastructure are indicated in Table 5.6.

Table 5.6 Flood economic damage losses estimations for the selected infrastructures

Infrastructure	Economic losses (US$)			
	Return Period (year)			
	2	10	50	100
Church	855,065	1,059,262	1,130,255	1,623,832
Academic institutions	459,741	708,104	772,855	1,116,149
Mosque	502,129	720,139	849,277	1,276,465
Health facilities	422,597	615,545	630,842	862,034

Churches exhibited the highest economic losses of US$ 855,065 and US$ 1,623,832 at 2-YRP and 100-YRP, respectively (Table 5.6). Heath facilities had the least economic losses of US$ 422,597 and US$ 862,034 at 2-YRP and 100-YRP, respectively (Table 5.6). For higher return periods beyond 100-years, the risk needs to be assessed in future when adequate flow data is available.

Improvement of catchment management can minimise the inundation of such key social infrastructures.

The major transport roads including highway are at a risk of inundation as presented in Figure 5.8.

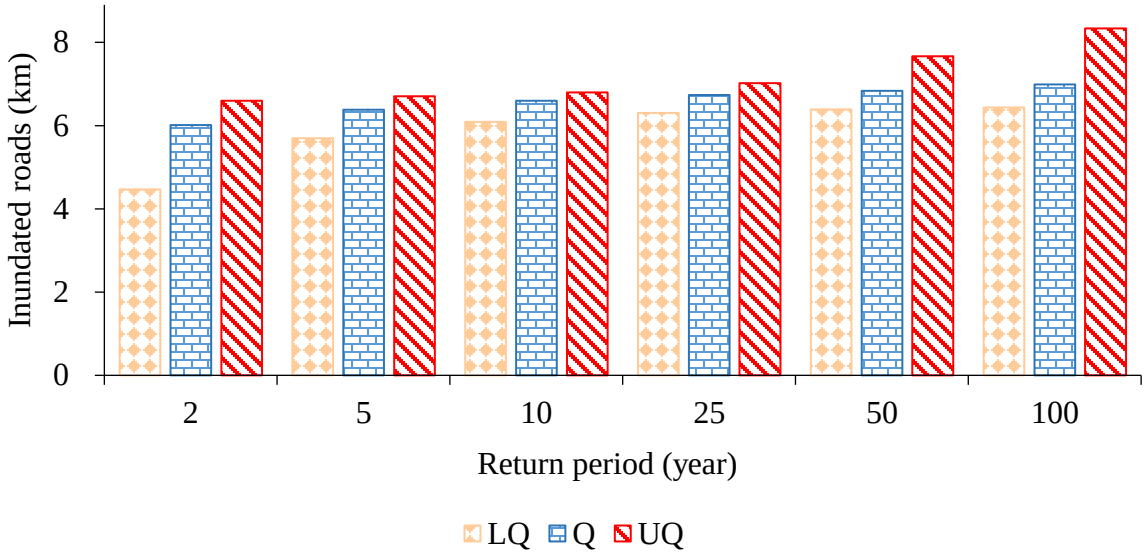

Figure 5.8 Estimated inundated roads for 2- to 100-year return periods.

A total of about 4.6 km and 6.7 km of road network are prone to inundation considering the LQ and UQ at 2-years return period, respectively. At 100-years return period, the affected roads will increase to approximately 6.54 km and 8.43 km for LQ and UQ, respectively (Figure 5.8). The affected sections of the roads have bridges and/or culverts. Inundation of the road infrastructure indicates probable inadequate capacity of the existing bridges and/or culverts. This puts the roads in danger of collapsing hence disrupting transport and livelihoods in the area. The authorities may use these findings as baseline information in development of more all-inclusive approaches for improving safety of these infrastructures.

5.4 Conclusion and implication of the findings

5.4.1 *Research questions addressed in this chapter*

Did land use land cover changes significantly influence flood dynamics? What is the spatial extent of inundation due to severe flooding events? What are the socio-economic impacts of flood in the study area?

5.4.2 *Conclusions*

The influence of land-use change on flood simulation was too insignificant ($p > 0.05$). therefore, flooding in the area could be influenced by other factors such as climate variability. Human settlements, land cover and several physical infrastructures (academic institutions, health facilities, worshiping places, roads) tend to be inundated due to severe flooding events.

The 2-year flood inundated about 17% of the low-lying area, while around 20% of the area was inundated by the severe 100-year flood. In US Dollar, around US$ 33 million and US$ 39 million losses were estimated at 2- and 100-year return period (YRP), respectively, due to inundated rice gardens and these indicate an impending high risk of household food insecurity and poverty. Amongst the infrastructure, churches showed the highest economic losses of US$ 855,065 and US$ 1,623,832 at 2-YRP and 100-YRP, respectively.

5.4.3 *Implication of the study findings*

With the above socio-economic losses, workable flood adaptation strategies need to be put in place. For instance, the government authorities can make use of these findings to identify the modelled floodplains and vulnerability, which can be circulated to the local establishments for effective land-use planning and management. Encourage of fast-growing crops and developing best agricultural management practices such as restoration of wetlands and embracing of cover crops in highly susceptible flood areas could be done. Besides, the community could be sensitised on the dangers of setting-up structures in flood-prone areas. In addition, several structural and non-structural sustainable management strategies including embankment/river training structures, flood forecasting and early warning, modification of farming practices, watershed management, relocation of personal property could be implemented to reduce on the flood-related loss of human life and property.

Chapter Six

6. Adaptation strategies, community willingness-to-pay and the influencing factors towards floodplain restoration

This chapter is based on the published paper:

Mubialiwo, A., Abebe, A., Onyutha, C., 2021. Analyses of community willingness-to-pay and the influencing factors towards restoration of River Malaba floodplains. *Environmental Challenges* 4, 1–14. https://doi.org/10.1016/j.envc.2021.100160

6.1 Introduction

Human life and property have unceasingly been affected by dramatic floods (Di Baldassarre *et al*., 2013). Effective management of floods require well informed adaptation strategies with an understanding of the community perception (Bomuhangi *et al*., 2016; Rakib *et al*., 2017; Sung *et al*., 2018). This enables developing flood adaptation strategies, with the society assigned the leading role in the entire process *(*Nyasimi *et al*., 2016; Rizvi *et al*., 2016). Brémond *et al.* (2013) noted that management of flooding impacts requires restoration of the floodplains by allocating more room for the water. This necessitates economic and environmental evaluation to guide in decision-making (Brémond *et al*., 2013). Adopting flood management mechanisms that depend on the willingness-to-pay (WTP) can boost community involvement particularly in Uganda where implementation of adaptation strategies to disasters remains a challenge (Ampaire *et al.*, 2017). In addition, the WTP approach is vital in countries, such as Uganda where there is a contest of low capacity at district and local levels to engage in adaptation planning (Echeverría *et al*., 2016). Government involvement is normally dependent upon the community efforts towards solving the existing problem (Kreibich *et al*., 2011; Nguyen and Robinson, 2015). This can be in form of community WTP towards supporting the government programs. The WTP tells the maximum value (e.g., amount of money) an individual is willing to offer for a service or good (Martín-Fernndez *et al*., 2010).

The contingent valuation (CV) method (Boyle, 2017; Cummings *et al*., 1986; Mitchell and Carson, 1989) tends to be preferred to other methods in establishing the community WTP contingent on provision of some imaginary service or good, for instance, in flood management (Wright, 2012). The community WTP for restoration of the floodplains, hence reduce the flood risk, is determined

by the anticipated damage, perception of flood risk, and attitude (Botzen *et al*., 2013; Khan *et al*., 2014). Mainly, a person compares the fringe benefits of getting protected against a risk with the marginal cost of investment to avoid the risk. This is entirely dependent on individual economic limitations. By the time of conducting this study, there were no studies that applied the CV method to determine community WTP towards restoration of River Malaba floodplains, moreover with identification of the influencing factors. Therefore, by using the shadow price, this study aimed at determining the community WTP for restoration of River Malaba floodplain based on the contingent valuation (CV) technique. Restoration meant putting in place several flood adaptation strategies. This was through identifying factors (demographics, socio-economic, institutional) and analysing their influence on community WTP towards the program.

6.2 The contingent valuation method

Several valuation methods exist including the Contingent Valuation (CV) (Boyle, 2017; Cummings *et al*., 1986; Mitchell and Carson, 1989), experimental auction (Vickrey, 1961), and conjoint analysis (Balderjahn, 1994; Green and Rao, 1971; Green and Srinivasan, 1990, 1978). Some of these methods (like the conjoint analysis) are found to offer high inducements for strategic behaviour on the part of survey respondents, hence overestimating the community WTP (Carson, 2000; Danso *et al.,* 2017). On the other hand, the CV method is applied to obtain information that may not be attained using the economic market-based instruments (Fujita *et al*., 2005; Ginsburgh, 2017; Khan *et al*., 2014). The CV method is an easy, flexible non-market valuation technique that has attracted an extensive application in cost-benefit analysis and environmental impact assessment in many countries (Venkatachalam, 2004). For example, Navrud *et al.* (2012) established that the application of CV method focusing on determining the WTP in generosity can eliminate the challenges associated with applying the method in developing countries (like Vietnam). Ghanbarpour *et al.* (2014) applied the CV technique to evaluate the community's WTP for flood insurance and structural flood control mechanisms in the Neka River Basin in Northern Iran, and with much confidence, applauded the method. In addition, the CV method has been used to approximate the environmental costs resulting from extreme floods in the Evros River basin, Greece (Markantonis *et al*., 2013). The method has similarly been applied to determine the United States community WTP for the reduction of greenhouse gas emission from the Glen Canyon Dam operations (Jones *et al.*, 2017), and to support policy making in solid waste management in Ikaria, Greece (Gaglias *et al*., 2016). With the CV technique, Zhao *et al*. (2013) estimated the WTP for

the protection of the Zhangjiabang Creek river ecosystem in China. Maghsood *et al*. (2019) also used the CV method to assess the community acceptability of flood management strategies under climate change in Talar River in northern Iran. Gravitiani and Suryanto (2017) further applied the CV approach to value the economic impact of flood mitigation in the Central Java, Indonesia. Besides, Wright, (2012) applied the CV method to analyse the society WTP for the operation and maintenance of an improved water source in the villages of Kigisu and Rubona in Uganda. Banga *et al.* (2011) used the CV method to establish the determinants of community WTP for an improvement in solid waste-collection services in Kampala, Uganda. Using the CV method, Chia *et al*. (2020) assessed the farmers' knowledge and WTP for insect-based feeds in Kenya. Angella *et al.* (2014) evaluated the farmers WTP for irrigation water at Doho rice irrigation scheme in Uganda. This scheme is located close to the study area. In this study, the CV technique was applied to determine to community WTP for the restoration of the floodplains of River Malaba. Floodplain restoration encompasses several adaptation strategies that can minimise the impacts of flooding such as loss of lives, destruction of houses, schools, hospitals, bridges, roads, and agriculture.

6.3 Methodology

6.3.1 *Flood adaptation strategies*

Using the techniques described in section 2.2.4, flood adaptation strategies that have been in existence were generated, mainly using the reconnaissance surveys. These included those locally developed by the community and those initiated by the government and other agencies. Through the household surveys, respondents were asked to score or rank the adaptation strategies in order of preference on a Likert scale of 1 to 5. In this study, values of 1 and 5 were used to denote the least efficient/preferred and very effectively/applicable, respectively. For guidance in the ranking of the strategies, respondents were presented with inundation maps of the study area. Likert scale (Likert, 1932) was initially developed by Rensis Likert and has had numerous application including modification in the field of social science and attitude research projects (Croasmun and Ostrom, 2011; Joshi *et al.*, 2015), particularly to measure the perception of the respondents. Based on the overall score of each adaptation strategy, ranking was made from the most desired to the least desired using the Weighted Average Index *WAI* (equation (6.1)) in order to analyse the respondents' level of agreement (Miah, 1993) as done by Simotwo *et al.* (2018), Thapa-Parajuli *et al.* (2018), and Ndamani and Watanabe (2016). *WAI* was generated by multiplying the total

number of declarations in each category with its corresponding weight and dividing it by the total number of responses

$$WAI = \frac{\sum F_i W_i}{\sum F_i} \tag{6.1}$$

where W = the weight applied to different response classes, i = score (1 = least preferred, 2 = less preferred, 3 = moderately preferably, 4 = very preferred, 5 =most preferred); F_i = frequency of responses for a particular response class i. WAI has previously been successfully applied for different studies in different countries (Chowdhury and Khairun, 2014; Zeleke and Assefa, 2017; Zhen and Zoebisch, 2006)

6.3.2 *Theoretical model for WTP*

To determine the community WTP, the CV method was applied. The CV technique was applied to generate information that may not be attained using the economic market-based instruments (Fujita *et al*., 2005; Ginsburgh, 2017; Khan *et al.*, 2014). Personal understanding, mindset, and preference concerning rain-induced flooding together with the associated non-market values were determined mainly using the household questionnaires. To assess the effect of flooding on the community well-being, respondents were asked for their WTP (Mitchell and Carson, 1989) towards the restoration of River Malaba floodplains. Restoration of the floodplains involves a series of adaptation strategies including structural to non-structural. The change in risk of being pretentious by the rain-induced floods was measured using money as the standard. This was defined as either positive or negative payment assuming the anticipated value constant under various risk levels (Khan *et al.*, 2014). Depending on the knowledge level of the targeted respondents, comprehending the hazards of being affected by rain-induced floods may be challenging (Khan *et al*., 2014). This could be further aggravated by differing risk levels across individual and communities (Loomis, 1990). However, in this study, by sampling in various risk zones differences in risk-alertness levels were identified. Subsequently, risk awareness regarding flooding and associated impacts was carried out during the reconnaissance survey. This eliminated the reasoning burden associated with understanding and interpreting probabilistic illustrations of the flooding risk particularly when it came to large groups of illiterate communities (Khan *et al.*, 2014). The danger of communities being affected by the rain-induced floods was categorised as exogenous (extrinsic), for those whose factors are outside the community controls and

endogenous, for which the community can get involved to reduce the possibility of unwanted events from occurring or reduce the cost of the events (Brouwer *et al*., 2009). The extent of damage a person is exposed to, determines the incentive to pay to reduce the risk (Khan *et al.*, 2014). Generally, a person compares the fringe benefits of getting protection against the risk with the marginal cost of investment to avoid the risk. This is entirely dependent on individual economic limitations.

Using the regression model in equation (6.2), the WTP was estimated as a function of several factors including comprehending the risk magnitude, which depends on the exogenous (extrinsic) factors, self-defence, individual income and person evasion from the risk (Bateman *et al.*, 2005)

$$WTP_i\left(X_i, \varepsilon_i\right) = X_i\beta + \varepsilon_i \tag{6.2}$$

where WTP_i is a dummy variable (having 1 for positive WTP and 0 for negative WTP), X_i is the vectors of descriptive variable, β are the matching vectors of the assessed parameter and ε_i is the subjective or marginal error which is considered to be normally distributed with a mean of zero and variance σ^2. The key assumption made was that, the WTP for floodplain restoration are consistent with differences in extrinsic risk grades across individual households. It was anticipated that the individual WTP towards the floodplain restoration would base on alertness and experience (Priest *et al.*, 2011; Reeser, 2016; Thistlethwaite *et al*., 2020). Diversity amongst individual preferences towards adaptation strategies was assumed to be influenced by several factors ranging from demographic, socio-economic and institutional (Table 6.1). These influenced individual mindset and perception towards the flooding hazard hence, their WTP for restoration program. In the regression model, a dummy variable for each category was coded for variables with more than 2 categories e.g., education, occupation, type of house.

Table 6.1 Explanatory variables applied in the logistic regression model

Variable	Definition of descriptive variable	Categorisation of the variable
G	Gender	Dummy variable [male =1 and female =0]
HAG	Household head age	Continuous variable
MS	Marriage status	Dummy variable [married =1, single = 0]
EL	Education level	Categorical variable [never went to school = 0, primary = 1, secondary = 2, tertiary (certificate/Diploma) = 3, University (Bachelors) = 4]
HHS	Household size	Continuous variable
OP	Occupation	Categorical variable [agricultural farming = 0, government job = 1, private firm (employed)= 2, small business (small shop) = 3]
TH	Type of house	Categorical variable [permanent = 0, semi-permanent = 1, mud house = 2]
HHI	Household income	Continuous variable
BR	Born respondent	Dummy variable [Yes = 1, No = 0]
FFL	Frequency of floods	Categorical variable [rainy season = 0, every year = 1, once in 5 years = 2]
BAFL	Business affected by floods	Dummy variable [Yes = 1, No = 0]
LPFL	Lost property due to floods	Dummy variable [Yes = 1, No = 0]
TP	Trend of production	Categorical variable [increased = 0, Decreased = 1, No change = 2]
RFES	One responsible for flood early warning system	Categorical variable [Government = 0, NGO = 1, charity group= 2, community = 3]
CGIP	Have confidence in government	Dummy variable [Yes = 1, No = 0]
FMP	Is flooding a major problem	Dummy variable [Yes = 1, No = 0]
CAC	Can Flooding be controlled	Dummy variable [Yes = 1, No = 0]

6.3.3 *Statistical analysis*

The starting question was to appreciate the insights of community WTP in principle for floodplain restoration without necessarily stating anything regarding money. The response obtained determined the proceeding question. The study ensured that respondents provided as honest responses as possible bearing in mind other personal demands that rely on their limited income (Khan e*t al*., 2014). Responses from the first question were considered as affirmative or negative, objection/protest or honest zero. Below are the WTP questions presented to respondents:

Qn. 1: *Assume the government of Uganda initiates a program dubbed* ***"Restoration of River Malaba Floodplains****", intended to minimise the impacts of flooding such as loss of lives, destruction of houses, agricultural and forest land, damage of roads and bridges. However, the program requires large amounts of money, and unfortunately, the government has limited funds due to other pressing demands. Therefore, suppose you are approached and requested you to contributed towards the program, in principle, would you be WTP?*
Yes/No (If Yes, answer question 2; If no, proceed to question 3)
Qn. 2: *If yes, what are some of the reasons for your WTP?*
Qn. 3: *If No, why are you not WTP?*

Following the response (yes or No) of WTP obtained from question 1, respondents with yes were asked for their WTP follow-up price bids to which they answered either yes or no. Several follow-up price bids were presented (5000, 10000, …, 500000 UGX). These follow-up bids were pre-tested prior to their usage in the WTP exercise through a dry run assessment on a trail representative sample of the intended respondents. This study adopted four starting bids of 10000, 100000, 350000 and 450000 UGX, which respectively correspond to 2.7, 27.0, 94.6 and 121.6 United States Dollars (US$) at an exchange rate of approximately 3700 UGX = 1 US$ according to Bank of Uganda as of 25 February 2021. The initial bids were randomly presented to avoid a fixed stating bid bias. Depending on the respondent's answer of either affirmative or negative to the starting bid, the follow-up bid presented was higher or lower, respectively (Ikeuchi *et al*., 2013). The study adopted the double-bound dichotomous choice (DBDC) CV approach instead of the single-bound dichotomous choice (SBDC). While SBDC approach considers a one-off choice, for the DBDC, the WTP relies on a series of variables X_i in equation (6.3) .This as well comprises

of the follow-up bid amount and hidden factors incorporated in the error parameter ε_i. The WTP of the second follow-up bid was computed using equation (6.4) subsequent to the first WTP bid.

$$WTP_i = X_i\beta + \varepsilon_i \tag{6.3}$$

$$WTP_i^2 = (1-\varphi)WTP_i + \varphi B^s + \sigma \tag{6.4}$$

where φ is the parameter reflecting on the first bid B^s and σ is a change parameter. Respondents were asked two different questions, (1) do you admit the first bid price B^s, and (2) do you admit the follow-up bid price B^f? (Khan *et al.*, 2014). Accordingly, four possible WTP intervals were generated using the DBDC CV approach (Haab and McConnell, 2002)

$WTP \geq B^2$ agree to both first bid B^s, and follow-up bid B^f (yes-yes responses, YY)

$B^s \leq WTP < B^f$ agree to first bid B^s, and reject follow-up bid B^f (yes-no responses, YN)

$B^f \leq WTP < B^s$ agree to follow-up bid B^f, and reject start bid B^s (no-yes responses, NY)

$WTP < B^2$ reject both first bid B^s, and follow-up bid B^f (no-no responses, NN)

YY = 1 for YY answer and zero (0) otherwise, YN = 1 for YN answer, NY =1 for NY answer, and NN = 1 for NN answer and 0 otherwise.

The maximum likelihood function is used to approximate the direct slope coefficient β and standard error σ. By defining $\varnothing_{\varepsilon/\varepsilon_2}$ as the standardised bivariate normal cumulative distribution function with zero mean, unit variance σ and correlation coefficient ρ, the j^{th} contribution to the bivariate probit probability function takes the form of (Haab and McConnell, 2002).

$$L_j\left(\frac{WTP_i}{\beta^i}\right) = \varnothing_{\varepsilon/\varepsilon_2}\left\{d_{1j}\left(\frac{B^s - WTP_1}{\sigma_1}\right), d_{2j}\left(\frac{B^f - WTP_2}{\sigma_2}\right), d_{1j}d_{2j}\rho\right\} \tag{6.5}$$

where $WTP_{1j} = 1$ if the reply to the first question is yes, and 0 otherwise, $WTP_{2j} = 1$ if the answer to the second question is yes, an 0 otherwise, $d_{1j} = 2WTP_{1j} - 1$ and $d_{2j} = 2WTP_{2j} - 1$ (Haab and McConnell, 2002).

The average WTP can be determined as $E(WTP) = X_i\hat{\beta}$, where $\hat{\beta}$ is the vector parameter estimate. To take into consideration the DBDC CV design, parameters were estimated by applying

the "doubleb" command in STATA suggested by Lopez-Feldman (2010). The "doubleb" command integrates both the starting and follow-up bids and considers the initial and follow-up response (Lopez-Feldman, 2012). Several studies (Budhathoki *et al.*, 2019; Galárraga *et al*., 2014; Jiang *et al.*, 2019; Mekonnen *et al.*, 2019; Ostermann *et al.*, 2015; Pakhtigian and Jeuland, 2019; Tien *et al.*, 2020) have embraced the use of "doubleb" command in STATA in difference areas across the world.

6.4 Results

6.4.1 *Characteristics of the household survey respondents*

The demographic and socio-economic characteristic with descriptive statistics such as parameter name, mean, minimum and maximum are included in Table 6.2. The planned sample size of respondents was 550 households. Nevertheless, 498 questionnaires (representing a 91% valid response rate) were administered. The remaining 52 chose not to participate in the research. The average age of respondents was 40 years with a range of 18 to 95 years, which indicates validity of the findings. The study conducted by Danso *et al.* (2017) in Kampala reported an average age of 39 years, while Angella *et al*. (2014) reported an average age of 42. During the field observations, the gender disparity was very small, despite the community practicing patrilineal system. For instance, there were 47.8% were male, and 52.2% females. This implies that the findings represent the views for both male and female. Banga *et al.* (2011) reported gender balance of 33.8% male, and 66.2% female in Kampala, Uganda. Wright (2012) reported 49% male respondents and 51% female in Mubende, Uganda.

The smallest household had 1 member while the largest family was composed of 40 members. The average size of families was 9.7 which is remarkably higher than the national average of 9.0 (Uganda Bureau of Statistics, 2020). Majority of the respondents were married registering a 97.2%, while only 2.8% were single (either unmarried, divorced, widowed or separated). A large number of the households had mud-houses (65.5%), while 26.7% had semi-permanent houses and only 7.8% had permanent houses. Interaction with the community revealed that they prefer mud-houses, mainly because those made out of bricks develop cracks (and/or collapse) due to settlements resulting from high water tables. A large number of respondents (59.4%) never went to school, only 21.3% had primary education, while 16.5% possessed secondary education. This shows that majority of the community lack basic education and so could not read and write.

Table 6.2 Demographic and socio-economic characteristics of the 498 respondents

Parameter	Category	Number	Percent	Mean ± STD Error	Min-Max
Age		498		40 ± 0.759	18-95
Gender	Male	238	47.8		
	Female	260	52.2		
Household size		498		9.7 ± 0.238	1-40
Civil status	Married	484	97.2		
	Single	14	2.8		
Type of household	Permanent	39	7.8		
	Semi-permanent	133	26.7		
	Mud-house	326	65.5		
Literacy level	Never went to school	296	59.4		
	Primary	106	21.3		
	Secondary	82	16.5		
	Technical	11	2.2		
	University (Degree)	3	0.6		
Occupation	Agricultural farming	412	82.7		
	Government job	15	3		
	Private firm (employed)	1	0.2		
	Small business (small shop)	26	5.2		
	Unemployed	44	8.8		
Household income (UGX)	Less than 5,000	91	18.5	155,161.23± 8,183.649	5,000-1,000,000
	5,000 – 1,000,000	396	80.7		
	Above 1,000,000	4	0.8		
Household expenditure (UGX)	Less than 5,000	72	6.6	167,852.06 ± 9,907.078	5,000-1,000,000
	5,000 – 1,000,000	419	89.6		
	Above 1,000,000	7	3.8		
Origin of respondent	Born in area	326	65.5		
	Migrated	172	34.5		
Reason for migration	Moved willingly	5	2.9		
	Moved because of disaster	7	4.1		
	Marriage	154	89.5		
	Employment	6	3.5		

STD denotes Standard Deviation, Min-Max stands for Minimum to Maximum.

The low literacy level in the study area is partly attributed to the involvement of children in rice growing, the major economic activity in the area. Besides there is the huge difference between rural and urban setting regarding education facilities (Tromp and Datzberger, 2021). During field

interactions, most of the respondents (the illiterates ones) could not comprehend flooding, its associated impacts and how to mitigate and/or implement proper adaptation strategies. Contrary, the Uganda bureau of statistics (2020) reported an average literacy level of 73% in Uganda, much higher than that in the study area. The study found that 82.7% of the respondents depend on agricultural farming as the main source of income. The other occupations reported in the study were small business (small shop) (5.2%), government job (3%) and private firm (0.3). 8.8% of the respondents are unemployed. While about 81% earn a monthly income between 5,000 to 1,000,000 UGX, nearly 90% have a monthly expenditure in the same range. This implies that some households spend more than their earnings. Those spending more than their earnings stated borrowing the extra money from either financial institution like Savings and Credit Co-operative Societies (SACCOs), micro finance or friends. Others reported selling some of their property like land, animals to pay debts. 65.5% of the respondents were born in the study area, while 34.5% migrated from other areas. Majority (89.5%) migrated to the study area for marriage, while only 4.1% migrated because of disasters (e.g., floods) in their previous places.

6.4.2 *Community perception of flooding in the area*

Table 6.3 shows the community perception of flooding in the study area. As seen from Table 6.3, 94.2% of the respondents have ever experienced floods, while only 5.8% reported to have never experienced flooding. Of those who experienced floods, 56.1%, stated that floods occur every rainy season, while 43.3% experience floods every year. The 56.1% were mainly residing along the river banks and/or the very low-laying areas. Only 6% reported experiencing floods once in 5 years.

While around 97% reported cultivating in the previously flooded area, about 86% of the households experienced a decrease in production, and only 12% reported an increase. FGDs revealed that decrease in production was due to soil erosion which washes away the fertile soils. Majority (84.0%) of the respondents did not have confidence in the government on the implementation of a flood management project. The community lost trust in the government because of the previously failed projects in the area coupled with high corruption. 77% of the respondents stayed in the same risky places during floods, mainly to protect their remaining property from theft. Only 23% migrated to safe places like schools, hospitals, and relatives' homes.

Table 6.3 Community perception of flooding in the study area

Variable	Category	Value	Percent	Mean ± STD Error	Min-Max
Do you experience floods in this area	Yes	469	94.2	0.94± 0.011	0-1
	No	29	5.8		
How frequent are the floods	Every rainy season	263	56.1	0.45± 0.024	0-2
	Every year	203	43.3		
	Once in 5 years	3	6		
What is the average depth of water logging	0 to 2 m	410	87.4	1.29± 0.042	0-3
	>2 m	59	12.6		
Has your business been affected by floods	Yes	463	98.7	0.99± 0.005	0-1
	No	6	1.3		
Have you ever lost property due to floods	Yes	456	97.2	0.97± 0.008	0-1
	No	13	2.8		
Do you cultivate in previously flooded land	Yes	454	96.8	0.97± 0.008	0-1
	No	15	3.2		
What is the trend of production when you cultivate in previously flooded land	Increased	54	11.9	0.90± 0.170	0-2
	Decreased	390	85.9		
	No change	10	2.2		
In case of a flood, which settlement option do you take	Stay in same place	361	77	0.23± 0.190	0-1
	Migrate	108	23		
Are you aware of any flood early warning system	Yes	307	65.5	0.65± 0.023	0-1
	No	162	34.5		
Do you utilise any flood prediction mechanism	Yes	360	76.8	0.77± 0.020	0-1
	No	109	23.2		
Do you have confidence in the government to implement this program	Yes	75	16.0	0.03±0.008	0-1
	No	394	84.0		
Is flooding a major problem to you	Yes	440	93.9	0.03±0.007	0-1
	No	29	6.1		
Can Flooding in this area be controlled	Yes	458	97.7	0.01±0.004	0-1
	No	22	2.3		

The study further revealed that majority (93.9%) of the respondents considered flooding as a major problem. However, 97.7% of the respondents believe flooding in the area can be controlled with God's intervention. 65.5% of the respondents were aware of the flood early warning system. The other respondents (34.5%) did not have any knowledge about the flood early warning system in their areas. However, there was only one flood early warning system (siren) in the entire study area located in Butaleja district which was been non-operational since 2017 due to damaged cables.

Besides, interaction with respondents revealed that by the time sound comes from the siren, the biggest part of the area is flooded. This was attributed to the inappropriate location of the sensors

The respondents' perception on the causes of floods and their impacts on different sectors/elements were explored as shown in Table 6.4. The causes and impacts on sectors were mainly generated during the reconnaissance surveys. Respondents scored them on a Likert scale of 1 to 5; with 1 (very small cause/impact) and 5 (very high cause/impact). The final score based on the WAI yielded "longer rainfall durations" as the main cause of flooding (WAI = 4.87), followed by "changes in the rainfall pattern" (WAI = 3.93). Respondents believed that "deforestation" was least influential in causing flooding, ranking it last (WAI = 1.69). It is noticeable that the first two causes (prolonged rainfall and changes in rainfall pattern) cannot be controlled by human. Generally, all the sectors/elements were significantly affected. However, respondents considered "farm and agricultural land" as the highly impacted element by floods (WAI = 4.78), followed by "roads, hospital and schools" (WAI = 4.58). While "domestic animals and poultry, households and settlement, and sources of drinking water" did not rank among the first two, these were equally impacted by floods (WAI>3.0) (Table 6.4).

Table 6.4 Respondents' insight on the causes of floods and their different impacts on elements (values in the table represent the number of respondents)

	Very high	High	Moderate	Small	Very small	WAI	Rank
Possible causes of floods							
Longer rainfall durations	423	34	10	0	2	4.87	I
Changes in rainfall pattern	309	27	24	10	99	3.93	II
Moving closer to the river	209	65	26	58	111	3.43	III
Poor agricultural practices	81	55	37	106	190	2.43	IV
Deforestation	17	14	24	165	249	1.69	V
Impacted sector/element							
Farm and agricultural land	389	66	5	8	1	4.78	I
Roads, hospital and schools	348	78	17	20	6	4.58	II
Domestic animals and poultry	227	95	42	40	65	3.81	III
Households and settlements	222	83	39	51	74	3.70	IV
Sources of drinking water	195	37	28	92	117	3.22	V

For brevity, the respondents' perception on effectiveness of flood alerting techniques and preference of the flood forecasting mechanisms are presented in Appendix E (Tables E.1 and E.2

). “Shouting out to neighbours” ranked the most effective alert mechanism (WAI = 4.35), followed by “door-to-door knocking” (WAI =3.48), while “alarm/siren at the monitoring point” came third (WAI = 3.33) (Tables E.1 of Appendix E). It sounded surprising why the quite difficult and time intensive mechanisms (“shouting out to neighbours” and “door-to-door knocking”), were considered most effective. However, respondents expressed that these were the cheap mechanisms that they could afford. The siren was not ranked most effective because it had been non-functional since 2017. Besides, interaction with respondents revealed that by the time sound comes from the siren, the biggest part of the area is flooded. This is attributed to the inappropriate location of the siren sensors. On the other hand, “radio stations, mobile phone text messages, television and newspapers” exhibited WAI <3.0, implying they were less-to-least effective early warning mechanisms. This was related to lack or inadequate access to the three mechanism by the communities as most respondents reported absence of radios and televisions in their homes. For the flood forecasting mechanisms, overall, respondents highly preferred the “observation of the rainfall duration” (WAI = 4.57), followed by “observing amount of rains in the mount Elgon area “(WAI = 4.41), while “sound from the early warning system/siren” was ranked third (WAI = 3.39) (Tables E.2 of Appendix E). “Too much heat” and “analysing magnitude of thunderstorms” had WAI<3.0, hence, considered less preferred.

6.4.3 *Flood adaptation strategies*

Several adaptation strategies have been in place for pre-flood, during-flood and post-flood management (Tables 6.5 and 6.6). These strategies were being practiced at household and community levels, as generated during the reconnaissance survey. Communities were asked to state their perception of preference and applicability of the different strategies.

“Relocation of personal property/materials” was the most applicable pre-flood strategy at household level. All the pre-flood strategies exhibited WAI with in a range of 3.0, having a close difference between them (Table 6.5). This implies that all the strategies have a moderate application. Similarly, during-flood, all strategies had WAI with in a range of 3.0, with a close difference between them (except “shout-out to neighbours and escape from flooding area”) However, all post-flood strategies have WAI above 4.0, indicating that all of them were highly applicable in the area (Table 6.5).

Table 6.5 Flood adaptation strategies at household (values in the table represent the percentage of respondents)

Adaptation strategy	MA	VA	MdA	LA	LSA	WAI	Rank
Pre-flood							
Relocate personal property/material including animals to safe areas	47.9	23.8	6.3	7.8	14.1	3.84	I
Build drainage channels around the house and other property	43.1	26.5	10.0	7.8	12.7	3.80	II
Raise the house floor level above the flooding levels	47.2	24.3	7.8	2.7	18.0	3.80	II
Stock basic items (food, drinking water, medicine, airtime)	45.7	19.2	8.8	10.0	16.3	3.68	IV
During-flood							
Shout-out to neighbours and escape from the flooding area	60.2	16.3	8.6	4.3	10.6	4.11	I
Remove valuable property from the house and relocating to safe places	51.1	18.0	7.9	8.4	14.6	3.82	II
Carrying away children and elderly on barks and set domestic animals free	51.1	18.2	6.7	8.2	15.8	3.81	III
Use sand bags to divert flood waters	33.6	26.9	16.5	11.3	11.8	3.59	IV
Climb on the nearby strong and tall trees, houses roof	29.0	19.2	7.2	14.4	30.2	3.02	V
Post-flood							
Repair of houses and destroyed structures at home	58.7	23.7	8.1	4.3	5.2	4.26	I
Replant crops in the affected gardens	58.7	23.7	8.1	4.3	5.2	4.26	I
Plant new food crops for animals	60.0	19.6	8.8	8.6	2.9	4.25	III
Manage food through continued diversion of flood waters	55.1	21.9	11.5	7.2	4.3	4.16	IV

MA stands for Most applicable, VA is very applicable, MdA is Moderately applicable, LA is less applicable and LSA is Least applicable

Regarding strategies at community level, all the pre-flood measures were less effective ($2.0 \leq WAI < 3.0$), while those practiced during-flood were moderately preferred ($3.0 \leq WAI < 4.0$). Nevertheless, two of the post-flood strategies were highly preferred ($WAI > 4.0$), while the other two were moderately preferred ($3.0 \leq WAI < 4.0$) (Table 6.6). Respondents were also asked to state the suitability and/or preference of various structural and non-structural strategies that could be employed to deal with floods aside from the current strategies being practiced at community and household levels.

Table 6.6 Flood adaptation strategies at Community level (values in the table represent the percentage of respondents)

Adaptation strategy	ME	VE	MdE	LE	LSE	WAI	Rank
Pre-flood							
Develop flood management plan	22.4	18.2	8.8	20.1	30.5	2.82	I
Organise human resources and train personnel on flood management	14.7	21.4	20.9	12.3	30.7	2.77	II
Put in place first aid facilities	10.1	26.5	14.0	10.3	39.1	2.58	III
Set up a contact office in case of floods	10.1	16.5	13.5	9.8	50.1	2.27	IV
Pre-estimation of flood risks	4.4	13.3	9.3	26.5	46.4	2.03	V
During-flood							
Provide food and other materials to the affected people	49.2	24.9	9.7	5.4	10.8	3.96	I
Provide health services to the affected people	49.0	21.6	11.5	3.4	14.6	3.87	II
Make immediate communication to the community through radios	36.4	20.2	14.8	18.4	10.1	3.54	III
Post-flood							
Involve the government and other agencies to provide support	56.3	16.5	13.7	7.2	6.3	4.09	I
Share the available resources with others such as settlement, food	52.1	24.0	7.4	6.7	9.8	4.02	II
Jointly repair the community access roads, clear drinking water areas	50.0	17.2	9.5	10.9	12.3	3.82	III
Set up temporary settlement for the affected community	47.7	19.1	10.2	8.8	14.2	3.77	IV

ME denotes Most effective, VE is very effective, MdE is Moderately effective, LE is less effective and LSE is Least effective.

The perceived preference/suitability of structural and non-structural strategies are presented in Tables 6.7 and 6.8. Assessment of structural adaptation strategies had 456 respondents while non-structural had 436. From Table 6.7, “Embankment/river training structures to prevent flood spread” was the most preferred structural strategy (WAI = 4.49). It was followed by “Reservoir/flow regulating structure e.g. weirs and barrages, dam” (WAI = 4.34), while “Gabion wall to protect river” came third (WAI = 4.21). “Bamboo mesh/mat with sand filled bag to prevent flood spread” and “Bio-dyke (bio engineering) – e.g. plant water resistant trees along river” has WAI of 4.16 and 4.10, receptively. It is noticeable that all the structural strategies had WAI>4 (>80%), with a minimal difference between them, implying that all the five strategies are highly preferred in flood management.

Table 6.7 Suitability of structural adaptation strategies for flood management (values in the table represent the percentage of respondents).

Adaptation strategy	MP	VP	MdP	LP	LSP	WAI	Rank
Embankment/river training structure to prevent flood spread	69.7	16.0	9.2	3.7	1.3	4.49	I
Reservoir/flow regulating structure e.g weirs and barrages, dam	65.6	15.6	10.5	3.9	4.4	4.34	II
Gabion wall to protect river	60.3	17.3	10.5	6.6	5.3	4.21	III
Bamboo mesh/mat with sand filled bag to prevent flood spread	53.9	21.5	13.6	8.6	2.4	4.16	IV
Bio-dyke (bio engineering) – e.g plant water resistant trees along river	55.7	18.6	7.7	15.8	2.2	4.10	V

MP is Most preferred, VP is very preferred, MdP is Moderately preferred, LP is less preferred and LSP is Least preferred

Among the non-structural (Table 6.8) "flood forecasting and warning" ranked the most preferred (WAI = 4.18), followed by "household level preparation /management like elevated houses" (WAI = 3.79). Contrary to structural strategies, the non-structural measures had WAI<4.0 (except "flood forecasting and warning"). This implies that five of the strategies were moderately preferred (3.0≤WAI<4.0), while only one was highly preferred (WAI>4.0).

Table 6.8 Suitability of non-structural adaptation strategies for flood management (values in the table represent the percentage of respondents).

Adaptation strategy	MP	VP	MdP	LP	LSP	WAI	Rank
Flood forecasting and warning	58.3	18.6	11.7	6.0	5.5	4.18	I
Household level preparation /management like elevated houses	43.3	21.3	15.4	11.0	8.9	3.79	II
Watershed management	50.5	11.7	11.9	17.2	8.7	3.78	III
Controlling flood level around the house & food storage (trench)	42.0	21.3	17.0	11.2	8.5	3.77	IV
Land use management to avoid damage from flood	39.0	22.0	19.0	11.9	8.0	3.72	V
Modification of the farming practices	41.3	18.6	17.9	13.5	8.7	3.70	VI

6.4.4 *Evaluation of the community willingness-to-pay*

Table 6.9 shows the household WTP responses for the program of restoring River Malaba floodplains. Restoration encompasses a series of adaptation strategies as described in section 6.4.3. The responses were categorised as affirmative, genuine zero and protest. The distribution of the

WTP responses was done for respondents who disclosed their household monthly income and those who did not disclose. Based on the reasons provided by respondents as to why they were not willing to pay for the program, a genuine zero was distinguished from a protest. For responses where the reason for not willing to pay was given as "I don't have money for the program, other expenditures are high" a genuine zero was assigned. Other responses were categorised as protests.

Table 6.9 Willingness-to-pay (WTP) responses for the program

	Reported Household monthly Income		
WTP	Yes	No	Total
Affirmative	272(0.55)	2(0.29)	274 (0.55)
Genuine Zero	172(0.35)	5(0.71)	177(0.36)
Protest	47(0.10)	0(0.00)	47(0.09)
Total	491(1.00)	7(1.00)	498(1.00)

From Table 6.9, 55% of the respondents were affirmative, while 36% presented a genuine zero. Only 9% of the respondents protested the idea of paying towards the program of restoring the River Malaba floodplain. However, Chia *et al*. (2020) achieved a response rate of 94% WTP for insect-based feeds in Kenya, Maghsood *et al.* (2019) reported an average WTP of 35% towards flood management strategies in Talar River Basin, northern Iran. Gaglias *et al.* (2016) reported 65% WTP to create a fund for financing social and environmental programs in Ikaria, Greece. In Uganda, Ojok *et al*. (2012) reported 48.1% WTP for improved municipal solid waste management service in Kampala, while Banga *et al.* (2011) on the other hand reported 79.8% WTP for a waste-collection service in Kampala.

Analysis of the WTP amounts was based on the respondents who had earlier-on disclosed their monthly incomes. Table 6.10 shows the statistical analysis of various WTP amounts.

Table 6.10 Breakdown of the WTP amount in UGX

WTP parameter	Mean	Median	Mode	Minimum	Maximum	Sum
Per month	97,080	50,000	10,000	5,000	500,000	38,249,500

3700 UGX is equivalent to 1US$ as of 30 December 2020. UGX denotes Uganda Shilling and US$ stands for United States Dollar.

Computation of the median was based on the presence extreme higher values in the responses, hence, making median more suitable than the mean value. The collected dataset on WTP amount was positively skewed (Cs =0.88) resulting in a smaller median value than the mean. This is a clear signal that the mean is sensitive to any score in the distribution and is prone to huge shifts from the true central value when the sample contains extreme scores (Sykes *et al*., 2016; Zheng *et al*., 2016). In addition, the mode value was used to show the most frequently occurring value in the data series. In this study, the average (mean) monthly WTP amount was 97,080 UGX, while the median was 50,000 UGX, and mode 10,000 UGX. The maximum and minimum monthly WTP amounts were 500,000 UGX, and 5,000 UGX, respectively. The respondent's WTP amount is further presented in Figure 6.1 with a liner trend line fitted on the probability of responses.

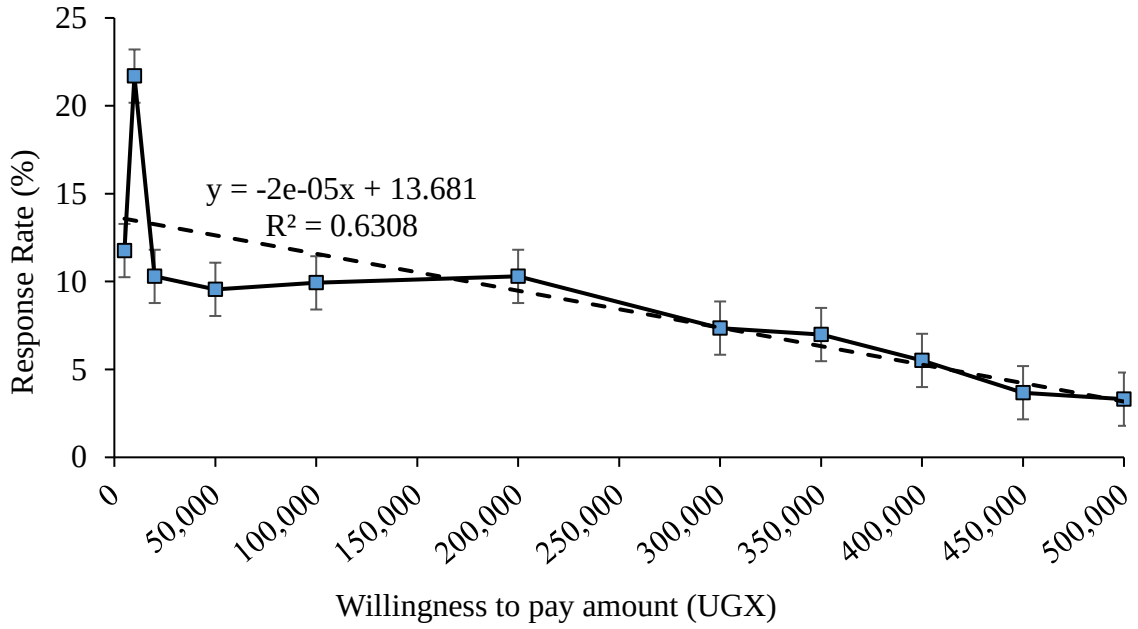

Figure 6.1 Analysis of the WTP amount in UGX

It is noticeable from the linear regression model on Figure 6.1 (y = -2e-05x + 13.681), that the response rate decreased with increasing WTP amount. The value of the regression model coefficient R^2 was obtained as 0.6308, which implies that the WTP amount influenced 63.1% changes in the response rate. It is further noticeable that the response rate varied from one WTP amount to another. The response rate increased from 11.8% to 21.7%, with an increase in WTP amount from UGX 5,000 (US$ 1.35) to UGX 10,000 (US$ 2.70). The highest response was at the WTP amount of UGX 10,000 (US$ 2.70), while the lowest was observed at UGX 500,000 (US$ 135.14). Largely the results reveal that the community were willing to contribute towards the

program for restoring River Malaba floodplain area. The individual monthly WTP amounts ranged from UGX 5,000 (US$ 1.35) to UGX 500,000 (US$ 135.14), with a monthly average of UGX 97,080 (US$ 26.24). Total monthly amount was UGX 38,249,500 (US$ 10,337.70) considering the 498 households.

Respondents gave various reasons for their choices of either affirmative or negative WTP responses as shown in Table 6.11. From Table 6.11, 55.0% were willing to pay towards the program, while 45.0% opposed. 36.2% of the respondents were WTP with anticipation that the program would result in management of floods hence, minimising the impacts on human and surrounding environment. 30.9% of the respondents agreed to pay with a hope that program's implementation would guarantee more protection of the residents living along the river banks. 16% of the respondents were WTP expressed that the program would mitigate rain-induced floods, while 16.8% voiced that the contributed money would help the authorities during budget constraints times.

Table 6.11 Reasons for negative and affirmative WTP responses towards the River Malaba floodplain restoration program

Item	Category	Number	Percent	Mean ± STD Error	Min-Max
WTP	Affirmative	274	55.0	0.55± 0.022	0-1
	Negative	224	45.0		
Reasons for WTP	Manage floods to minimise impacts	271	36.2	0.38± 0.021	1-5
	Mitigate floods	120	16.0		
	Contribute money to authorities	126	16.8		
	Protect residents along river banks	231	30.9		
Reasons for not WTP	Flooding is a minor problem to me	29	6.5	0.09± 0.009	1-5
	I don't have money	177	39.6		
	Uganda government should pay	23	5.1		
	Those affected should pay	4	0.4		
	No confidence in government	194	43.4		
	Flooding is beyond any one's control effort (be left to God)	22	4.9		

However, of the 45.0% respondents who were not WTP, 30.6% did not have money due to other high expenses. 5.1% stated that it was the government responsibility to restore the river floodplains, while a small percentage (0.4%) expressed that those affected by floods should pay

for the program. On the other hand, 6.5% of the respondents were not WTP because flooding from the river is a minor challenge to them, while about 43.4% explained that they could not pay for the program because they have no trust in the government programs. A small number (of about 5%) believed that floods in the area are beyond any human control effort and should only be left to God.

6.4.5 *Factors influencing the community Willingness to Pay*

The factors categorised under demographic, socio-economic and descriptive statistics were verified for multicollinearity to establish if there was no high correlation prior to their use in the regression model. The analysis revealed a weak correlation between most of the explanatory variables, hence making them suitable for use in the regression model. However, some variables such as "frequency of floods once in 5 years", and "no change in production trend" exhibited collinearity. These were excluded from the regression model. Table 6.12, presents results of the probability of a respondent being willing to pay for the restoration of River Malaba floodplains.

The value of R-square demonstrates how better the data fits in the regression model, and it varies between 0 and 1.0, with the value of 1.0 denoting a perfect match, while higher values indicate a better fit (Barnnett *et al.*, 1998). From the analysis of the Wald chi-squared test, the null hypothesis was rejected with $R^2 = 0.531$, $p = 0.000$. Therefore, the variables coefficients included in the regression model were statistically different from zero. Almost 50% of the variables had significant influences on community WTP (Table 6.12). The respective variable influences are described in section 6.5.

Table 6.12 Analysis of the effect of explanatory variables in the logistic regression model

Variable	Coefficient *(β)*	Std. error (σ)
Gender	0.1794***	0.5233
Age	0.0031***	0.0013
Marital Status	0.4335***	0.1817
Education (Never went to school)	-0.2237 ^{ns}	0.3177
Education (Primary)	0.015**	0.3111
Education (Secondary)	0.145**	0.3104
Education (Tertiary)	0.1527***	0.3264
Household size	-0.0057 ^{ns}	0.0043
Occupation (agriculture)	0.0283***	0.1526
Occupation (government)	0.2568*	0.3846
Occupation (small business)	0.0969*	0.1704
Type of house (semi-permanent)	0.1331 ^{ns}	0.0925
Type of house (Mud)	0.0705 ^{ns}	0.0830
Household income	0.2388**	0.0838
Respondent born in study area	0.0749 ^{ns}	0.0515
Flood frequency (rainy season)	0.0085 ^{ns}	0.2654
Flood frequency (every year)	0.0312 ^{ns}	0.2646
Business affected by floods	0.2622***	0.0564
Loss of property in floods	0.1507***	0.0496
Production trend (increase)	0.0589 ^{ns}	0.1685
Production trend (decrease)	0.0855 ^{ns}	0.0656
Responsible for early warning (government)	0.1614 ^{ns}	0.1660
Responsible for early warning (NGO)	0.1275 ^{ns}	0.2067
Responsible for early warning (charity)	0.141 ^{ns}	0.2056
Responsible for early warning (community)	0.1222 ^{ns}	0.3071
Confidence in government	-0.3268***	0.0628
Flooding a major problem	0.2251***	0.5510
Can flood be controlled	-0.124 ^{ns}	0.1902
Constant	-0.709**	0.5296

***, ** and * denote significance at 1%, 5% and 10% level, respectively, while ^{ns} indicates none significance at the three levels (1%, 5% and 10%). "Std. error" stands for standard error.

6.5 Discussion

During the reconnaissance surveys, it was observed that flooding is a major problem in River Malaba sub-catchment. For instance, interaction with some of the households revealed the following: "…*after the worst flood (locally known as Somalia flood) of 1997, the number of*

flooding events had reduced until 2010, when the frequency started increasing to date, with at least 3 to 4 flooding events annually…". During the FGDs and KIIs, some of the respondents expressed that increasing bends along the river, cultivation near the river banks were some of the key factors contributing to the rising number of flooding damages in the area. This conforms to the findings by Mayega *et al*. (2015), who attributed most disasters in Uganda to human factors. Similarly, in other areas across the worlds, several studies have reported the influence of human factors in causing rain-induced disasters, such as floods. For instance, the current poor urban planning practice and insufficient to absence of environmental set-ups have aggravated Nigeria's flooding (Echendu, 2020). In Dire Dawa city, Ethiopia, apart from the natural factors, anthropogenic effects have resulted in flash floods (Erena and Worku, 2018). Besides, in China, Lyu *et al*. (2018) noted that human factors including degradation of rivers and lakes and construction of three dams are among the significant factors influencing the occurrence of floods. During field observations, water crossing roads (rendering them impassable), standing waters in compounds and gardens even after 5 days of rainfall were key indicators of flooding. On average, the flood water height was 2 m as measured from the marks on some of the features like houses and school structures. However, in other areas, it went up to 4 m.

At the household and community levels, the post-flood adaptation strategies were found to be more efficient than those practiced before- and during-floods. Regarding the suggested structural and non-structural strategies, "embankment/river training structures to prevent flood spread" and "flood forecasting and early warning" were highly preferred, respectively. The above implies that the community preferred strategies that are to be implemented by someone else (e.g. government, NGO, charity organisations) than themselves. This signifies lack of responsibility, commitment and ownership by the community to take a leading role in the entire process. This conduct could be attributed to absence of material, monetary and logistical facilitation in addition to lack of community awareness (Nguimalet, 2018). Therefore, education/sensitisation of the community on the benefits of performing a key role in developing and implementing flood adaptation strategies is vital (Rizvi *et al.*, 2016). Besides authorities need to extend social and material requirements to community levels, and improving society sense of belonging (Simon *et al*., 2020).

10% of the respondents protested WTP towards the program despite them disclosing their monthly incomes. During the survey, most of these stated that "they do not have confidence in the implementation of this project by the government due to corruption exhibited on the previous

projects". Graphically (Figure 6.1), a decreasing trend is noticeable in the response rate from the highest (21.7%) to lowest (3.3%). This is because, as the WTP amount increases, the response rate decreases. The study by Jofre-bonet and Kamara (2018) also reported a reduced WTP response (percentage) at higher WTP amount for health insurance in Sierra Leone. Therefore, the respondents in this study acted in a way that is consistent with the ideal situation. The increase in response rate from 11.8% to 21.7%, with an increase in WTP amount from UGX 5,000 (US$ 1.35) to UGX 10,000 (US$ 2.70) could sound abstruse. In a normal situation, the response rate would be expected to decrease as the WTP amount increases. However, a low response rate at UGX 5,000 than UGX 10,000 was because respondents expressed that contributing only UGX 5,000 could not raise enough money to support the program, hence opting for a slightly higher amount. According to Carson and Groves (2011) some respondents may opt to go for higher WTP amount to ensure that the program serves the intended purpose than merely choosing WTP values below anticipated cost. With total monthly amount would be UGX 38,249,500 (US$ 10,337.70) for the sample size of 498, assuming that all factors remain constant and that all households in the study area were willing to pay towards the restoration program, a reasonable sum of money can be generated.

The different regression coefficients *(β)* and standard errors (σ) can be found in Table 6.12. Six independent variables (education, occupation, type of house, flood frequency, production trend and responsibility for early warning) were categorical and therefore, a dummy variable for each category was coded. Gender had a positive regression coefficient at 1% significance level. This implied that males were more likely to pay for the program than females. This sounds true because in Uganda there is customary marriage which gives more powers to males on financial decisions (Banga *et al.*, 2011; Wright, 2012). Although reported on a different sector, results of this study were in treaty with the findings from Banga *et al.,* (2011). The studies by Twerefou (2014) in Ghana and Eridadi *et al*. (2021) in Ethiopia reported similar results. The respondents' age had a significant positive influence on their WTP for the restoration program. This inferred that respondents' WTP increases as they attain an old age. Similar results can be found in previous studies e.g., Eridadi *et al*. (2021) in Ethiopia and Jiang *et al.* (2019) in China. However, this study findings contradicted with those of Banga *et al.* (2011) in Uganda, Eskandari-Damaneh *et al.* (2020) in Iran and in a transnational study by Funahashi *et al*., (2020) who reported negative impact of age on community WTP. Respondents who never went to school exhibited a negative attitude toward the program. However, respondents' education level from primary upwards had a

significant ($p < \alpha$) positive influence on their WTP for the restoration of River Malaba floodplains. The highest education class (tertiary) respondents were willing to contribute more compared to their counterparts in lower education categories. The studies by Nguyen and Robinson (2015), Zhao *et al*. (2013), and Banga *et al.* (2011) reported that respondents with higher education yielded relatively higher WTP in China, Vietnam, and Uganda, respectively. This indicates the need to improve education standards in the study area which could possibly help community attain additional acquaintance of the benefits of floodplains restoration.

The respondent's marital status had a significant positive influence on their WTP. It was statistically significant at 1% significance level. This revealed that married respondents were more likely to pay for the restoration program as they are obliged to meet their family expenditures compared to their counterparts (the singles). This study findings were similar to those of Eridadi *et al.* (2021). However, the study by Acey *et al.* (2019) reported that married people were less likely to pay for water utility in Kenya. Although statistically insignificant, respondents who were born in the area were likely to pay towards the program. This implied that being a born of an area enables an individual to comprehend the various challenges within the community.

The three variables of respondents' occupation (agriculture, government and small business) had significant positive influences on their WTP. These results indicated that having a source of income could increase an individual's potential to contribute towards the government program aimed at solving community challenges. Previous study by Eridadi *et al*. (2021) reported positive impact (though insignificant) of occupation on community WTP towards improving water services in Sebeta town, Ethiopia. The relationship between the probability of respondents WTP and the continuous variable "household income" was positive. The regression coefficient was significantly positive at 5% significance level. This indicated that respondents with high income value were more willing to pay towards restoring the floodplains compared to lower income earners. These results agreed with several other studies (Eridadi *et al*., 2021; Eskandari-Damaneh *et al*., 2020; Jones *et al*., 2017; Kikulwe and Asindu, 2020; Maghsood *et al*., 2019; Makwinja *et al*., 2019; Twerefou, 2014) that reported significant positive impact of income on WTP. Therefore, empowering the community economically could potentially motivate them to always contribute towards government programs. Socio-economic variables of "effect on business", "loss of property due to floods" and "flooding being a major problem" had a significant ($p < 0.01$) positive impact on the community WTP for the program. This implied that respondents had hope that by

contributing towards the program would enable the government handle the flooding problem hence, minimising on the future losses due to floods. Some of the socio-economic variables such as "production trend", "responsibility for early warning" exhibited positive (but insignificant) impacts on WTP.

The institutional variable "confidence in government" had a significant ($p < 0.01$) negative impact on WTP. Confidence refers to the amount of trust that respondents have in government institutions and actions towards managing floods and associated impacts. During the study, it was pointed out by some respondents that those with authority such as chairpersons, treasurers on the management committees were corrupt. Other respondents stated that some of the committees created to manage floods were donor-driven and their interests to restore floodplains were tagged on the monetary paybacks than the will of the community. Generally, various independent variables of gender, age, marital status, education, occupation, income, effect on business, loss of property in floods, confidence in governance and flood as a major problem influence (mostly significant) on the community WTP towards restoring River Malaba floodplains.

6.6 Conclusion and implication of the findings

6.6.1 *Research questions addressed in this chapter*

Is the community willing to pay for flood adaptation strategies? What factors influence the community WTP?

6.6.2 *Conclusion*

In general, the community was willing to pay for flood adaptation strategies with about 55% of the households expressing WTP an individual amount between UGX 5,000 (US$ 1.35) to UGX 500,000 (US$ 135.14). Several factors including age, gender, marital status, education level, occupation, household income, business affected, lost property due to floods, flooding a major problem had significant ($p < 0.01$) positive impact on WTP.

6.6.3 *Implication of the study findings*

The findings of this study are pertinent in supporting stakeholders' decision regarding predictive planning of flood adaptation strategies in the study area. It was realised that a fixed value of the estimated WTP amount can be applied across the entire community towards restoration of the

floodplains. However, in most cases, findings may not be used as obtained at the assessment time due to budget constraints that may materialise during the implementation stage (Khan *et al*., 2014; Venkatachalam, 2004).

While 55% expressed WTP, a considerable number (45%) was not affirmative. This could be that, they are not aware of the benefits related to flood management. Hence, the government needs to sensitise the community. Community support can boost success of government intervention on flood management as their ownership by the community. Various factors including demographic, socio-economic and institutional can affect WTP at different levels. Therefore, consideration of all the necessary factors while analysing WTP in necessary.

Chapter Seven

7. Conclusion and recommendations

7.1 Conclusion

Both rainfall and evapotranspiration exhibited trends and oscillatory variation in sub-trends over multi-decadal time scales. The number of wet days and sum of rainfall exhibited a decreasing trend with $p > 0.05$ and $p < 0.05$, respectively. However, annual maxima rainfall series were increasing ($p > 0.05$). This indicated that it may be raining less frequently but with some events having very high intensity. The sub-catchment PET had an insignificant ($p > 0.05$) positive trend. In general, a common pattern was exhibited by both rainfall and PET over the entire area. The conceptual hydrological models displayed satisfactory performance when forced with PGF reanalyses meteorological data. Australian Water Balance Model (AWBM) with Nash–Sutcliffe efficiency (NSE) of 0.837 was best performing model in reproducing observed extreme peak flows, while Soil Moisture Accounting and Routing (SMAR) performed unsatisfactory (NSE of 0.436).

Flooding was highly noticeable in the low-lying areas and the extent of inundation increased with increasing years of return period. The influence of land-use change on flood simulation was too insignificant ($p > 0.05$). Human settlements, land cover and several physical infrastructures (academic institutions, health facilities, worshiping places, roads) tend to be inundated due to severe flooding events. In US Dollar, around US$ 33 million and US$ 39 million losses were estimated at 2- and 100-year return period (YRP), respectively, due to inundated rice gardens and these indicate an impending high risk of household food insecurity and poverty. Amongst the infrastructure, churches showed the highest economic losses of US$ 855,065 and US$ 1,623,832 at 2-YRP and 100-YRP, respectively

In general, the local community of the River Malaba sub-catchment were aware of the flood. According to them, variability in rainfall pattern and longer rainfall durations were considered the main cause of floods in the study area. At household and community level, the post-flood strategies were more efficient than those practiced before- and during-floods. Among the suggested structural and non-structural strategies, “embankment/river training structures” and “flood forecasting and early warning” were highly preferred, respectively. However, these strategies necessitate considerable logistical requirements, such as materials and money which may be a

challenge to the local community. Therefore, authorities need to extend social and material support to community levels, and improve society sense of belonging through sensitisation drives.

In general, the community was willing to pay for flood adaptation aimed at restoring floodplains hence, minimising the flooding impacts. About 55% of the households expressed WTP an individual amount between UGX 5,000 (US$ 1.35) to UGX 500,000 (US$ 135.14). However, it should be noted that a large proportion expressed lack of ability to pay. Several factors including age, gender, marital status, education level, occupation, household income, business affected, lost property due to floods, flooding a major problem had significant ($p < 0.01$) positive impact on the community WTP.

7.2 Recommendations

i) It is recommended that possible drivers of rainfall and evapotranspiration variability over the study area be quantified to support local communities to predict upcoming periods of wet conditions. This could be done by investigating delayed influence of large-scale atmospheric conditions on the rainfall and evapotranspiration variability. Climate change impacts on rainfall and evapotranspiration across the study area should also be investigated

ii) Apart from using the uncalibrated Hargreaves method in estimating PET which might yield biased results, and thereby influence the outcomes of analyses of trend and variability, the application of other PET estimation methods that have less data needs should be explored.

iii) Omitting seasonal difference in the computation of bias correction factors of reanalysed data might yield unreliable results due to blind temporal relationship. Estimation of bias correction factors for PGF data over the study area was confined to monthly-scale. It is therefore recommended that the possible uncertainties in the computed bias factors be investigated considering other time-scales, such as daily, hourly. Besides, it is recommended to evaluate the performance of hydrological models when forced with uncorrected reanalyses dataset (e.g. PGF). In addition, other bias correction methods that can ably correct peak rainfall should be explored in future.

iv) Instead of using the coarse physiographic data, finer spatial resolution LULC data and high-resolution terrain data, for instance, by processing aerial images acquired by unmanned aerial vehicle (UAV) flights over the flood risk area is recommended for investigation.

v) As opposed to the assumed damage functions considered in this study, it is recommended that further analyse be conducted when site-specific damage functions become available. Besides, future studies should explore applying flood loss models to estimate crop losses.

vi) A hybrid 1D-2D HEC-RAS model may be faster to simulate than a full 2D. However, this requires overflow locations to be used in defining the connection between 1D and 2D models. It is therefore recommended that a hybrid 1D-2D model be applied when the overflow locations information over the study area become available. Preferably an initiative to collect this information for at least 5 years should be considered.

vii) To strengthen insights from this study, in addition to quantitative evaluation of the results of 2D HEC-RAS model using the five metrics including False Alarm Ratio (FAR), Hit Rate (HR), Critical Success Index (CSI) and Bias Error (Be), spatial location of the inundation should be verified, especially when adequate observed flood events extent data covering the entire area become available.

viii) WTP is a new concept to communities especially in developing countries. This can jeopardise data collection process especially explaining the benefits of the study to the affected communities and interesting them to participate in the survey. It is therefore recommended that responsible authorities sensitise the community on the benefits of the WTP approach and promote future research studies following the same approach.

ix) A related study could be conducted while focusing on the integration of society, policy and hydrology.

x) Apart from focusing on managing floods, it is recommended that equally other important weather-induced disasters in the area be considered. For instance, research focusing on investigating how much the community would be willing to pay for drought and landslides resilience programs. Consideration of other areas which are equally prone to weather-induced disasters, such as the Rwenzori region in western Uganda and other regions in Africa is recommended.

References

Abbott, M.B., Bathurst, J.C., Cunge, J.A., O'connell, P.., Rasmussen, J., 1986. An introduction to the European hydrological system - Systeme Hydrologique Europeen, 'SHE', 1: History and philosophy of a physically-based, distributed modelling system. Journal of Hydrology 87, 45–59.

Abtew, W., 1996. Evapotranspiration measurements and modeling for three wetland systems in south Florida. Journal of the American Water Resources Association 32, 465–473. https://doi.org/10.1111/j.1752-1688.1996.tb04044.x

Acey, C., Kisiangani, J., Ronoh, P., Delaire, C., Makena, E., Norman, G., Levine, D., Khush, R., Peletz, R., 2019. Cross-subsidies for improved sanitation in low income settlements: Assessing the willingness to pay of water utility customers in Kenyan cities. World Development 115, 160–177. https://doi.org/10.1016/j.worlddev.2018.11.006

Adler, R.F., Sapiano, M.R.P., Huffman, G.J., Wang, J.-J., Gu, G., Bolvin, D., Chiu, L., Schneider, U., Becker, A., Nelkin, E., Xie, P., Ferraro, R., Shin, D.-B., 2018. The Global Precipitation Climatology Project (GPCP) Monthly Analysis (New Version 2.3) and a Review of 2017 Global Precipitation. Atmosphere 9, 1–27. https://doi.org/10.3390/atmos9040138

Adnan, R.M., Liang, Z., Heddam, S., Kermani, M.Z.-, Kisi, O., Li, B., 2020. Least square support vector machine and multivariate adaptive regression splines for streamflow prediction in mountainous basin using hydro-meteorological data as inputs. Journal of Hydrology 586. https://doi.org/10.1016/j.jhydrol.2019.124371

Aghelpour, P., Varshavian, V., 2020. Evaluation of stochastic and artificial intelligence models in modeling and predicting of river daily flow time series. Stochastic Environmental Research and Risk Assessment 34, 33–50. https://doi.org/10.1007/s00477-019-01761-4

Alaska Satellite Facility, 2021. Alos Palsar. https://asf.alaska.edu/data-sets/sar-data-sets/alos-palsar/ (accessed 4.11.21).

Alemu, H., Kaptué, A.T., Senay, G.B., Wimberly, M.C., Henebry, G.M., 2015. Evapotranspiration in the Nile Basin: Identifying Dynamics and Drivers, 2002–2011. Water 7, 4914–4931. https://doi.org/10.3390/w7094914

Alexandersson, H., 1986. A homogeneity test applied to precipitation data. Journal of Climatology 6, 661–675.

Alkema, D., 2007. Simulating floods on the application of a 2D-hydraulic model for flood hazard and risk assessment. University of Utrecht.

Allen, R.G., Pereira, L.S., Raes, D., Smith, M., 1998. Crop evapotranspiration - Guidelines for computing crop water requirements - FAO Irrigation and drainage paper 56. FAO – Food and Agriculture Organization of the United Nations, Rome, Italy.

Alvi, M.H., 2016. A Manual for Selecting Sampling Techniques in Research. University of Karachi, Iqra University, Karachi, Pakistan.

Amadio, M., Rita Scorzini, A., Carisi, F., Essenfelder, H.A., Domeneghetti, A., Mysiak, J., Castellarin, A., 2019. Testing empirical and synthetic flood damage models: The case of Italy. Natural Hazards and Earth System Sciences 19, 661–678. https://doi.org/10.5194/nhess-19-661-2019

Amir, M.S.I.I., Khan, M.M.K., Rasul, M.G., Sharma, R.H., Akram, F., 2013. Automatic Multi-

Objective Calibration of a Rainfall Runoff Model for the Fitzroy Basin, Queensland, Australia. International Journal of Environmental Science and Development 4, 313–315.

Ampaire, E.L., Jassogne, L., Providence, H., Acosta, M., Twyman, J., Winowiecki, L., Astena, P. van, 2017. Institutional challenges to climate change adaptation: A case study on policy action gaps in Uganda. Environmental Science and Policy 75, 81–90. https://doi.org/10.1016/j.envsci.2017.05.013

Angella, N., Dick, S., Fred, B., 2014. Willingness to pay for irrigation water and its determinants among rice farmers at Doho Rice Irrigation Scheme (DRIS) in Uganda. Journal of Development and Agricultural Economics 6, 345–355. https://doi.org/10.5897/jdae2014.0580

Antolini, F., Tate, E., Dalzell, B., Young, N., Johnson, K., Hawthorne, P.L., 2020. Flood Risk Reduction from Agricultural Best Management Practices. Jounral of American Water Resources Association 56, 161–179. https://doi.org/10.1111/1752-1688.12812

Arnal, L., Ramos, M., Perez, E.C. De, Cloke, H.L., Stephens, E., Wetterhall, F., Andel, S.J. van, Pappenberger, F., 2016. Willingness-to-pay for a probabilistic flood forecast: a risk-based decision-making game. Hydrology and Earth System Sciences 20, 3109–3128. https://doi.org/10.5194/hess-20-3109-2016

Arnold, J.G., Moriasi, D.N., Gassman, P.W., Abbaspour, K.C., White, M.J., Srinivasan, R., Santhi, C., Harmel, R.D., Van Griensven, A., Van Liew, M.W., Kannan, N., Jha, M.K., 2012. SWAT: Model use, calibration, and validation. Transactions of the ASABE 55, 1491–1508.

Asadi, A., 2013. The Comparison of lumped and distributed models for estimating flood hydrograph (study area: Kabkian basin). Journal of Electronics and Communication Engineering Research 1, 7–13.

Ashouri, H., Hsu, K.L., Sorooshian, S., Braithwaite, D.K., Knapp, K.R., Cecil, L.D., Nelson, B.R., Prat, O.P., 2015. PERSIANN-CDR: Daily precipitation climate data record from multisatellite observations for hydrological and climate studies. Bulletin of the American Meteorological Society 96, 69–83. https://doi.org/10.1175/BAMS-D-13-00068.1

Assessment Capacity Project (ACAPS), 2018. Uganda: Flooding and landslides in Bududa. https://www.acaps.org/sites/acaps/files/products/files/20181018_acaps_start_briefing_note_uganda_flooding_and_landslides_in_bududa.pdf (accessed 10.15.20).

Atuyambe, L.M., Ediau, M., Orach, C.G., Musenero, M., Bazeyo, W., 2011. Land slide disaster in eastern Uganda: Rapid assessment of water, sanitation and hygiene situation in Bulucheke camp, Bududa district. Environmental Health 10, 1–22. https://doi.org/10.1186/1476-069X-10-38

Baan, P.J.A., Klijn, F., 2004. Flood risk perception and implications for flood risk management in the Netherlands. International Journal of River Basin Management 2, 113–122. https://doi.org/10.1080/15715124.2004.9635226

Baig, M.R.I., Ahmad, I.A., Shahfahad, Tayyab, M., Rahman, A., 2020. Annals of GIS Analysis of shoreline changes in Vishakhapatnam coastal tract of Andhra Pradesh, India: an application of digital shoreline analysis system (DSAS). Annals of GIS 26, 361–376. https://doi.org/10.1080/19475683.2020.1815839

Balderjahn, I., 1994. Der Einsatz der Conjoint-Analyse zur empirischen Bestimmung von Preisresponsefunktionen in. Marketing ZFP 16, 12–20.

Banga, M., Lokina, R.B., Mkenda, A.F., 2011. Households' willingness to pay for improved solid waste collection services in Kampala city, Uganda. Journal of Environment and Development 20, 428–448. https://doi.org/10.1177/1070496511426779

Barasa, B., Kakembo, V., Mugagga, F., Egeru, A., 2013. Comparison of extreme weather events and streamflow from drought indices and a hydrological model in River Malaba, Eastern Uganda. International Journal of Environmental Studies 70, 940–951. https://doi.org/10.1080/00207233.2013.862463

Barasa, B., Kakembo, V., Mwololo Waema, T., Laban, M., 2017. Effects of heterogeneous land use/cover types on river channel morphology in the Solo River catchment, Eastern Uganda. Geocarto International 32, 155–166. https://doi.org/10.1080/10106049.2015.1132480

Barnnett, J., Marrison, M., Blamey, R., 1998. Testing the validity of responses to contingency valuation questionnaire. Australia Journal of Agricultural Resources Economics 42, 131–148.

Bartlett, R.F., 1993. Linear Modelling of Pearson's Product Moment Correlation Coefficient: An Application of Fisher's z Transformation. Journal of the Royal Statistical Society 42, 45–53.

Bashar, K.E., 2012. Comparative Performance of Soil Moisture Accounting Approach in Continuous Hydrologic Simulation of the Blue Nile. Nile Basin Water Science & Engineering Journal 5, 1–10.

Bateman, I.J., Brouwer, R., Georgiou, S., Hanley, N., Machado, F., Mourato, S., Saunders, C., 2005. A 'natural experiment' approach to contingent valuation of private and public UV health risk reduction strategies in low and high-risk countries. Environmental and Resource Economics 31, 47–72. https://doi.org/10.1007/s10640-004-6978-7

Bedient, B.P., Huber, C.W., 2002. Hydrology and Floodplain Analysis. Prentice- Hall, Upper Saddle River, United States of America.

Beirland, J., Teugels, J.L., Vynckier, P., 1996. Practical analysis of extreme values, Insurance: Mathematics and Economics. Leuven University Press, Leuven, Belgium. https://doi.org/10.1016/s0167-6687(97)00022-x

Beirlant, J., Teugels, J., Vynckier, P., 1996. Practical analysis of extreme values. Leuven, University Press, Leuven, Belgium.

Bergström, S., 1992. The HBV model - its structure and applications, SMHI reports Hydrology. SMHI, NORRKÖPING Sweden.

Beven, K.J., Binley, A.M., 1992. The future role of distributed models: Model calibration and predictive uncertainty. Hydrological Processes 6, 279–298.

Birhanu, D., Kim, H., Jang, C., Park, S., 2018. Does the Complexity of Evapotranspiration and Hydrological Models Enhance Robustness? Sustainability 10, 1–34. https://doi.org/10.3390/su10082837

Blackman, R.B., Tukey, J.W., 1959. The Measurement of Power Spectra, Dover Publications. New York.

Blaney, H.F., Criddle, W.D., 1950. Determining water requirements in irrigated areas from climatological and irrigation data, 48th ed. U.S. Soil Conservation Service, Washington, DC.

BMT-WBM, 2018. TUFLOW 1D/2D Fixed Grid Hydraulic Modelling. TUFLOW and TUFLOW HPC hydrodynamic computational engines.

Bomuhangi, A., Nabanoga, G., Namaalwa, J.J., Jacobson, M.G., Abwoli, B., 2016. Local

communities' perceptions of climate variability in the Mt. Elgon region, eastern Uganda. Cogent Environmental Science 2, 1–16. https://doi.org/10.1080/23311843.2016.1168276

Botzen, W.J.W., Aerts, J.C.J.H., van den Bergh, J.C.J.M., 2013. Individual preferences for reducing flood risk to near zero through elevation. Mitigation and Adaptation Strategies for Global Change 18, 229–244. https://doi.org/10.1007/s11027-012-9359-5

Boughton, W., 2004. The Australian water balance model. Environmental Modelling & Software 19, 943–956. https://doi.org/10.1016/j.envsoft.2003.10.007

Boyle, K.J., 2017. Contingent Valuation in Practice, in: Champ P., Boyle K., B.T. (Ed.), A Primer on Nonmarket Valuation. The Economics of Non-Market Goods and Resources. Springer, Dordrecht. https://doi.org/10.1007/978-94-007-7104-8_4

Brémond, P., Grelot, F., Agenais, A.-L., 2013. Review Article: Economic evaluation of flood damage to agriculture - Review and analysis of existing methods. Natural Hazards and Earth System Sciences 13, 2493–2512. https://doi.org/10.5194/nhess-13-2493-2013

Brereton, R.G., 2015. The t -distribution and its relationship to the normal distribution. Journal of Chemometrics Columnist 29, 481–483. https://doi.org/10.1002/cem.2713

Brouwer, R., Akter, S., Brander, L., Haque, E., 2009. Economic valuation of flood risk exposure and reduction in a severely flood prone developing country. Environment and Development Economics 14, 397–417. https://doi.org/10.1017/S1355770X08004828

Brunner, G.W., 2016. HEC-RAS, River Analysis System Hydraulic Reference Manual. US Army Corps of Engineers Hydrologic Engineering Center (HEC), Davis, CA, USA.

Budhathoki, N.K., Lassa, J.A., Pun, S., Zander, K.K., 2019. Farmers' interest and willingness-to-pay for index-based crop insurance in the lowlands of Nepal. Land Use Policy 85, 1–10. https://doi.org/10.1016/j.landusepol.2019.03.029

Buishand, T.A., 1982. Some methods for testing the homogeneity of rainfall records. Journal of Hydrology 58, 11–27.

Burnash, R., 1995. The NWS River Forecast System-Catchment Modeling, in: Singh, V. (Ed.), Computer Models of Watershed Hydrology. Water Resources Publication, Colorado, pp. 311–366.

Caloiero, T., Coscarelli, R., Ferrari, E., 2018. Analysis of Monthly Rainfall Trend in Calabria (Southern Italy) through the Application of Statistical and Graphical Techniques. Proceedings 2. https://doi.org/10.3390/proceedings2110629

Camberlin, P., 2009. Nile Basin Climates, in: Dumont, H.J. (Ed.), The Nile: Origin, Environments, Limnology and Human Use. Springer, Berlin, Germany, pp. 307–333.

Carson, R.T., 2000. Contingent valuation: A user's guide. Environmental Science and Technology 34, 1413–1418. https://doi.org/10.1021/es990728j

Carson, R.T., Groves, T., 2011. Incentive and information properties of preference questions : commentary and extensions, in: The International Handbook on Non-Market Environmental Valuation. pp. 300–321.

Cengiz, T.M., Tabari, H., Onyutha, C., Kisi, O., 2020. Combined use of graphical and statistical approaches for analyzing historical precipitation changes in the black sea region of Turkey. Water 12, 1–19. https://doi.org/10.3390/w12030705

Charan, J., Biswas, T., 2013. How to calculate sample size for different study designs in medical

research? Indian Journal of Psychological Medicine 35, 121–126. https://doi.org/10.4103/0253-7176.116232

Chelangat, C., Abebe, A., 2021. Reservoir operation for optimal water use of Kabalega reservoir in Uganda. International Journal of Energy and Water Resources. https://doi.org/10.1007/s42108-020-00109-x

Chen, J., 2007. Flood Damage Map for the Huong River Basin. University of Twente, The Netherland.

Chen, T., Ren, L., Yuan, F., Yang, X., Jiang, S., Tang, T., Liu, Y., Zhao, C., Zhang, L., 2017. Comparison of spatial interpolation schemes for rainfall data and application in hydrological modeling. Water 9, 1–18. https://doi.org/10.3390/w9050342

Chia, S.Y., Macharia, J., Diiro, G.M., Kassie, M., Ekesi, S., van Loon, J.J.A., Dicke, M., Tanga, C.M., 2020. Smallholder farmers' knowledge and willingness to pay for insect-based feeds in Kenya. PLoS ONE 15, 1–25. https://doi.org/10.1371/journal.pone.0230552

Chowdhury, M.A., Khairun, Y., 2014. Farmers' Local Knowledge in Extensive Shrimp Farming Systems in Coastal Bangladesh. APCBEE Procedia 8, 125–130. https://doi.org/10.1016/j.apcbee.2014.03.013

City of Vancouver, 2020. Climate Change Adaptation Strategy.

Ciullo, A., Viglione, A., Castellarin, A., Crisci, M., Di Baldassarre, G., 2017. Socio-hydrological modelling of flood-risk dynamics: comparing the resilience of green and technological systems. Hydrological Sciences Journal 62, 880–891. https://doi.org/10.1080/02626667.2016.1273527

Cochran, W.G., 1977. SamplingTechniques, Third. ed, Sampling Techniques. John Wiley & Sons, Inc., New York, NY USA.

Cochran, W.G., 1963. Sampling Techniques, 2nd ed. John Wiley and Sons Inc., New York.

Costabile, P., Ostanzo, C., Ferraro, D., Macchione, F., Petaccia, G., 2020. Performances of the New HEC-RAS Version 5 for 2-D Hydrodynamic-Based Rainfall-Runoff Simulations at Basin Scale: Comparison with a State-of-the Art Model. Water 12, 1–19. https://doi.org/10.3390/w12092326

Croasmun, J.T., Ostrom, L., 2011. Using Likert-Type Scales in the Social Sciences. Jounral of Adult Education 40, 19–22.

Croke, B., Andrew, F., Spate, J., Cuddy, S., 2005. IHACRES User Guide. Technical Report 2005/19. Second Edition. iCAM, School of Resources, Environment and Society, The Australian National University, Canberra. Australia.

Cummings, R.G., Brookshire, D.S., Schulze, W.D., 1986. Valuing Environmental Goods—An Assessment of the Contingent Valuation Method. Rowman & Allanheld, Totowa NJ.

Daily Monitor, 2019. Famine looms as floods ravage gardens in eastern region. https://www.monitor.co.ug/uganda/news/national/famine-looms-as-floods-ravage-gardens-in-eastern-region-1855692 (accessed 6.15.21).

Danso, G.K., Otoo, M., Ekere, W., Ddungu, S., Madurangi, G., 2017. Market Feasibility of Faecal Sludge and Municipal Solid Waste-Based Compost as Measured by Farmers' Willingness-to-Pay for Product Attributes: Evidence from Kampala, Uganda. resources 6, 1–17. https://doi.org/10.3390/resources6030031

Das, S., 2019. Extreme rainfall estimation at ungauged sites: Comparison between region-of-influence approach of regional analysis and spatial interpolation technique. International Journal of Climatology 39, 407–423. https://doi.org/10.1002/joc.5819

David Ford, Pingel, N., DeVries, J.J., 2008. Hydrologic Modeling System - HEC-HMS - Applications Guide. US Army Corps of Engineers Hydrologic Engineering Center, HEC, Davis, CA, USA.

Deltares systems, 2019. SOBEK Hydrodynamics, Rainfall Runoff and Real Time Control-User Manual. Deltares, Delft, Netherlands.

Devkota, S., Shakya, M.N., Sudmeier-rieux, K., Jaboyedoff, M., Westen, C.J. Van, Mcadoo, B.G., Adhikari, A., 2018. Development of Monsoonal Rainfall Empirical Model for Data-Scarce Situations: The Case of the Central-Western Hills (Panchase Region) of Nepal. Hydrology 5, 1–27. https://doi.org/10.3390/hydrology5020027

DHI, 2017. MIKE 21 Flow Model User Manual. DHI.

Dhungel, S., Barber, M.E., Mahler, R.L., 2019. Comparison of one-and two- dimesnional flood modelling in urban environments. International Journal of Sustainable Development and Planning 14, 356–366. https://doi.org/10.2495/SDP-V14-N4-356-366

Di Baldassarre, G., Viglione, A., Carr, G., Kuil, L., Salinas, J.L., Blöschl, G., 2013. Socio-hydrology: Conceptualising human-flood interactions. Hydrology and Earth System Sciences 17, 3295–3303. https://doi.org/10.5194/hess-17-3295-2013

Downer, C.W., Ogden, F.L., Martin, W.D., Harmon, R.S., 2002. Theory, development, and applicability of the surface water hydrologic model CASC2D. Hydrological Processes 16, 255–275. https://doi.org/10.1002/hyp.338

Duan, Q.Y., Gupta, V.K., Sorooshian, S., 1993. Shuffled complex evolution approach for effective and efficient global minimization. Journal of Optimisation and Theory Appllication 76, 501–521.

Ebtehaj, I., Zeynoddin, M., Bonakdari, H., 2020. Discussion of "Comparative assessment of time series and artificial intelligence models to estimate monthly streamflow: A local and external data analysis approach" by Saeid Mehdizadeh, Farshad Fathian, Mir Jafar Sadegh Safari and Jan F. Adamowski. Journal of Hydrology 583. https://doi.org/10.1016/j.jhydrol.2020.124614

Echendu, A.J., 2020. The impact of flooding on Nigeria's sustainable development goals (SDGs). Ecosystem Health and Sustainability 6, 1–13. https://doi.org/10.1080/20964129.2020.1791735

Echeverría, D., Terton, A., Alec, C., 2016. Review of Current and Planned Adaptation Action in Uganda, CARIAA Working Papers#19. London, United Kingdom.

Ednah, M.C., 2018. Sustainable Water use in Lake Edward-George Basin: a case study of River Mubuku-Sebwe sub-catchments. MSc. Thesis, Department of Environmental Management, Makerere University.

Ehret, U., Zehe, E., Wulfmeyer, V., Warrach-Sagi, K., Liebert, J., 2012. HESS Opinions "Should we apply bias correction to global and regional climate model data?" Hydrology and Earth System Sciences 16, 3391–3404. https://doi.org/10.5194/hess-16-3391-2012

Entorf, H., Jensen, A., 2020. Willingness-to-pay for hazard safety – A case study on the valuation of flood risk reduction in Germany. Safety Science 128, 10. https://doi.org/10.1016/j.ssci.2020.104657

Erena, S.H., Worku, H., 2018. Flood risk analysis: causes and landscape based mitigation strategies in Dire Dawa city, Ethiopia. Geoenvironmental Disasters 5, 1–19. https://doi.org/10.1186/s40677-018-0110-8

Eridadi, H.M., Yoshihiko, I., Alemayehu, E., Kiwanuka, M., 2021. Evaluation of willingness to pay toward improving water supply services in Sebeta town, Ethiopia. Journal of Water 11, 282–294. https://doi.org/10.2166/washdev.2021.204

Eskandari-Damaneh, H., Noroozi, H., Ghoochani, O.M., Taheri-Reykandeh, E., Cotton, M., 2020. Evaluating rural participation in wetland management: A contingent valuation analysis of the set-aside policy in Iran. Science of the Total Environment 747, 1–10. https://doi.org/10.1016/j.scitotenv.2020.141127

Far, S.S., Wahab, A.K.A., 2016. Evaluation of Peaks-Over-Threshold Method. Ocean Science Discussions 1–25. https://doi.org/10.5194/os-2016-47

Feizollahi, S., Shirmohammadi, A., Kahreh, Z.S., Kahreh, M.S., 2014. Investigation the effect of Internet Technology on Performance of services organizations with e-commerce orientations. Procedia - Social and Behavioral Sciences 109, 605–609. https://doi.org/10.1016/j.sbspro.2013.12.514

Floodlist, 2021. Uganda - severe flooding affects thousands in Butaleja. http://floodlist.com/africa/uganda-flooding-butaleja-may-2021 (accessed 6.14.21).

Floodlist, 2019. Uganda – Deadly Floods and Landslides in Eastern Region (updated). http://floodlist.com/africa/uganda-floods-bududa-sironko-december-2019 (accessed 1.10.20).

Fujita, Y., Fujii, A., Furukawa, S., Ogawa, T., 2005. Estimation of Willingness-to-Pay (WTP) for Water and Sanitation Services through Contingent Valuation Method (CVM) A Case Study in Iquitos City, The Republic of Peru. JBICI Review 10, 59–87.

Funahashi, H., Shibli, S., Sotiriadou, P., Mäkinen, J., Dijk, B., De Bosscher, V., 2020. Valuing elite sport success using the contingent valuation method: A transnational study. Sport Management Review 23, 548–562. https://doi.org/10.1016/j.smr.2019.05.008

Gaglias, A., Mirasgedis, S., Tourkolias, C., Georgopoulou, E., 2016. Implementing the Contingent Valuation Method for supporting decision making in the waste management sector. Waste Management 53, 237–244. https://doi.org/10.1016/j.wasman.2016.04.012

Galárraga, O., Sosa-Rubí, S.G., Infante, C., Gertler, P.J., Bertozzi, S.M., 2014. Willingness-to-accept reductions in HIV risks: conditional economic incentives in Mexico. National Institute of Health Public Access 15, 41–55. https://doi.org/10.1007/s10198-012-0447-y

Garcia, M., Juan, A., Bedient, P., 2020. Integrating reservoir operations and flood modeling with HEC-RAS 2D. Water 12, 1–8. https://doi.org/10.3390/w12082259

Ghanbarpour, M.R., Saravi, M.M., Salimi, S., 2014. Floodplain Inundation Analysis Combined with Contingent Valuation: Implications for Sustainable Flood Risk Management. Water Resources Management 28, 2491–2505. https://doi.org/10.1007/s11269-014-0622-2

Ghimire, E., 2019. Evaluation of One-Dimensional and Two-Dimensional HEC-RAS Models for Flood Travel Time Prediction and Damage Assessment Using HAZUS-MH: A Case Study of Grand River, Ohio. Youngstown State University.

Ginsburgh, V., 2017. Economic ideas you should forget, in: Frey, B.S., Iselin, D. (Eds.), Economic Ideas You Should Forget. Springer International Publishing AG. https://doi.org/10.1007/978-

3-319-47458-8_26

Glenn, I.D., 1992. Sampling the evidence of extension program impact. Program Evaluation and Organizational Development (PEOD-5), IFAS Extension, University of Florida.

Goodarzi, M.S., Amiri, B.J., Azarneyvand, H., Khazaee, M., Mahdianzadeh, N., 2020. Assessing the Performance of a Hydrological Tank Model at Various Spatial Scales. Journal of Water Management Modeling 29, 1–8. https://doi.org/10.14796/JWMM.C472

Gravitiani, E., Suryanto, 2017. Valuing the Economic Impact of Flood Mitigation in Central Java, Indonesia. Journal of Business and Economics Review 2, 49–55.

Green, P.E., Rao, V.R., 1971. Conjoint Measurement for Quantifying Judgmental Data. Journal of Marketing Research 8, 355–363. https://doi.org/10.2307/3149575

Green, P.E., Srinivasan, V., 1990. Conjoint Analysis in Marketing: New Developments with Implications for Research and Practice. Journal of Marketing 54, 3–19. https://doi.org/10.2307/1251756

Green, P.E., Srinivasan, V., 1978. Conjoint Analysis in Consumer Research: Issues and Outlook. Journal of Consumer Research 5, 103–123. https://doi.org/10.1086/208721

Griensven, A. Van, Ndomba, P., Yalew, S., Kilonzo, F., 2012. Critical review of SWAT applications in the upper Nile basin countries. Hydrology and Earth System Sciences 16, 3371–3381. https://doi.org/10.5194/hess-16-3371-2012

Grimaldi, S., Nardi, F., Piscopia, R., Petroselli, A., Apollonio, C., 2020. Continuous hydrologic modelling for design simulation in small and ungauged basins: a step forward and some tests for its practical use. Journal of Hydrology 125664. https://doi.org/10.1016/j.jhydrol.2020.125664

Gupta, H. V, Kling, H., Yilmaz, K.K., Martinez, G.F., 2009. Decomposition of the mean squared error and NSE performance criteria: Implications for improving hydrological modelling. Journal of Hydrology 377, 80–91. https://doi.org/10.1016/j.jhydrol.2009.08.003

Haab, T.C., McConnell, K.E., 2002. Valuing environmental and natural resources. The econometrics of non-market valuation. Edward Elgar Publishing, Chetenham, UK.

Haan, C.T., 1977. Statistical Methods in Hydrology. Ames: Iowa State University Press.

Hamon, W.R., 1963. Computation of direct runoff amounts from storm rainfall. International Association of Sciences Hydrological Publications 63, 52–62.

Hansen, K.S., Pedrazzoli, D., Mbonye, A., Clarke, S., Cundill, B., Magnussen, P., Yeung, S., 2013. Willingness-to-pay for a rapid malaria diagnostic test and artemisinin-based combination therapy from private drug shops in Mukono district, Uganda. Health Policy and Planning 28, 185–196. https://doi.org/10.1093/heapol/czs048

Hargreaves, G.H., Allen, R.G., 2003. History and evaluation of hargreaves evapotranspiration equation. Journal of Irrigation and Drainage Engineering 129, 53–63. https://doi.org/10.1061/(ASCE)0733-9437(2003)129:1(53)

Hargreaves, G.H., Samani, Z.A., 1985. Reference crop evapotranspiration from temperature. Transactions - American Society of Agricultural Engineers 1, 96–99.

Hargreaves, G.H., Samani, Z.A., 1982. Estimation of potential evapotranspiration. Journal of Irrigation and Drainage Division 108, 225–230.

Harris, I., Jones, P.D., Osborn, T.J., Lister, D.H., 2014. Updated high-resolution grids of monthly

climatic observations - the CRU TS3.10 Dataset. International Journal of Climatology 34, 623–642. https://doi.org/10.1002/joc.3711

Harris, I., Osborn, T.J., Jones, P., Lister, D., 2020. Version 4 of the CRU TS monthly high-resolution gridded multivariate climate dataset. Scientific data 7, 1–18. https://doi.org/10.1038/s41597-020-0453-3

Hill, B.M., 1975. Institute of Mathematical Statistics is collaborating with JSTOR to digitize, preserve, and extend access to The Annals of Statistics. ® www.jstor.org. The Annals of Statistics 3, 1163–1174.

Höffken, J., Vafeidis, A.T., MacPherson, L.R., Dangendorf, S., 2020. Effects of the Temporal Variability of Storm Surges on Coastal Flooding. Frontiers in Marine Science 7, 1–14. https://doi.org/10.3389/fmars.2020.00098

Huang, Y., Qin, X., 2014. Uncertainty analysis for flood inundation modelling with a random floodplain roughness field. Environmental Systems Research 3, 1–7.

Huffman, G.J., Adler, R.F., Bolvin, D.T., Gu, G., Nelkin, E.J., Bowman, K.P., Hong, Y., Stocker, E.F., Wolff, D.B., 2007. The TRMM Multisatellite Precipitation Analysis (TMPA): Quasi-global, multiyear, combined-sensor precipitation estimates at fine scales. Journal of Hydrometeorology 8, 38–55. https://doi.org/10.1175/JHM560.1

Huizinga, J., De Moel, H., Szewczyk, W., 2017. Global flood depth-damage functions: Methodology and the database with guidelines, EUR 28552 EN, Publications Office of the European Union, Luxembourg. https://doi.org/10.2760/16510, JRC105688

Ialongo, C., 2019. Confidence interval for quantiles and percentiles. Biochemia Medica 29, 1–13. https://doi.org/10.11613/BM.2019.010101

Ikeuchi, A., Tsuji, K., Yoshikane, F., Ikeuchi, U., 2013. Double-bounded Dichotomous Choice CVM for Public Library Services in Japan. Procedia - Social and Behavioral Sciences 73, 205–208. https://doi.org/10.1016/j.sbspro.2013.02.042

Insitute of Hydrology, 1980. Low flow studies report1. Insitute of Hydrology, Wallingford, United Kingdom.

Jaiswal, R.K., Ali, S., Bharti, B., 2020. Comparative evaluation of conceptual and physical rainfall – runoff models. Applied Water Science 10, 1–14. https://doi.org/10.1007/s13201-019-1122-6

Jakeman, A.J., Hornberger, G.M., 1993. How Much Complexity Is Warranted in a Rainfall-Runoff Model? Water Resources Research 29, 2637–2649.

Jakeman, A.J., Littlewood, I.G., Whitehead, P.G., 1990. Computation of the instantaneous unit hydrograph and identifiable component flows with application to two small upland catchments. Journal of Hydrology 117, 275–300. https://doi.org/10.1016/0022-1694(90)90097-H

Jiang, D., Bai, D., Yin, Z., Fan, G., 2019. Willingness to Pay for Enhanced Water Security in a Rapidly Developing Shale Gas Region in China. Water 11, 1–14. https://doi.org/10.3390/w11091888

JICA, 2011. The development study on water resources development and management for Lake Kyoga Basin in the Republic of Uganda. Final report, Supporting report. JICA, Kampala, Uganda.

Jofre-bonet, M., Kamara, J., 2018. Willingness to pay for health insurance in the informal sector

of Sierra Leone. PLoS ONE 13, 1–18. https://doi.org/10.1371/journal.pone.0189915

Jones, B.A., Ripberger, J., Jenkins-Smith, H., Silva, C., 2017. Estimating willingness to pay for greenhouse gas emission reductions provided by hydropower using the contingent valuation method. Energy Policy 111, 362–370. https://doi.org/10.1016/j.enpol.2017.09.004

Joshi, A., Kale, S., Chandel, S., Pal, D.K., 2015. Likert Scale: Explored and Explained. British Journal of Applied Science & Technology 7, 396–403. https://doi.org/10.9734/BJAST/2015/14975

Jury, M.R., 2018. Uganda rainfall variability and prediction. Theoretical and Applied Climatology 132, 905–919. https://doi.org/10.1007/s00704-017-2135-4

Kalnay, E., Kanamitsu, M., Kistler, R., Collins, W., Deaven, D., Gandin, L., Iredell, M., Saha, S., White, G., Woollen, J., Zhu, Y., Chelliah, M., Ebisuzaki, W., Higgins, W., Janowiak, J., Mo, K.C., Ropelewski, C., Wang, J., Leetmaa, A., Reynolds, R., Jenne, R., Joseph, D., 1996. The NCEP NCAR 40-Year Reanalysis Project. Bulletin of the American Meteorological Society 77, 437–472. https://doi.org/10.1175/1520-0477(1996)077<0437:TNYRP>2.0.CO;2

Kangieser, P.C., Blackadar, A., 1994. Estimating the likelihood of extreme events. Weatherwise 47, 38–40.

Kansiime, M.K., Wambugu, S.K., Shisanya, C.A., 2013. Perceived and Actual Rainfall Trends and Variability in Eastern Uganda: Implications for Community Preparedness and Response. Journal of Natural Sciences Research 3, 179–195.

Kendall, M.G., 1975. Rank correlation methods, 4th ed. Charles Griffin, London.

Khan, N., Shahid, S., Ismail, T., Ahmed, K., Nawaz, N., 2018. Trends in heat wave related indices in Pakistan. Stochastic Environmental Research and Risk Assessment 33, 287–302. https://doi.org/10.1007/s00477-018-1605-2

Khan, N.I., Brouwer, R., Yang, H., 2014. Household's willingness to pay for arsenic safe drinking water in Bangladesh. Journal of Environmental Management 143, 151–161. https://doi.org/10.1016/j.jenvman.2014.04.018

Kikulwe, E.M., Asindu, M., 2020. A contingent valuation analysis for assessing the market for genetically modified planting materials among banana producing households in Uganda. GM Crops and Food 11, 113–124. https://doi.org/10.1080/21645698.2020.1720498

Kitutu, M.G., Muwanga, A., Poesen, J., Deckers, J.A., 2009. Influence of soil properties on landslide occurrences in Bududa district, Eastern Uganda. African Journal of Agricultural Research 4, 611–620.

Kiyengo, R., Majaliwa, M., Twinomuhangi, R., Waswa, H., 2019. Spatio-temporal flood trends & settlement choice in flood-prone areas. A case study of Lubiji micro-catchment, Kampala City. International Journal of Environmental Studies 1–13. https://doi.org/10.1080/00207233.2019.1686910

Kizza, M., Rodhe, A., Xu, C.Y., Ntale, H.K., Halldin, S., 2009. Temporal rainfall variability in the Lake Victoria Basin in East Africa during the twentieth century. Theoretical and Applied Climatology 98, 119–135. https://doi.org/10.1007/s00704-008-0093-6

Knoben, W.J.M., Freer, J.E., Woods, R.A., 2019. Technical note: Inherent benchmark or not? Comparing Nash-Sutcliffe and Kling-Gupta efficiency scores. Hydrology and Earth System Sciences 23, 4323–4331. https://doi.org/10.5194/hess-23-4323-2019

Knoema, 2021. Uganda - Paddy rice yield.

https://knoema.com/atlas/Uganda/topics/Agriculture/Crops-Production-Yield/Paddy-rice-yield (accessed 6.15.21).

Kocsis, T., Kovács-Székely, I., Anda, A., 2020. Homogeneity tests and non-parametric analyses of tendencies in precipitation time series in Keszthely, Western Hungary. Theoretical and Applied Climatology 139, 849–859. https://doi.org/10.1007/s00704-019-03014-4

Koenig, T.A., Bruce, J.L., O'Connor, J., McGee, B.D., Holmes, R.R., Hollins, R.J., Forbes, B.T., Kohn, M.S., Schellekens, M.F., Martin, Z.W., Peppler, M.C., 2016. Identifying and preserving high-water mark data, in: Surface-Water Techniques Book 3, Applications of Hydraulics. U.S. Geological Survey, Science Information Delivery, Denver, Colorado, p. 60.

Krause, P., Boyle, D.P., Bäse, F., 2005. Comparison of different efficiency criteria for hydrological model assessment. Advances in Geosciences 5, 89–97. https://doi.org/10.5194/adgeo-5-89-2005

Kreibich, H., Christenberger, S., Schwarze, R., 2011. Economic motivation of households to undertake private precautionary measures against floods. Natural Hazards and Earth System Sciences 11, 309–321. https://doi.org/10.5194/nhess-11-309-2011

Krishnaswamy, J., Bonell, M., Venkatesh, B., Purandara, B.K., Rakesh, K.N., Lele, S., Kiran, M.C., Reddy, V., Badiger, S., 2013. The groundwater recharge response and hydrologic services of tropical humid forest ecosystems to use and reforestation: Support for the '"infiltration-evapotranspiration trade-off hypothesis"'. Journal of Hydrology 498, 191–209. https://doi.org/10.1016/j.jhydrol.2013.06.034

Kroonenberg, P.M., Verbeek, A., 2018. The Tale of Cochran's Rule: My Contingency Table has so Many Expected Values Smaller than 5, What Am I to Do? The American Statistician 72, 175–183. https://doi.org/10.1080/00031305.2017.1286260

Kumar, K., 1989. Conducting Key Informant Interviews in Developing Countries; A.I.D. Program Design and Evaluation Methodology Report No. 13. https://doi.org/10.1190/segam2013-0137.1

Kumar, N., Kumar, M., Sherring, A., Suryavanshi, S., Ahmad, A., Lal, D., 2019. Applicability of HEC - RAS 2D and GFMS for flood extent mapping: a case study of Sangam area, Prayagraj, India. Modeling Earth Systems and Environment 9. https://doi.org/10.1007/s40808-019-00687-8

Lam, K.C., Bryant, R.G., Wainright, J., 2015. Application of spatial interpolation method for estimating the spatial variability of rainfall in Semiarid New Mexico, USA. Mediterranean Journal of Social Sciences 6, 108–116. https://doi.org/10.5901/mjss.2015.v6n4s3p108

Lang, M., Ouarda, T.B.M.J., Bobée, B., 1999. Towards operational guidelines for over-threshold modeling. Journal of Hydrology 225, 103–117. https://doi.org/10.1016/S0022-1694(99)00167-5

Langbein, W.., 1949. Annual Floods and the Partial-Duration Flood Series. Transactions American Geophysical Union 30, 879–881.

Leavesley, G.H., Restrepo, P.J., Markstrom, S.L., Dixon, M., Stannard, L.G., 1996. The Modular Modeling System (MMS): User's manual. Geological Survey (U.S.) Open-File Report 96-151, Denver, Colorado. https://doi.org/10.3133/ofr96151

Lehmann, E.L., 1975. Nonparametrics: Statistical Methods Based on Ranks. Holden-Day, San-Francisco, Calif, USA.

Lehmann, N., Finger, R., Klein, T., Calanca, P., 2013. Sample Size Requirements for Assessing Statistical Moments of Simulated Crop Yield Distributions. Agriculture 3, 210–220. https://doi.org/10.3390/agriculture3020210

Levina, E., Tirpak, D., 2006. Adaptation to Climate Change: Key Terms. Paris, France.

Li, B., Rodell, M., Sheffield, J., Wood, E., Sutanudjaja, E., 2019. Long-term, non-anthropogenic groundwater storage changes simulated by three global-scale hydrological models. Scientific Reports 9, 1–13. https://doi.org/10.1038/s41598-019-47219-z

Li, C., Wang, H., Liu, J., Yan, D., Yu, F., Zhang, L., 2010. Effect of calibration data series length on performance and optimal parameters of hydrological model. Water Science and Engineering 3, 378–393. https://doi.org/10.3882/j.issn.1674-2370.2010.04.002

Li, H., Beldring, S., Xu, C., 2015. Stability of model performance and parameter values on two catchments facing changes in climatic conditions. Hydrological Sciences Journal 60, 1317–1330. https://doi.org/10.1080/02626667.2014.978333

Li, Z., Yang, Y., Kan, G., Hong, Y., 2018. Study on the applicability of the Hargreaves potential evapotranspiration estimation method in CREST distributed hydrological model (version 3.0) applications. Water 10, 1–15. https://doi.org/10.3390/w10121882

Likert, R., 1932. A Technique for the Measurement of Attitude, Archives of Psychology. New York. https://doi.org/2731047

Linacre, E.T., 1977. A simple formula for estimating evaporation rates in various climates, using temperature data alone. Agricultural Meteorology 18, 409–424. https://doi.org/10.1016/0002-1571(77)90007-3

Link, K.G., Stobb, M.T., Paola, J. Di, Neeves, K.B., Fogelson, A.L., Sindi, S.S., Leiderman, K., 2018. A local and global sensitivity analysis of a mathematical model of coagulation and platelet deposition under flow. PLoS ONE 13, 1–38. https://doi.org/10.1371/journal.pone.0200917

Lloyd, C.D., 2005. Assessing the effect of integrating elevation data into the estimation of monthly precipitation in Great Britain. Journal of Hydrology 308, 128–150. https://doi.org/10.1016/j.jhydrol.2004.10.026

Loomis, J.B., 1990. Comparative Reliability of the Dichotomous Choice and Open-Ended Contingent Valuation Techniques. Journal of Environmental Economics and Management 18, 78–85.

Lopez-Feldman, A., 2010. 'DOUBLEB: Stata module to compute Contingent Valuation using Double-Bounded Dichotomous Choice,' Statistical Software Components S457168, Boston College Department of Economics, revised 14 Oct 2013.

Lopez-Feldman, A.C., 2012. Introduction to contingent valuation using Stata. Munich Personal RePEc Archive. https://mpra.ub.uni-muenchen.de/41018/ (accessed 5.24.21).

Lorenz, N.E., 1956. Empirical Orthogonal Functions and Statistical Weather Prediction. Scientific report No.1. Statistical Forecasting Project. Department of Meteorology, Massachusetts Institute of Technology, Cambridge.

Lu, G.Y., Wong, D.W., 2008. An adaptive inverse-distance weighting spatial interpolation technique. Computers and Geosciences 34, 1044–1055. https://doi.org/10.1016/j.cageo.2007.07.010

Luwa, J.K., Majaliwa, J.-G.M., Bamutaze, Y., Kabenge, I., Pilesjo, P., Oriangi, G., Mukengere,

E.B., 2021. Variabilities and Trends of Rainfall, Temperature, and River Flow in Sipi Sub-Catchment on the Slopes of Mt. Elgon, Uganda. Water 13, 1–17. https://doi.org/10.3390/w13131834

Lyu, H., Xu, Y., Cheng, W., Arulrajah, A., 2018. Flooding Hazards across Southern China and Prospective Sustainability Measures. Sustainability 10, 1–18. https://doi.org/10.3390/su10051682

Ma, Q., Dai, C., Jin, H., Liang, S., Bense, V.F., Lan, Y., Marchenko, S.S., Wang, C., 2021. Streamflow changes in the headwater area of Yellow river, NE Qinghai-Tibet plateau during 1955–2040 and their implications. Water 13, 1–17. https://doi.org/10.3390/w13101360

Ma, Z., Liu, Z., Zhao, Y., Zhang, L., Liu, D., Ren, T., Zhang, I., Li, S., 2020. An unsupervised crop classification method based on principal components isometric binning. International Jounral of Geo-Information 9, 124. https://doi.org/10.3390/ijgi9110648

Macleod, D.A., Dankers, R., Graham, R., Guigma, K., Jenkins, L., Todd, M.C., Kiptum, A., Kilavi, M., Njogu, A., Mwangi, E., 2021. Drivers and subseasonal predictability of heavy rainfall in equatorial east africa and relationship with flood risk. Journal of Hydrometeorology 22, 887–903. https://doi.org/10.1175/JHM-D-20-0211.1

Maghsood, F.F., Moradi, H., Berndtsson, R., Panahi, M., Daneshi, A., Hashemi, H., Bavani, A.R.M., 2019. Social acceptability of flood management strategies under climate change using contingent valuation method (CVM). Sustainability 11, 1–18. https://doi.org/10.3390/su11185053

Majaliwa, J.G.., Tenywa, M.., Bamanya, D., Majugu, W., Isabirye, P., Nandozi, C., Nampijja, J., Musinguzi, P., Nimusiima, A., C, L.K., Rao, K., Bonabana, J., Bagamba, F., Sebuliba, E., Azanga, E., Sridher, G., 2015. Characterization of historical seasonal and annual rainfall and temperature trends in selected climatological homogenous rainfall zones of Uganda. Global Journal of Science Frontier Research 15, 1–21.

Makkink, G.F., 1957. Testing the Penman formula by means of lysimeters. Journal Institute of Water Engineers 11, 277–288.

Makwinja, R., Kosamu, I.B.M., Kaonga, C.C., 2019. Determinants and Values of Willingness to Pay for Water Quality Improvement: Insights from Chia Lagoon, Malawi. Sustainability 11, 26.

Mann, H.B., 1945. Nonparametric Test Against Trend. Econometrica 13, 245–259.

Markantonis, V., Meyer, V., Lienhoop, N., 2013. Evaluation of the environmental impacts of extreme floods in the Evros River basin using Contingent Valuation Method. Natural Hazards 69, 1535–1549. https://doi.org/10.1007/s11069-013-0762-3

Martín-Fernndez, J., Del Cura-Gonzlez, M.I., Gámez-Gascán, T., Oliva-Moreno, J., Domínguez-Bidagor, J., Beamud-Lagos, M., Pérez-Rivas, F.J., 2010. Differences between willingness to pay and willingness to accept for visits by a family physician: A contingent valuation study. BMC Public Health 10, 1–11. https://doi.org/10.1186/1471-2458-10-236

Martínez-Gomariz, E., Forero-Ortiz, E., Guerrero-Hidalga, M., Castán, S., Gómez, M., 2020. Flood depth-damage curves for Spanish urban areas. Sustainability 12, 1–25. https://doi.org/10.3390/su12072666

Mathers, N., Fox, N., Hunn, A., 2007. Surveys and Questionnaires. The NIHR RDS for the East Midlands / Yorkshire & the Humber.

Mayega, R.W., Tumuhamye, N., Atuyambe, L., Okello, D., Bua, G., Ssentongo, J., Bazeyo, W., 2015. Qualitative Assessment of Resilience to the Effects of Climate Variability in the Three Communities in Uganda. RAN Secretariat and East African Resilience Innovation Lab (EA RILab), Kampala, Uganda.

McGrath, H., Abo El Ezz, A., Nastev, M., 2019. Probabilistic depth–damage curves for assessment of flood-induced building losses. Natural Hazards 97, 1–14. https://doi.org/10.1007/s11069-019-03622-3

McKenna, S.A., Main, D.S., 2013. The role and influence of key informants in community-engaged research: A critical perspective. Action Research 11, 113–124. https://doi.org/10.1177/1476750312473342

Mekonnen, A., Gebreegziabher, Z., Beyene, A.D., Hagos, F., 2019. Valuation of Access to Irrigation Water in Rural Ethiopia: Application of Choice Experiment and Contingent Valuation Methods. World Economics and Policy 26. https://doi.org/10.1142/S2382624X19500073

Mesić, I.K., 2016. Comparison of Ordinary and Universal Kriging interpolation techniques on a depth variable (a case of linear spatial trend), case study of the Šandrovac Field. The Mining-Geology-Petroleum Engineering Bulletin 41–58. https://doi.org/10.17794/rgn.2016.2.4

Miah, M.Q., 1993. Applied Statistics for Human Settlement Planning, Asian Insititute of Technology. Bangkok, Thailand.

Ministry of Water and Environment, 2018a. Mpologoma Catchment Management Plan. Ministry of Water and Environment, Kampala, Uganda.

Ministry of Water and Environment, 2018b. Uganda National Climate Change Policy (Summary Version): Transformation through Climate Change Mitigation and Adaptation, Ministry of Water and Environment. Kampala, Uganda.

Ministry of Water and Environment, 2015. Water and Environment Sector Performance Report 2015. Ministry of Water and Environment, Kampala, Uganda.

Ministry of Water and Environment, 2014a. Uganda Second National Communication to the United Nations Framework Convention on Climate Change. Kampala, Uganda.

Ministry of Water and Environment, 2014b. Uganda Catchment Management Planning Guidelines. Ministry of Water and Environment, Kampala, Uganda.

Mitchell, R.C., Carson, R.T., 1989. Using surveys to value public goods. The Contingent valuation method. Resources for the Future, Washington, DC, USA.

Molinari, D., Rita Scorzini, A., Arrighi, C., Carisi, F., Castelli, F., Domeneghetti, A., Gallazzi, A., Galliani, M., Grelot, F., Kellermann, P., Kreibich, H., Mohor, G.S., Mosimann, M., Natho, S., Richert, C., Schroeter, K., Thieken, A.H., Paul Zischg, A., Ballio, F., 2020. Are flood damage models converging to 'reality'? Lessons learnt from a blind test. Natural Hazards and Earth System Sciences 20, 2997–3017. https://doi.org/10.5194/nhess-20-2997-2020

Morgan, S.J., Pullon, S.R.H., Macdonald, L.M., Mckinlay, E.M., Gray, B. V, 2017. Case Study Observational Research: A Framework for Conducting Case Study Research Where Observation Data Are the Focus. Qualitative Health Research 27, 1060–1068. https://doi.org/10.1177/1049732316649160

Mubialiwo, A., Abebe, A., Kawo, N.S., Ekolu, J., Nadarajah, S., Onyutha, C., 2022. Hydrodynamic modelling of floods and estimating socio-economic impacts of floods in

Ugandan River Malaba sub-catchment. Earth Systems and Environment 6, 45–67. https://doi.org/10.1007/s41748-021-00283-w

Mubialiwo, A., Abebe, A., Onyutha, C., 2021a. Performance of rainfall – runoff models in reproducing hydrological extremes: a case of the River Malaba sub-catchment. SN Applied Sciences 3, 24. https://doi.org/10.1007/s42452-021-04514-7

Mubialiwo, A., Abebe, A., Onyutha, C., 2021b. Analyses of community willingness-to-pay and the influencing factors towards restoration of River Malaba floodplains. Environmental Challenges 4, 1–14. https://doi.org/10.1016/j.envc.2021.100160

Mubialiwo, A., Chelangat, C., Onyutha, C., 2021c. Changes in precipitation and evapotranspiration over Lokok and Lokere catchments in Uganda. Bulletin of Atmospheric Science and Technology 2, 1–23. https://doi.org/10.1007/s42865-021-00031-y

Mubialiwo, A., Onyutha, C., Abebe, A., 2020. Historical Rainfall and Evapotranspiration Changes over Mpologoma Catchment in Uganda. Advances in Meteorology 2020, 1–19. https://doi.org/10.1155/2020/8870935

Mugume, I., Mesquita, M.D.S., Basalirwa, C., Bamutaze, Y., Reuder, J., Nimusiima, A., Waiswa, D., Mujuni, G., Tao, S., Ngailo, T.J., 2016. Patterns of dekadal rainfall variation over a selected region in Lake Victoria Basin, Uganda. Atmosphere 7, 1–23. https://doi.org/10.3390/atmos7110150

Mwaura, F.M., Okoboi, G., 2014. Climate Variability and Crop Production in Uganda. Journal of Sustainable Development 7, 159–172. https://doi.org/10.5539/jsd.v7n2p159

Naing, L., Winn, T., Rusli, B.N., 2016. Practical Issues in Calculating the Sample Size for Prevalence Studies. Archives of Orofacial Sciences 1, 9–14. https://doi.org/10.1016/j.dld.2018.11.003

Nair, S., Srinivasan, G., Nemani, R., 2009. Evaluation of multi-satellite TRMM derived rainfall estimates over a western state of India. Journal of the Meteorological Society of Japan 87, 927–939. https://doi.org/10.2151/jmsj.87.927

Nash, J.. ., Sutcliffe, J. V, 1970. River flow forecasting through conceptual models: Part I - A discussion of principles. Hydrology 10, 282–290.

Nashwan, M.S., Shahid, S., 2019. Spatial distribution of unidirectional trends in climate and weather extremes in Nile river basin. Theoretical and Applied Climatology 137, 1181–1199. https://doi.org/10.1007/s00704-018-2664-5

Nashwan, M.S., Shahid, S., Rahim, N.A., 2018. Unidirectional trends in annual and seasonal climate and extremes in Egypt. Theoretical and Applied Climatology 136, 457–473. https://doi.org/10.1007/s00704-018-2498-1

Navrud, S., Tuan, T.H., Tinh, B.D., 2012. Estimating the welfare loss to households from natural disasters in developing countries: A contingent valuation study of flooding in Vietnam. Global Health Action 5, 12. https://doi.org/10.3402/gha.v5i0.17609

Ndamani, F., Watanabe, T., 2016. Determinants of farmers' adaptation to climate change: A micro level analysis in Ghana. Scientia Agricola 73, 201–208. https://doi.org/10.1590/0103-9016-2015-0163

Neema, S., Mongo Bua, G., Tuhebwe, D., Ssentongo, J., Tumuhamye, N., Mayega, R.W., Fishkin, J., Atuyambe, L.M., Bazeyo, W., 2018. Community Perspective on Policy Options for Resettlement Management: A Case Study of Risk Reduction in Bududa, Eastern Uganda.

PLOS Currents Disasters 1–20. https://doi.org/10.1371/currents.dis.49e8e547de25ca1c1f9edbbfc8b9efa5

Neumann, J. Von, 1941. Distribution of the ratio of the mean successive difference to the variance. Annals of Mathematical Statistics 12, 367–395. https://doi.org/10.1214/aoms/1177731677

Ngoma, H., Wen, W., Ojara, M., Ayugi, B., 2021. Assessing current and future spatiotemporal precipitation variability and trends over Uganda, East Africa, based on CHIRPS and regional climate model datasets. Meteorology and Atmospheric Physics 21. https://doi.org/10.1007/s00703-021-00784-3

Nguimalet, C.R., 2018. Comparison of community-based adaptation strategies for droughts and floods in Kenya and the Central African Republic. Water International 43, 183–204. https://doi.org/10.1080/02508060.2017.1393713

Nguyen, T.C., Robinson, J., 2015. Analysing motives behind willingness to pay for improving early warning services for tropical cyclones in Vietnam. Meteorological Applications 22, 187–197. https://doi.org/10.1002/met.1441

Nhat, L.M., Tachikawa, Y., Takara, K., 2006. Establishment of Intensity-Duration-Frequency Curves for Precipitation in the Monsoon Area of Vietnam. Annals of Disaster Prevention Research Institute Kyoto University 49, 93–103.

Nielsen, J.P., 1998. Multiplicative Bias Correction in Kernel Hazard Estimation. Scandinavian Journal of Statistic 25, 541–553.

Novella, N.S., Thiaw, W.M., 2013. African rainfall climatology version 2 for famine early warning systems. Journal of Applied Meteorology and Climatology 52, 588–606. https://doi.org/10.1175/JAMC-D-11-0238.1

Nsubuga, F.W., Olwoch, J.M., Rautenbach, H., 2014. Variability properties of daily and monthly observed near-surface temperatures in Uganda: 1960 – 2008. International Journal of Climatology 34, 303–314. https://doi.org/10.1002/joc.3686

Ntegeka, V., Willems, P., 2008. Trends and multidecadal oscillations in rainfall extremes, based on a more than 100-year time series of 10 min rainfall intensities at Uccle, Belgium. Water Resources Research 44, 1–15. https://doi.org/10.1029/2007WR006471

Nyasimi, M., Radeny, M., Mungai, C., Kamini, C., 2016. Uganda's National Adaptation Programme of Action: Implementation, challenges and Emerging Lessons. CGIAR Research Program on Climate Change, Agriculture and Food Security (CCAFS), Copenhagen, Denmark.

Nyeko-Ogiramoi, P., Willems, P., Ngirane-Katashaya, G., 2013. Trend and variability in observed hydrometeorological extremes in the Lake Victoria basin. Journal of Hydrology 489, 56–73. https://doi.org/10.1016/j.jhydrol.2013.02.039

Nyumba, T.O., Wilson, K., Derrick, C.J., Mukherjee, N., 2018. The use of focus group discussion methodology: Insights from two decades of application in conservation. Methods in Ecology and Evolution 9, 20–32. https://doi.org/10.1111/2041-210X.12860

O'Connell, P.E., Nash, J.E., Farrell, J.P., 1970. River flow forecasting through conceptual models part II - The Brosna catchment at Ferbane. Journal of Hydrology 10, 317–329. https://doi.org/10.1016/0022-1694(70)90221-0

Obada, E., Alamou, E.A., Chabi, A., Zandagba, J., Afouda, A., 2017. Trends and changes in recent and future Penman-Monteith potential evapotranspiration in Benin (West Africa). Hydrology

4, 1–18. https://doi.org/10.3390/hydrology4030038

OCHA, 2010. Eastern Uganda Landslides and Floods Situation Report#3. https://reliefweb.int/sites/reliefweb.int/files/resources/81D1CDAB49713514C12576EA003098A5-Full_Report.pdf (accessed 10.3.20).

Odongo, C.O., Bisaso, R.K., Byamugisha, J., Obua, C., 2014. Intermittent use of sulphadoxine-pyrimethamine for malaria prevention: a cross-sectional study of knowledge and practices among Ugandan women attending an urban antenatal clinic. Malaria Journal 13, 1–8.

Ojok, J., Koech, M.K., Tole, M., Okumu, J.O., 2012. Households' Willingness to Pay for Improved Municipal Solid Waste Management Services in Kampala, Uganda. Science Journal of Environmental Engineering Research 2013, 1–8. https://doi.org/10.7237/sjeer/143

Ongdas, N., Akiyanova, F., Karakulov, Y., Muratbayeva, A., Zinabdin, N., 2020. Application of HEC-RAS (2D) for flood hazard maps generation for Yesil (Ishim) river in Kazakhstan Nurlan. Water 12, 20. https://doi.org/10.3390/w12102672

Ongoma, V., Chen, H., Omony, G.W., 2016. Variability of extreme weather events over the equatorial East Africa, a case study of rainfall in Kenya and Uganda. Theoretical and Applied Climatology 131, 295–308. https://doi.org/10.1007/s00704-016-1973-9

Onyutha., C., Amollo, C.J., Nyende, J., Nakagiri, A., 2021. Suitability of averaged outputs from multiple rainfall-runoff models for hydrological extremes: a case of River Kafu catchment in East Africa. International Journal of Energy and Water Resources 5, 43–56. https://doi.org/10.1007/s42108-020-00075-4

Onyutha, C., 2021a. Graphical-statistical method to explore variability of hydrological time series. Hydrology Research 52, 266–283. https://doi.org/10.2166/nh.2020.111

Onyutha, C., 2021b. Trends and Variability of Temperature and Evaporation Over the African Continent: Relationships with Precipitation. Atmosfera 34, 267–287. https://doi.org/10.20937/ATM.52788

Onyutha, C., 2020a. Analyses of rainfall extremes in East Africa based on observations from rain gauges and climate change simulations by CORDEX RCMs. Climate Dynamics 24. https://doi.org/10.1007/s00382-020-05264-9

Onyutha, C., 2020b. From R-squared to coefficient of model accuracy for assessing " goodness-of-fits ". Geoscientific Model Development Discussions 1–25. https://doi.org/10.5194/gmd-2020-51

Onyutha, C., 2019. Hydrological Model Supported by a Step-Wise Calibration against Sub-Flows and Validation of Extreme Flow Events. Water 11(244), 1–23. https://doi.org/10.3390/w11020244

Onyutha, C., 2018. Trends and variability in African long-term precipitation. Stochastic Environmental Research and Risk Assessment 32, 2721–2739. https://doi.org/10.1007/s00477-018-1587-0

Onyutha, C., 2017a. Variability of Rainfall and River Flow in the Nile Basin. Ku Leuven.

Onyutha, C., 2017b. On rigorous drought assessment using daily time scale: Non-Stationary Frequency Analyses, revisited concepts, and a new method to yield non-parametric indices. Hydrology 4(48), 1–43. https://doi.org/10.3390/hydrology4040048

Onyutha, C., 2016a. Geospatial trends and decadal anomalies in extreme rainfall over Uganda, East Africa. Advances in Meteorology 2016, 1–15. https://doi.org/10.1155/2016/6935912

Onyutha, C., 2016b. Statistical analyses of potential evapotranspiration changes over the period 1930-2012 in the Nile River riparian countries. Agricultural and Forest Meteorology 226–227, 80–95. https://doi.org/10.1016/j.agrformet.2016.05.015

Onyutha, C., 2016c. Identification of sub-trends from hydro-meteorological series. Stochastic Environmental Research and Risk Assessment 30, 189–205. https://doi.org/10.1007/s00477-015-1070-0

Onyutha, C., 2016d. Influence of Hydrological Model Selection on Simulation of Moderate and Extreme Flow Events: A Case Study of the Blue Nile Basin. Advances in Meteorology 2016, 1–28. https://doi.org/10.1155/2016/7148326

Onyutha, C., 2012. Statistical modelling of FDC and return periods to characterise QDF and design of threshold of hydrological extremes. Journal of Urban and Environmental Engineering 6, 132–148. https://doi.org/10.4090/juee.2012.v6n2.132148

Onyutha, C., Acayo, G., Nyende, J., 2020. Analyses of Precipitation and Evapotranspiration Changes across the Lake Kyoga Basin in East Africa. Water 12, 1–23. https://doi.org/10.3390/w12041134

Onyutha, C., Asiimwe, A., Ayugi, B., Ngoma, H., Ongoma, V., Tabari, H., 2021a. Observed and future precipitation and evapotranspiration in water management zones of uganda: Cmip6 projections. Atmosphere 12, 1–25. https://doi.org/10.3390/atmos12070887

Onyutha, C., Asiimwe, A., Muhwezi, L., Mubialiwo, A., 2021b. Water availability trends across water management zones in Uganda. Atmospheric Science Letters 1–14. https://doi.org/10.1002/asl.1059

Onyutha, C., Nyesigire, R., Nakagiri, A., 2021c. Contributions of Human Activities and Climatic Variability to Changes in River Rwizi Flows in Uganda, East Africa. Hydrology 8, 145. https://doi.org/10.3390/hydrology8040145

Onyutha, C., Turyahabwe, C., Kaweesa, P., 2021d. Impacts of climate variability and changing land use/land cover on River Mpanga flows in Uganda, East Africa. Environmental Challenges 5, 1–14. https://doi.org/10.1016/j.envc.2021.100273

Onyutha, C., Willems, P., 2018. Investigation of flow-rainfall co-variation for catchments selected based on the two main sources of River Nile. Stochastic Environmental Research and Risk Assessment 32, 623–641. https://doi.org/10.1007/s00477-017-1397-9

Onyutha, C., Willems, P., 2017a. Space-time variability of extreme rainfall in the River Nile basin. International Journal of Climatology 37 (14), 4915–4924. https://doi.org/10.1002/joc.5132

Onyutha, C., Willems, P., 2017b. Influence of spatial and temporal scales on statistical analyses of rainfall variability in the River Nile basin. Dynamics of Atmospheres and Oceans 77, 26–42. https://doi.org/10.1016/j.dynatmoce.2016.10.008

Onyutha, C., Willems, P., 2015a. Uncertainty in calibrating generalised Pareto distribution to rainfall extremes in Lake Victoria basin. Hydrology Research 46, 356–376. https://doi.org/10.2166/nh.2014.052

Onyutha, C., Willems, P., 2015b. Empirical statistical characterization and regionalization of amplitude–duration–frequency curves for extreme peak flows in the Lake Victoria Basin, East Africa. Hydrological Sciences Journal 60, 997–1012. https://doi.org/10.1080/02626667.2014.898846

Onyutha, C., Willems, P., 2013. Uncertainties in Flow-Duration-Frequency Relationships of High

and Low Flow Extremes in Lake Victoria Basin. Water 5, 1561–1579. https://doi.org/10.3390/w5041561

Ostermann, J., Brown, D.S., Mühlbacher, A., Njau, B., Thielman, N., 2015. Would you test for 5000 Shillings? HIV risk and willingness to accept HIV testing in Tanzania. Health Economics Review 5, 1–11. https://doi.org/10.1186/s13561-015-0060-8

Osuret, J., Atuyambe, L.M., Mayega, R.W., Ssentongo, J., Tumuhamye, N., Bua, G.M., Tuhebwe, D., Bazeyo, W., 2016. Coping Strategies for Landslide and Flood Disasters: A Qualitative Study of Mt. Elgon Region, Uganda. PLOS Currents Disasters 1–13. https://doi.org/10.1371/currents.dis.4250a225860babf3601a18e33e172d8b

Page, E.S., 1961. Cummultive sum charts. Technometrics 3, 1–9.

Pakhtigian, E.L., Jeuland, M., 2019. Valuing the Environmental Costs of Local Development: Evidence From Households in Western Nepal. Ecological Economics 158, 158–167. https://doi.org/10.1016/j.ecolecon.2018.12.021

Pande, S., Arkesteijn, L., Savenije, H.H.G., Bastidas, L.A., 2014. Hydrological model parameter dimensionality is a weak measure of prediction uncertainty. Hydrology and Earth System Sciences Discussions 11, 2555–2582. https://doi.org/10.5194/hessd-11-2555-2014

Pandžić, K., Kobold, M., Oskoruš, D., Biondić, B., Biondić, R., Bonacci, O., Likso, T., Curić, O., 2020. Standard normal homogeneity test as a tool to detect change points in climate-related river discharge variation: case study of the Kupa River Basin. Hydrological Sciences Journal 65, 227–241. https://doi.org/10.1080/02626667.2019.1686507

Pellicone, G., Caloiero, T., Modica, G., Guagliardi, I., 2018. Application of several spatial interpolation techniques to monthly rainfall data in the Calabria region (southern Italy). International Journal of Climatology 38, 3651–3666. https://doi.org/10.1002/joc.5525

Pérez-Sánchez, J., Senent-aparicio, J., Segura-Méndez, F., Pulido-velazquez, D., Srinivasan, R., 2019. Evaluating Hydrological Models for Deriving Water Resources in Peninsular Spain. Sustainability 11(2872), 1–36. https://doi.org/10.3390/su11102872

Persson, G., Bärring, L., Kjellström, E., Strandberg, G., Rummukainen, M., 2007. Climate indices for vulnerability assessments, SMHI Reporst Metereology and Climatology, RKM No.111. Swedish Meteorological and Hydrological Institute, Norrköping, Sweden.

Pettitt, A.N., 1979. A non-parametric approach to the change-point problem. Applied Statistics 28, 126–135.

Phillips, J., Mcintyre, B., 2000. ENSO and Internal Rainfall Variability in Uganda: Implications for Agricultural management. International Journal of Climatology 20, 171–182. https://doi.org/10.1002/(SICI)1097-0088(200002)20:2<171:AID-JOC471>3.0.CO;2-O

Piani, C., Haerter, J.O., Coppola, E., 2010. Statistical bias correction for daily precipitation in r egional climate models over Europe. Theoretical and Applied Climatology 99, 187–192. https://doi.org/10.1007/s00704-009-0134-9

Pickands, J., 1975. Statistical inference using extreme order statistics. The Annals of Statistics 3, 119–131.

Pinos, J., Orellana, D., Timbe, L., 2020. Assessment of microscale economic flood losses in urban and agricultural areas: case study of the Santa Bárbara River, Ecuador. Natural Hazards 103, 2323–2337. https://doi.org/10.1007/s11069-020-04084-8

Pinos, J., Timbe, L., 2019. Performance assessment of two-dimensional hydraulic models for

generation of flood inundation maps in mountain river basins. Water Science and Engineering 12, 11–18. https://doi.org/10.1016/j.wse.2019.03.001

Pirnia, A., Golshan, M., Darabi, H., Adamowski, J., Rozbeh, S., 2018. Using the mann–kendall test and double mass curve method to explore stream flow changes in response to climate and human activities. Journal of Water and Climate Change 10, 725–742. https://doi.org/10.2166/wcc.2018.162

Pitman, W. V, 1973. A mathematical model for generating monthly river flows from meteorological data in South Africa. University of the Witwatersrand, Hydrological Research Unit.

Podger, G., 2004. User Guide - Rainfall Runoff Library, Catchment Modelling Toolkit, CRC for Catchment Hydrology. CRC for Catchment Hydrology, Australia.

Porter, J.W., McMahon, T.A., 1971. A model for the simulation of Streamflow data from cimatic records. Journal of Hydrology 13, 297–324.

Priest, S.J., Parker, D.J., Tapsell, S.M., 2011. Modelling the potential damage-reducing benefits of flood warnings using European cases. Environmental Hazards 10, 101–120. https://doi.org/10.1080/17477891.2011.579335

Priestley, C.H.B., Taylor, R.J., 1972. On the assessment of surface heat flux and evaporation using large-scale parameters. Monthly Weather Review 100, 81–92. https://doi.org/10.1175/1520-0493(1972)100<0081:OTAOSH>2.3.CO;2

Rakib, M.A., Islam, S., Nikolaos, I., Bodrud-Doza, M., Bhuiyan, M.A.H., 2017. Flood vulnerability, local perception and gender role judgment using multivariate analysis: A problem-based "participatory action to Future Skill Management" to cope with flood impacts. Weather and Climate Extremes 18, 29–43. https://doi.org/10.1016/j.wace.2017.10.002

Ramiaramanana, F.N., Teller, J., 2021. Urbanization and floods in sub-saharan africa: Spatiotemporal study and analysis of vulnerability factors—case of antananarivo agglomeration (Madagascar). Water 13, 1–23. https://doi.org/10.3390/w13020149

Rangari, V.A., Umamahesh, N. V., Bhatt, C.M., 2019. Assessment of inundation risk in urban floods using HEC RAS 2D. Modeling Earth Systems and Environment 5. https://doi.org/10.1007/s40808-019-00641-8

Reeser, C., 2016. Homeover Willingness to pay for a pre-flood buyout agreement. University of Illinois at Urbana-Champaign.

Refsgaard, J.., Storm, B., 1995. MIKE SHE, in: Singh, V.P. (Ed.), Computer Models of Watershed Hydrology. Water Resources Publications, Highlands Ranch, Colorado, USA, pp. 809–846.

Reliefweb, 2020. Map showing Districts Affected by the February, March, April and May (MAM) Rainy Season (Flood and Landslide Prone) including Landing Sites/Lake shores which have experienced rising water levels as of 6th May 2020. https://reliefweb.int/map/uganda/map-showing-districts-affected-february-march-april-and-may-mam-rainy-season-flood-and (accessed 6.26.21).

Reliefweb, 2019. Floods, landslides: Gov't speaks out on disaster situation. https://reliefweb.int/report/uganda/floods-landslides-govt-speaks-out-disaster-situation (accessed 6.14.21).

Reliefweb, 2007. Uganda: Flood - affected areas (as of 19 Sep 2007). OCHA Services. https://reliefweb.int/map/uganda/uganda-flood-affected-areas-19-sep-2007 (accessed

6.26.21).

Rizvi, A.R., Barrow, E., Zapata, F., Gomez, A., Podvin, K., Kutegeka, S., Gafabusa, R., Adhikari, A., 2016. Learning from Participatory Vulnerability Assessments – key to identifying Ecosystem based Adaptation options.

Rodrigues, E.L., Jacobi, C.M., Côrtes, J.F.E., 2019. Wild fires and their impact on the water supply of a large neotropical metropolis: A simulation approach. Science of the Total Environment 651, 1261–1271. https://doi.org/10.1016/j.scitotenv.2018.09.289

Rohwer, C., 1931. Evaporation from free water surfaces. USDA Technical Bulletin 271, 1–96.

Romali, N.S., Yusop, Z., 2021. Flood damage and risk assessment for urban area in Malaysia. Hydrology Research 52, 142–159. https://doi.org/10.2166/nh.2020.121

Rosbjerg, D., 1985. Estimation in partial duration series with independent and dependent peak values. Journal of Hydrology 76, 183–195. https://doi.org/10.1016/0022-1694(85)90098-8

Saber, M., Yilmaz, K.K., 2018. Evaluation and Bias Correction of Satellite-Based Rainfall Estimates for Modelling Flash Floods over the Mediterranean region: Application to Karpuz River Basin, Turkey. Water 10, 1–24. https://doi.org/10.3390/w10050657

Salas, J.D., Obeysekera, J., 2014. Revisiting the concepts of return period and risk for nonstationary hydrologic extreme events. Journal of Hydrologic Engineering 19, 554–568. https://doi.org/10.1061/(ASCE)HE.1943-5584.0000820

Sampson, C.C., Smith, A.M., Bates, P.D., Neal, J.C., Alfieri, L., Freer, J.E., 2015. A high-resolution global flood hazard model. Water Resources Research 7358–7381. https://doi.org/10.1002/2015WR016954

Santhi, C., Arnold, J.G., Williams, J.R., Dugas, W.A., Srinivasan, R., Hauck, L.M., 2001. Validation of the SWAT model on a large river basin with point and nonpoint sources. Journal of the American Water Resources Association 37, 1169–1188. https://doi.org/10.1111/j.1752-1688.2001.tb03630.x

Sarchani, S., Seiradakis, K., Coulibaly, P., Tsanis, I., 2020. Flood inundation mapping in an ungauged basin. Water 12, 1–21. https://doi.org/10.3390/W12061532

Sassen, M., Sheil, D., 2013. Human impacts on forest structure and species richness on the edges of a protected mountain forest in Uganda. Forest Ecology and Management 307, 206–218. https://doi.org/10.1016/j.foreco.2013.07.010

Schulz, K., Bernhardt, M., 2016. The end of trend estimation for extreme floods under climate change? Hydrological Processes 30, 1804–1808. https://doi.org/10.1002/hyp.10816

Scorzini, A.R., Frank, E., 2017. Flood damage curves: new insights from the 2010 flood in Veneto, Italy. Journal of Flood Risk Management 10, 381–392. https://doi.org/10.1111/jfr3.12163

Segers, J., 2005. Generalized Pickands estimators for the extreme value index. Journal of Statistical Planning and Inference 128, 381–396. https://doi.org/10.1016/j.jspi.2003.11.004

Sen, P.K., 1968. Estimates of the regression coefficient based on Kendall's tau. Journal of the American Statistical Association 63, 1379–1389. https://doi.org/10.1080/01621459.1968.10480934

Seong, C., Sridhar, V., Billah, M.M., 2018. Implications of potential evapotranspiration methods for streamflow estimations under changing climatic conditions. International Journal of Climatology 38, 896–914. https://doi.org/10.1002/joc.5218

Sharifi, E., Saghafian, B., Steinacker, R., 2018. Bias Correction of Satellite Precipitation Products based on Concept of Copula. Geophysical Research Abstracts 20.

Sheffield, J., Goteti, G., Wood, E.F., 2006. Development of a 50-year high-resolution global dataset of meteorological forcings for land surface modeling. Journal of Climate 19, 3088–3111. https://doi.org/10.1175/JCLI 3790.1

Shepard, D., 1968. A two- dimensional interpolation function for irregularly- spaced data, in: Proceedings of the 23rd National Conference. Havard College-Cambridge, Massachusetts, pp. 517–524. https://doi.org/10.1145/800186.810616

Shustikova, I., Domeneghetti, A., Neal, J.C., Bates, P., Castellarin, A., 2019. Comparing 2D capabilities of HEC-RAS and LISFLOOD-FP on complex topography. Hydrological Sciences Journal 64, 1769–1782. https://doi.org/10.1080/02626667.2019.1671982

Simon, K., Diprose, G., Thomas, A.C., 2020. Community-led initiatives for climate adaptation and mitigation. Kotuitui 15, 93–105. https://doi.org/10.1080/1177083X.2019.1652659

Simotwo, H.K., Mikalitsa, S.M., Wambua, B.N., 2018. Climate change adaptive capacity and smallholder farming in Trans-Mara East sub-County, Kenya. Geoenvironmental Disasters 5, 1–14. https://doi.org/10.1186/s40677-018-0096-2

Singh, A.S., Masuku, M.B., 2014. Sampling Techniques and determination of sample size in applied statistics research: An overview. International Journal of Economics, Commerce and Management 2, 22.

Sneyers, R., 1990. On the statistical analysis of series of observations. Technical Note No.143, WMO No. 415, Secretariat of the World Meteorological Organization. Geneva, Switzerland.

Spearman, C., 1904. The proof and measurement of association between two things. The American Journal of Psychology 15, 72–101.

Sugawara, M., 1995. Tank model, in: Singh, V.P. (Ed.), Computer Models of Watershed Hydrology. Water Resources Publications, Littleton, CO, USA, pp. 165–214.

Sule, B.F., Alabi, S.A., 2013. Application of synthetic unit hydrograph methods to construct storm hydrographs. International Journal of Water Resources and Environmental Engineering 5, 639–647. https://doi.org/10.5897/IJWREE2013.0437

Sung, K., Jeong, H., Sangwan, N., Yu, D.J., 2018. Effects of Flood Control Strategies on Flood Resilience Under Sociohydrological Disturbances. Advanced Earth and Space Science 1–20. https://doi.org/10.1002/2017WR021440

Sykes, L., Gani, F., Vally, Z., 2016. Statistical terms Part 1: The meaning of the MEAN, and other statistical terms commonly used in medical research. South African Dental Journal 71, 274–278.

Tabari, H., Talaee, P.H., 2011. Local calibration of the Hargreaves and Priestley-Taylor equations for estimating reference evapotranspiration in arid and cold climates of Iran based on the Penman-Monteith model. Journal of Hydrologic Engineering 16, 837–845. https://doi.org/10.1061/(ASCE)HE.1943-5584.0000366

Tang, L., Zhang, Y., 2018. Considering abrupt change in rainfall for flood season division: A case study of the Zhangjia Zhuang reservoir, based on a new model. Water 10, 1–16. https://doi.org/10.3390/w10091152

Tassew, B.G., Belete, M.A., K.Miegel, 2019. Application of HEC-HMS Model for Flow Simulation in the Lake Tana Basin: The Case of Gilgel Abay Catchment, Upper Blue Nile

Basin, Ethiopia. Hydrology 6, 1–17. https://doi.org/10.3390/hydrology6010021

Tegegne, G., Park, D.K., Kim, Y., 2017. Comparison of hydrological models for the assessment of water resources in a data-scarce region, the Upper Blue Nile River Basin. Journal of Hydrology: Regional Studies 14, 49–66. https://doi.org/10.1016/j.ejrh.2017.10.002

Teng, J., Jakeman, A.J., Vaze, J., Croke, B.F.W., Dutta, D., Kim, S., 2017. Flood inundation modelling: A review of methods, recent advances and uncertainty analysis. Environmental Modelling and Software 90, 201–216. https://doi.org/10.1016/j.envsoft.2017.01.006

Thapa-Parajuli, R., Devkota, R., Bhattarai, U., Maraseni, T., 2018. A Preference-based Analysis of Community Level Flood Early Warning Techniques in the West Rapti River Basin, Nepal. Journal of Geography & Natural Disasters 08, 1–5. https://doi.org/10.4172/2167-0587.1000230

Theil, H., 1950. A rank-invariant method of Linear and Polynomial regression analysis, in: Nederlandse Akademie van Wetenschappen, Series A, A. Statistical Department of the Mathematisch Centrum, Amsterdam, Netherlands, pp. 386–392.

Thiessen, A.H., 1911. Precipitation Averages for Large Areas. Monthly Weather Review 39, 1082–1084.

Thistlethwaite, J., Henstra, D., Brown, C., Scott, D., 2020. Barriers to Insurance as a Flood Risk Management Tool: Evidence from a Survey of Property Owners. International Journal of Disaster Risk Science 11, 263–273. https://doi.org/10.1007/s13753-020-00272-z

Thomas, V., López, R., 2015. Global increase in climate-related disasters (No. 466), ADB Economic Working paper Series. Metro Manila, Philippines.

Thornthwaite, C.W., 1948. An Approach toward a Rational Classification of Climate. Geographical Review 38, 55–94.

Tian, Y., Huffman, G.J., Adler, R.F., Tang, L., Sapiano, M., Maggioni, V., Wu, H., 2013. Modeling errors in daily precipitation measurements: Additive or multiplicative? Geophysical Research Letters 40, 2060–2065. https://doi.org/10.1002/grl.50320

Tien, H., Ariyawardana, A., Ratnasiri, S., 2020. Forest plantation owners' willingness to pay for hybrid nursery stock: The case of Acacia hybrids in Central Vietnam. Forest Policy and Economics 116, 1–19. https://doi.org/10.1016/j.forpol.2020.102184

Tiwari, H., Balvanshi, A., 2020. Hydrological Modelling of Bina River Basin in Madhya Pradesh, India. Global Journal of Engineering Sciences 6, 1–7. https://doi.org/10.33552/GJES.2020.06.000639

Tromp, R.E., Datzberger, S., 2021. Global Education Policies versus local realities. Insights from Uganda and Mexico. Compare 51, 356–374. https://doi.org/10.1080/03057925.2019.1616163

Twerefou, D.K., 2014. Willingness to Pay for Improved Electricity Supply in Ghana. Modern Economy 5, 489–498. https://doi.org/10.4236/me.2014.55046

Uganda Bureau of Statistics, 2020. Uganda Bureau of Statistics 2020 statistical abstract. Uganda Bureau of Statistics. https://www.ubos.org/wp-content/uploads/publications/11_2020STATISTICAL__ABSTRACT_2020.pdf (accessed 11.24.20).

Uganda Bureau of Statistics, 2018. Uganda Bureau of Statistics: Statistical Abstract. Kampala, Uganda.

Uganda Radio Network, 2020. Floods Destroy Crop Gardens in Butaleja. https://ugandaradionetwork.net/story/floods-destroy-crop-gardens-in-butaleja- (accessed 6.15.21).

UNISDR, 2018. Annual Report on Substantial Reduction of Disasters Risk and Losses for a Sustainable Future. United Nations Office for Disaster Risk Reduction (UNISDR), Geneva, Swtizerland.

Venkatachalam, L., 2004. The contingent valuation method: A review. Environmental Impact Assessment Review 24, 89–124. https://doi.org/10.1016/S0195-9255(03)00138-0

Vickrey, W., 1961. Counter speculation, auctions and competitive sealed tenders. Journal of Finance 16, 8–37.

Vido, J., Nalevanková, P., Valach, J., Šustek, Z., Tadesse, T., 2019. Drought Analyses of the Horné Po žitavie Region (Slovakia) in the Period 1966-2013. Advances in Meteorology 2019, 1–10. https://doi.org/10.1155/2019/3576285

Wackernagel, H., 1995. Ordinary Kriging, in: Multivariate Geostatistics. Springer, Berlin, Heidelberg, pp. 74–81.

Wafana, B., Sidney, S., Kemigisha, C., Kisakye, E., Kuddiza, A., Wakabi, S., Wambi, I., Musiime, I., Nekaka, R., Gavamukulya, Y., 2019. Data in brief Towards universal health coverage: Data for determinants of immunization coverage of Pneumococcal and Rota virus vaccines among under five children in Busolwe Town Council, Butaleja District, Eastern Uganda. Data in brief 25, 1–5. https://doi.org/10.1016/j.dib.2019.104269

Wasswa, P., Nalwadda, C.K., Buregyeya, E., Gitta, S.N., Anguzu, P., Nuwaha, F., 2015. Implementation of infection control in health facilities in Arua district, Uganda: a cross-sectional study. BMC Infectious Diseases 15, 1–9. https://doi.org/10.1186/s12879-015-0999-4

Willems, P., 2009. Environmental Modelling & Software A time series tool to support the multi-criteria performance evaluation of rainfall-runoff models. Environmental Modelling and Software 24, 311–321. https://doi.org/10.1016/j.envsoft.2008.09.005

Willems, P., Guillou, A., Beirlant, J., 2007. Bias correction in hydrologic GPD based extreme value analysis by means of a slowly varying function. Journal of Hydrology 338, 221–236. https://doi.org/10.1016/j.jhydrol.2007.02.035

Willmott, C.J., 1981. On the validation of models. Physical Geography 2, 184–194. https://doi.org/10.1080/02723646.1981.10642213

WMO, 2009. Hydrological Data, in: Manual on Low-Flow Estimation and Prediction. Operational Hydrology Report No. 50. WMO-No. 1029. WMO, Geneva, p. 138.

Wright, S.G., 2012. Using contingent valuation to estimate willingness to pay for improved water source in rural Uganda. Michigan Technological University.

Xu, X., Wang, Y., Kalcic, M., Logsdon, R., Yang, Y.C.E., Scavia, D., 2017. Evaluating the impact of climate change on fl uvial fl ood risk in a mixed-used watershed. Environmental Modelling and Software 1–11. https://doi.org/10.1016/j.envsoft.2017.07.013

Yu, B., Zhu, Z., 2015. A comparative assessment of AWBM and SimHyd for forested watersheds. Hydrological Sciences Journal 60 (7-8), 1200–1212. https://doi.org/10.1080/02626667.2014.961924

Zarekarizi, M., Srikrishnan, V., Keller, K., 2020. Neglecting uncertainties biases house-elevation

decisions to manage riverine flood risks. Nature Communications 11, 1–11. https://doi.org/10.1038/s41467-020-19188-9

Zeleke, T., Assefa, D., 2017. Think Tanks and University Relations in Ethiopia. Journal of Adavanced Public and International Affairs (JAPPIA) 4, 66–90.

Zhang, G., Xie, T., Zhang, L., Hua, X., Liu, F., 2017. Application of Multi-Step Parameter Estimation Method Based on Optimization Algorithm in Sacramento Model. Waste Management 9, 1–21. https://doi.org/10.3390/w9070495

Zhang, Q., Tang, Q., Liu, X., Hosseini-Moghari, S.M., Attarod, P., 2020. Improving princeton forcing dataset over iran using the delta-ratio method. Water 12, 1–15. https://doi.org/10.3390/w12030630

Zhang, X., Alexander, L., Hegerl, G.C., Jones, P., Tank, A.K., Peterson, T.C., Trewin, B., Zwiers, F.W., 2011. Indices for monitoring changes in extremes based on daily temperature and precipitation data. Wiley Interdisciplinary Reviews: Climate Change 2, 851–870. https://doi.org/10.1002/wcc.147

Zhang, Y., Zheng, H., Chiew, F.H.S., Peña-Arancibia, J., Zhou, X., 2016. Evaluating Regional and Global Hydrological Models against Streamflow and Evapotranspiration Measurements. American Meteorological Society 17 (3), 995–1010. https://doi.org/10.1175/JHM-D-15-0107.1

Zhao, J., Liu, Q., Lin, L., Lv, H., Wang, Y., 2013. Assessing the comprehensive restoration of an urban river: An integrated application of contingent valuation in Shanghai, China. Science of the Total Environment 458–460, 517–526. https://doi.org/10.1016/j.scitotenv.2013.04.042

Zhen, L., Zoebisch, M., 2006. Resource Use and Agricultural Sustainability: Risks and Consequences of Intensive Cropping in China. Journal of Agriculture and Rural Development in the Tropics and Subtropics 1–117.

Zheng, S., Mogusu, E., Veeranki, S.P., Quinn, M., Cao, Y., 2016. The relationship between the mean, median, and mode with grouped data. Communications in Statistics - Theory and Methods 46, 4285–4295. https://doi.org/10.1080/03610926.2015.1081948

Zhou, Y., Guo, S., Chang, F., 2019. Explore an evolutionary recurrent ANFIS for modelling multi-step-ahead flood forecasts. Journal of Hydrology 570, 343–355. https://doi.org/10.1016/j.jhydrol.2018.12.040

Appendices

Appendix A: Homogeneity testing of observed precipitation data set and observed flow and Validation of PGF-based precipitation data series

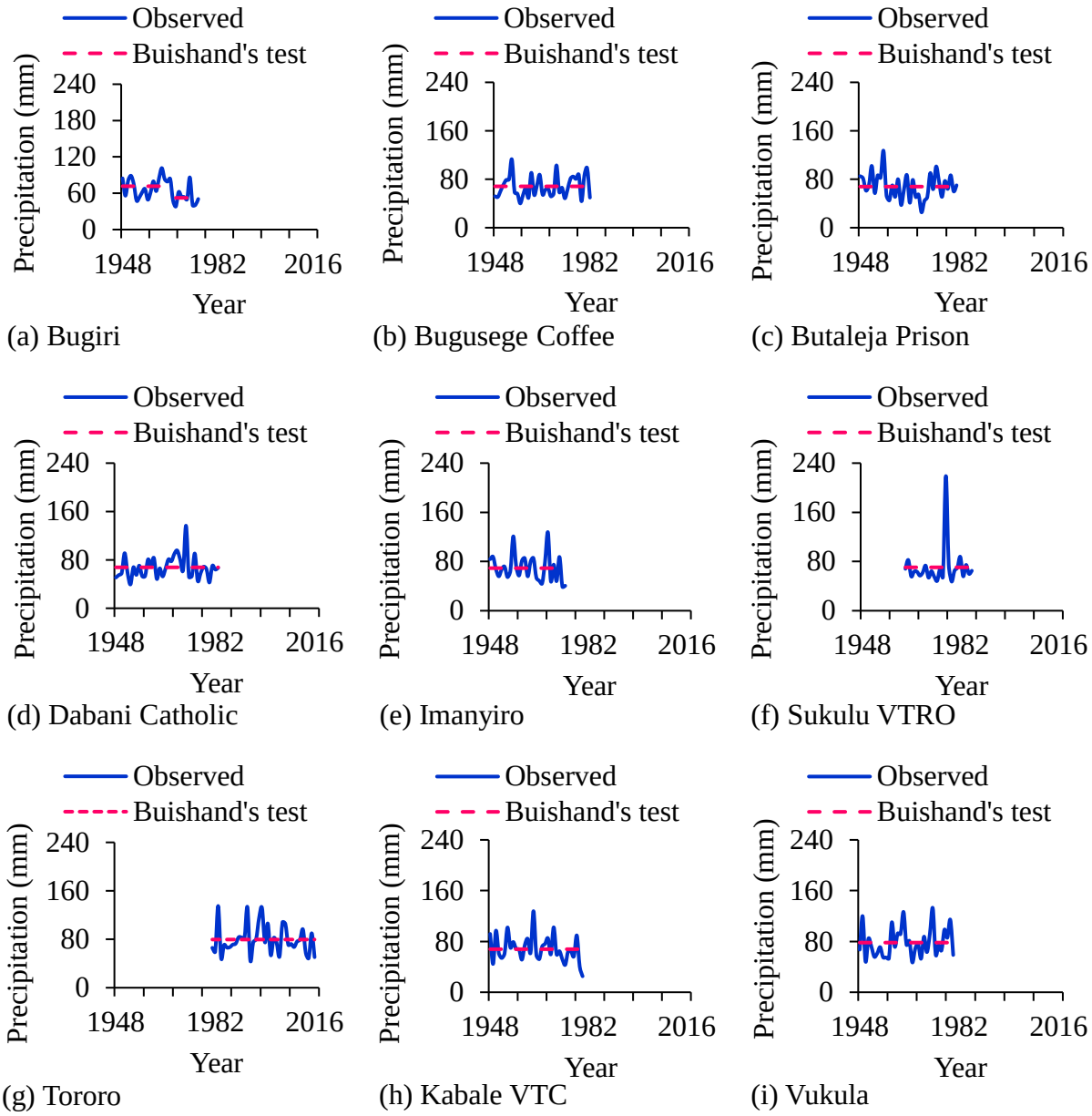

Figure A.1 Buishand's test on the annual maximum precipitation for observation station (a) 1, (b) 2, (c) 3, (d) 4, (e) 5, (f) 6, (g) 7, (h) 8, and (i) 9. Details of station 1-9 can be found in Table 2.1.

.

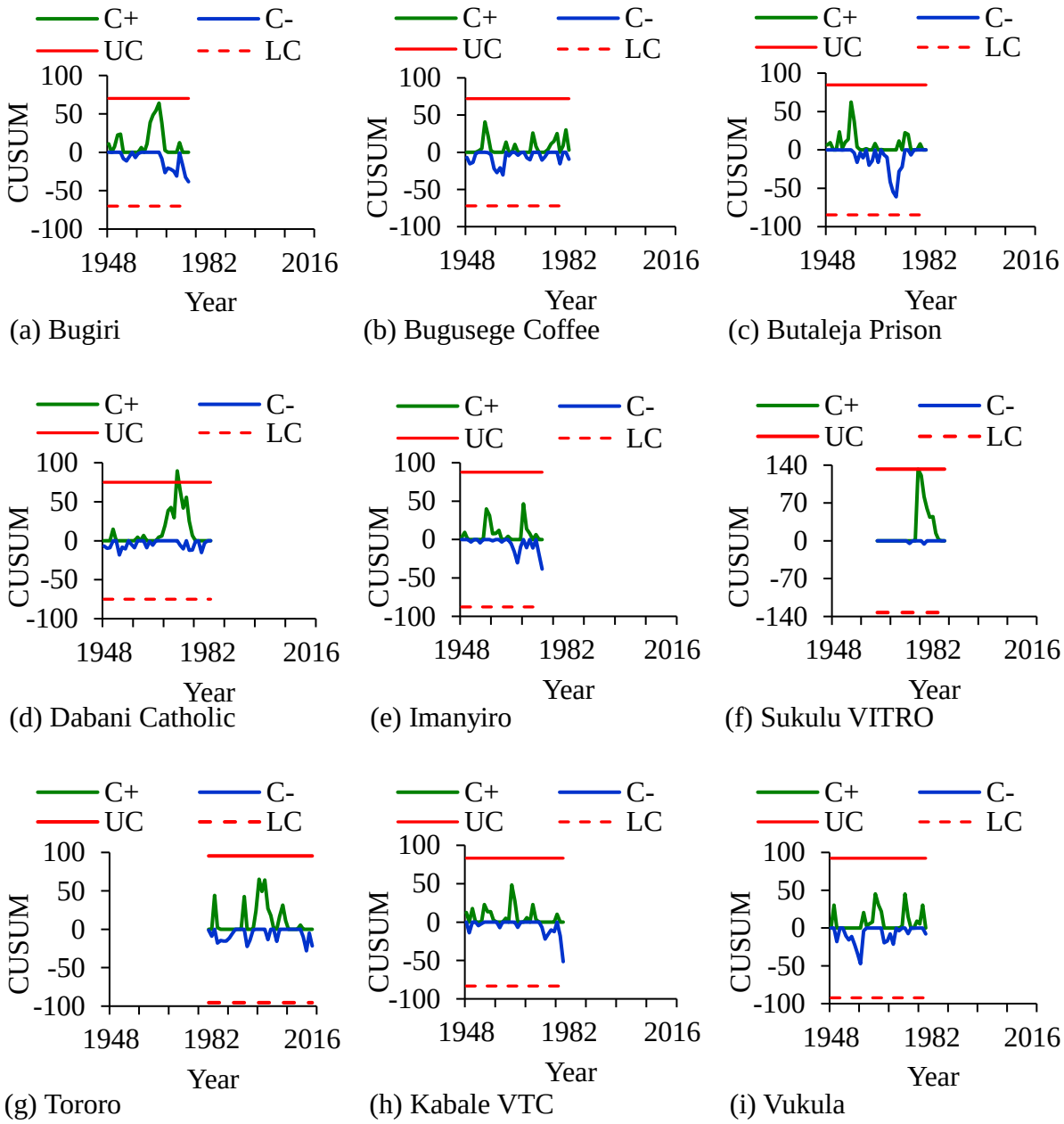

Figure A.2 CUSUM charts for annual maximum precipitation at station (a) 1, (b) 2, (c) 3, (d) 4, (e) 5, (f) 6, (g) 7, (h) 8, and (i) 9. Details of station 1-9 can be found in Table 2.1. On the legend, UC and LC denote th upper and lower CUSUM limits, respectively while, C+ and C- indicate positive and negative shift, respectively.

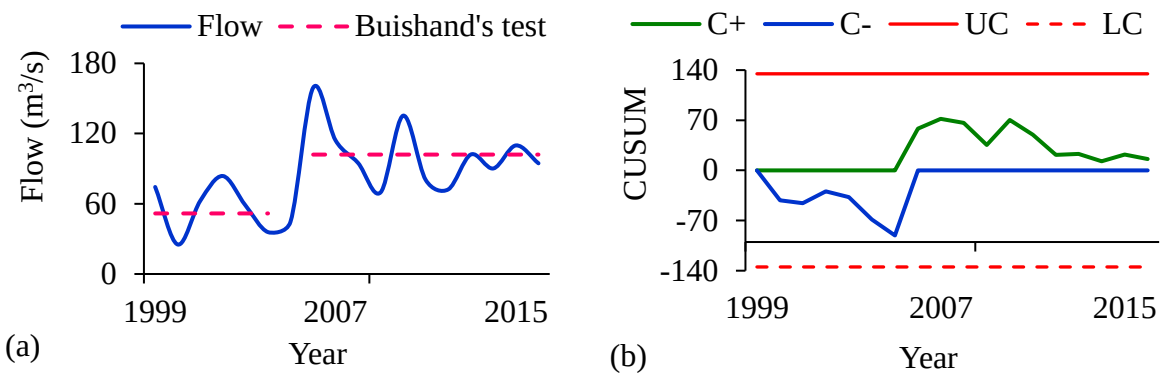

Figure A.3 (a) Buishand's test on the annual maximum flow (b) CUSUM chart for annual maximum flow. On the legend of (b), UC and LC denote th upper and lower CUSUM limits, respectively while, C+ and C- indicate positive and negative shift, respectively.

Table A.1 Homogeneity test on annual maximum flow

p-value			
Pettit's test	SNHT	Buishand's test	Von Neumann test
0.008*	0.008*	0.007*	0.037*

*Denotes that H_o (homogenous flow data) was rejected ($p < 0.05$).

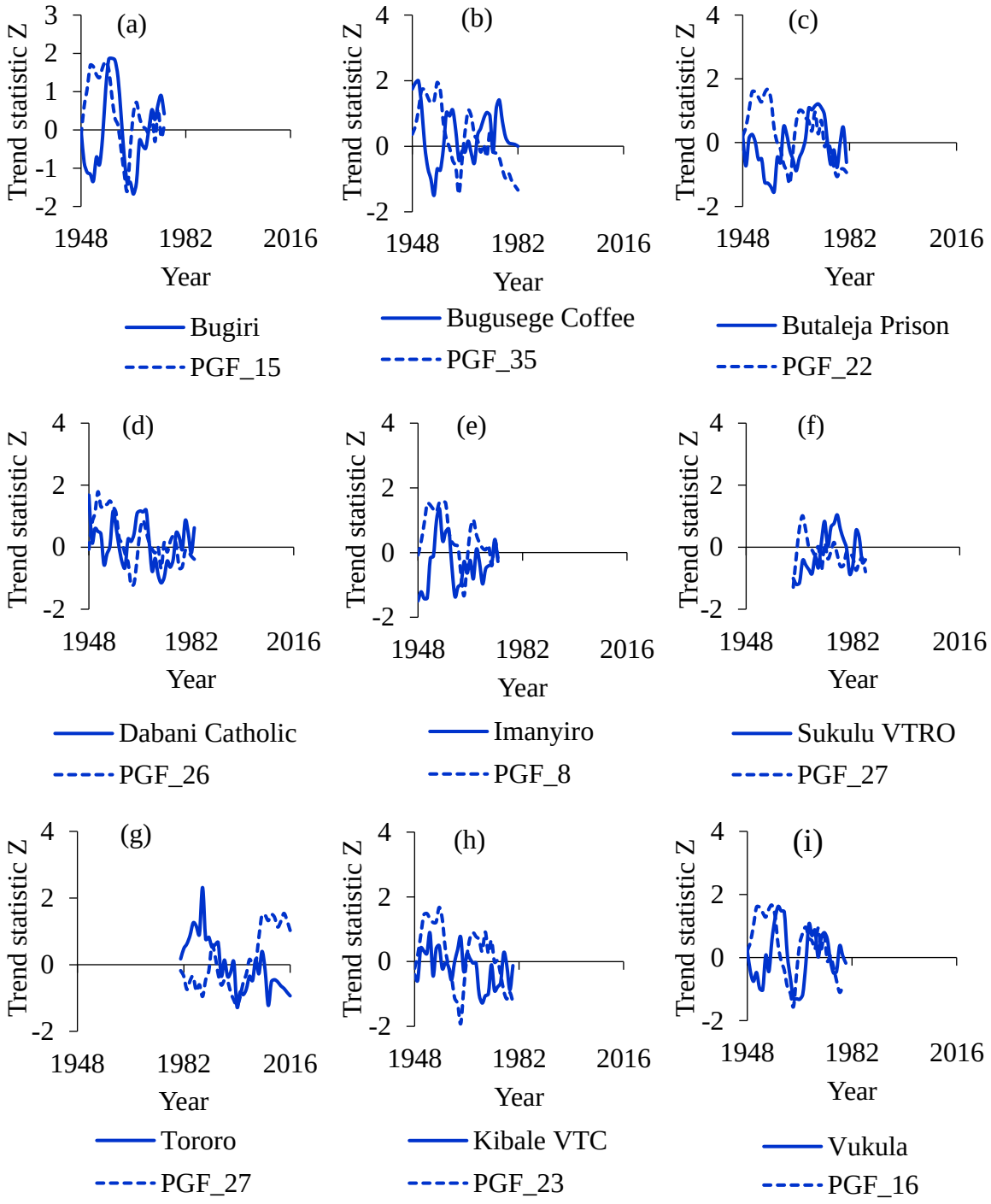

Figure A.4 Variability of ANMS from PGF and observed rainfall at station (a) 1, (b) 2, (c) 3, (d) 4, (e) 5, (f) 6, (g) 7, (h) 8, and (i) 9. Details of station 1-9 can be found in Table 2.1.

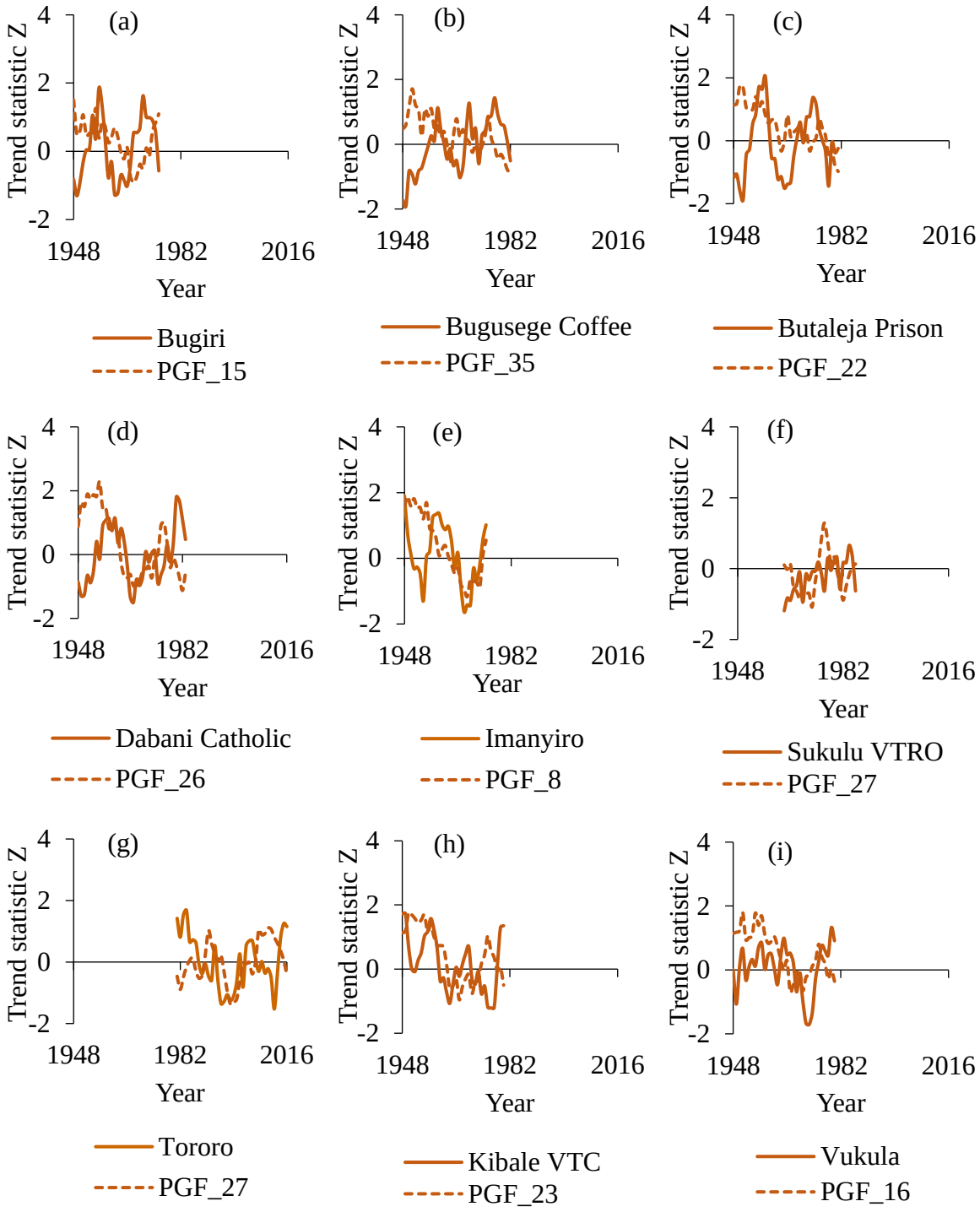

Figure A.5 Variability of NWD10 from PGF and observed rainfall at station (a) 1, (b) 2, (c) 3, (d) 4, (e) 5, (f) 6, (g) 7, (h) 8, and (i) 9. Details of station 1-9 can be found in Table 2.1.

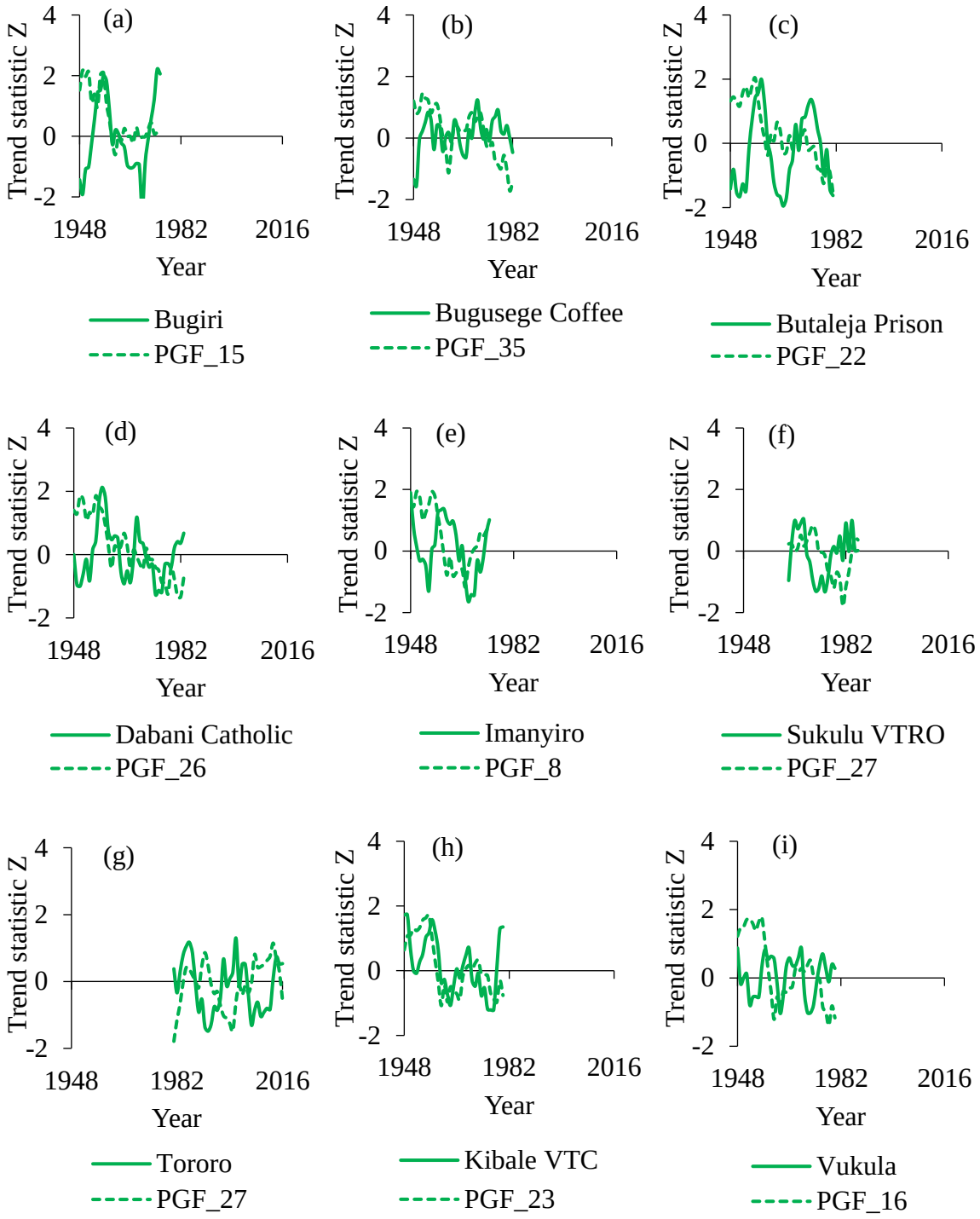

Figure A.6 Variability of NWD5 from PGF and observed rainfall at station (a) 1, (b) 2, (c) 3, (d) 4, (e) 5, (f) 6, (g) 7, (h) 8, and (i) 9. Details of station 1-9 can be found in Table 2.1.

.

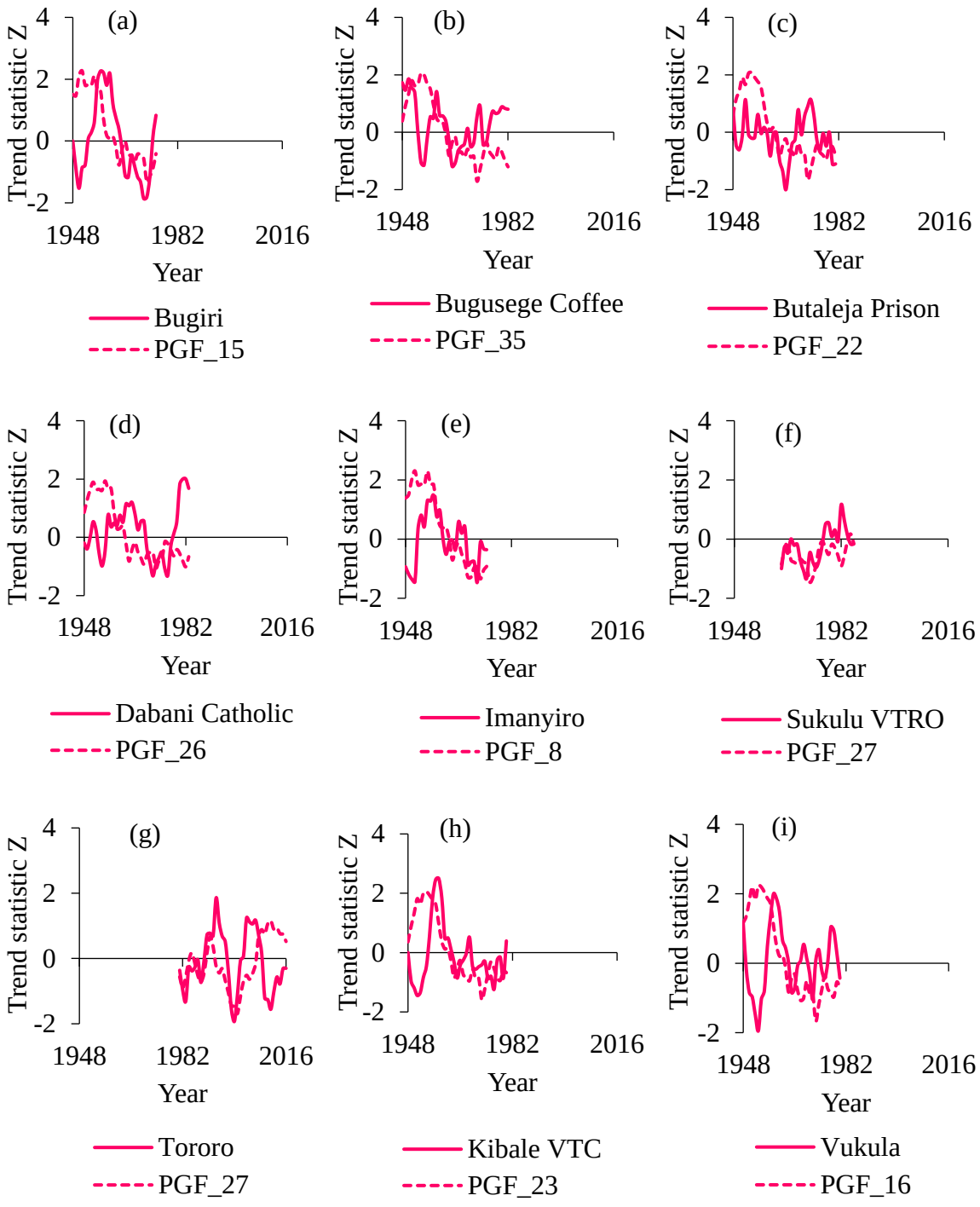

Figure A.7 Variability of SPre10 from PGF and observed rainfall at station (a) 1, (b) 2, (c) 3, (d) 4, (e) 5, (f) 6, (g) 7, (h) 8, and (i) 9. Details of station 1-9 can be found in Table 2.1.

.

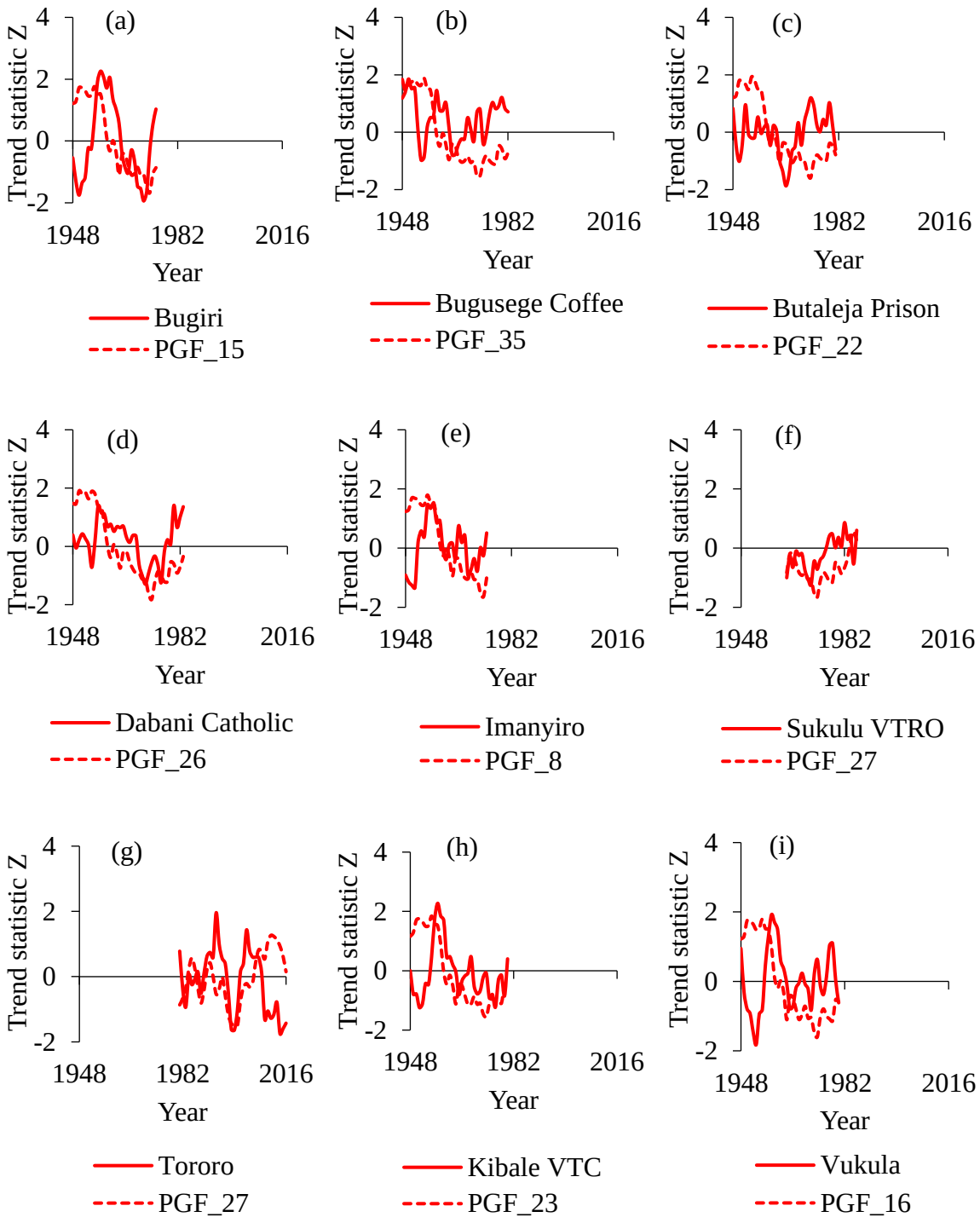

Figure A.8 Variability of SPre5 from PGF and observed rainfall at station (a) 1, (b) 2, (c) 3, (d) 4, (e) 5, (f) 6, (g) 7, (h) 8, and (i) 9. Details of station 1-9 can be found in Table 2.1.

Appendix B: Model calibrated parameters

Table B.1 Calibrated parameters for Australian Water Balance Model (AWBM)

S/N	Description and parameter symbol	Unit	Calibrated value
1	Fraction of catchment area for the first store (A1)	(–)	0.372
2	Fraction of catchment area for the second store (A2)	(–)	0.032
3	Base flow index (BFI)	(–)	0.567
4	Storage capacity of first store (C1)	(mm)	0.065
5	Storage capacity of second store (C2)	(mm)	199.00
6	Storage capacity of third store (C3)	(mm)	392.006
7	Base flow recession constant (K_{base})	(day)	0.997
8	Surface flow recession constant (K_{surf})	(day)	0.953

Table B.2 Calibrated parameters for Sacramento (SAC) model

S/N	Description and parameter symbol	Unit	Calibrated value
1	Additional fraction of pervious area (Adimp)	(–)	0.001
2	Lower Zone Free Water Primary Maximum (Lzfpm)	(mm)	49.990
3	Lower Zone Free Water Supplemental Maximum (Lzfsm)	(mm)	49.755
4	Ratio of water in LZFPM (Lzpk)	(mm)	0.010
5	Ratio of water in LZFSM (Lzsk)	(mm)	0.055
6	Lower Zone Tension Water Maximum (Lztwm)	(mm)	389.10
7	Impervious fraction of the basin (Pctim)	(–)	0.003
8	Minimum proportion of percolation (Pfree)	(–)	0.476
9	Exponential percolation rate (*R*exp)	(–)	0.090
10	Fraction of water unavailable for transpiration (Rserv)	(–)	0.107
11	Catchment portion that loses water by evaporation (Sarva)	(–)	0.000
12	Fraction of base flow which is groundwater flow (Side)	(–)	0.771
13	Flow volume through porous material (Ssout)	($m^3/s/km^2$)	0.000
14	Upper Zone Free Water Maximum (Uzfwm)	(1/day)	9.334
15	Ratio of water in UZFWM (Uzk)	(1/day)	0.040
16	Upper Zone Tension Water Maximum (Uztwm)	(1/day)	0.000
17	Factor applied to PBASE (Zperc)	(–)	38.657

Table B.3 Calibrated parameters for TANK model

S/N	Description and parameter symbol	Unit	Calibrated value
1	Overland runoff from the top outlet of first tank ($a11$)	(m^3/s)	0.846
2	Overland runoff from the lower outlet of first tank ($a12$)	(m^3/s)	0.687
3	Intermediate runoff ($a21$)	(m^3/s)	0.008
4	Subbase runoff ($a31$)	(m^3/s)	0.992
5	Base flow ($a41$)	(m^3/s)	3.7e-5
6	Alpha	(–)	3.000
7	Outflow from the bottom of the first tank ($b1$)	(m^3/s)	0.640
8	Outflow from the bottom of the second tank ($b2$)	(m^3/s)	0.025
9	Outflow from the bottom of the third tank ($b3$)	(m^3/s)	0.437
10	Water depth in the first tank ($C1$)	(mm)	95.564
11	Water depth in the second tank ($C2$)	(mm)	7.528
12	Water depth in the third tank ($C3$)	(mm)	59.580
13	Water depth in the fourth tank ($C4$)	(mm)	99.300
14	Depth below the top outlet of the first tank ($H11$)	(mm)	199.921
15	Depth below the lower outlet of the first tank ($H12$)	(mm)	99.089
16	Depth below the outlet of the second tank ($H21$)	(mm)	0.000
17	Depth below the outlet of the third tank ($H31$)	(mm)	99.846
18	Depth below the outlet of the fourth tank ($H41$)	(mm)	96.187

Table B.4 Calibrated parameters for Identification of Unit Hydrographs and Component Flows from Rainfall, Evaporation and Stream (IHACRES)

S/N	**Description and parameter symbol**	**Unit**	**Calibrated value**
1	Delay	day	0
2	Recession rate 1 ($\alpha^{(s)}$)	1/day	-0.969
3	Peak response 1 ($\beta^{(s)}$)	(–)	0.031
4	Time constant 1 ($T^{(s)}$)	day	31.764
5	Volume proportion 1 ($V^{(s)}$)	°C	1.000
6	Mass balance term (c)	(–)	0.0002
7	Drying rate at reference temperature (t_w)	°C/day	22.00
8	Temperature dependence of drying rate (f)	(–)	3.000
9	Reference temperature (t_{ref})	°C	20.00
10	Moisture threshold for producing flow (l)	mm	0.000
11	Power on soil moisture (p)	(–)	1.000

Table B.5 Calibrated parameters for SIMHYD model

S/N	Description and parameter symbol	Unit	Calibrated value
1	Baseflow coefficient	(–)	0.021
2	Impervious threshold	(–)	0.000
3	Infiltration Coefficient	(–)	400.0
4	Infiltration Shape	(–)	3.000
5	Interflow Coefficient	(–)	0.000
6	Pervious Fraction	(–)	0.986
7	Rainfall Interception Store Capacity	(mm)	0.000
8	Recharge Coefficient	(–)	0.570
9	Soil Moisture Store Capacity	(mm)	500.0

Table B.6 Calibrated parameters for Soil Moisture and Accounting Model (SMAR)

S/N	Description and parameter symbol	Unit	Calibrated value
1	Groundwater evaporation rate (C)	(–)	0.677
2	Groundwater runoff coefficient (G)	(–)	1.000
3	Proportion direct runoff (H)	(–)	0.035
4	Storage loss coefficient (Kg)	(–)	0.004
5	Unit Hydrograph linear routing (N)	(–)	1.000
6	Unit Hydrograph linear routing component (NK=N x K)	(–)	1.000
7	Evaporation conversion parameter (T)	(–)	0.650
8	Infiltration rate (Y)	(mm/day)	209.00
9	Soil moisture total storage depth (Z)	(mm)	50.000

Table B.7 Calibrated parameters for Hydrological Model focusing on Sub-flows' Variation (HMSV)

S/N	Description and parameter symbol	Unit	Calibrated value
	Baseflow sub-model		
1	Initial soil moisture storage (S_{m1})	mm	87.46
2	Maximum limit of soil moisture storage deficit (S_{max})	mm	136.72
3	Baseflow parameter (a_1)	(–)	6.37
4	Baseflow recession constant (t_{b1})	day	194.00
	Interflow sub-model		
5	Interflow parameter (a_2)	(–)	6.37
6	Interflow recession constant (t_{b2})	day	69
	Overland flow sub-model		
7	Overland flow parameter 1 (a_3)	(–)	5.59
8	Overland flow recession constant 1 (t_{b3})	day	4.00
9	Overland flow parameter 2 (c_3)	(–)	4.39
10	Overland flow recession constant 2 (t_{b4})	day	3.00

Appendix C: Amplitude-Duration Frequency Analyses

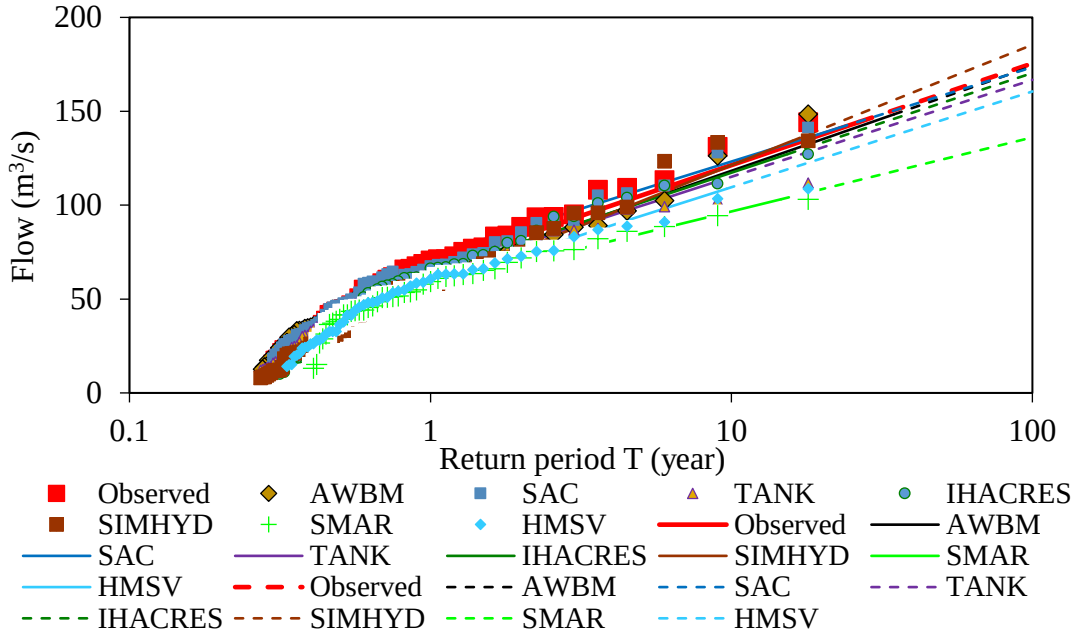

Figure C.1 Comparison of exponential quantile-quantile plot for the high flow POT events considering 5-days aggregation level. The markers represent the empirical quantiles, solid lines signify theoretical (calibrated distribution) quantiles, while dashed lines denote extrapolated quantiles

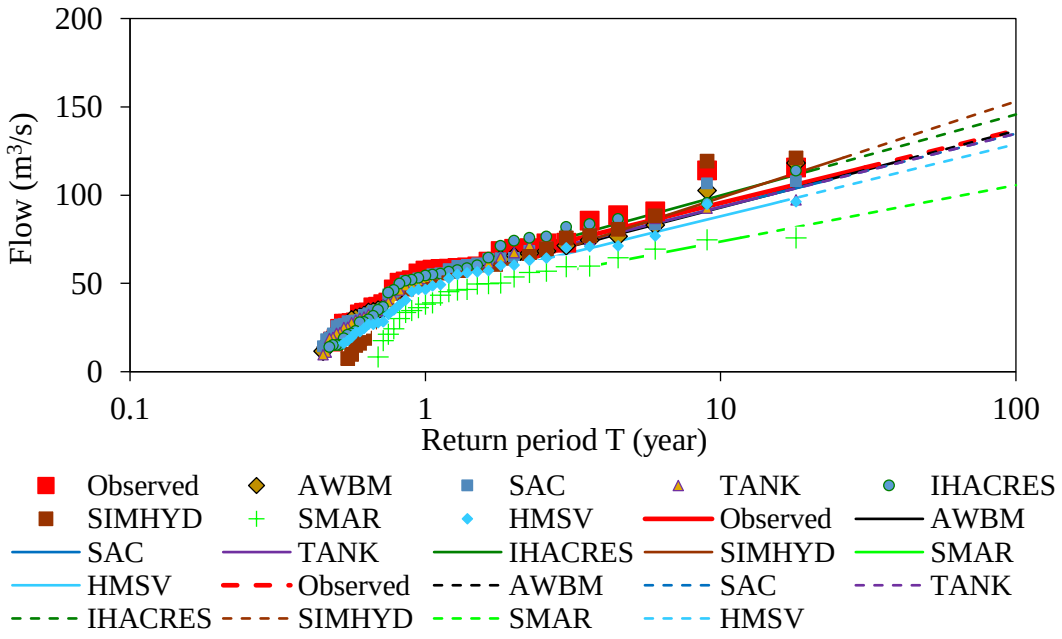

Figure C.2 Comparison of exponential quantile-quantile plot for the high flow POT events considering 30-days aggregation level. The markers represent the empirical quantiles, solid lines

signify theoretical (calibrated distribution) quantiles, while dashed lines denote extrapolated quantiles

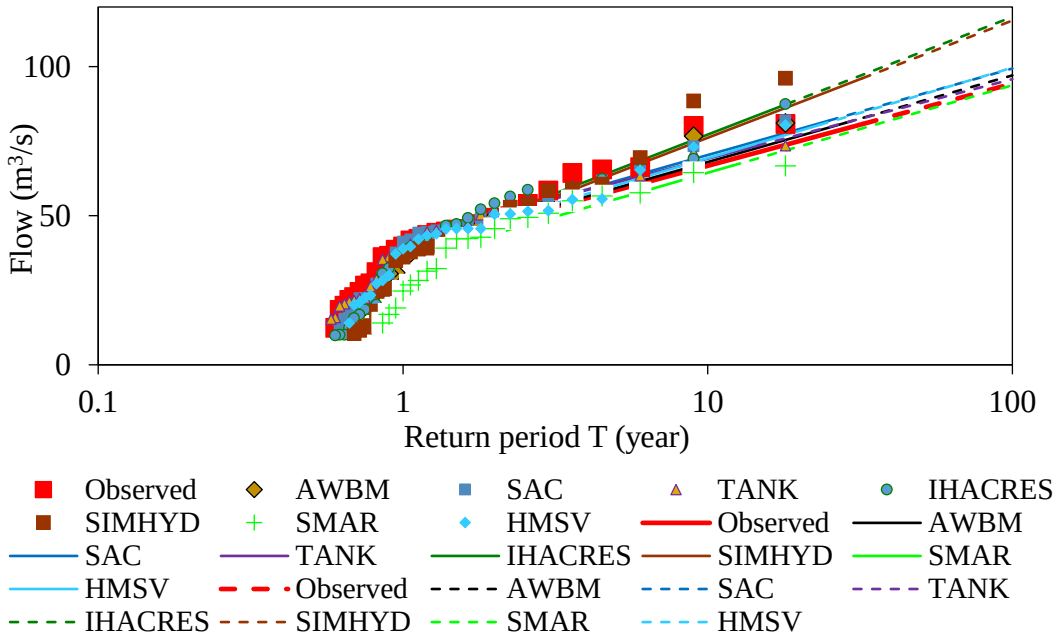

Figure C.3 Comparison of exponential quantile-quantile plot for the high flow POT events considering 90-days aggregation level. The markers represent the empirical quantiles, solid lines signify theoretical (calibrated distribution) quantiles, while dashed lines denote extrapolated quantiles.

Appendix D: Spatial Inundation Extent Analyses

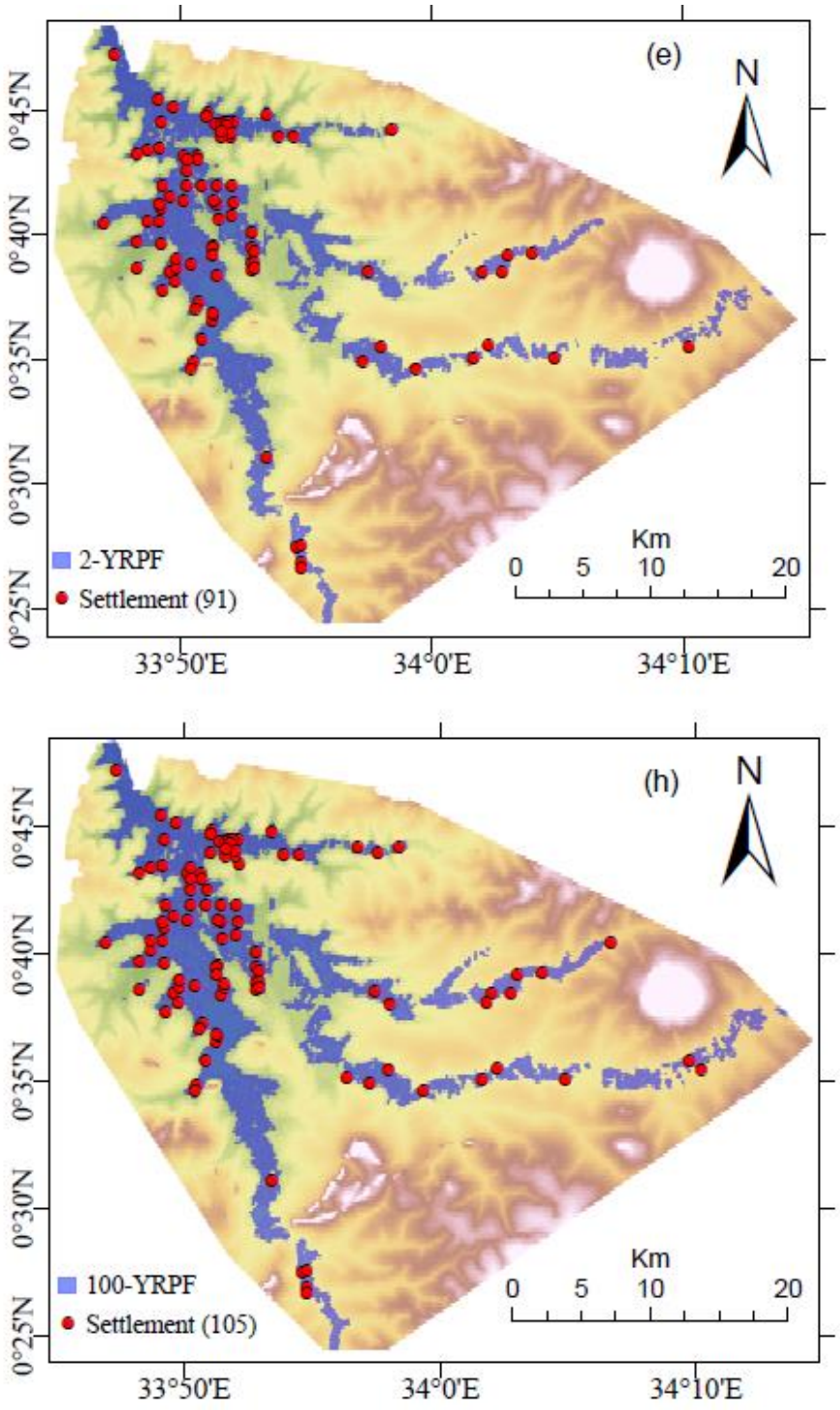

Figure D.1 Inundation extent of human settlement based on extreme flows (Q) at (e) 2-YRP and (h)100-YRP. "YRPF" denotes "year return period flood". The number of settlements in the brackets represent number of settlement clusters with each cluster having an average 10 households (Mubialiwo et al., 2021b)

Appendix E: Community perception of flood alerting and forecasting mechanisms

Table E.1 Responses on the effectiveness of flood alerting mechanisms (values in the table represent the number of respondents)

Flood early warning system	ME	VE	MdE	LE	LSE	WAI	Rank
Shouting out to neighbours	228	29	6	16	28	4.35	I
Door-to-door knocking by the alert team	155	41	6	5	100	3.48	II
Alarm/siren at the monitoring point	117	44	25	64	57	3.33	III
Radios stations	102	34	18	60	93	2.97	IV
Mobile phone text messages	6	32	18	79	172	1.77	V
Televisions	3	1	3	19	281	1.13	VI
Newspapers	2	0	2	20	283	1.10	VII

ME is Most effective, VE is very effective, MdE is Moderately effective, LE is less effective and LSE is Least effective.

Table E.2 Respondents' preference of the flood forecasting mechanisms (values in the table represent the number of respondents)

Flood prediction mechanism	MP	VP	MdP	LP	LSP	WAI	Rank
Observation of the duration of rains	257	72	17	6	8	4.57	I
Observation the amount of rains in the mountain areas of Elgon	261	43	18	20	18	4.41	II
Sound from flood early warning system	164	36	27	41	92	3.39	III
Too much heat indicating rains	74	72	40	35	139	2.74	IV
Analysing the magnitude of thunderstorms before and at beginning of the storm	29	55	49	74	153	2.26	V

MP is Most preferred, VP is very preferred, MdP is Moderately preferred, LP is less preferred and LSP is Least preferred

About the author and a list of peer reviewed publications

About the author

Personal details

Name	Ambrose Mubialiwo
Date of Birth	20 November 1986
Nationality	Ugandan
Email address	mambroze@gmail.com amubialiwo@kyu.ac.ug ambrose.mubialiwo@aau.edu.et

Education background

Addis Ababa University Ethiopia	Ph.D. in Water Management (Hydrology and Water Resources Management)
Katholieke Universiteit Leuven / VUB, Belgium	MSc. Water Resources Eng.
Kyambogo University, Ug	BEng. Civil and Building Eng.

Professional Bodies

1. Registered Engineer with Uganda Engineers Registration Board

2. Corporate Member of the Uganda Institution of Professional Engineers

Academic working experience

Kyambogo University	Assistant Lecturer	Dec 2015-Present
Kyambogo University	Teaching Assistant	Aug 2010-Nov 2015
Ndejje University	Part-timer Lecturer	Aug 2014-Nov 2015

List of the peer reviewed publications that formed different chapters of the dissertation.

Mubialiwo A., Onyutha C., Abebe A., 2020. Historical rainfall and evapotranspiration changes over Mpologoma catchment in Uganda. *Advances in Meteorology* 2020 (Article ID 8870935): 1–19. https://doi.org/10.1155/2020/8870935

Mubialiwo, A., Abebe, A., Onyutha, C., 2021. Performance of rainfall – runoff models in reproducing hydrological extremes: a case of the River Malaba sub-catchment. *SN Applied Sciences* 3, 24. https://doi.org/10.1007/s42452-021-04514-7

Mubialiwo, A., Abebe, A., Onyutha, C., 2021. Analyses of community willingness-to-pay and the influencing factors towards restoration of River Malaba floodplains. *Environmental Challenges* 4, 1–14. https://doi.org/10.1016/j.envc.2021.100160

Mubialiwo, A., Abebe, A., Kawo, N.S., Ekolu, J., Nadarajah, S., Onyutha, C., 2022. Hydrodynamic modelling of floods and estimating socio-economic impacts of floods in Ugandan River Malaba sub-catchment. *Earth Systems and Environment* 6, 45-67. https://doi.org/10.1007/s41748-021-00283-w